

Inorganic-Organic Hybrid Polymers: Solution-Processible Coating Materials for Defined Surface Functionalization

Dissertation

zur Erlangung des Grades
“Doktor der Naturwissenschaften”
im Promotionsfach Chemie

am Fachbereich Chemie, Pharmazie und Geowissenschaften
der Johannes Gutenberg-Universität Mainz

Daniel Keßler

geb. in Bendorf

Mainz, 2009

Die vorliegende Arbeit wurde unter Betreuung von [REDACTED] in der Zeit von Oktober 2006 bis Juli 2009 am Institut für Organische Chemie der Johannes Gutenberg-Universität Mainz angefertigt.

Dekan:
Erster Berichterstatter:
Zweiter Berichterstatter:
Tag der mündlichen Prüfung:

[REDACTED]

18.08.2009

	List of Abbreviations	III
1	Introduction	1
1.1	Surface Coatings	1
1.1.1	Functional Surface Coatings	5
1.1.2	Reactive Surface Coatings	6
1.1.3	Semi-Conductive Polymer Films and Their Applications	7
1.2	Coating Adhesion and Coating/Thin Film Characterization	10
1.2.1	Coating Adhesion	10
1.2.2	Standardization of Adhesion Tests	12
1.2.3	Coating/Thin Film Characterization	13
1.3	Polymeric Materials	22
1.3.1	Atom Transfer Radical Polymerization (ATRP)	23
1.3.2	Reversible Addition Fragmentation Chain Transfer (RAFT)	24
1.3.3	Silicon-Containing Materials as Adhesion Promoters	26
1.3.4	Sol-Gel Coatings and Poly(silsesquioxanes)	27
1.3.5	Hybrid Polymers based on Poly(silsesquioxanes)	30
2	Aim of Work	33
3	Results and Discussion	35
3.1	Synthesis of Inorganic-Organic Hybrid Polymers	35
3.1.1	Hybrid Polymer Synthesis Using ATRP	35
3.1.2	Hybrid polymer Synthesis Using RAFT	37
3.1.3	Microreactor Based Synthesis of Poly(methylsilsesquioxanes)	38
3.1.4	Synthesis of Hybrid Polymers Starting from Organic Polymers	39
3.2	General Coating Properties	41
3.3	Functional Coating Materials	43
3.3.1	Temperature-Responsive Coatings	43
3.3.2	Semi-Conductive Coatings	43
3.4	Reactive Coating Materials	45
3.4.1	Surface-Analogous Reaction	45
3.4.2	Modification on the Surface	46
4	Publications	49
4.1	“Synthesis of Processable Inorganic-Organic Hybrid Polymers Based on Poly(silsesquioxanes): Grafting from Polymerization Using ATRP”	51
4.2	“Synthesis of Functional Inorganic-Organic Hybrid Polymers Based on Poly(silsesquioxanes) and Their Thin Film Properties”	69
4.3	“Synthesis of Defined Poly(silsesquioxane)s: Fast Polycondensation of Trialkoxysilanes in a Continuous-Flow Microreactor”	89

4.4	“Surface Coatings Based on Polysilsesquioxanes: Grafting-from Approach Starting from Organic Polymers”	101
4.5	“Temperature-Responsive Surface Coatings Based on Poly(methylsilsesquioxane)-Hybrid Polymers”	109
4.6	“Surface Coatings Based on Polysilsesquioxanes: Solution Processible Smooth Hole-Injection-Layers for Optoelectronic Applications”	117
4.7	“Substrate-Independent Stable and Adherent Reactive Surface Coatings and Their Conversion with Amines”	127
4.8	“Reactive Surface Coatings Based on Polysilsesquioxanes: Defined Adjustment of Surface Wettability”	137
4.9	“Reactive Surface Coatings Based on Polysilsesquioxanes: Controlled Functionalization for Specific Protein Immobilization”	159
4.10	“Modular Approach toward Multi-Functional Surfaces with Adjustable and Dual-Responsive Wettability Using a Hybrid Polymer Toolbox”	185
5	Conclusion	199
6	Publications – Overview	201
7	Acknowledgements	207

A	ampere
a.u.	arbitrary units
AFM	atomic force microscopy
A_H	Hamaker constant
AIBN	azoisobutyronitrile
ATR	attenuated total reflectance
ATRP	atom transfer radical polymerization
BPO	benzoyl peroxide
br	broad peak in NMR spectrum
CA	contact angle
$CDCl_3$	chloroform, deuterized
CPMAS NMR	charge polarized magic angle spinning nuclear magnetic resonance
CTA	chain transfer agent
CV	cyclovoltammetry
δ	chemical shift (NMR spectroscopy)
d	duplet (splitting in NMR spectroscopy)
D, d	distance
DCB	dichlorobenzene
DCM	dichloromethane
DMF	dimethylformamide
DSC	differential scanning calorimetry
EA	elemental analysis
ETL	electron transport layer
eV	electron volt
FBP	folate-binding protein
FD	field desorption (mass spectrometry)
FPA	pentafluorophenylacrylate
FPVB	pentafluorophenyl vinylbenzoate
FTIR	Fourier transform infrared spectroscopy
FTO	fluorine tin oxide
GPC	gel permeation chromatography
h	hours
HIL	hole injection layer
HIM	hole injection material
HOMO	highest occupied molecular orbital
HTL	hole transport layer
Hz	hertz
IPM	initiating groups per molecule
ITO	indium tin oxide
J	coupling constant (NMR spectroscopy)
LCST	lower critical solution temperature
LUMO	lowest unoccupied molecular orbital

m	multiplet (splitting in NMR spectroscopy)
MA	methacrylate
mCTA	macro chain transfer agent
M_e	molecular weight of entanglement
MI	macroinitiator
MMA	methylmethacrylate
M_N, M_n	molecular weight (number average)
MTMS	methyltrimethoxysilane
M_w, M_w	molecular weight (weight average)
n	refractive index
NBD	7-nitro-2,1,3-benzoxadiazole
NIPAM	<i>N</i> -isopropylacrylamide
NMP	nitroxide mediated polymerization
NMR	nuclear magnetic resonance
OLED	organic light-emitting diode
OPVC	organic photovoltaic cell
ORMOCER®	organically modified ceramic
OTFT	organic thin film transistor
PA	pre-albumin
PAN	polyacrylonitrile
PBS	phosphate buffered saline
PC	polycarbonate
PDI	polydispersity index (M_w/M_n)
PDMA	poly(decylmethacrylate)
PDMS	poly(dimethylsiloxane)
PEG	poly(ethylene glycol)
PEHA	poly(ethylhexylacrylate)
PFFA	poly(pentafluorophenylacrylate)
PFPVB	poly(pentafluorophenyl vinylbenzoate)
P_{gel}	gel point
PHAH	polyhalogenated aromatic hydrocarbons
PLED	polymer light-emitting diode
PMA	poly(methylacrylate)
PMMA	poly(methylmethacrylate)
PMSSQ	poly(methylsilsesquioxane)
PNIPAM	poly(<i>N</i> -isopropylacrylamide)
POSS	polyhedral oligomeric silsesquioxane ($Si_8O_{12}R_8$)
P_{ox}	oxidation potential (CV)
ppm	parts per million (NMR spectroscopy)
PPSSQ	poly(phenylsilsesquioxane)
PPVB	poly(propargyl vinylbenzoate)
P_{red}	reduction potential (CV)

PS	polystyrene
PSSQ	poly(silsesquioxane)
PTFE	polytetrafluoroethylene
PVB	propargyl vinylbenzoate
PVC	polyvinylchloride
q	quartet (splitting in NMR spectroscopy)
Θ_a	advancing contact angle
Θ_r	receding contact angle
RAFT	reversible addition fragmentation chain transfer
RMS	root mean square
rpm	rounds per minute
RT	room temperature
s	singlet (splitting in NMR spectroscopy)
SEC	size exclusion chromatography
SEM	scanning electron microscopy
SPR	surface plasmon resonance
t	triplet (splitting in NMR spectroscopy)
τ	transit time (time-of-flight)
T1	T1 branch in silsesquioxane network (two free silanol groups)
T2	T2 branch in silsesquioxane network (one free silanol group)
T3	T3 branch in silsesquioxane network (completely condensed)
T4	thyroxine
TCO	transparent conductive oxide
TEOS	tetraethoxysilane
T_g	glass transition temperature
TGA	thermo gravimetical analysis
THF	tetrahydrofurane
TOF	time-of-flight
UV/Vis	ultra violet/visible light
V	volt
wt% , wt.-%	weight percent
XPS	X-ray photoelectron spectroscopy

1 Introduction

Looking at every single item people use in everyday life, its properties are not only determined by the bulk material but to a large extent by its surface properties. Especially when thinking of device miniaturization, e.g. in electronic devices, defined adjustment of surface properties becomes more and more important as the surface-to-volume ratio increases.

As the application spectrum of coatings reaches from large-area coverage (e.g. in automotive industry or building exteriors) to defined functionalization of (sub-)micrometer surfaces (e.g. microelectronics or microfluidics) also various methods were investigated for coating formulation. Especially when applied from solution, polymers are the materials of choice to realize defined surface properties.

The present thesis describes different synthetic approaches toward highly cross-linkable hybrid polymers and their ability to form stable and adherent coatings that are independent from the underlying material. Furthermore, new concepts of surface functionalization based on these hybrid polymers were investigated and successfully applied for various purposes.

1.1 Surface Coatings

The increasing need for more sophisticated materials, devices and products increases the difficulties to implement defined or unique surface characteristics, which determine the materials characteristics to a large extent.¹

To realize these desired specific surface characteristics coatings are applied on almost any kind of object. Every single application determines the requirements on the intended coating material, e.g. specific wettability; scratch, abrasion or chemical resistance; transparency; conductivity; color; defined permeability; corrosion protection; etc.² Besides the specific function, a strong adhesion and stability of the coating on the underlying material as well as a cost effective and simple processability have to be guaranteed. These two issues are usually determined by the underlying material (substrate) and the geometrical shape of the object to be coated. Various adhesion phenomena can occur on different materials due to specific chemical functions at the interface (which are sometimes determined by pre-treatment of the interface) and different degrees of surface roughness (for a detailed introduction to adhesion phenomena see chapter 1.2).

These broad spectra of underlying materials and desired surface functions lead to different coating formation protocols: physical or chemical vapor deposition; powder coatings; electrochemical deposition; electroplated metals; plasma coatings; etc.^{3,4}

Besides the mentioned methods, deposition from a liquid state (e.g. solution or melt) is the most common technique used for coating (see 1.2). The main advantage of the application from a liquid state is the formation of a continuous liquid film on top of the surface, which is

¹ Almeida, E. *Ind. Eng. Chem. Res.* **2001**, *40*, 3.

² Cartier, M. (Ed.), *Handbook of Surface Treatment and Coatings*, John Wiley & Sons, New York, USA, **2003**.

³ Swaraj, P., *Surface Coatings. Science and Technology*, John Wiley & Sons, New York, USA, **1995**.

⁴ Freund, L. B.; Suresh, S., *Thin Films: Stress, Defect Formation and Surface Evolution*, Cambridge University Press, Cambridge, UK, **2003**.

able to even out defects.⁵ The most important step in the coating process is the film formation, meaning the conversion of the continuous liquid film into an integral solid film. This transition from the liquid state to a continuous solid film is usually realized by a shift of the glass transition temperature (T_g) of polymers in the coating material.⁶ The T_g of the polymeric coating material is increased (exceeding ambient temperature or the operating temperature of the coated object) either by solvent evaporation or chemical reactions during the film formation.^{7,8} A film formation that is only based on solvent evaporation (thermoplastic coating) seems to become less important nowadays. Effective polymer entanglement only occurs if the molecular weight is high (entanglement molecular weight M_e varies significantly for different polymers and is usually in the range of several 10^5 g/mol), resulting in highly viscous polymer solutions which lead to problems in processability. Furthermore, without covalent attachment to the underlying material delamination of the polymer from the substrate may occur. Figure 1.1 demonstrates the delamination of polystyrene (PS) on silicon wafers, right after coating a continuous film is formed, upon annealing PS delaminated from the surface.



Figure 1.1. Delamination of polystyrene on silicon wafers. Polystyrene ($M_w = 25$ kg/mol) was spin-coated onto Si wafers (1 wt% in THF, 4000 rpm, 15 s). The left wafer was just coated, whereas the right wafer was annealed at 130 °C for 1 h.

Another disadvantage of thermoplastic coatings is the low diffusion of residual solvent after the polymer reaches the glassy state, meaning the coating will emit significant amounts of solvent vapor for very long periods. Especially for coatings in contact with food and beverage this solvent retention is not acceptable. Furthermore, this emission of volatile organic carbons

⁵ Reynolds, P. A. „Rheology“ in Marrion, A. R. (Ed.), *The Chemistry and Physics of Coatings 2nd Ed.*, RSC, Cambridge, UK, **2004**.

⁶ Proveder, T.; Urban, M. W. (Eds.), *Film Formation in Coatings. Mechanism, Properties, and Morphology*, ACS Symp. Series 790, ACS, Washington, DC, USA, **2001**.

⁷ Pascault, J. P.; Sautereau, H.; Verdu, J.; Williams, R. J. J., *Thermosetting Polymers*, Marcel Dekker, New York, USA, **2002**.

⁸ Port, A. B.; Cameron, C. „Film Formation“ in Marrion, A. R. (Ed.), *The Chemistry and Physics of Coatings 2nd Ed.*, RSC, Cambridge, UK, **2004**.

(VOC), contributing to current or potential atmospheric pollution, is restricted by various national emission ceilings.^{9,10}

An advanced method of thermoplastic film formation widely used in paint and coating industry is a dispersed phase polymer system (latex). Polymer particles are applied from a stabilized dispersion in water. After application, water and additional co-solvents evaporate and the particles pack closely. Driven by capillary forces, the particles overcome the repulsive inter-particle stabilization forces and coalesce into a continuous film. Finally, polymer inter-particle diffusion causes film formation. Usually coalescing aids are used to reduce the T_g at the particle – particle interface and thus allows chain diffusion. Film formation from a latex reduces the VOC emission over time effectively and allows application of high molecular weight polymers.

Film formation from solutions of cross-linkable polymers combines solvent evaporation and chemical cross-linking reactions between several functional groups, resulting in molecular weight increase (thermosetting resins).^{11,12} The main classes of cross-linking reactions are step-growth or chain growth reactions and usually require radiation or stoving.¹³ Most thermosetting coatings use step-growth cross-linking reactions between two functionalities (A+B). Infinite molecular weight (MW) is reached at the gel point. According to the theory of Flory and Stockmeyer,¹⁴ the gel point (P_{gel}) is only determined by the number of functionalities A and B and their ratio r .⁷ For stoichiometric mixtures the sol fraction should completely be converted into the gel fraction, which is practically not reached and thus a residual sol fraction remains. However, controlling the emission of residual low-molecular-weight polymers or solvent is much easier for thermosetting coatings in comparison to thermoplastic coatings.¹⁵

In industrial applications the used cross-linkable molecules (either small molecules or polymers) are called binders. Typical examples are melamine formaldehyde or isocyanates, which are able to cross-link acrylate-based copolymers, containing hydroxyl groups.¹⁶ Also random copolymers of styrene or methylmethacrylate with incorporated benzocyclobutenes showed promising coating properties after cross-linking of the cyclobutene groups.¹⁷

Besides the mentioned procedures to coat substrates with polymers, which are well established in industry, different specialized approaches are used to create well defined polymeric layers in various academic applications. Since the first report of monomolecular layer formation by adsorption of surfactants onto clean metal surfaces, those self-assembled

⁹ Council Directive on the limitation of emission of volatile organic compounds due to the used of organic solvents in certain additives and installations, *Official Journal of the European Communities*, L 85/1, 23-3-1999.

¹⁰ Directive 2001/81/EC on national emission ceilings for certain atmospheric pollutants, *Official Journal of the European Communities*, L 309/22, 27-11-2001.

¹¹ Stepto, R. F. T. (Ed.), *Polymer Networks*, Blackie, London, UK, **1998**.

¹² Wicks, Z. W.; Jones, F. N.; Pappas, S. P.; Wicks, D. A., *Organic Coatings. Science and Technology 3rd ed.*, John Wiley & Sons, Hoboken, NJ, USA, **2007**.

¹³ Koleske, J. V., *Radiation-Cured Coatings in Tracton*, A. A. (Ed.), *Coatings Technology Handbook 3rd ed.*, CRC press, Boca Raton, FL, USA, **2006**.

¹⁴ Flory, P. J., *Principles of Polymer Chemistry*, Cornell University Press, Ithaca, NY, USA, **1953**.

¹⁵ Tracton, A. A. (Ed.), *Coatings Materials and Surface Coatings*, CRC press, Boca Raton, FL, USA, **2007**.

¹⁶ Chung, R. P.-T.; Solomon, D. H. *Prog. Org. Coat.* **1992**, *21*, 227.

¹⁷ Ryu, D. Y.; Shin, K.; Drockenmuller, E.; Hawker, C. J.; Russell, T. P. *Science* **2005**, *308*, 236.

monolayers (SAM) became a useful tool to create defined surface properties.¹⁸ The basis for this method is the controlled adsorption of specific functionalities, designed to match with the desired substrate (see figure 1.2). Most popular are SAMs of thiols (or disulfides) on gold surfaces¹⁹ and chloro- or alkoxy-silanes on glass or silicon surface (generally on hydroxylated surfaces).^{20,21} A detailed review about formation and structure of various types of self-assembled monolayers was given by Ulman.²² In case of organosulfur on metal surfaces (e.g. thiols on gold) no covalent bonding between Au and S can be observed and thus the organosulfur compounds can be substituted on the surface by exchange reactions with other thiols or disulfides.^{23,24,25} The chemisorption is most likely due to Au(I) thiolate (RS⁻) species.^{26,27} In comparison, the SAM formation of organosilicon derivatives on metal oxide surfaces relies on the in situ covalent attachment to surface silanol groups (Si-OH) via Si-O-Si bonds, which does not allow further substitution reactions with other silanols in solution. Substrates on which silanol monolayers have been successfully prepared include silicon oxide,²⁸ aluminium oxide,²⁹ quartz,³⁰ glass,²⁸ mica,³¹ zinc selenide,²⁸ germanium oxide²⁸ and gold (activated by UV/ozone exposure).³² As a consequence of the covalent attachment, no flexibility of position during film formation is observed as for thiols on Au. This complicates the formation of high-quality organosilicon SAMs, and may lead to incomplete coverage or to facile polymerization in solution and polysiloxane deposition on the surface.³³

Effective methods of functionalization of surfaces with polymers, based on the SAM formation, are polymer brushes, either grafted from or grafted to the surface. For the grafting from approach, initiator molecules form a SAM on the surface, giving defined starting points from which polymers can grow. Polymers with functional end groups capable to adsorb on the surface are used to graft polymers to a given surface (see figure 1.2).³⁴

Other methods for covalent attachment of polymers on surfaces rely on photoinitiators, e.g. benzophenones, to bind to polymeric surfaces³⁵ or on electrografting from conductive surfaces.³⁶

¹⁸ Bigelow, W. C.; Pickett, D. L.; Zisman, W. A. *J. Colloid Interface Sci.* **1946**, *1*, 513.

¹⁹ Nuzzo, R. G.; Allara, D. L. *J. Am. Chem. Soc.* **1983**, *105*, 4481.

²⁰ Sagiv, J. *J. Am. Chem. Soc.* **1980**, *102*, 92.

²¹ Wasserman, S. R.; Tao, Y.-T.; Whitesides, J. M. *Langmuir* **1989**, *5*, 1074.

²² Ulman, A. *Chem. Rev.* **1996**, *96*, 1533.

²³ Biebuyck, H. A.; Whitesides, G.M. *Langmuir* **1993**, *9*, 1766.

²⁴ Mohri, N.; Inoue, M.; Arai, Y.; Yoshikawa, K. *Langmuir* **1995**, *11*, 1612.

²⁵ Fenter, P.; Eberhardt, A.; Eisenberger, P. *Science* **1994**, *266*, 1216.

²⁶ Walczak, M. W.; Chung, C.; Stole, S. M.; Widrig, C. A.; Porter, M. D. *J. Am. Chem. Soc.* **1991**, *113*, 2370.

²⁷ Porter, M. D.; Bright, T. B.; Allara, D. L. *J. Am. Chem. Soc.* **1987**, *109*, 3559.

²⁸ Gun, J.; Sagiv, J. *J. Colloid Interface Sci.* **1986**, *112*, 457.

²⁹ Tilman, N.; Ulman, A.; Schildkraut, J. S.; Penner, T. L. *J. Am. Chem. Soc.* **1988**, *110*, 6136.

³⁰ Mathauser, K.; Frank, C. W. *Langmuir* **1993**, *9*, 3446.

³¹ Schwartz, D. K.; Steinberger, S.; Israelachvili, J.; Zasadzinski, Z. A. N. *Phys. Rev. Lett.* **1992**, *69*, 3354.

³² Finklea, H. O.; Robinson, L. R.; Blackburn, A.; Richter, B.; Allara, D. L.; Bright, T. *Langmuir* **1986**, *2*, 239.

³³ Brandriss, S.; Margel, S. *Langmuir* **1993**, *9*, 1232.

³⁴ Advincula, R. C.; Brittain, W. J.; Caster, K. C.; R  he, J. (Eds.), *Polymer Brushes*, Wiley-VCH, Weinheim, Germany, **2004**.

³⁵ Prucker, O.; Naumann, C. A.; R  he, J.; Knoll, W.; Frank, C. W. *J. Am. Chem. Soc.* **1999**, *121*, 8766.

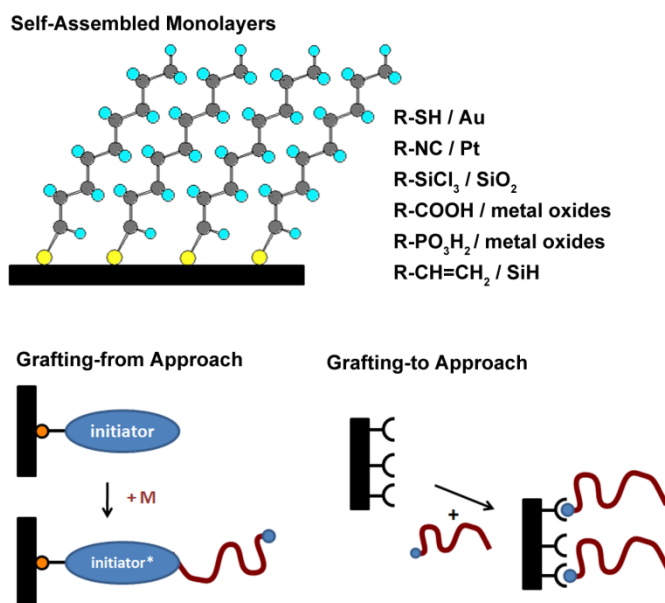


Figure 1.2. Different approaches to functionalize specific surfaces with small molecules or polymers.

1.1.1 Functional Surface Coatings

Usually every coating could be understood as functional coating, because the aim of the coating application is to fulfill a certain function on the surface (e.g. corrosion protection).

Using a more specific definition, a functional coating consists of a defined chemical moiety, attached to the surface. This defined surface chemistry is directly responsible for the coating's function. A first example was already pointed out by Langmuir in 1938; the spatial arrangement of ligands and atoms in the top surface region of a coating defines the surface wettability.³⁷ Thus, wettability of a coating is determined to a large extent by the chemical structures immobilized on the surface (furthermore topological roughness and chemical heterogeneity also have influence on wetting, see chapters 3.4 and 4.8). By adjusting functional moieties in a coating material the resulting surface coating showed the desired permanent wettability, adjustable in a range between hydrophilic and hydrophobic behavior, in respect to the used chemical functions.^{38,39} Besides permanently altered wettability also various surface coatings featuring stimuli-responsive wetting behavior could be realized using defined functional coatings. The resulting change in surface wetting may be observed by monitoring the change in contact angle (CA) (see chapter 1.2.3) between a droplet of water or aqueous solution and the surface. Changes to surface wetting have a significant effect on interfacial interactions with other materials, e.g. liquids, gases, biomolecules or cells and

³⁶ Cuenot, S.; Gabriel, S.; Jerome, R.; Jerome, C.; Fustin, C.-A.; Jonas, A. M.; Duwez, A.-S. *Macromolecules* **2006**, *39*, 8428.

³⁷ Langmuir, I. *Science* **1938**, *87*, 493.

³⁸ Howarter, J. A.; Youngblood, J. P. *Macromol. Rapid Commun.* **2008**, *29*, 455.

³⁹ Gao, L.; McCarthy, T. J. *Langmuir* **2006**, *22*, 2966.

tissues.⁴⁰ Poly(*N*-isopropylacrylamide) (PNIPAM) usually acts as surface-immobilized function to realize temperature-responsive wetting behavior because of its lower critical solution temperature (LCST) at approx. 32 °C. Below LCST PNIPAM is soluble in water, meaning if immobilized on a surface the surface is more hydrophilic (CA ≈ 80°). Heated above LCST PNIPAM collapse, changing the surface to a more hydrophobic one (CA ≈ 100°).⁴¹ Further examples for stimuli-responsive surfaces and their responsible functional coatings are: poly(acrylic acid) (PAA) or poly(styrene sulfonate) coatings exhibiting pH-responsive surfaces;⁴² azobenzene containing polymer films as light-responsive coatings⁴³ or redox-active groups like ferrocene as electrochemically responsive coatings.⁴⁴ Various other surface-responsive materials, including more complex architectures like block-copolymers,⁴⁵ end-group functionalized polymer brushes⁴⁶ or even dual-responsive coatings⁴⁷ can be found in the literature.

Besides adjustment of wettability, various functional coatings are used in different biochemical or bio-medical applications. Specific functional coatings were successfully used to enhance tissue growth on artificial implants.^{48,49} Furthermore, biosensors and microfluidic analysis devices need specific binding sites for various biomolecules or cells on the surface.⁵⁰ Among others, coatings to immobilize catalysts for various reactions⁵¹ are another example for functional or smart surface coatings.^{52,53}

1.1.2 Reactive Surface Coatings

Similar to reactive polymers in solution,⁵⁴ reactive coatings can be converted or functionalized by further chemical reactions. Reactive coatings offer a variety of possibilities for further tailoring of surface properties. Reactive coatings offer a variety of possibilities for further tailoring of surface properties. The coating material expresses reactive sites at the interface, which should react fast and quantitative with the desired functionalized molecule. Usually this surface-analogous reaction is carried out by dipping the coated substrate into a solution containing the function to be immobilized.

⁴⁰ Gras, S. L.; Mahmud, T.; Rosengarten, G.; Mitchell, A.; Kalanta-zadeh, K. *ChemPhysChem* **2007**, *8*, 2036.

⁴¹ Sun, T.; Wang, G.; Feng, L.; Liu, B.; Ma, Y.; Jiang, L.; Zhu, D. *Angew. Chem. Int. Ed.* **2004**, *43*, 357.

⁴² Papaefthimiou, V.; Steitz, R.; Findenegg, G. H. *Chem. Unserer Zeit* **2008**, *42*, 102.

⁴³ Siewierski, L. M.; Brittain, W. J.; Petrash, S.; Foster, M. D. *Langmuir* **1996**, *12*, 5838.

⁴⁴ Sondag-Huethorst, J. A. M.; Fokkink, L. G. J. *Langmuir* **1994**, *10*, 4380.

⁴⁵ Russell, T. P. *Science* **2002**, *297*, 964.

⁴⁶ Lahann, J.; Mitragotri, S.; Tran, T.-N.; Kaido, H.; Sundaram, J.; Choi, I. S.; Hoffer, S.; Somorjai, G. A.; Langer, R. *Science* **2003**, *209*, 371.

⁴⁷ Xia, F.; Feng, L.; Wang, S.; Sun, T.; Song, W.; Jiang, W.; Jiang, L. *Adv. Mater.* **2006**, *18*, 432.

⁴⁸ Dong, J.; Foley, J. D.; Frethem, C. D.; Hoerr, R. A.; Matuszewski, M. J.; Puskas, J. E.; Haugstad, G. *Langmuir* **2009**, *25*, 5442.

⁴⁹ Rickert, D.; Moses, M. A.; Lendlein, A.; Kelch, S.; Franke, R. *Clinical Hemorheology and Microcirculation* **2003**, *28*, 175.

⁵⁰ Huber, D. L.; Manginell, R. P.; Samara, M. A.; Kim, B.-I.; Bunker, B. C. *Science* **2003**, *301*, 352.

⁵¹ Mukhutdinov, R. K.; Samoilov, N. A.; Sinelnikova, V. K.; Gubasayan, S. M.; Sultanova, L. G. *Chem. Petro. Eng.* **1988**, *24*, 75.

⁵² Ghosh, S. K. (Ed.), *Functional Coatings*, Wiley-VCH, Weinheim, Germany, **2006**.

⁵³ Provder, T.; Baghdachi, J., *Smart Coatings I*, ACS Symp. Series 957, **2007** and *Smart Coatings II*, ACS Symp. Series 1002, **2009**, Washington, DC, USA.

⁵⁴ Theato, P. *J. Polym. Sci., Part A: Polym. Chem.* **2008**, *46*, 6677.

Coatings composed of copolymers of vinyl isocyanates and maleic anhydride groups have successfully been used to coat metal oxide surfaces while maintaining reactive isocyanates and maleic anhydrides on the surface, which could be converted with amines in solution.⁵⁵ Other reactive coatings, which can be functionalized with amines are based on activated esters, like *N*-succinimidyl esters⁵⁶ or pentafluorophenyl esters,⁵⁷ or plasma-polymerized maleic anhydrides.⁵⁸ Especially pentafluorophenyl esters showed complete and fast conversion with aliphatic amines, even without additional base.⁵⁹ Langer and coworkers introduced the CVD polymerization of [2.2]paracyclophane pentafluorophenol ester to create chemically and topologically uniform reactive polymer coatings.⁶⁰ Their method could successfully be used to pattern surfaces onto a broad range of different materials. However, this solvent free process is not applicable toward large structured surfaces or devices and the reaction conditions must be controlled very precisely to avoid the decomposition of the reactive groups.^{61,62}

Besides reactive sites capable to bind amino-functionalized molecules, copper-catalyzed 1,3-dipolar cycloaddition between azides and acetylene⁶³ is a very popular reaction to attach defined functions to a reactive coating.^{64,65} Reactive coatings expressing either acetylenes or azides have been developed.⁶⁶

Other reactive coatings are based on aldehyds (addition of hydroxylamines),⁶⁷ epoxides (addition of alcohols),⁶⁸ maleimides (Michael addition with thioles)⁶⁹ or dienes (Diels-Alder reaction with dienophiles).⁷⁰

1.1.3 Semi-Conductive Polymer Films and Their Applications

Most functional coatings, like in bio-chemical analysis devices, mainly focuses on a specific function expressed directly at the interface. Semi-conductive coatings need defined polymeric functionalities, which are well distributed throughout the whole film, mostly in specific morphologies (As the main function is not limited to the interface but through the whole deposited material, usually the term “semi-conductive film” is used rather than “coating”, even if deposition methods and principal properties are similar.)

⁵⁵ Beyer, D.; Bohanon, T. M.; Knoll, W.; Ringsdorf, H. *Langmuir* **1996**, *12*, 2514.

⁵⁶ Jerome, C.; Gabriel, S.; Voccia, S.; Detrembleur, C.; Ignatova, M.; Gouttebaron, R.; Jerome, R. *Chem. Commun.* **2003**, 2500.

⁵⁷ Lahann, J.; Choi, I. S.; Lee, J.; Jensen, K. F.; Langer, R. *Angew. Chem. Int. Ed.* **2001**, *40*, 3166.

⁵⁸ Schiller, S.; Hu, J.; Jenkins, A. T. A.; Timmons, R. B.; Sanchez-Estrada, F. S.; Knoll, W.; Förch, R. *Chem. Mater.* **2002**, *14*, 235.

⁵⁹ Eberhardt, M.; Theato, P. *Macromol. Rapid Commun.* **2005**, *26*, 1488.

⁶⁰ Lahann, J.; Balcells, M.; Lu, H.; Rodon, T.; Jensen, K. F.; Langer, R. *Anal. Chem.* **2003**, *75*, 2117.

⁶¹ Lahann, J.; Balcells, M.; Rodon, T.; Lee, J.; Choi, I. S.; Jensen, K. F.; Langer, R. *Langmuir* **2002**, *18*, 3632.

⁶² Chen, H.-Y.; Elkasabi, Y.; Lahann, J. *J. Am. Chem. Soc.* **2006**, *128*, 374.

⁶³ Kolb, H. C.; Finn, M. G.; Sharpless, K. B. *Angew. Chem. Int. Ed.* **2001**, *40*, 2004.

⁶⁴ Schlossbauer, A.; Schaffert, D.; Kecht, J.; Wagner, E.; Bein, T. *J. Am. Chem. Soc.* **2008**, *130*, 12558.

⁶⁵ Barner-Kowollik, C.; Inglis, A. J. *Macromol. Chem. Phys.* **2009**, doi: 10.1002/macp.200900139.

⁶⁶ Evans, R. A. *Australian Journal of Chemistry* **2006**, *60*, 384.

⁶⁷ MacBeath, G.; Schreiber, S. L. *Science* **2000**, *289*, 1760.

⁶⁸ Chen, B.; Pernodet, N.; Rafailovich, M. H.; Bakhtina, A.; Gross, R. A. *Langmuir* **2008**, *24*, 13457.

⁶⁹ Viitala, T.; Vikholm, I.; Pelton, J. *Langmuir* **2000**, *16*, 4953.

⁷⁰ Houseman, B. T.; Huh, J. H.; Kron, S. J.; Mrksich, M. *Nat. Biotechnol.* **2002**, *20*, 270.

Recently, organic or polymeric semi-conductors are used in organic thin film transistors (OTFT),⁷¹ photochromic devices,⁷² organic light emitting diodes (OLED)⁷³ or organic photovoltaic cells (OPVC).⁷⁴ Semi-conductive polymer films have the advantage of allowing an easy, low-cost manufacture of large-area displays using solution processing of film-forming polymers. Most of these devices require a multi-layer built-up of different semi-conductive films on top of each other, usually a cascade of polymeric films having p-type (electron donor, hole transport) and n-type (electron acceptor, electron transport) properties (see Figure 1.3).⁷⁵ As the semi-conductive properties usually arise from π -conjugated molecules or polymers (especially their HOMO-, LUMO-levels and charge carrier mobilities), the films also have to fulfill different mechanical properties or fabrication requirements.⁷⁶

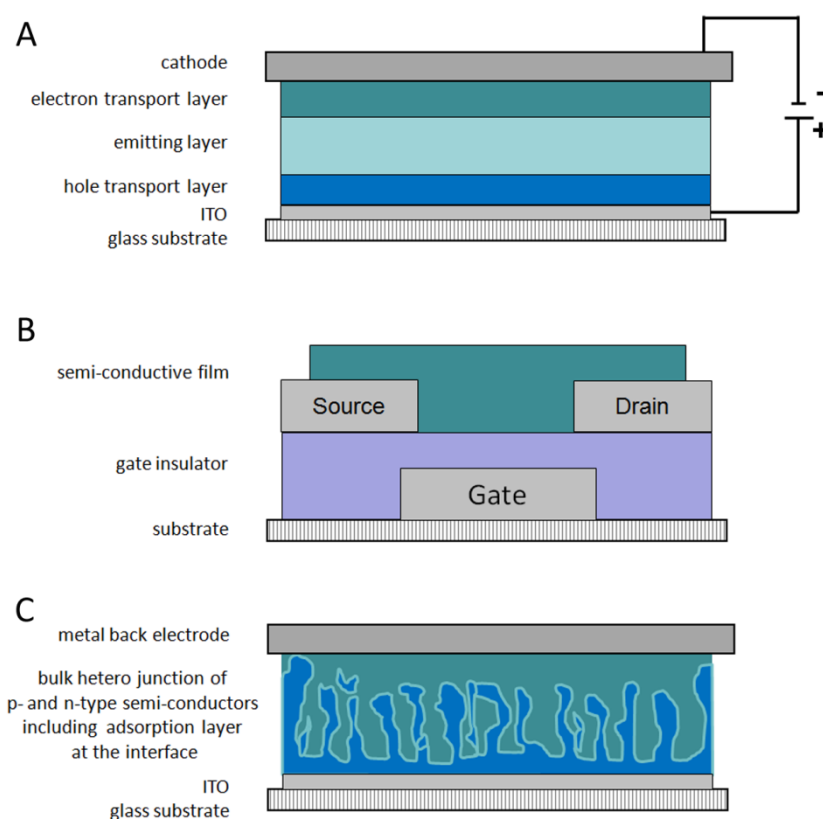


Figure 1.3. Examples of different organic electronic devices (schematically). A: device setup of a three layer OLED. B: device setup of an OTFT (bottom-gate, bottom-contact setup). C: device setup of a bulk-heterojunction organic solar cell.

⁷¹ Sirringhaus, H.; Tessler, N.; Friend, R. H. *Science* **1998**, *280*, 1741.

⁷² Sapp, S. A.; Sotzing, G. A.; Reynolds, J. R. *Chem. Mater.* **1998**, *10*, 2101.

⁷³ Tang, C. W.; Van Slyke, S. A. *Appl. Phys. Lett.* **1987**, *51*, 913.

⁷⁴ Yu, G.; Gao, J.; Hummelen, J. C.; Wudl, F.; Heeger, A. J. *Science* **1995**, *267*, 1969.

⁷⁵ Shinar, J. (Ed.), *Organic Light-Emitting Devices. A Survey*, Springer-Verlag, New York, USA, **2004**.

⁷⁶ Cui, J.; Huang, Q.; Veinot, J. C. G.; Yan, H.; Wang, Q.; Hutchison, G. R.; Richter, A. G.; Evmenenko, G.; Dutta, P.; Marks, T. J. *Langmuir* **2002**, *18*, 9958.

Organic electronics need contact with different types of electrodes; mostly one transparent conductive oxide (TCO) electrode (e.g. indium tin oxide, ITO) and one metallic electrode (e.g. aluminum, gold, silver). A good adhesion of the organic layer on top of the metal or metal oxide electrode to prevent physical delamination or decohesion is needed.⁷⁷ The organic coating should produce a smooth amorphous film-forming morphology to achieve an effective planarization of the electrodes.⁷⁸ Furthermore, a semi-conductive coating material needs to possess very good solvent resistance in order to facilitate a multilayer processing.

Cross-linkable semi-conductive polymers are a common method to produce stable films, which do not redissolve during multi-layer deposition.⁷⁵ To guarantee efficient contact with the electrodes, trialkoxysilane- or trichlorosilane- functionalized small molecules were deposited, resulting in stable silsesquioxane-like networks on top of the electrodes.⁷⁹

⁷⁷ Yu, W.; Pei, J.; Cao, Y.; Huang, W. *J. Appl. Phys.* **2001**, *89*, 2343.

⁷⁸ Liu, M. S.; Niu, Y.-H.; Ka, J.-W.; Yip, H.-L.; Huang, F.; Luo, J.; Kim, T.-D.; Jen, A. K. Y. *Macromolecules* **2008**, *41*, 9570.

⁷⁹ Li, J.; Marks, T. J. *Chem. Mater.* **2008**, *20*, 4873.

1.2 Coating Adhesion and Coating/Thin Film Characterization

1.2.1 Coating Adhesion

Adhesion is the most essential characteristic of a coating. The most critical issue to create very strong adhesion is the formation of a continuous film on top of the surface, which is able to fill the surface roughness of the substrate and create an integral solid film. If one considers an atomically smooth interface between surface coating and substrate (see Figure 1.4 left) and adhesion only by van der Waals forces, the force to separate the coating from its substrate can be calculated as $F/\text{mm}^2 \approx 100 \text{ N}$.⁸⁰ Considering surface roughness at the interface of the dry coating and on the surface which is not filled by the coating, the contact area decreases tremendously and thus does the adhesion force (right scheme, figure 1.4).⁸¹



Figure 1.4. Scheme of coating application onto a substrate. Left: atomically flat interfaces; right: rough interfaces, not filled by the coating.

If the coating does not completely penetrate into the microscopic pores and grooves in the surface, the actual interfacial contact area is smaller than the geometric area. Furthermore, when water permeates through the film, or through defects in the film to the substrate, areas of contact of water with the uncovered surface will cause major problems (e.g. if the coating is meant to protect steel against corrosion).⁸²

Adhesion of a coating on a certain substrate can be traced back on different adhesion phenomena (schematically shown in figure 1.5).

Filling the immanent surface roughness of a given substrate by a continuous coating film already leads to the first adhesion phenomenon of *mechanically interlocked interfaces* (Fig. 1.5 A). If the complete surface is covered by the coating, the actual interface for attraction forces becomes larger than the geometric area, yielding in higher adhesion forces. Furthermore, the mechanical interlocking is analogous to using a dovetail joint to hold two pieces of wood together. To pull the coating off the substrate, one would either have to break the substrate or the coating. This interlocking effect increases with the stiffness, achieved by cross-linking, of the coating material in these dovetail-like surface areas.⁸³

⁸⁰ Force per unit area $f = A_H/(6\pi D^3)$, with $A_H = 10^{-20} \text{ J}$ (Hamaker constant), $D = \text{distance}$

⁸¹ *Adhesion*, in Wicks, Z. W.; Frank, Jones, J. F. N.; Pappas, S. P.; Wicks, D. A., *Organic Coatings: Science and Technology*, 3rd ed., John Wiley & Sons, Hoboken, NJ, USA, **2007**.

⁸² Pulker, H. K.; Perry, A. J.; Berger, R. *Surface Technology* **1981**, *14*, 25.

⁸³ Possart, W., *Adhesion – Current Research and Application*, Wiley-VCH, Weinheim, Germany, **2005**.

Further adhesion phenomena, depending on the underlying material, are *electric double layer formation* (B), *chemical bonding interfaces* (either consisting of covalent bonds or hydrogen bonds) (C) (see chapter 1.3.3 for details) or *pure van der Waals interaction* (D).⁸⁴

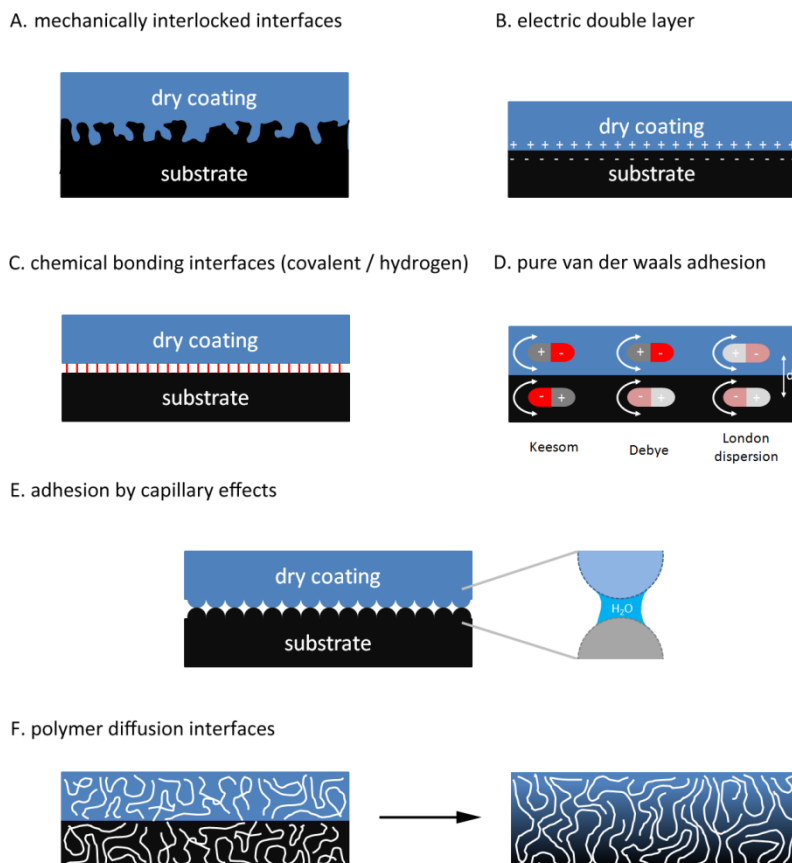


Figure 1.5. Adhesion phenomena between a coating and a certain substrate.⁸⁵

If water vapor is present (humidity) adhesion can be caused by *capillary effects* (E) between a coating and the surface; usually this effect is not important in coating technology. Especially on polymeric substrates, adhesion is achieved by *polymer diffusion interfaces* (F). Polymer chains from the substrate and from the coating can diffuse in the other layer, respectively. This implies that the polymeric phases do not undergo phase separation and are miscible. To allow the polymer chains to move, the T_g at the interfaces have to be decreased, which is usually achieved by the presence of solvent from which the coating material is applied or by an additional heating step.⁸⁶ Usually a coating procedure relies on several of these adhesion phenomena at the same time, depending on the coating material itself and the substrate to be coated. In principal, a coating material that is able to utilize different phenomena enlarges its

⁸⁴ Butt, H.-J.; Graf, K.; Kappl, M., *Physics and Chemistry of Interfaces*, Wiley-VCH, Weinheim, Germany, **2006**.

⁸⁵ Butt, H.-J., *Tutorial: Two Aspects of Adhesion: Bridging and Contact Adhesion*, IRTG Spring Meeting **2009**, Seoul, Korea.

⁸⁶ Packham, D. H., *Handbook of Adhesion*, John Wiley & Sons, Chichester, UK, **2005**.

scope of possible substrates (e.g. metals, metal oxides, wood, plastics, etc.) and if different phenomena are present on one substrate, adhesion is enhanced.⁸⁷

Several causes of failure of the adhesion may occur, depending very much on a certain application. The main causes of failure are mechanical stress (combination of tensile and shear forces), thermal stress (difference in contraction and expansion) and chemical stress (penetration of media and adsorption at the interface). Depending on the application, the coating material has to be designed accordingly. Furthermore, the substrate material usually inhibits rigidity higher than that of the coating, which may cause cohesive failure (fracture will occur within the coating).⁸⁸

1.2.2 Standardization of Adhesion Tests

Considering the complexity of adhesion phenomena, devising suitable test to quantify the adhesion between a coating and a given substrate is difficult. As often the case with coatings, the only really conclusive way of telling whether adhesion is satisfactory is to use the product and see whether the coating adheres over its lifetime.⁸⁹

Since a specification for the degree of adhesion must be provided especially in industrial applications, several routine tests have been established in the field of quality testing. Typically, the cross-cut and the pull-off method are mostly used to determine adhesion specifications.

*Cross-Cut Test.*⁹⁰

To obtain an idea of the adhesion of the coating onto a given substrate, a lattice pattern is cut into it, penetrating through the film and into the substrate. Usually 6 cuts are performed parallel with a distance of 1 to 2 mm, similar 6 cuts are performed perpendicular to those. Afterwards an adhesive tape is pasted over the pattern and removed with a certain force. The classification of the adhesion is based on estimating the area where the coating is removed by this procedure. The classification protocol is shown in figure 1.6. Class 0 indicates perfect adhesion, classifications 1 and 2 indicates partial decohesion, whereas classifications 3 and 4 indicates poor adhesion to the substrate.

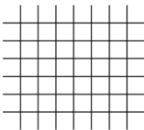
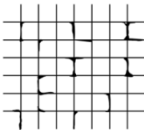
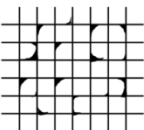
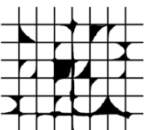
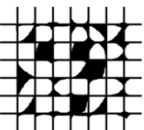
appearance					
percentage of flaking	0%	< 5%	< 15%	< 35%	< 65%
classification	0	1	2	3	4

Figure 1.6. Principle of classifying film adhesion in the cross-cut test.

⁸⁷ Ebnesajjad, S. (Ed.), *Adhesives Technology Handbook 2nd Ed.*, William Andrew, Norwich, NY, USA, **2008**.

⁸⁸ Good, R. J. J. *Adhes.* **1972**, *4*, 133.

⁸⁹ *Testing for adhesion*, in Wicks, Z. W.; Jones, F. N.; Pappas, S. P.; Wicks, D. A., *Organic Coatings. Science and Technology 3rd ed.*, John Wiley & Sons, Hoboken, NJ, USA, **2007**.

⁹⁰ *Paints and varnishes – Cross-cut test (ISO 2409:2007)*.

*Pull-Off Test.*⁹¹

To perform a pull-off test, a stud is glued with the coating and is subject to axial tension until detachment of the film occurred. The result is the maximum tensile stress that is possible at the interface. Additionally, also a torque can be applied about the axis of the stud, thus the process of detachment reveals the maximum shear stress.

Other tests for adhesion are based on delamination procedures (i.e. the knife-cutting method, the peel test or the blister method) or on local debonding systems (i.e. scratch technique, indentation debonding).⁹²

1.2.3 Coating/Thin Film Characterization

Depending on the coating, its desired function and application, several characterization methods for the determination of characteristic properties of coatings or thin films are in use.⁹³ Several surface-analytical methods, which were used in the presented work, will be introduced in detail.

*Ellipsometry.*⁹⁴

Ellipsometry measures a change in polarization (light wave's electric field behavior in space and time) as light reflects from an interface. The polarization change is represented as an amplitude ratio Ψ , and a phase difference, Δ . The measured response depends on optical properties and thickness of individual films on the surface. Thus, ellipsometry is primarily used to determine film thickness and optical constants. However, it is also applied to characterize composition, roughness, and other material properties associated with a change in optical response.

The electric field \vec{E} can be split into two orthogonal electric waves: \vec{E}_p , parallel to the sample surface (with phase ξ_p) and \vec{E}_s , perpendicular to the sample (with phase ξ_s). Depending on the magnitude of E_p and E_s as well as their difference in phase $\Delta\xi$, three different states of polarization are possible: linear ($E_s \neq E_p$, $\Delta\xi = 0$), circular ($E_s = E_p$, $\Delta\xi = 90^\circ$), and elliptical ($E_s \neq E_p$, $\Delta\xi \neq 0$). Ellipsometry is primarily interested in how p- and s- components change upon reflection or transmission in relation to each other. The sample is irradiated with a known polarization of light and the reflected polarization is measured.⁹⁵ Thus, the fundamental equation of ellipsometry is the following ($R_{(p,s)}$: reflectivity):

$$\tan(\Psi)e^{i\Delta} = \frac{R_p}{R_s}$$

⁹¹ Paints and varnishes – Pull-off test for adhesion (ISO 4624:2002).

⁹² Zorll, U., *Adhesion Testing*, in Tracton, A. A. (Ed.), *Coatings Technology. Fundamentals, Testing, and Processing Techniques*, CRC Press, Boca Raton, FL, USA, **2007**.

⁹³ Anderson, D. G. *Anal. Chem.* 1999, **71**, 21.

⁹⁴ Gutmann, J. S., *Tutorial: Determination of Film Thickness*, IMPRS School, Oberwesel, Germany, Nov. 2007.

⁹⁵ Azzam, R. M. A.; Bashara, N. M., *Ellipsometry and Polarized Light*, Elsevier Science B. V., Amsterdam, Netherlands, **1987**.

In practical use, the common measurement techniques are the “Null-Ellipsometer” setups.⁹⁶ The PSCA (polarizer-sample-compensator-analyzer) and the PCSA (polarizer-compensator-sample-analyzer) setup are shown in figure 1.7.

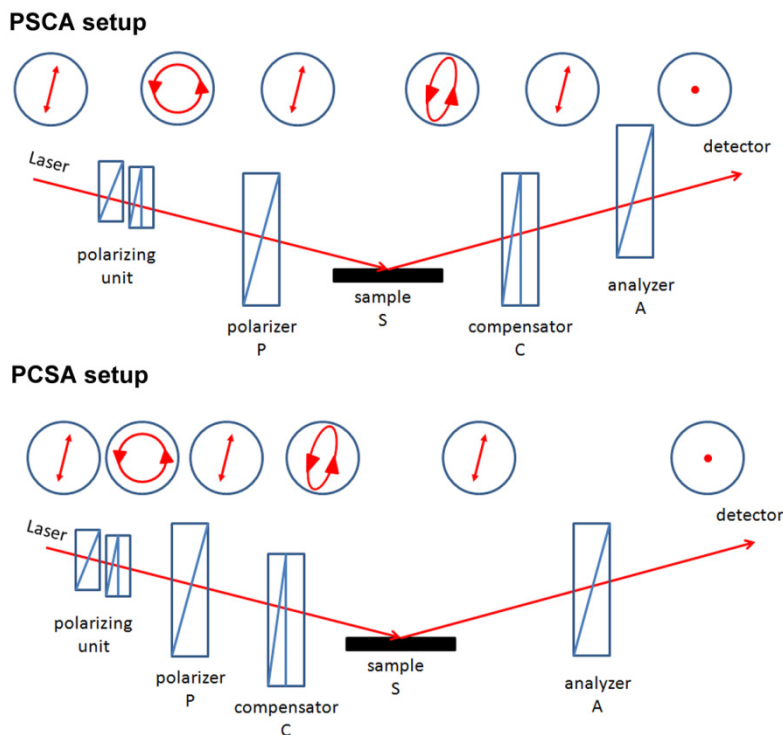


Figure 1.7. PSCA and PCSA setups in null-ellipsometry.

The angles of the polarizer (P) and the analyzer (A) were adjusted to match the condition $I(P,A) = 0$; the intensity at the detector is 0. If a quarter-wave-plate is used as compensator (C) and fixed in 45° , Ψ and Δ are given by the following equations:

$$\begin{aligned} \Psi &= |A| & \Delta &= 2P \pm 90^\circ & \text{for } C = -45^\circ \\ \Psi &= |A| & \Delta &= -2p \pm 90^\circ & \text{for } C = +45^\circ \end{aligned}$$

A model, based on Fresnel's equations, is used to fit the film thickness d and the refractive index n .⁹⁷

ATR-FTIR spectroscopy.⁹⁸

Attenuated-total-reflectance Fourier-transform infrared (ATR-FTIR) spectroscopy is a non-destructive method to probe the chemical composition of solid or liquid samples. IR spectroscopy measures the frequencies at which the sample absorbs, as well as the

⁹⁶ Tompkins, H., *A User's Guide to Ellipsometry*, Academic Press, San Diego, USA, **1993**.

⁹⁷ Tompkins, H.; Haber, E. A., *Handbook of Ellipsometry*, William Andrew Publishing, New York, USA, **2005**.

⁹⁸ Gremlich, H.-U., *IR-Spektroskopie*, Wiley-VCH, Weinheim, Germany, **2003**.

intensities of these absorptions. Determining these frequencies allows identification of the sample's chemical composition, since chemical functional groups are known to absorb radiation at specific frequencies. ATR-FTIR spectra are obtained by pressing small pieces of a material against an “internal reflection element” (IRE). IR radiation is focused onto the end of the IRE and reflects across the length of the crystal. Thus, the evanescent IR radiation penetrates several ten to hundred nanometers from the surface of the IRE into the material.

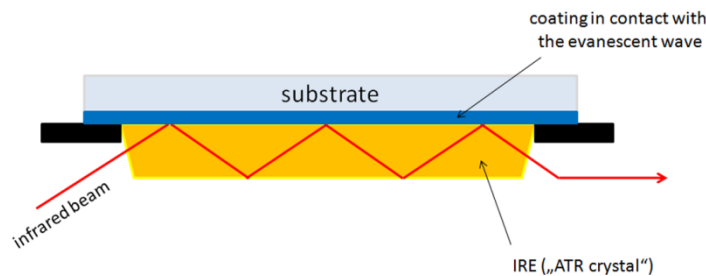


Figure 1.8. ATR-FTIR setup to measure coating characteristics on the coated substrate.

The ATR-FTIR setup (figure 1.8) is ideal to determine different coating characteristics, like the chemical composition or the presence of different chemical functions. After application onto a substrate, for example on glass or on plastics, the coating is pressed on the IRE to ensure contact to the evanescent IR field.⁹⁹ By applying the coating directly onto the ATR crystal, changes with time can be observed. The evaporation of solvents, curing reactions, and migration of additives to the surface are some of the possibilities.¹⁰⁰

Contact angle measurements.¹⁰¹

Wetting includes all phenomena involving contacts between three phases, usually a solid, a liquid and a gas or non-mixable liquid phase. If a drop of a liquid is placed on a solid surface, two different possibilities may happen; either the liquid spreads the solid completely or a finite contact angle (CA, Θ) is established. In the second case a three-phase contact line is formed, at which all three phases are in contact. Young's equation relates the contact angle to the interfacial tensions γ_s , γ_l , and γ_{sl} (see figure 1.9).

$$\text{Young's equation: } \gamma_l \cos \theta = \gamma_s - \gamma_{sl}$$

Two different cases have to be distinguished. First, $\gamma_s < \gamma_{sl}$, the interfacial tension of the wetted surface is higher than the interfacial tension of the solid surface in contact to the gas phase. The resulting contact angle will be larger than 90° . If the liquid was water, the solid surface is

⁹⁹ Kendall, D. S., *Infrared Spectroscopy of Coatings*, in Tracton, A. A. (Ed.), *Coatings Technology. Fundamentals, Testing, and Processing Techniques*, CRC Press, Boca Raton, FL, USA, 2007.

¹⁰⁰ Popli, R.; Dwivedi, A. M. *J. Appl. Polym. Sci.* **1989**, *37*, 2469.

¹⁰¹ Chapter 7 „Contact Angle Phenomena and Wetting“ in Butt, H.-J.; Graf, K.; Kappl, M., *Physics and Chemistry of Interfaces*, Wiley-VCH, Weinheim, Germany, 2006.

considered to be hydrophobic. In the second case, the wetted surface is energetically more favorable than the “dry” surface ($\gamma_s > \gamma_{sl}$). The resulting contact angle will be smaller than 90° ; if the liquid was water, the solid surface is considered to be hydrophilic.

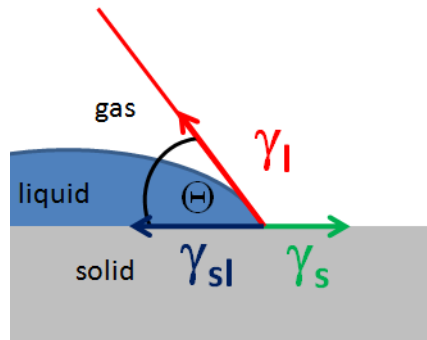


Figure 1.9. Contact angle and interface tensions at the three-phase contact line.

As most coatings are supposed to come into contact with liquids, the contact angle and the interface tension are important characteristics of a coating. Depending on the application the contact angle of different liquids may be important; in the following the focus lies on the contact angle of water on a solid/coated surface under ambient conditions (usual humidity).

The common method to determine the contact angle is to observe the sessile drop with a camera in front of the drop and a light source behind. Nowadays, the angle is fitted by a computer using the Laplace equation. Alternative methods are, for instance, the captive bubble method, where a gas bubble is placed under the substrate within the liquid, or the capillary rise method, the liquid rises inside a thin coated capillary (the CA can be calculated from the meniscus height).

If the contact angle is measured while the drop volume is continuously increasing and the wetting line is just before starting to advance toward the non-wetted surface, the obtained CA is called the advancing contact angle (Θ_a). While decreasing the drop volume, just before the contact line moves toward the wetted surface, the receding CA (Θ_r) is measured. Usually the advancing angle is higher than the receding CA. This difference $\Delta\Theta$ is called contact angle hysteresis. This hysteresis is influenced by different factors, for example, surface roughness,¹⁰² chemical heterogeneity,¹⁰³ adsorbed molecules on the surface,¹⁰⁴ changes of the surface structure caused by the wetting line,¹⁰⁵ etc.

In addition to the influence of surface roughness and chemical heterogeneity on the hysteresis, it does also affect the mean contact angle. Surface roughness is usually described as a factor R_{rough} , which is the ratio between the actual and the projected surface area. Thus,

¹⁰² Shuttleworth, R.; Bailey, G. L. *J. Disc. Faraday. Soc.* **1948**, 3, 16.

¹⁰³ Brandon, S.; Marmur, A. *J. Colloid Interface Sci.* **1996**, 183, 351.

¹⁰⁴ Drelich, J.; Miller, J. D.; Good, R. J. *J. Colloid Interface Sci.* **1996**, 179, 37.

¹⁰⁵ Kern, R.; Müller, P. *Surface Sci.* **1992**, 264, 467.

R_{rough} is either equal to 1 (for atomically flat surfaces) or larger than 1 for rough surfaces. The effect of the surface roughness on the contact angle is described by the Wenzel equation.

$$\text{Wenzel equation:}^{106} \quad \cos \theta_{\text{app}} = R_{\text{rough}} \cos \theta$$

In here, Θ_{app} is the apparent contact angle which can be measured and Θ is the corresponding contact angle on smooth surfaces. For $\Theta < 90^\circ$ (hydrophilic surfaces), the apparent contact angle will be decreased by surface roughness; in the opposite case for $\Theta > 90^\circ$ it will be increased if roughness is present. The influence of chemical heterogeneity, present at the interface, is expressed by Cassie and Baxter.¹⁰⁷ A smooth but chemically patchwise heterogeneous surface is considered with two different kinds of regions with contact angles Θ_1 and Θ_2 , which occupy the surface ratios f_1 and f_2 .¹⁰⁸

$$\cos \theta_{\text{app}} = f_1 \cos \theta_1 + f_2 \cos \theta_2$$

The most prominent example of rough and chemically heterogeneous surfaces is probably the "Lotus-effect". The surface of a leaf can be viewed as a surface covered with hydrophobic spikes. These spikes are responsible for the roughness, furthermore, between the spikes air is trapped, which gives chemical heterogeneity. Using this effect, super-water-repellent (superhydrophobic) surface coatings could be made.¹⁰⁹

Surface Plasmon Resonance (SPR).^{110,111}

Surface plasmons are charge-density oscillations that may exist at the interface of two media with dielectric constants of opposite signs, for instance, a metal and a dielectric. The charge density wave is associated with an electromagnetic wave; the field vectors reach their maximum at the interface and decay evanescently into both media. This surface plasmon wave is polarized (the magnetic vector is perpendicular to the direction of propagation of the wave and parallel to the plane of the interface). The spectroscopy of surface plasmons is based on the attenuation of total internal reflection (ATR). From Snell's law, the critical angle of total internal reflection (TIR) can be calculated.¹¹² Above the angle of TIR, the incident light gives rise to the surface plasmon wave with an evanescent wave perpendicular to the metal interface. Changes in the refractive index within the evanescent field by a dielectric layer lead to corresponding changes in the intensity of the reflected light. To detect the resonance between the light wave and the plasmon, the wave vectors have to be identical (Maxwell's

¹⁰⁶ Wenzel, R. N. *Ind. Eng. Chem.* **1936**, *28*, 988.

¹⁰⁷ Cassie, A. B. D.; Baxter, S. *Trans. Faraday Soc.* **1944**, *40*, 546.

¹⁰⁸ Cassie, A. B. D. *Discus. Faraday Soc.* **1948**, *3*, 11.

¹⁰⁹ Onda, T.; Shibuichi, S.; Satoh, N.; Tsujii *Langmuir* **1996**, *12*, 2125.

¹¹⁰ Homola, J.; Yee, S. S.; Gauglitz, G. *Sens. Actuators B* **1999**, *54*, 3.

¹¹¹ Homola, J. *Chem. Rev.* **2008**, *108*, 462.

¹¹² Homola, J. *Anal. Bioanal. Chem.* **2003**, *377*, 528.

equation).¹¹³ Usually the wave vector of the plasmon will exceed the wave vector of light in air, therefore the metal has to be deposited on an optically denser medium (commonly a glass prism is used). One possible setup is the Kretschmann-configuration, shown in figure 1.10. Using this setup, the wave vector of the incident light depends on the angle of incidence. Thus, the surface plasmon resonance can be measured using a goniometer; after reaching the angle of TIR at a specific angle the vector of the laser light matches the plasmon vector and the reflection is minimized. Adsorbed molecules, either directly on the metal layer or on a thin coating ($d < 10$ nm), shift the field of the plasmon and thus the resonance angle, respectively. This shift is proportional to the dielectric constant and the thickness of the adsorbed layer. The shift can be monitored either by several scans or in a kinetic mode (figure 1.10, right), measuring the intensity at a constant angle (usually at one flank of the minimum) with time. To determine thicknesses or thickness increase, SPR requires the knowledge of the refractive index. Within this thesis the refractive index of all measured materials, either deposited on the metal or adsorbed at the interface is assumed to be $n = 1.5$.¹¹⁴

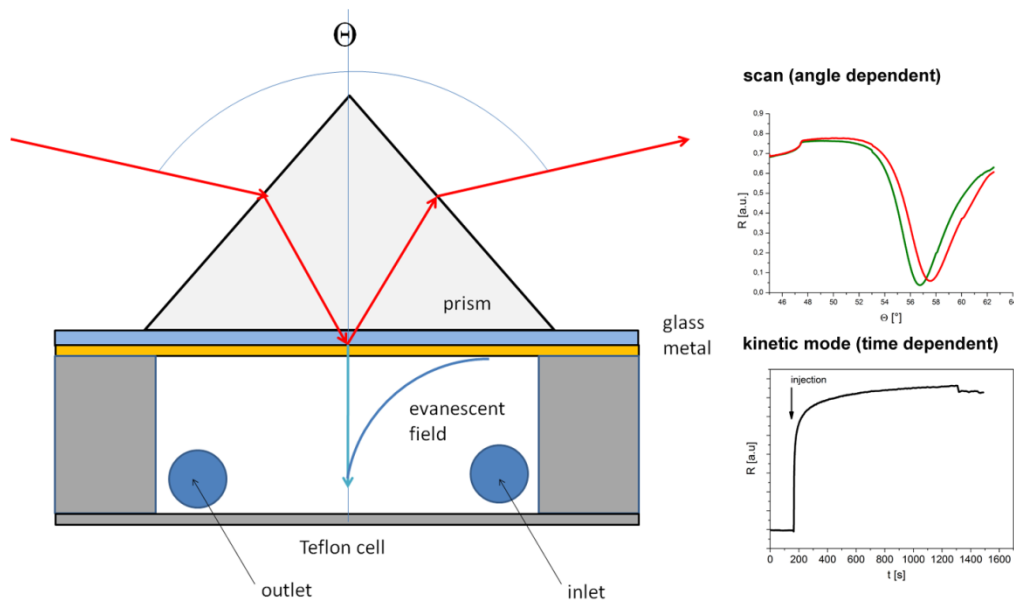


Figure 1.10. Kretschmann-configuration mounted on a teflon cell, which allows injection of solutions.¹¹⁵

¹¹³ Mittler-Neher, S.; Spinke, J.; Liley, M.; Nelles, G.; Weisser, M.; Back, R.; Wenz, G.; Knoll, W. *Biosens. Bioelectr.* **1995**, *10*, 903.

¹¹⁴ Liedberg, B.; Nylander, C.; Lundström, I. *Biosens. Bioelectr.* **1995**, *10*, i.

¹¹⁵ Knoll, W., *SPR-Tutorial*, IRTG Spring Meeting, Ringberg, Germany, **2008**.

X-ray photoelectron spectroscopy (XPS).^{116,117}

XPS is a surface chemical analysis technique that can be used to analyze the surface chemistry of a coating. The quantitative elemental composition of the top 1 – 10 nm is detected (detection of all elements with $Z \geq 3$).¹¹⁸ Besides synchrotron-based light sources, monochromatic aluminum $K\alpha$ X-rays or polychromatic magnesium X-rays are used in laboratory XPS systems. The general setup is shown in figure 1.11.

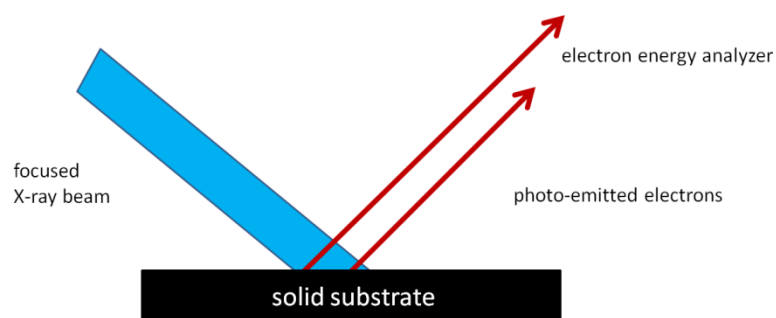


Figure 1.11. XPS setup.

An X-ray beam is focused onto the solid substrate (the substrate usually has to be solid due to an ultra-high vacuum applied to the measurement chamber). Electrons inside the material are excited and might be emitted from the substrate and detected in an electron energy analyzer. From the X-ray wavelength and the kinetic energy of the detected electron E_{kin} , the binding energy of the electron in the material E_b can be calculated using the following equation.

$$E_b = E_p - (E_{kin} + \varphi)$$

E_p is the energy of the X-ray photons and φ is an apparatus constant.¹¹⁹ The binding energy of each electron is not only characteristic for each element, but also for the electron's binding state, the electron orbital. Thus, XPS provides information about the elements present at the surface and also their binding states in molecules.¹²⁰

As XPS only detects electrons that have escaped from the solid surface, only the elemental composition of the top interface (usually < 10 nm) is detected. The deeper electrons, which

¹¹⁶ Moulder, J. F.; Stickle, W. F.; Sobol, P. E.; Bomben, K. D., *Handbook of X-ray Photoelectron Spectroscopy*, Perkin-Elmer Corp., Eden Prairie, MN, USA, **1992**.

¹¹⁷ Wagner, C. D.; Riggs, W. M.; Davis, L. E.; Moulder, J. F.; Mullenberger, G. E., *Handbook of X-ray Photoelectron Spectroscopy*, Perkin-Elmer Corp., Eden Prairie, MN, USA, **1979**.

¹¹⁸ Christ (Ed.), *Handbook of Monochromatic XPS Spectra*, XPS International LLC, Mountain View, CA, USA, **2003**.

¹¹⁹ Seah, M.P.; Briggs, D. (Ed.), *Practical Surface Analysis by Auger and X-ray Photoelectron Spectroscopy*, John Wiley & Sons, Chichester, UK, **1983**.

¹²⁰ Davis, L.E. (Ed.), *Modern Surface Analysis: Metallurgical Applications of Auger Electron Spectroscopy (AES) and X-ray Photoelectron Spectroscopy (XPS)*, The Metallurgical Society of AIME, Warrendale, USA, **1980**.

were also excited by the X-ray beam, entering approx. 2 μm into the substrate, are either recaptured or trapped within the material.¹²¹

Besides determination of the elemental compositions across the top interface (mapping) also the elemental profile as a function of depth can be obtained either by ion beam etching or by tilting the sample (angle resolved XPS).¹²²

Atomic Force Microscopy (AFM).¹²³

The atomic force microscope is one type of scanning probe microscopes (SPM), which allows true 3D-profiling of non-conductive surfaces¹²⁴ (in comparison to a scanning tunneling microscope, which was invented earlier, but is only capable to probe conductive surfaces).¹²⁵

The main principle is based on a small tip which is scanned across the surface and thus probes attractive and repulsive forces on a flat spring (cantilever) arising from the surface. The widely used beam deflection detection setup of an AFM is shown in figure 1.12. Depending on the forces on the cantilever it will bend in z-direction according to Hook's law (not considering lateral forces which will also cause torsion), the bending is detected by a laser beam, deflected from the cantilever onto a split photodiode detector. An electrical feedback loop controls the interaction between a piezo scanner and the photodiode, resulting in a topographical image of the surface.

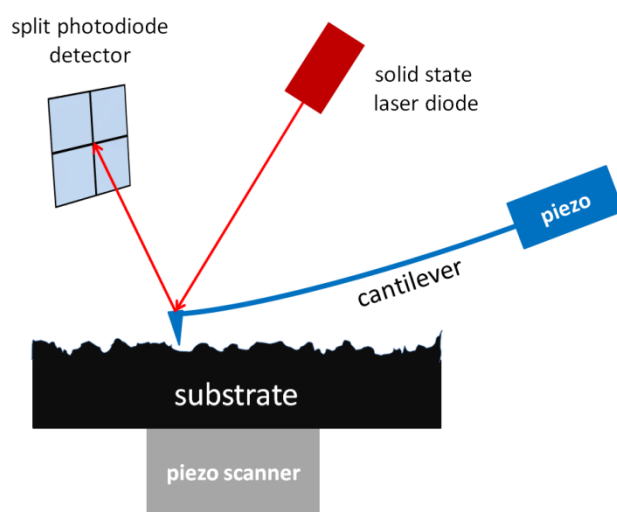


Figure 1.12. General setup of an atomic force microscope with beam deflection detection.

¹²¹ Oura, K.; Lifshits, V. G.; Saranin, A. A.; Zotov, A. V.; Katayama, M., *Surface Science: An Introduction*, Springer, Berlin, Germany, **2003**.

¹²² Worthington, C.R.; Tomlin, G. *Proc. Phys. Soc. A* **1956**, *69*, 401.

¹²³ Berger, R., *SPM-Tutorial*, IRTG Workshop, Nierstein, Germany, **2007**.

¹²⁴ Binnig, G.; Quate, C. F.; Gerber, C. *Phys. Rev.Lett.* **1986**, *56*, 930.

¹²⁵ Binnig, G.; Rohrer, H.; Gerber, C.; Weibel, E. *Phys. Rev. Lett.* **1982**, *50*, 120.

Depending on the nature of the sample and the desired information about the surface, different modes can be applied.¹²⁶

In contact mode, the feedback loop regulates a constant cantilever deflection, thus the force between tip and sample remains constant. The distance the scanner moves vertically at each (x,y) data point is stored by the computer to form the topographical image. The advantages are high scanning speed and atomic resolution. Disadvantages arise from shear forces and capillary forces which may damage soft samples. In non-contact mode, the tip oscillates (induced by a piezo at the cantilever) with an amplitude of a few nanometer, it does not contact the surface. The cantilever's oscillating amplitude is decreased by van der Waals forces, the feedback loop maintains a constant amplitude by vertically moving the scanner at each (x,y) position until a setpoint amplitude is reached. From this information the topographical image is calculated. The main drawback of the non-contact mode is unstable feedback and scraping if a thin fluid layer on top of the surface is present (for example due to usual humidity). Thus, the application for non-contact mode AFM is limited.

The tapping mode is commonly used for polymeric substrates or other soft materials. The cantilever is oscillating similar to the non-contact mode but near its resonance frequency, resulting in amplitudes of 20 nm to 100 nm. The tip lightly "taps" on the sample surface during scanning, contacting the surface at the bottom of its swing. When imaging in air, the typical amplitude of the oscillation allows the tip to contact the surface through the adsorbed fluid layer without getting stuck. By vertical movement of the piezo scanner, a constant oscillation amplitude is maintained. Thus, information about the topography is obtained, as well as information about a phase shift during oscillation due to different mechanical properties of the sample surface.¹²⁷

¹²⁶ Hinterdorfer, P.; Dufrene, Y. F. *Nature Methods* **2006**, 3,5.

¹²⁷ Giessibl, F. *Rev. Modern Phys.* **2003**, 75, 949.

1.3 Polymeric Materials

Polymers are usually the first choice to attach various functions to surfaces and thus are the main component in most coating materials. However, every class of coating formulation requires different types of polymers, polymer architectures or functionalities within the polymer (e.g. thermosetting resins require cross-linkable moieties within the polymer, polymers which will be grafted to a surface need one certain end-group functionality).

Different polymeric materials with different architectures or functionalities usually require different polymerization techniques.

Generally, polymerization techniques can be divided into two classes: step-growth polymerization and chain growth polymerization.

In *step-growth polymerization* two defined functionalities undergo condensation or addition reaction. These two functionalities can either be combined in one molecule (A-B monomer) or a mixture of two monomers, each with two identical functions, is used (A-A and B-B monomers). Incorporation of monomers with three or more functionalities (e.g. A₃ or B₄ monomers) will lead to cross-linking and gelation, whereas step-growth of A-B₂ monomers will yield hyperbranched polymers. The main characteristics of linear step-growth polymerizations are: no initiator is necessary to start the polymerization, high molecular weight is only reached with high conversion, and the ends remain active (no termination). Typical examples for step-growth polymers are: polyester, polyamides, polyurethanes, polysiloxanes, polycarbonates or phenol formaldehyde resins (Bakelite).¹²⁸

A radical, anionic, or cationic reactive center, once produced, starts to add monomers in a *chain-growth polymerization*. The main differences to step-growth are: high molecular weight is reached almost instantaneously, the chain reaction has to be initiated, and chains can terminate each other or branch themselves. Typical monomers for chain-growth polymerization are usually unsaturated molecules, e.g. vinyl or acrylate based. Although radical, cationic, and anionic initiators are used in chain polymerization, they cannot be used indiscriminately, since they prefer certain monomers. Most monomers will undergo polymerization by radical initiation, which also tolerates high functionality of the monomer and makes fewer demands on purity and inert reaction conditions.¹²⁹ Due to these advantages, the free radical polymerization is actually the most common technique to produce synthetic polymers. The main part of the global production of polymers consists of polyethylene (LDPE, HDPE), polystyrene (PS), polyvinylchloride (PVC), polyacrylonitrile (PAN) and polymethylmethacrylate (PMMA), all synthesized in large scale by free radical polymerization.

The mechanism of the *free radical polymerization* can be divided into 4 steps: initiation, chain growth, chain transfer and termination. Common initiators are based on azo- or peroxy-compounds, e.g. azoisobutyronitrile (AIBN) or benzoyl peroxide (BPO). Decomposition at reasonable rates occurs between 40 °C and 90 °C. Besides thermal decomposition also electrochemical or photo activation are used. After decomposition, the generated free radical

¹²⁸ Allock, H. R.; Lampe, F. W.; Mark, J. E., *Contemporary Polymer Chemistry 3rd ed.*, Pearson Education Inc., Upper Saddle River, NJ, USA, **2003**.

¹²⁹ Odian, G., *Principles of Polymerization 4th ed.*, John Wiley & Sons, Hoboken, NJ, USA, **2004**.

(R·) initiates the polymerization by addition of the first monomer (R-M·), this active chain end propagates further polymerization of monomers (P_n·). The radical of the growing chain may be transferred to another molecules (e.g. to a solvent molecule, to a chain transfer agent or another polymer, monomer or initiator). By radical transfer, the chain growth of one chain is stopped, but the concentration of radicals remained equal. The polymerization proceeds until termination of the radical chain end occurs. Two radical chain ends may undergo recombination or disproportionation. In case of recombination the molecular weight doubles whereas disproportionation has no influence on the molecular weight. The rate constant of the termination reaction (k_T) is usually five orders of magnitude higher than the rate constant of the propagation reaction (k_p).¹³⁰ In ideal case the resulting molecular weight distribution follows a Schulz-Flory distribution with $1.5 < \text{PDI} < 2.0$ (with PDI = polydispersity index M_w/M_n).¹³¹ The propagation rate is directly proportional to the concentration of active growing chain ends; the termination rate is proportional to the concentration of active growing chain ends squared. The concept of controlled/“living” radical polymerization is based on decreasing the number of active growing chain ends, which results in stronger depression of termination as depression of propagation. In most types of living radical polymerization techniques, this is realized by a reversible reaction between the active growing chain end and a corresponding dormant chain end which is not capable to propagate or terminate. The most popular methods for living radical polymerization are Atom Transfer Radical Polymerization (ATRP), Nitroxide-Mediated Polymerization (NMP) and Reversible Addition Fragmentation Chain Transfer (RAFT) polymerization.

Besides the advantages of controlling the molecular weight and obtaining narrow molecular weight distributions, living radical polymerizations allow a defined built-up of specific polymer architectures, as they usually have defined end groups which can also be activated in a second polymerization step (e.g. for block-copolymer synthesis).¹³²

1.3.1 Atom Transfer Radical Polymerization (ATRP)

The Atom Transfer Radical Polymerization (ATRP) is derived from the transition-metal-catalyzed Atom Transfer Radical Addition (ATRA) reaction and was first published by Matyjaszewski.¹³³ As transition-metal-catalysts copper (I) salts are used,¹³⁴ but also Ru, Fe,¹³⁵ Co and Rh¹³⁶ salts could successfully be applied in ATRP. Usually, suitable monomers for free radical polymerization polymerize also under ATRP conditions.

As initiators organic halogenides (R-X) are used, in a halogen atom transfer reaction the organic halogenide reacts reversibly with the $\text{Cu}^{(I)}\text{X}(\text{Lig})_2$ salt (usually stabilized in solution by specific ligands, Lig) to a radical (R·) and $\text{Cu}^{(II)}\text{X}_2(\text{Lig})_2$. This radical initiates the polymerization by

¹³⁰ Wang, J. S.; Matyjaszewski, K. *Macromolecules* **1995**, *28*, 7901.

¹³¹ Elias, H. G., *Makromoleküle Bd. 1 Grundlagen 5. Aufl.*, Hüthig & Wepf, Basel, Switzerland, **1990**.

¹³² Matyjaszewski, K. (Ed.), *Controlled/Living Radical Polymerization: Progress in ATRP, NMP, and RAFT*, ACS Symp. Series 768, Washington, DC, USA, **2000**.

¹³³ Wang, J. S.; Matyjaszewski, K. *J. Am. Chem. Soc.* **1995**, *117*, 5614.

¹³⁴ Grimaud, T.; Matyjaszewski, K. *Macromolecules* **1997**, *30*, 2216.

¹³⁵ Sawamoto, M. *Macromolecules* **1996**, *29*, 1070.

¹³⁶ Percec, V.; Kim, H.J.; Barboiu, B. *Macromolecules* **1995**, *28*, 7970.

adding monomers ($RM_n\cdot$) until it undergoes the reversible halogen transfer reaction again to form the corresponding dormant polymer chain with a halogenic end group (RM_nX) and $Cu^{(I)}X(Lig)_2$. By this reversible activation of the growing chain end, the actual concentration of free radicals is kept low during the whole polymerization. The equilibrium constant of the reversible halogen transfer reaction is approximately $K_{eq} = 10^{-8}$, thus the majority of chain ends is dormant.^{137,138} The cooper (II) species act as a persistent radical.¹³⁹ The obtained low concentration of active growing chain ends almost suppresses the rate of termination, even though it cannot completely be neglected. As the ATRP relies on solubility products of various species in solution, the composition of the reaction mixture (initiator, monomer, solvent, copper salt, ligands) have to be adjusted very precisely. Furthermore, other factors like the sequence of adding all components into the flask, the way of mixing and the amount of residual oxygen have an impact on the final polymer.¹⁴⁰ In summary, ATRP allows good control of molecular weight by initiator concentration and conversion, yields in narrow molecular weight distributions, and benefits of easy functionalization possibilities of the organic halogenides to create defined architectures like block-copolymers, polymer brushes, etc.¹⁴¹

1.3.2 Reversible Addition Fragmentation Chain Transfer (RAFT)

Another promising method to perform controlled/"living" radical polymerization of vinyl- or acrylate- based monomers is the Reversible Addition Fragmentation Chain Transfer (RAFT) polymerization.¹⁴² In contrast to ATRP (and also to NMP), the RAFT process does not control the amount of active growing chain ends by reversible termination (no radical is present) but by reversible chain transfer (the persistent radical in the dormant species is a real radical species). Similar to a free radical polymerization; RAFT needs common radical initiators like AIBN or BPO; additionally a chain transfer agent (CTA) is added to the reaction mixture. Typically thiocarbonylthio compounds are used as CTA, i.e. dithioesters, trithiocarbonates, dithiocarbamates or xanthogenates. The first studies about controlled radical polymerization by dithioester derivatives of the general formula $Z-(C=S)-SR$ were made by Rizzardo.^{143,144}

The mechanism of the RAFT polymerization is based on a sequence of addition and fragmentation reactions, which allow transferring the active growing chain end to a dormant radical species and further to a new active growing chain end (see figure 1.13).

The initiation is similar to the free radical polymerization, an initiator (I) decomposes into two free radicals ($R\cdot$) which might start to polymerize first monomer molecules. In a first reversible addition reaction the growing chain end ($P_n\cdot$) reacts with the CTA to form an intermediate

¹³⁷ Matyjaszewski, K.; Patten, T.E.; Xia, J. *J. Am. Chem. Soc.* **1997**, *119*, 674.

¹³⁸ Tang, W.; Kwak, Y.; Braunecker, W.; Tsarevsky, N. V.; Coote, M. L.; Matyjaszewski, K. *J. Am. Chem. Soc.* **2008**, *130*, 10702.

¹³⁹ Fischer, H. *Chem. Rev.* **2004**, *101*, 3581.

¹⁴⁰ Shipp, D.A.; Matyjaszewski, K. *Macromolecules* **2000**, *33*, 1553.

¹⁴¹ Matyjaszewski, K.; Xia, J. *Chem. Rev.* **2001**, *101*, 2921.

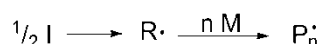
¹⁴² Barner-Kowollik, C. (Ed.), *Handbook of RAFT Polymerization*, Wiley-VCH, Weinheim, Germany, **2008**.

¹⁴³ Chiefari, J.; Chong, Y.; Ercole, F.; Krstina, J.; Jeffery, J.; Le, T.; Mayadunne, R.; Meijs, G.; Moad, C.; Moad, G.; Rizzardo, E.; Thang, S. *Macromolecules* **1998**, *31*, 5559.

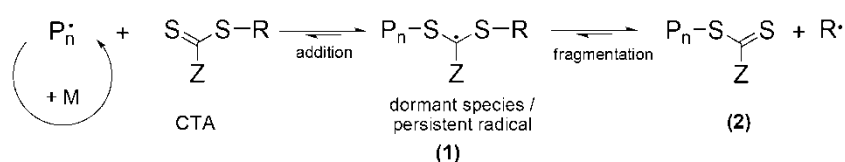
¹⁴⁴ Mayadunne, R.; Rizzardo, E.; Chiefari, J.; Chong, Y.; Moad, G.; Thang, S. *Macromolecules* **1999**, *32*, 6977.

radical (1) which is not able to propagate or to terminate. By fragmentation of (1), a polymeric dithioester (2) and a new free radical $R\cdot$ is formed. $R\cdot$ can initiate a new chain $P_m\cdot$. The chain equilibrium between $P_m\cdot$, the persistent radical (3) and $P_n\cdot$ allows propagation of all chains with the same probability (the radical is passed like in a torch relay). Thus, polymers with narrow molecular weight distribution and mostly dithioester-functionalized ω -groups and R-functionalized α -groups are obtained. The defined end groups can be characterized by NMR or UV/Vis spectroscopy.

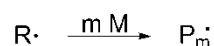
Initiation:



1. Addition / Reversible Chain Transfer:



Reinitiation:



Propagation / Chain Equilibrium

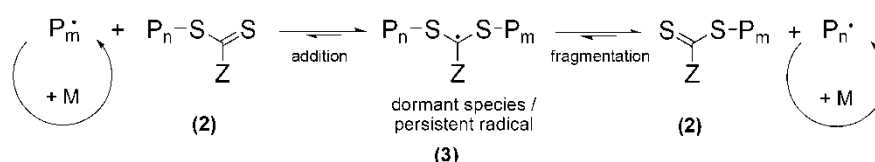


Figure 1.13. Mechanism of the RAFT polymerization.¹⁴⁵

In general, the RAFT technique is very tolerant against different (functional) monomers, solvent, ambient atmosphere, etc. But to obtain PDI < 1.1 and high conversions, the CTA has to be tuned properly for the desired polymerization. Especially the radical leaving group R should be designed similar to an active growing chain radical to allow species (1) to fragmentate in both directions. Furthermore, the Z-group has to be designed in order to stabilize the intermediate radicals (1, 3) and to activate or deactivate the thiocarbonyl double bond. Side reactions of the intermediate radicals (1, 3) have to be suppressed effectively.

¹⁴⁵ Moad, G.; Rizzardo, E.; Thang, S. *Polymer* **2008**, *49*, 1079.

Similar to the ATRP, RAFT allows a variety of possibilities to built-up polymer architectures like polymeric stars, micro-arm stars, microgels, block copolymers, polymer brushes, etc. just by choosing the right CTA (or to functionalize the CTA accordingly).^{146,147} Also defined endgroup-functionalization can be achieved, which allows further derivatization.^{148,149}

A related polymerization method is the *initiator-transfer-terminator* (Inifiter) polymerization method, introduced by Otsu in 1982.^{150,151} The inifiter method does not yield in controlled M_w with narrow PDI as the RAFT polymerization does, but similar to RAFT it allows to start the polymerization from a defined starting group. *N,N*-diethyldithiocarbamoyl compounds are used as photochemical initiators ($\text{Et}_2\text{N}(\text{C}=\text{S})\text{SR}$). Further CTA molecules are not necessary. The bond between C and S is weak enough to break under UV irradiation; monomers are inserted in this bond.

1.3.3 Silicon-Containing Materials as Adhesion Promoters

Silane adhesion promoters are ambifunctional silicon compounds of the general structure $(\text{H}_3\text{CO})_3\text{Si-X}$, where X is an organofunctional group chosen for compatibility with the organic coating. These adhesion promoters are generally formulated into primers or added at relatively low levels to coatings. They promote adhesion of coatings to substrates, especially improving their resistance to debonding under humid conditions.

The alkoxy silanes are able to hydrolyze to the corresponding silanols that are able to condensate with hydroxyl groups present at the surface. Methoxy silanes also react directly with metal hydroxides and then cross-link in the present of atmospheric moisture.¹⁵²

Silane adhesion promoters had their first breakthrough in coatings applied to inorganic metal oxides, like glasses, etc.¹⁵³ Before those reactive silanes came up, it was difficult to formulate coatings that maintain adhesion to glass after exposure to a humid atmosphere. Usually, inorganic metal oxides express hydroxyl groups at the interface (sometimes the amount of hydroxyl groups present at the interface can be increased by oxygen-plasma exposure). These hydroxyl groups condensate with the present silanols or methoxy silanes to form covalent bonds, leading to enormous increase of adhesion.

Besides covalent attachment between metal oxide substrates and organic coatings, silane adhesion promoters also found applications on other substrates.

The surface of clean steel is not iron; rather, hydrated iron oxides are present as a monolayer on the iron (this is not a layer of rust particles).¹⁵⁴ Adhesion of usual organic coatings to this layer is usually based on hydrogen bonds between the hydroxylated surface and carboxylic

¹⁴⁶ Barner-Kowollik, C.; Davis, T.; Heuts, J.; Stenzel, M.; Vana, P.; Whittaker, M. *J. Polym. Sci.: Part A: Polym. Chem.* **2003**, *41*, 365.

¹⁴⁷ Lechmann, M. C.; Kessler, D.; Gutmann, J. S. *Langmuir* **2009**, accepted.

¹⁴⁸ Roth, P.; Kessler, D.; Zentel, R.; Theato, P. *Macromolecules* **2008**, *41*, 8316.

¹⁴⁹ Roth, P.; Kessler, D.; Zentel, R.; Theato, P. *J. Pol. Sci. Part A: Pol. Chem.* **2009**, *47*, 3118.

¹⁵⁰ Otsu, T.; Yoshida, M. *Makromol. Chem. Rapid Commun.* **1982**, *3*, 127.

¹⁵¹ Otsu, T. *J. Polym. Sci.: Part A: Polym. Chem.* **2000**, *38*, 2121.

¹⁵² Plueddemann, E. P., *Chapter 25: Silane Adhesion Promoters*, in Tracton, A. A. (Ed.), *Coating Materials and Surface Coatings*, CRC Press, Boca Raton, FL, USA, **2007**.

¹⁵³ Plueddemann, E. P., *Silane Coupling Agents*, Plenum Press, New York, USA, **1982**.

¹⁵⁴ Reinhard, G. *Prog. Org. Coat.* **1987**, *15*, 125.

functions of the organic resin.¹⁵⁵ Using trialkoxysilane adhesion promoters, these hydroxyl groups on metal surfaces can be used to create a covalent bond interface between the organic coating and metals. Besides several reports on silane-containing coatings onto iron or steel,^{156,157} also coatings on pure aluminum show an increase in adhesion.¹⁵⁸

As adhesion (or sometimes even wetting) of plastic substrates is a problem of coatings on polymeric substrates and also of intercoating adhesion (adhesion between two coatings on top of each other, i.e. multi-layer electronic devices, chapter 1.1.3) silane adhesion promoters also found application on plastics. Only a few polymeric materials express hydroxyl groups at the interface, thus polymeric substrates are usually pre-treated by oxidation processes like oxygen-plasma or flame treatment with gas burners using air/gas ratios such that the flames are oxidizing.¹⁵⁹ Depending on the procedure hydroxyl, ketone and/or carboxylic groups are generated, which may interact with the silane adhesion promoters.¹⁶⁰

1.3.4 Sol-Gel Coatings and Poly(silsesquioxanes)

Since trialkoxysilanes are promising adhesion promoters and are established on metal oxide surfaces as well as on metals or plastics, sol-gel coatings may be understood as a coating material consisting of inherent adhesion promoters. Since the last 30 years, the sol-gel method has emerged as a versatile method for preparing various oxide materials, e.g. silica-, alumina- or titania-based systems.¹⁶¹ The sol-gel approach consists of simultaneous hydrolysis and condensation reactions, originating from alkoxyde precursors, to form glassy polymer networks.¹⁶² Sol-gel materials are well established protective coatings, as it is possible to form highly adherent, chemically inert films on metal or metal oxide surfaces.¹⁶³ Single and multicomponent sol-gel coatings can be prepared from a variety of different alkoxy precursors which are commercially available. Furthermore, the preparation from a sol allows incorporation of water- or alcohol-soluble dopants into the final coating.

Common coating techniques, like spraying, dipping or spinning can be applied to a sol-gel material, yielding in thin films of submicrometer thickness. Thicker films can be produced by multiple layer deposition.¹⁶⁴ Especially the corrosion resistance behavior of sol-gel derived thin films deposited onto stainless steel has been extensively studied. A variety of compositions, including SiO_2 , ZrO_2 , $\text{SiO}_2 - \text{TiO}_2$, $\text{ZrO}_2 - \text{Y}_2\text{O}_3$ have been found to improve the resistance to oxidation and corrosion under acidic conditions.¹⁶⁵ Good coating properties of sol-gel derived

¹⁵⁵ Jacobasch, H. J. *Prog. Org. Coat.* **1989**, *17*, 115.

¹⁵⁶ Plueddemann, E. P. *Prog. Org. Coat.* **1983**, *11*, 297.

¹⁵⁷ Sathyanarayana, M. N.; Yassen, M. *Prog. Org. Coat.* **1995**, *26*, 275.

¹⁵⁸ Witucki, G. L. *J. Coat. Technol.* **1993**, *65*, 57.

¹⁵⁹ Ryntz, R. A., *Painting of Plastics*, Federation of Societies for Coating Technology, Blue Bell, PA, USA, **1994**.

¹⁶⁰ Mittal, K. L. (Ed.), *Adhesion Aspects of Polymeric Coatings*, Plenum Press, New York, USA, **1983**.

¹⁶¹ Brinker, C. J.; Scherer, G. W., *Sol-Gel Science*, Academic Press, San Diego, CA, USA, **1990**.

¹⁶² Aleman, J.; Chadwick, A. V.; He, J.; Hess, M.; Horie, K.; Jones, R. G.; Kratochvil, P.; Meisel, I.; Mita, I.; Moad, G.; Penczek, S.; Stepto, R. F. T. *Pure Appl. Chem.* **2007**, *79*, 1801.

¹⁶³ Metroke, T. L.; Parkhill, R. L.; Knobbe, E. T. *Prog. Org. Coat.* **2001**, *41*, 233.

¹⁶⁴ Brinker, C. J.; Hurd, A.J.; Frye, G. C.; Ashley, A. S. *J. Non-Cryst. Solids* **1992**, *147/148*, 424.

¹⁶⁵ Guglielmi, M. J. *Sol-Gel Sci. Tech.* **1997**, *8*, 443.

materials were also found on glass and silicon surfaces,¹⁶⁶ aluminum substrates¹⁶⁷ as well as on plastics.¹⁶⁸

Besides pure inorganic sol-gel derived coatings, like SiO₂ derived from tetraethylorthosilicate (TEOS) also partially organically modified sol-gel materials show excellent coating abilities. Organically modified ceramics (ORMOCER®s) are probably the most prominent examples for sol-gel hybrid coating materials.¹⁶⁹ Generally, the hybrid material is formed through the hydrolysis and condensation of organically modified silicates with traditional alkoxide precursors. The incorporated Si-R functionalities allow organic modification of the hybrid material characteristics between those of silicones, polymers and glass ceramics. Today's applications of ORMOCER®s are mainly as protective coating on various substrates, but also as dental fillers or as polymeric ion conductor in fuel cells. Similar to ORMOCER®s, inorganic-organic hybrid materials enlarged the accessible scope of characteristics and functionalities of sol-gel derived coatings.

Especially poly(silsesquioxanes) (PSSQ) are ideal materials for defined inorganic organic hybrid coating materials.¹⁷⁰ Like silicates, they allow the formation of three dimensional networks due to three possible access points for further silanol condensation; furthermore every silicon atom is connected to one organic moiety. The general composition of PSSQ is RSiO_{3/2}, whereas R can be hydrogen, alkyl-, alkylene-, aryl- or organically interconnecting groups.

Poly(silsesquioxanes) are usually prepared by acid-catalyzed hydrolytic polycondensation from the corresponding trialkoxy- or trichloro silanes (see figure 1.14). The resulting microstructure is usually a mixture of the typical PSSQ structures: random structure, T8 cage structure, ladder-like structure or partial cage structure (see figure 1.15). To obtain a specific microstructure, the reaction conditions have to be tuned very precisely.¹⁷¹

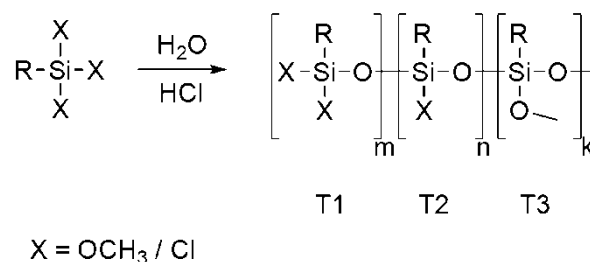


Figure 1.14. Polycondensation reaction of trimethoxy- or trichloro silanes to poly(silsesquioxane). The general structure of PSSQ shows the three possible branching T1, T2 and T3.

Using defined reaction parameters, especially temperature and reaction time, soluble pre-condensed PSSQ materials with molecular weight between 500 g/mol and 10.000 g/mol can be

¹⁶⁶ den Toonder, J.; Malzbender, J.; de With, G.; Balkenende, R. *J. Mater. Res.* **2002**, *17*, 224.

¹⁶⁷ Kato, K. *J. Mater. Sci.* **1992**, *27*, 1445.

¹⁶⁸ Chan, C. M.; Cao, G. Z.; Fong, H.; Sarikaya, M.; Robbinson, T.; Nelson, L. *J. Mater. Res.* **2000**, *15*, 148.

¹⁶⁹ ORMOCER®s, Fraunhofer-Institut für Silicatforschung ISC Würzburg, Germany

¹⁷⁰ Gunji, T.; Iizuka, Y.; Arimitsu, K.; Abe, Y. *J. Poly. Sci.: Part A: Polym. Chem.* **2004**, *42*, 3676.

¹⁷¹ Baney, R. H.; Itoh, M.; Sakaibara, A.; Suzuki, T. *Chem. Rev.* **1995**, *95*, 1409.

obtained. The solubility of this pre-condensed PSSQ is determined by the degree of branching, which can be determined by ^{29}Si CPMAS NMR spectroscopy (chemical shifts δ : -47 ppm for T1, -57 ppm for T2 and -64 ppm for T3 branches).¹⁷² The sol-gel process of trifunctional silanes and the mechanism of the formation of PSSQ were extensively studied by Tripp^{173,174} and Macosko.^{175,176}

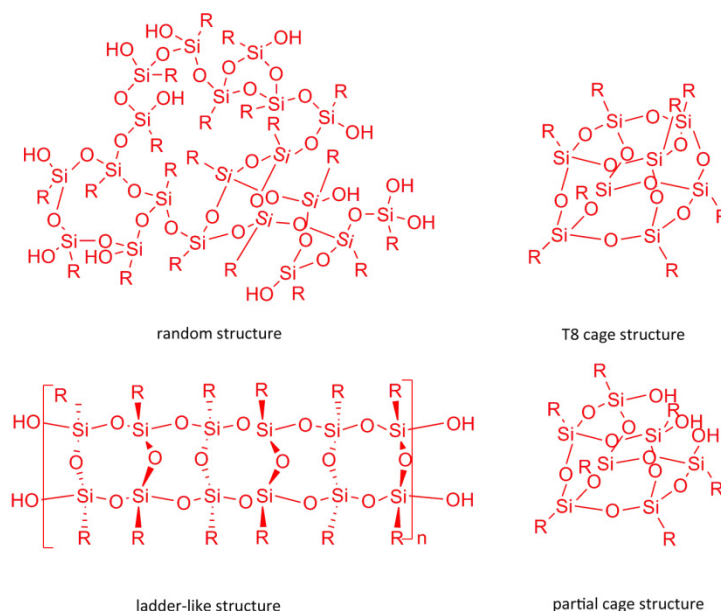


Figure 1.15. Typical microstructures of poly(silsesquioxanes).

Most used PSSQ gels in coating applications are either poly(methylsilsesquioxanes) (PMSSQ), poly(alkylsilsesquioxanes) or poly(phenylsilsesquioxanes) (PPSSQ). Besides these organic functionalities carrying one silane moiety, also organic molecules with two or even more silanes are actually used as hybrid materials.^{177,178} Main applications are in optics and electronics,¹⁷⁹ or as precursor for fabrication of porous silica layers.¹⁸⁰

¹⁷² Gomez-Romero, P.; Sanchez, C., *Functional Hybrid Materials*, Wiley-VCH, Weinheim, Germany, **2004**.

¹⁷³ White, L. D.; Tripp, C. P. *J. Colloid Interface Sci.* **2000**, *227*, 237.

¹⁷⁴ C. P. Tripp, Veregin, R. P. N.; McDougall, M. N. V.; Osmond, D. *Langmuir* **1995**, *11*, 1858.

¹⁷⁵ Rankin, S. E.; Macosko, C. W.; McCormick, A. V. *AIChE Journal* **1998**, *44*, 1141.

¹⁷⁶ Rankin, S. E.; Macosko, C. W.; McCormick, A. V. *Chem. Mater.* **1998**, *10*, 2037.

¹⁷⁷ Loy, D. A.; Shea, K. J. *Chem. Rev.* **1995**, *95*, 1431.

¹⁷⁸ Shea, K. J.; Loy, D. A. *Chem. Mater.* **2001**, *13*, 3306.

¹⁷⁹ Shea, K. J.; Loy, D. A.; Webster, O. J. *Am. Chem. Soc.* **1992**, *114*, 6700.

¹⁸⁰ Sugizaki, T.; Kashio, M.; Kimura, A.; Yamamoto, S.; Moriya, O. *J. Polym. Sci.: Part A: Polym. Chem.* **2004**, *42*, 4212.

1.3.5 Hybrid Polymers based on Poly(silsesquioxanes)

Inorganic-organic hybrid materials combine structural elements of inorganic oxide glasses/ceramics (mainly silica based), polysiloxanes, and organic polymers.¹⁸¹ The concept is to combine properties of organic polymers (functionalization, ease of processing at low temperatures, toughness) with properties of glass-like materials (hardness, chemical and thermal stability, transparency) in order to generate new/synergetic properties not accessible otherwise with classical composites.¹⁸²

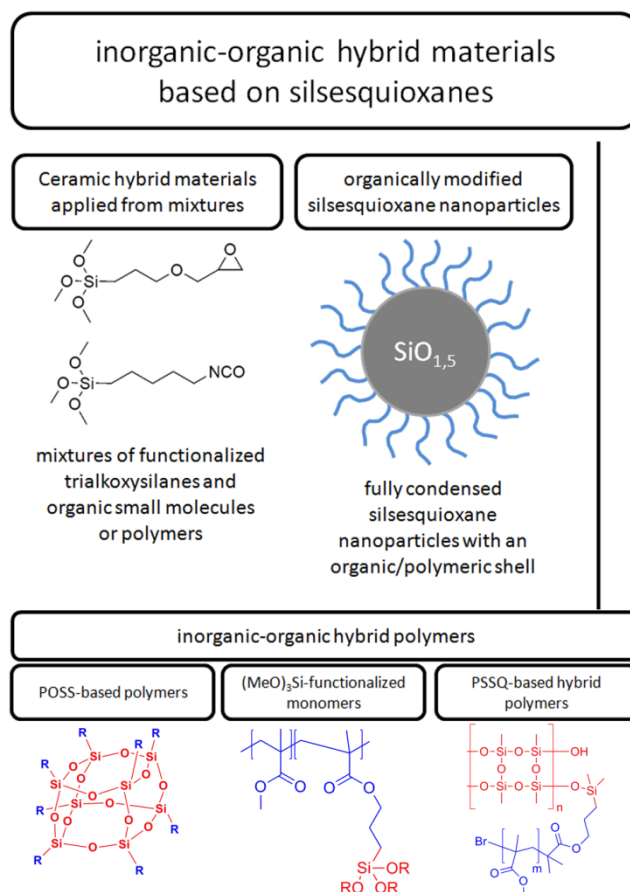


Figure 1.16. Classification of inorganic-organic hybrid materials based on silsesquioxanes with several examples.^{183, 187, 191, 197, 201}

Most inorganic-organic hybrid materials are actually based on silicon as inorganic network forming agent, but in principle other inorganic elements can be incorporated during the sol-gel process. Various methods were introduced to create inorganic-organic hybrid materials. Most approaches consist of a mixture of an organic polymer, or block copolymer, with a silicon precursor (usually functionalized to bind to the organic polymers, e.g. carrying epoxy-, amine-,

¹⁸¹ Kickelbick, G. (Ed.), *Hybrid Materials. Synthesis, Characterization, and Applications*, Wiley-VCH, Weinheim, Germany, **2007**.

¹⁸² Haas, K.-H. *Adv. Engin. Mater.* **2000**, 2, 571.

acrylate-functions). The real inorganic-organic connection is not made until the material is applied and finally cross-linked.^{183,184} Main drawbacks of application from a mixture of an organic polymer and an inorganic precursor are maintaining the right mixing procedure and guarantee similar diffusion of the different moieties (e.g. in dip-coating application of spherical objects or capillaries).¹⁸⁵ To overcome these disadvantages of unstructured inorganic-organic hybrid materials, several methods were developed to combine inorganic moieties and organic moieties already during synthesis. Silsesquioxane-based nanoparticles, synthesized by hydrolytic condensation of a functionalized precursor,¹⁸⁶ could successfully be used as macroinitiator to graft glycomethacrylate stars with approx. 25 arms via ATRP.^{187,188} Similarly, a silica shell could be grown around a SiOH-functionalized polystyrene latex.¹⁸⁹ Starting from those silica hybrid nanoparticles functionalized sol-gel coatings for optical applications could be produced.¹⁹⁰ Besides the introduced ceramic hybrid materials from a mixture of precursors and hybrid nanoparticles, inorganic-organic hybrid polymers are the third class of hybrid materials (the boundaries between these different classes are not defined exactly).

The different methods in the active field of research of combining inorganic moieties with an organic polymer will be presented in the following.

Polyhedral oligomeric silsesquioxanes (POSS; $\text{Si}_8\text{O}_{12}\text{R}_8$)¹⁹¹ (structure shown in figure 1.15, top, right) are well defined monomeric systems which can be functionalized easily.¹⁹² POSS can either be functionalized with one acrylic function, and thus be polymerized to form a homo or block copolymer, or it can be functionalized with initiators, allowing grafting polymers from a POSS core.^{193,194} The main drawback of using POSS as inorganic moiety is the absence of Si-OH groups which would allow 3D-network formation by cross-linking, an intrinsic feature which should be implied in silicon-based hybrids.

Several modified approaches could increase the number of free silanol groups capable to cross-link or to promote surface adhesion by a secondary condensation. Partial cage structures (T-POSS) could be incorporated in urethane or siloxane polymers; by cross-linking residual SiOH groups stable coatings on metal substrates could be obtained.^{195,196} Acrylate or methacrylate functionalized trialkoxysilanes could be polymerized to yield highly reactive homo or diblock copolymers. Well defined block copolymers with one highly trialkoxysilane-

¹⁸³ Simon, P. F. W.; Ulrich, R.; Spiess, H. W.; Wiesner, U. *Chem. Mater.* **2001**, *13*, 3464.

¹⁸⁴ Ogoshi, T.; Chujo, Y. *Composite Interfaces* **2005**, *11*, 539.

¹⁸⁵ Harreld, J. H.; Esaki, A.; Stucky, G. D. *Chem. Mater.* **2003**, *15*, 3481.

¹⁸⁶ Mori, H.; Lanzendörfer, M. G.; Müller, A. H. E. *Macromolecules* **2004**, *37*, 5228.

¹⁸⁷ Muthukrishnan, S.; Plamper, F.; Mori, H.; Müller, A. H. E. *Macromolecules* **2005**, *38*, 10631.

¹⁸⁸ Mori, H.; Müller, A. H. E.; Klee, J. E. *J. Am. Chem. Soc.* **2003**, *125*, 3712.

¹⁸⁹ Tissot, I.; Reymond, J. P.; Lefebvre, F.; Bourgeat-Lami, E. *Chem. Mater.* **2002**, *14*, 1325.

¹⁹⁰ Penard, A.-L.; Gacoin, T.; Boilot, J.-P. *Acc. Chem. Res.* **2007**, *40*, 895.

¹⁹¹ Zhang, L.; Abbenhuis, H.C.L.; Yang, Q.; Wang, Y.-M.; Magusin, P.C.M.M.; Mezari, B.; van Santen, R.A.; Li, C. *Angew. Chem. Int. Ed.*, **2007**, *46*, 5003.

¹⁹² Zhang, C.; Laine, R. M. *J. Am. Chem. Soc.*, **2000**, *122*, 6979.

¹⁹³ Costa, R.O.R.; Vasconcelos, W.L.; Tamaki, R.; Laine, R.M. *Macromolecules*, **2001**, *34*, 5398.

¹⁹⁴ Pyun, J.; Matyjaszewski, K. *Macromolecules* **2000**, *33*, 217.

¹⁹⁵ Oaten, M.; Choudhury, N. R. *Macromolecules* **2005**, *38*, 6392.

¹⁹⁶ Han, S. H.; Lee, J. Y.; Koo, S. M. *J. Ind. Eng. Chem.* **2004**, *10*, 813.

functionalized block could be built-up using either ATRP¹⁹⁷ or RAFT polymerization.¹⁹⁸ Like other block copolymers also these inorganic-organic hybrid block copolymers showed the expected aggregation phenomena. By induced cross-linking of these aggregates nanohybrids could be obtained (sol-gel chemistry in micelles).¹⁹⁹

Solution processible poly(methylsilsesquioxane) (PMSSQ) can be produced by adjusting specific reaction parameters like temperature, amount of water, amount of acid, etc. properly.²⁰⁰ These preformed randomly structured inorganic networks still contain a lot of free silanol groups for secondary condensation. During the sol-gel process to produce this soluble PMSSQ networks, mono- or trichlorosilane-functionalized ATRP initiators could be co-condensed into the network.²⁰¹ By grafting methylmethacrylate (MMA) from these macro ATRP initiators, hybrid polymers consisting of PMSSQ and PMMA were obtained which could successfully be applied as low-dielectric-constant coating.²⁰²

In general, the different synthetic strategies to create inorganic-organic hybrid materials benefits a lot of the concepts of controlled radical polymerization techniques, like ATRP²⁰³ or the inifiter method²⁰⁴ because of the defined starting point of the organic polymerization. The impact of controlled/"living" radical polymerization on the formation of inorganic-organic hybrid materials was summarized by Pyun et al.²⁰⁵

¹⁹⁷ Du, J.; Chen, Y.; Zhang, Y.; Han, C. C.; Fischer, K.; Schmidt, M. *J. Am. Chem. Soc.* **2003**, *125*, 14710.

¹⁹⁸ Mellon, V.; Rinaldi, D.; Boureat-Lami, E.; D'Adosto, F. *Macromolecules* **2005**, *38*, 1591.

¹⁹⁹ Chen, Y.; Du, J.; Xiong, M.; Zhang, K.; Zhu, H. *Macromol. Rapid Commun.* **2006**, *27*, 741.

²⁰⁰ Lee, J.-K.; Char, K.; Rhee, H.-W.; Ro, H. W.; Yoo, D. Y.; Yoon, D. Y. *Polymer* **2001**, *42*, 9085.

²⁰¹ Theato, P.; Kim, K. J.; Yoon, D. Y. *Phys. Chem. Chem. Phys.* **2004**, *6*, 1458.

²⁰² Ro, H. W.; Kim, K. J.; Theato, P.; Gidley, D. W.; Yoon, D. Y. *Macromolecules* **2005**, *38*, 1031.

²⁰³ Pyun, J.; Jia, S.; Kowalewski, T.; Patterson, G. D.; Matyjaszewski, K. *Macromolecules* **2003**, *36*, 5094.

²⁰⁴ Bai, J.; Qiu, K.-Y.; Wie, Y. *Polymer International* **2003**, *52*, 853.

²⁰⁵ Pyun, J.; Matyjaszewski, K. *Chem. Mater.* **2001**, *13*, 3436.

2 Aim of Work

In general, the key requirements on a versatile coating material are strong adhesion and stability on various underlying substrates, as well as easy access to a broad range of functionalities incorporated in the coating material.

As briefly explained in the introduction, sol-gel coatings based on trifunctional silanes showed extraordinary adhesion on a wide range of materials, e.g. silicon, inorganic oxide glasses, metals and also polymeric substrates. The combination with organic polymers to yield hybrid materials is seen as the most promising approach to introduce chemical functions and their by creating functional surface coatings.

To obtain an easy processible material, the inorganic part (offering adhesion) and the organic part (functionality) should be combined in one hybrid polymer, which should be applicable from solution, e.g. by dip-coating or spin-coating.

As inorganic part, a pre-formed soluble poly(methylsilsesquioxane) (PMSSQ) should guarantee adhesion due to a large amount of free silanol groups, capable for secondary condensation to form a cross-linked film. Besides the mechanically interlocking and the van der Waals adhesion phenomena, PMSSQ should further be able to form a covalent bond interface or a polymer diffusion interface, for adhesion enhancement.

To afford a direct connection to an organic polymer, the pre-formed PMSSQ should contain defined starting points for a controlled radical polymerization step (e.g. initiating species for ATRP or chain transfer groups for RAFT). Having those PMSSQ-macroinitiators or macro CTAs in hands, functional hybrid coating materials can be obtained by grafting accordingly functionalized organic polymers from PMSSQ.

The adhesion properties of the obtained hybrid polymers after spin- or dip-coating and annealing should be tested using different underlying materials, reaching from metals, metal oxides to plastics. Also the long-term stability should be evaluated.

To confirm the variable applicability, the tolerance of the controlled radical polymerization procedures towards functional moieties should be utilized. Imaginable are, for instance, functional surface coatings, enabling defined wetting or stimuli-responsive wetting, and also semi-conductive films.

Besides the direct functionalization strategy, by polymerization of functional monomers during hybrid polymer synthesis, also a post-coating functionalization is desirable, which would allow attachment of defined moieties to the surface by a simple surface-analogous reaction. Reactive surface coatings could be realized by grafting activated esters or acetylene based monomers from a PMSSQ precursor; it has to be assured that the reactive moieties are maintained during the coating process and can be addressed finally at the interface or throughout the deposited film. Those reactive coatings would allow adjustment of defined surface characteristics, e.g. defined wetting, switchable wetting, but also to attach defined recognition motives allowing application in bio-chemical analytical devices.

Overall, the scope of this work can be divided in three parts: (1) defined synthesis of hybrid polymers based on PMSSQ, (2) implantation of different functions during the synthesis and characterization of the resulting functional or semi-conductive surface coatings, (3) design of reactive surface coatings and thereby enlarging the range of possible applications.

3 Results and Discussion

The presented concept to create a new class of substrate-independently adherent functional coating materials relies on hybrid polymers combining the inherent characteristics of sol-gel derived silsesquioxane networks and the broad functionalities, which can be incorporated into different organic polymers.

Sol-gel materials, like poly(methylsilsesquioxane), are promising coating materials, due to their ability to act as inherent adhesion promoter on various substrates (see chapters 1.3.3 and 1.3.4). However, to guarantee maximum adhesion the sol-gel materials have to be processed from solution to form a continuous layer which can be converted to an integral solid film by annealing afterwards. Thus, solubility and cross-linkability have to be maintained during hybrid polymer synthesis. Various organically modified moieties could be incorporated into the PMSSQ network, which were capable as defined starting points to graft organic polymers. Using different controlled radical polymerization methods yielded a broad scope of functional hybrid materials.

These different hybrid materials could successfully be applied to various substrates, producing functional or reactive surface coatings.

In the following, the synthetic concept based on different polymerization techniques will be presented, followed by a summary of the general coating properties. Afterwards the realized functional and reactive surface coatings will be demonstrated.

The detailed procedures are given in the corresponding publications (see chapter 4), respectively.

3.1 Synthesis of Inorganic-Organic Hybrid Polymers

Different synthetic strategies were elaborated to produce hybrid polymers based on poly(silsesquioxanes). The two main concepts were: (A) pre-condensation of modified PMSSQ starting from methyltrimethoxysilane (MTMS) and an organically modified trifunctionalized silane, capable to initiate an ATRP or to promote a RAFT polymerization, followed by grafting the organic polymer (chapter 3.1.1 and 3.1.2); (B) endgroup functionalization of organic polymers, enabling incorporation into a PMSSQ network afterwards (chapter 3.1.4).

3.1.1 Hybrid Polymer Synthesis Using ATRP

Three different functionalized ATRP initiators (2-bromoisobutyric acid 5-(trichlorosilyl)pentyl ester, *p*-chloromethylphenyl trichlorosilane, *p*-(chloromethyl)-phenylethyltrichlorosilane) were co-condensed with methyltrimethoxysilane (MTMS) to yield a series of macro initiators PMSSQ-MI-1, PMSSQ-MI-2, and PMSSQ-MI-3, respectively (see figure 3.1), which provide a high functionality of unreacted silanol groups and initiating groups for the atom transfer radical polymerization. The synthesis of different macro initiators allows us to investigate differences between three PMSSQ matrices as well as differences during ATRP polymerization.

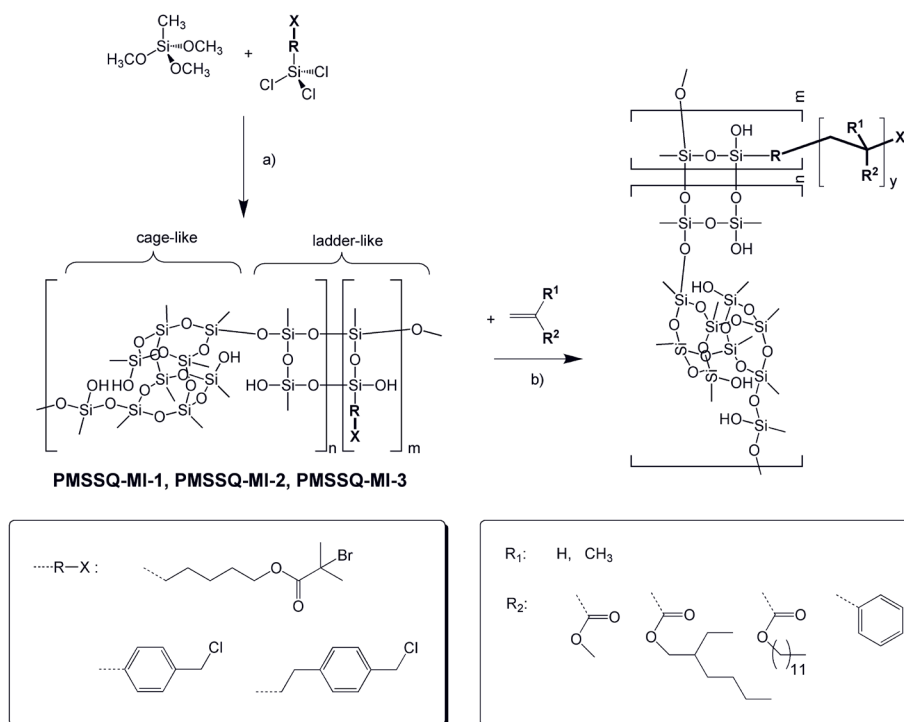


Figure 3.1. Synthetic pathway towards PMSSQ based hybrid polymers: a) co-condensation of the ATRP initiators with MTMS yielding the macro initiators classes PMSSQ-MI-1, PMSSQ-MI-2 and PMSSQ-MI-3, and b) controlled radical polymerization of vinyl monomers under ATRP conditions.

Using common ATRP conditions, each PMSSQ based macro initiator was used to initiate the polymerization of methyl acrylate (MA), ethyl hexyl acrylate (EHA), methyl methacrylate (MMA), decyl methacrylate (DMA) and styrene (S). PMSSQ-MI-1 was activated using CuBr where as PMSSQ-MI-2 and PMSSQ-MI-3 were activated using CuCl, all other reaction conditions were kept identical for all polymerizations.

All analyzed macro initiators and the corresponding hybrid polymers showed similar thermal behaviors. A highly reactive inorganic macro initiator was obtained through a co-condensation process. After the controlled radical polymerization, which had been performed under equivalent conditions, the inorganic blocks still showed reactive T1 and T2 branches in ²⁹Si CPMAS NMR spectroscopy. As a consequence thereof, the hybrid polymers could be cross-linked by thermal annealing. After heating to 200 °C for 24 h, fully condensed materials were obtained, which were completely insoluble in n-hexane, chloroform, methylene chloride, THF, dioxane, acetone and ethyl acetate.

Thin films of the hybrid polymers were prepared on silicon, glass, steel, copper, polycarbonate and PMMA surfaces via spin-coating (4000 rpm, 15 s) from a solution of 10 wt% in THF, followed by annealing at 130 °C for 1 h. Excellent adhesion characteristics were found by the tape test. All materials showed a successful surface functionalization, which is not influenced by the substrate. Further details can be found in publication 1, chapter 4.1.

3.1.2 Hybrid Polymer Synthesis Using RAFT

Similar to the ATRP approach chain transfer agents for the RAFT polymerization were functionalized with trialkoxysilanes. After co-condensation with MTMS various PMSSQ-RAFT macro chain transfer agents (mCTAs) were obtained (see figure 3.2).

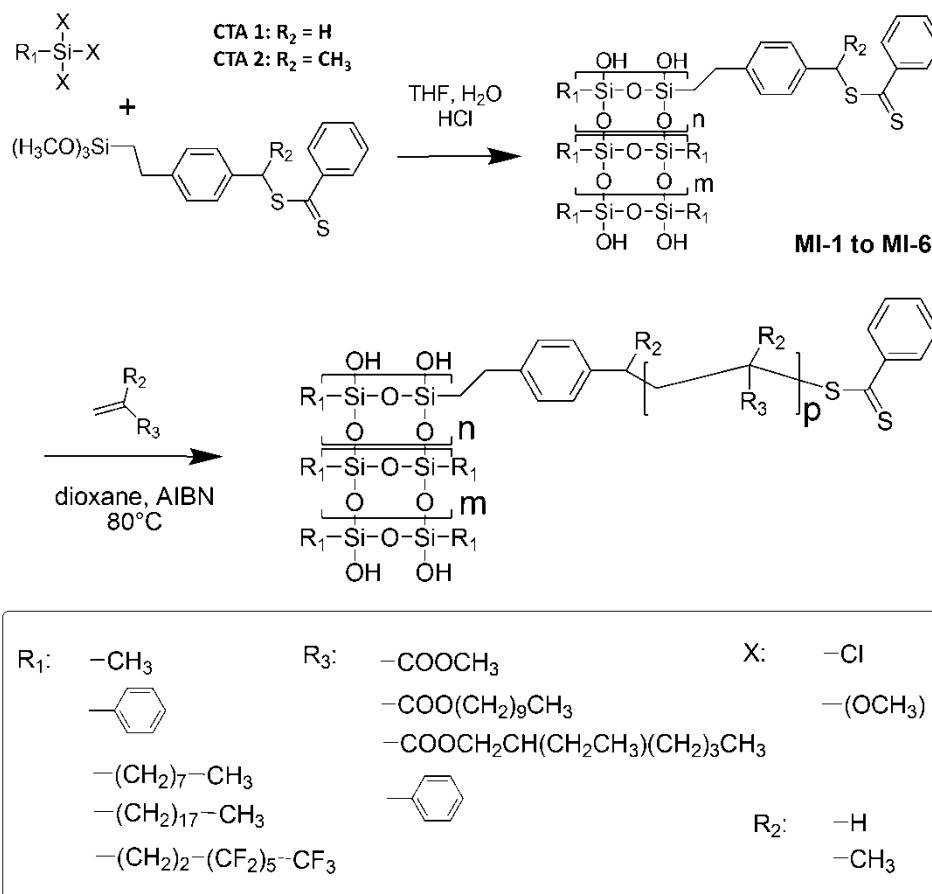


Figure 3.2. Synthetic pathway towards PSSQ based hybrid polymers. The first steps shows the co-condensation of the macro-CTA, the second step shows the grafting from polymerization via RAFT to yield in an inorganic/organic hybrid polymer.

Dithiobenzoic acid benzyl-(4-ethyltrimethoxysilyl) ester (CTA 1) and dithio benzoic acid 1-ethylphenyl-4-(ethyltrimethoxysilyl) ester (CTA 2) were investigated as chain transfer agents in the RAFT polymerization. CTA 1 was used in polymerizations of acrylates, while CTA 2 was applicable for methacrylates; the grafting from polymerization of styrene was possible with both types.

Besides grafting different polymers from the PMSSQ network, also the network itself could be modified by co-condensing different trialkoxysilanes instead of MTMS (compare R_1 in figure 3.2). Furthermore, not only one monomer could be grafted from the silsesquioxane macro-CTA, also a mixture could be used, yielding a random copolymer in the organic part, which enlarges the accessible scope of functional hybrid materials even further.

As described in the introduction, ideal coating materials should be applicable on a wide range of substrates, thus stable and adherent films should be formed on any surface type. The different obtained hybrid polymers were spin coated from a 10 wt% solution in THF as described above on silicon, glass, steel, copper, polycarbonate and poly(methyl methacrylate) surfaces. The successful surface coating of the substrate was analyzed by contact angle measurements. While the advancing contact angles of water on different substances vary dramatically, depending on the nature of the material, all surfaces showed after coating with the respective hybrid polymers similar advancing contact angles. In other words, the contact angle is determined only by the hybrid coating agent used and not by the substrate, indicating not only a successful surface modification but also the potential of hybrid polymers as coating materials.

Similarly as described for the hybrid polymers by ATRP, good adhesion of the coating materials after annealing was observed during tape test.

The detailed synthetic procedure, as well as all surface characterization data can be found in publication 2, chapter 4.2.

3.1.3 Microreactor Based Synthesis of Poly(methylsilsesquioxanes)

As described briefly above, hybrid polymer synthesis starting from a pre-formed PMSSQ network resulted in a broad range of new coating materials, capable to be functionalized in different manners. The crucial step during the synthesis is the formation of the PMSSQ network. During the batch synthesis of PMSSQ, the composition can be controlled by the initial ratio of initiating species to MTMS, but the final molecular weight of the PMSSQ cannot be adjusted reproducibly.

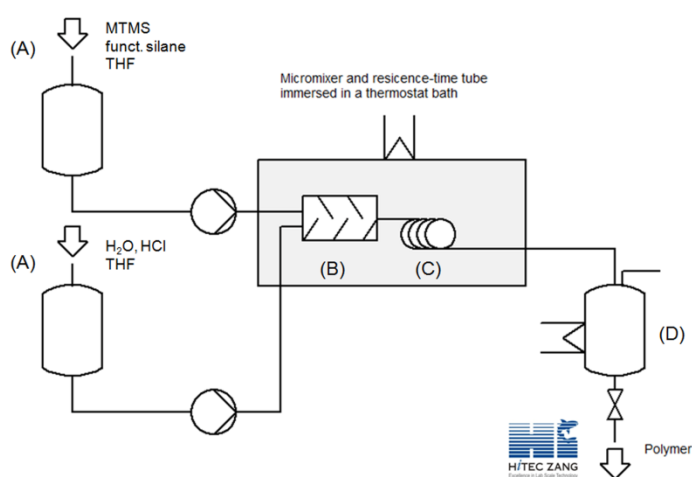


Figure 3.3. Microreactor setup: (A) syringe pumps; (B) IMM micromixer; (C) delay loops; (D) cooled flask

Therefore, the co-condensation step has been studied using microreactors in order to achieve a better thermal control and to reduce mass transfer effects during the polycondensation,

which resulted in an improved control over molecular weight and in narrower molecular weight distributions. The setup, shown in figure 3.3, was used for the studies.

The dependency between the molecular weight and the residence time is shown in figure 3.4. The detailed reaction parameters are explained in publication 3, see chapter 4.3.

For the first time a very precise adjustment of molecular weight was demonstrated for functionalized PMSSQ. The co-condensation in microreactors may be used for further hybrid polymer synthesis.

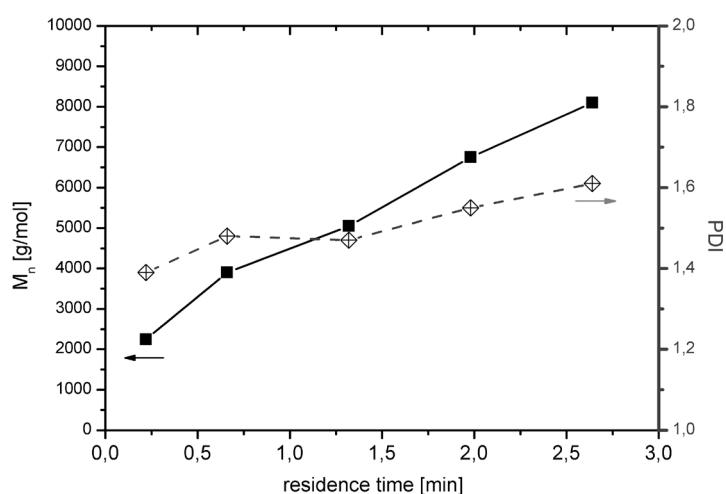


Figure 3.4. Dependence of the molecular weight on the residence time of the co-condensation of MTMS and an alkoxysilane-functionalized chain transfer agent.

3.1.4 Synthesis of Hybrid Polymers starting from Organic Polymers

PMSSQ-based hybrid polymers obtained in an ATRP or RAFT process showed an excellent adherence on various substrates offering convenient access to defined surface properties on different substrates. However, stable and adherent polymeric coatings of non-radically formed polymers like polycarbonate (PC) (produced via polycondensation) or polyethyleneglycol (PEG) (produced via anionic polymerization) could not be produced by covalent attachment of those polymers to PMSSQ.

Thus, a different synthetic concept to attach pre-formed polymers to a PMSSQ network consisting of a trichlorosilyl-endgroup functionalization of PC or PEG and further co-condensation with methyl trimethoxysilane (MTMS) to yield a PMSSQ network (route B) was investigated.

To synthesize endgroup-functionalized PC, the polycondensation reaction of bisphenol A and diphenyl carbonate was quenched with *o*-allylphenol and the successful introduction of the allyl-endgroups was confirmed by ^1H NMR spectroscopy. Hydrosilylation with silicochloroform and further co-condensation with MTMS yielded in the desired PMSSQ-PC hybrid polymer. ^1H NMR spectroscopy of PMSSQ-PC shows the additional Si-CH₃ signal at 0.16 ppm, whereas

the allyl signals vanished. The molecular weight increased from 5 kg/mol to 47 kg/mol and showed a monomodal distribution, indicating that PC segments were incorporated in a PMSSQ network. The ability of this hybrid material to undergo further cross-linking was checked by ^{29}Si CPMAS NMR spectroscopy, 62% of all silicon atoms still carry two or one free OH group (T1 and T2 branches). Cross-linking occurred, similar to other PMSSQ systems, between 100 °C and 130 °C and took less than 70 min at 130 °C (measured by TGA).

A PMSSQ-PEG hybrid polymer was synthesized by endgroup-functionalization of PEG-diol (2 kg/mol) with isocyanatopropyltriethoxysilane, yielding - similar to the functionalization of PC - a di-(trichlorosilyl)-functionalized PEG. Further co-condensation with MTMS led to the PMSSQ-PEG hybrid polymer. GPC showed a monomodal molecular weight distribution with $M_n = 39$ kg/mol. ^{29}Si CPMAS NMR spectroscopy showed 60% T1 and T2 branches, cross-linking occurred under similar conditions as explained above. PMSSQ-PC and PMSSQ-PEG could be used to produce surface coatings on a wide range of substrates. Successful surface modification and high long-term stability of the coatings could be demonstrated by contact angle measurements and ISO tape test.

Detailed reaction parameters are given in chapter 4.4 (publication 4).

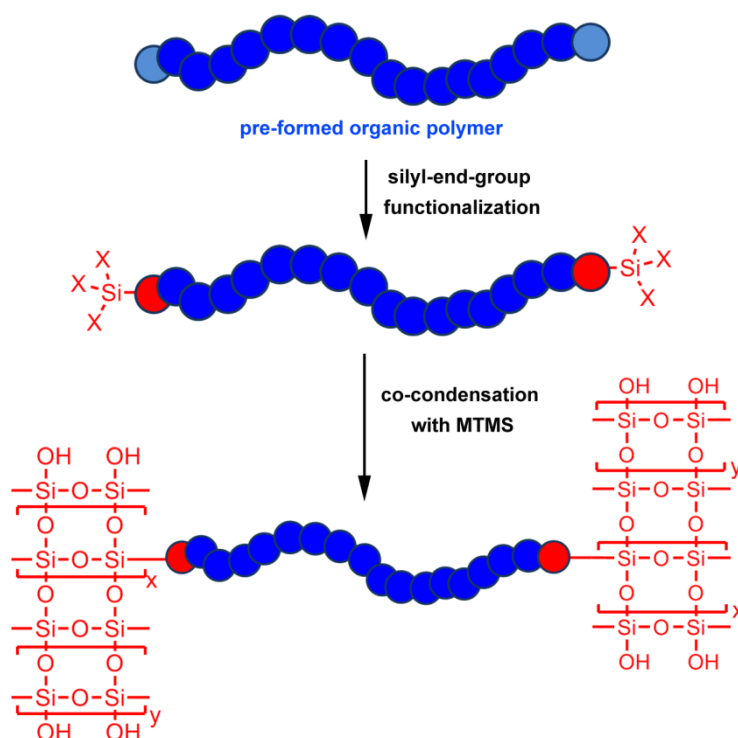


Figure 3.5. Reaction pathway to create inorganic-organic hybrid polymers, starting from pre-formed organic polymers.

3.2 General Coating Properties

Using the different presented synthetic approaches to create new hybrid polymers, a variety of different polymers could be included into a PMSSQ-based hybrid. During the first strategy (A) a functional PMSSQ was formed in a first step, which was capable as a defined starting point for either ATRP or RAFT polymerization. The scope of monomers which can be grafted reached from acrylates, methacrylates to styrenes.

The strategy B started from the pre-formed organic polymer which was endgroup functionalized to be able to undergo co-condensation with MTMS and thus resulted in the corresponding hybrid polymer.

Independently from the used method and the used organic polymer, all coatings showed some intrinsic characteristics, which are summarized below.

- All coating materials were still soluble and thus allowed application from solution by either spin-coating or dip-coating.
- The PMSSQ part of all hybrid polymers maintained approximately between 40% and 50% silicons with at least one free silanol function. This high amount of SiOH groups guaranteed a high cross-linking density after annealing.
- Annealing conditions were found to be independent from the organic part. Meaning all coating materials could be cross-linked efficiently by annealing at 130 °c for 1h.
- Stable and adherent films could be prepared from all tested hybrid polymers; physical characteristics of the organic part (e.g. T_g) showed no influence.
- 10 – 20 wt% of the inorganic part is sufficient to create stable films.
- Tape Test indicated strong adhesion on Si, glass, steel, PDMS, PMMA, etc.
- Very smooth surfaces were obtained by AFM measurements (in all measurements the root mean square surface roughness was below 1 nm on an area of 1 μm^2 for all coating materials) (see figure 3.6).
- The final coatings did not rededolve in water or any common organic solvent.
- The wetting behavior of coated substrates is only determined by the applied coating and thus also determined by the ratio between inorganic and organic part (see figure 3.7)

Details concerning tape test results and AFM topography images can be found in chapter 4.

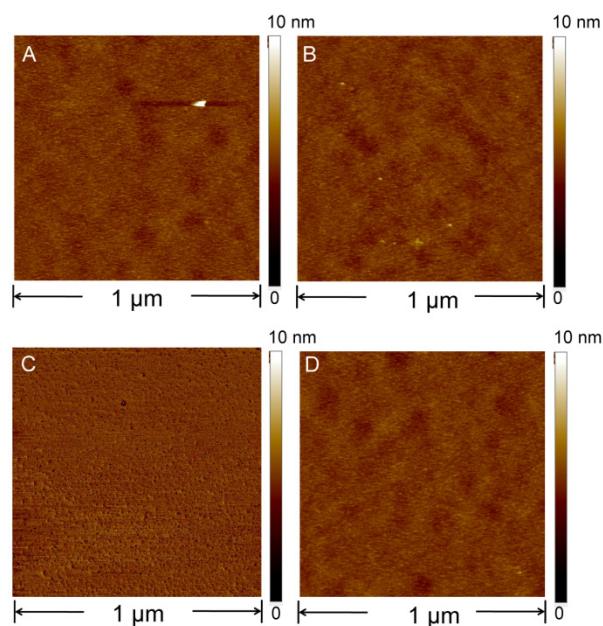


Figure 3.6. AFM topography of PMSSQ-PFPA hybrid polymers on various substrates. (A) gold substrate; (B) PC substrate; (C) PDMS substrate; (D) PMMA.

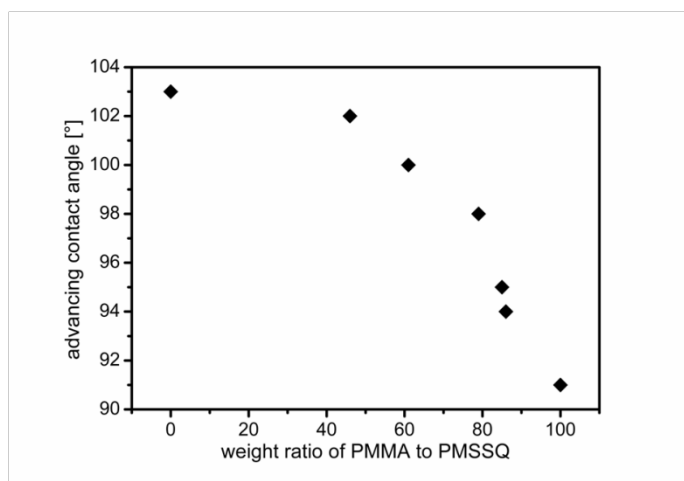


Figure 3.7. Influence of the variation of the organic to inorganic weight ratio on the observed contact angle after spin coating on a silicon substrate (spin-coated from 10 wt% solution in THF).

3.3 Functional Coating Materials

To create surface coatings with defined functionalities present at the interface, a polymer expressing the desired function has to be grafted either from or to the PMSSQ network. Several examples of functional surface coatings will be presented in the following.

3.3.1 Temperature-Responsive Coatings

Poly(*N*-isopropylacrylamide) (PNIPAM) exhibits a reversible temperature-dependent soluble/insoluble transition at its lower critical solution temperature (LCST) in aqueous media. The LCST of PNIPAM in water was found to be 32 °C. It is known, that the phase transition of PNIPAM accompanies not only a drastic confirmation change from a coil to a globule, but also a rapid change in interfacial properties. Below the LCST a PNIPAM coated surface shows a hydrophilic behavior, when heated above the LCST the behavior changes to hydrophobic. This effect on substrates offers the ability to control important interfacial phenomena such as wetting, fluid flows and adhesion. Further, the reversible adsorption of biomolecules on surfaces is of special interest.

Following the presented coating strategy, PNIPAM was grafted from a PMSSQ macroCTA yielding a PMSSQ-PNIPAM hybrid polymer. By simple spin-coating or dip-coating procedures a PNIPAM modified surface could be obtained in one step. To check the temperature-responsive behavior of the surfaces, capillary rise experiments with water of different temperatures have been carried out. The coated glass tubes were placed over a water surface just touching it. The meniscus height was measured as an indication of the surface hydrophobicity. Below LCST ($T = 15$ °C) PNIPAM exhibits a hydrophilic behavior, indicated by a high meniscus, when measured above LCST ($T = 40$ °C) PNIPAM turns to a hydrophobic behavior, resulting in a drop of meniscus height in the capillary.

For detailed information see publication 5 (Chapter 4.5).

3.3.2 Semi-Conductive Coatings

As already explained in detail in chapter 1.1.3 the common difference between functional surface coatings and semi-conductive films is the fact that semi-conductive films need certain functionality throughout the whole deposited film.

As PMSSQ-based hybrid polymers are directly cross-linked after application, a randomly cross-linked coating should be obtained. The whole deposited film consists mainly of the organic polymer which is pervaded with the inorganic cross-linker. Usually 10 - 20 wt% inorganic part is sufficient for cross-linking of the whole film, this amount should not disturb the pathway of charge carriers and their mobility.

In optoelectronic applications, PMSSQ hybrid polymers are the ideal candidates for the interfacial design between the inorganic electrodes and the organic semiconductors. Interfacial engineering of electrical devices between the anode surface and the overlying organic layer is an important method for tuning electronic properties. In particular, the need for precise control of the electrode/organic semiconductor interface is apparent in the area of polymer light-emitting diodes (PLED). The typical chemical approach is to deposit an

intermediate layer of an organic semiconductor as a hole-injection layer (HIL) or hole-transport layer (HTL), which features a HOMO level between that of the ITO work function and the desired organic emitting layer. Besides the electronic properties of an effective HIL, there are further important requirements on a high-quality thin film: minimum number of defects, such as aggregates or pinholes, good adhesion of the organic layer on top of the hydrophilic oxide anode to prevent physical delamination or decohesion, and a smooth amorphous film-forming morphology to achieve an effective planarization of the ITO surface. Furthermore, for an efficient use of HILs in multilayer PLEDs, the material needs to possess very good solvent resistance in order to facilitate a multilayer processing.

In the presented approach, the mechanical properties were addressed by the PMSSQ part, whereas for electronic properties we grafted *N,N*-di-4-methylphenylamino styrene (TPA), which is known as a monomer yielding hole-conductive polymers.

The obtained hole injection material (HIM) features a HOMO level of -5.6 eV and a hole mobility of $1 \cdot 10^{-6} \text{ cm}^2/\text{Vs}$. PMSSQ-PTPA is an ideal coating material, achieving an effective planarization of the ITO substrate (see figure 3.8). By spin-coating and annealing of the HIM, surface roughness was decreased from 2.33 nm to 0.357 nm (image RMS $1 \times 1 \mu\text{m}^2$). High stability, adhesion and surface functionalization was preserved even after solvent treatment, thus the described HIL fabrication strategy is capable for a further spin-on multilayer device fabrication.

Further details concerning semi-conductive coatings can be found in publication 6 (chapter 4.6).

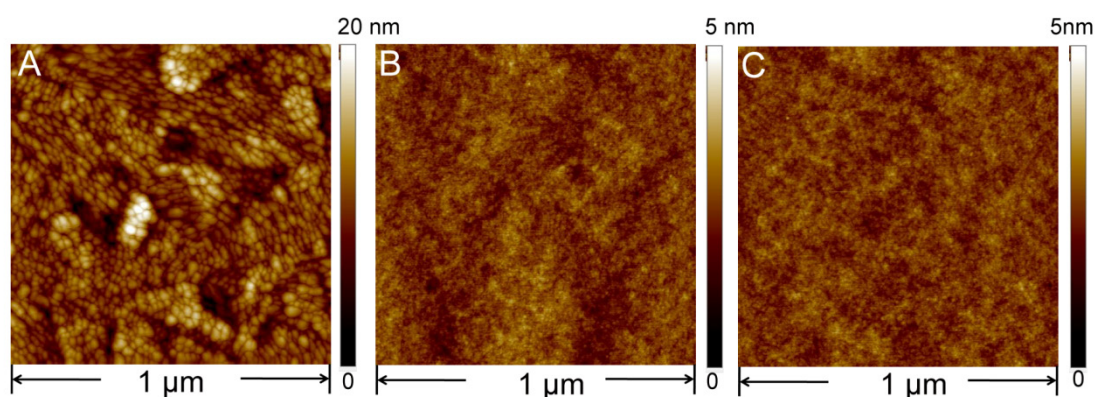


Figure 3.8. Left image: AFM topography of bare ITO (RMS roughness 2.33 nm), middle image: AFM topography of PMSSQ-PTPA coated ITO (RMS roughness 0.36 nm), right image: PMSSQ-PTPA coated ITO after 1 h toluene treatment (RMS roughness 0.31 nm).

3.4 Reactive Coating Materials

The most challenging task in coating design is the formulation of reactive coatings. Reactive sites have to be included into the coating without decomposition during film formation or curing. As cross-linking of PMSSQ based coating materials is induced by thermal curing, a thermo-labile group could not be integrated. Further requirements were quantitative and fast conversion of the reactive site and polymerizability under controlled radical polymerization conditions.

As monomers we choose, pentafluorophenyl (meth)acrylate (FP(M)A), pentafluorophenyl vinylbenzoate (FPVB) and propargylvinylbenzoate (PVB). All four monomers could successfully be grafted from a PMSSQ macro CTA using the RAFT technique. Poly(FP(M)A) is known to react fast and quantitative with primary aliphatic amines to amides; additionally poly(FPVB) also reacts with primary aromatic amines to amides, whereas poly(PVD) undergoes copper-catalyzed 1,3-dipolar cycloaddition with azides to the corresponding triazole (Huisgen reaction). The reactive sites of the obtained hybrid polymers showed no decomposition during the usual annealing time.

3.4.1 Surface-Analogous Reaction

Figure 3.9 shows the surface-analogous conversion of a reactive surface coating, here as example the conversion of a poly(methylsilsesquioxane)-poly(pentafluorophenylacrylate) (PMSSQ-PFPA) coating. The coated substrate is dipped into a solution of an amine which should be attached to the surface (depending on the nature of the reactive coating the solution may also contain an azide and the corresponding copper catalyst for cycloaddition). The conversion could be monitored using either FTIR spectroscopy or XPS. Both methods indicated a complete conversion in the top range of the coating. Using piperazidyl functionalized NDB (pip NBD), the conversion of the whole film could be monitored using UV/Vis spectroscopy. In conversion experiments of reactive coatings of different thicknesses with pipNBD, we found a linear behavior between film thickness and the resulting absorption up to a film thickness of 670 nm. This indicated that the entire reactive film was converted by the amine. For films thicker than 670 nm, the adsorption did not increase linearly anymore, even for conversion times longer than one day. A similar conversion experiment with amino-functionalized perylene showed complete conversion up to a film thickness of 400 nm. This indicates that different molecules diffuse with different rates into the reactive coating.[‡]

The surface reactions had no influence on the surface-roughness of the coating. The image RMS value (image size $1 \times 1 \mu\text{m}^2$) after conversion with $\text{H}_2\text{N-PEG}$ was 0.479 nm. Also the stability of the coatings was not affected by the surface-analogous reactions. ISO cross-cut test results remained 0 after conversion, indicating a complete adhesion onto any tested substrate. The adsorption process of $\text{H}_2\text{N-PEG}$ onto the thin reactive coating could be monitored using surface plasmon resonance (SPR). PMSSQ-PFPA coated gold-covered glass slides (spin coated from 0.04 wt% solution, equivalent to 3.8 nm film thickness, fitted by Winspall) were allowed to

[‡] Amino-functionalized perylene was synthesized as explained briefly in: Kaiser, H.; Lindner, J.; Langhals, H. *Chem. Ber.* **1991**, *124*, 529-535

react in situ with a solution of 0.1 mg/ml H₂N-PEG in water. A thickness increase of 0.9 nm was calculated for the binding of amino-PEG onto the reactive coating. The surface-analogous reaction using other water-soluble amines could also be detected by SPR.

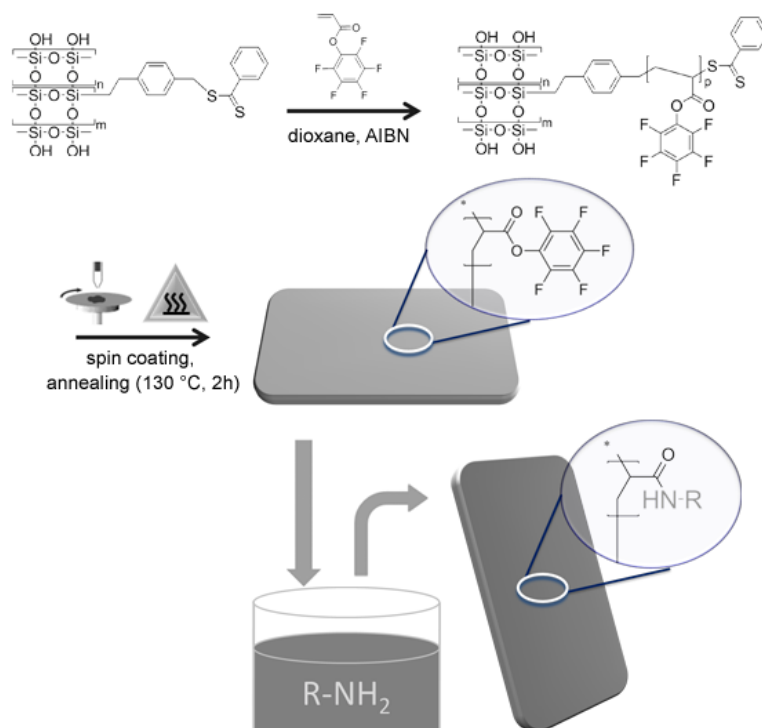


Figure 3.9. To build up the PFPA hybrid polymer, pentafluorophenyl acrylate was polymerized under RAFT conditions, using AIBN as initiator and PMSSQ-mCTA as chain transfer agent. Afterwards the PMSSQ-PFPA hybrid polymer is spin coated onto the substrate and annealed at 130°C for 2h, yielding the desired reactive surface. By surface analogues reaction the reactive coating can be converted with various amines in a wet chemical process.

For further details concerning the conversion of reactive coatings by surface-analogous reactions see publications 7, 8 and 10 (chapter 4).

3.4.2 Modification on the Surface

Reactive surface coatings are an ideal platform to create surface coatings with defined chemical structures. Publication 8 (chapter 4.8) gives several examples for tuning the surface wettability between hydrophilic and hydrophobic behavior (see figure 3.10). Not only by conversion with different amines (e.g. glutamic acid for hydrophilic surfaces and perfluorinated amines for hydrophobic amines), but also by controlled assembly of amino-functionalized nanoparticles on the surface and further activation in a layer-by-layer like process, defined wetting could be tuned. By conversion with isopropylamine, a PNIPAM coating is formed insitu (compare chapters 3.3.1 or 4.5). The switching of contact angle by temperature could be enhanced effectively by nanoparticle incorporation. Those reactive

coatings may find application in built-up of microfluidic devices where controlled wetting is needed on a micrometer scale.

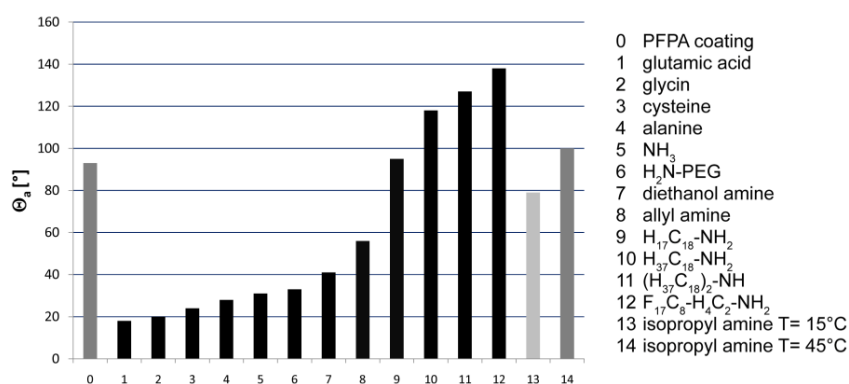


Figure 3.10. Via surface analogues reaction of the reactive coatings, the wetting behavior could be permanently altered (advancing contact angle values given for coatings on silicon, contact angles on other substrates only vary $\pm 3^\circ$). Bar 13 and 14 show the reversible switching behavior after conversion with isopropyl amine at different temperatures.

Publication 9 (chapter 4.9) gives several examples how reactive coatings could be used in biochemical analysis devices. Specific binding sites for various proteins could be attached to the surface (see figure 3.11). Afterwards the immobilization of the desired proteins could be studied using different analytical techniques.

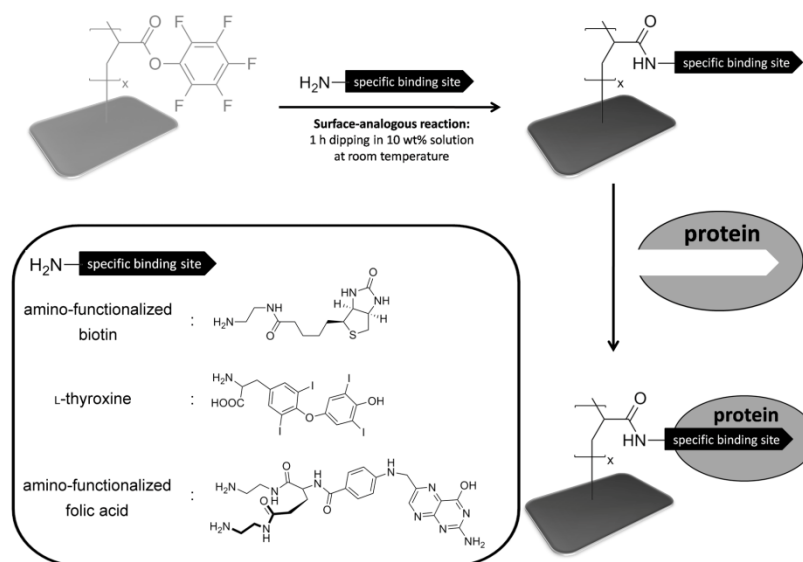


Figure 3.11. Spin coating PMSSQ-PFPA hybrid polymers onto a given substrates resulted in thin reactive surface coatings. After surface-analogous reaction with amino-functionalized specific binding sites proteins were assembled on top.

The versatile strategy allowed the attachment of various linkers, e. g. biotin, L-thyroxine and folic acid. The adsorption processes of streptavidin, pre-albumin and folate-binding protein were monitored using SPR, FTIR, fluorescence spectroscopy, and AFM. The presented protein immobilization strategy, consisting of four steps (a) spin-coating of PMSSQ-PFPA hybrid polymer from THF solution, (b) annealing at 130 °C for 2 h to induce thermal cross-linking of the PMSSQ part, (c) surface-analogues reaction with different amino-functionalized specific binding sites for proteins and (d) controlled assembly of proteins on the surface, may find various applications in future biosensor design.

Publication 10 (chapter 4.10) shows the combination of different reactive sites combined in one coating material and how they can be addressed orthogonally, as shown in figure 3.12.

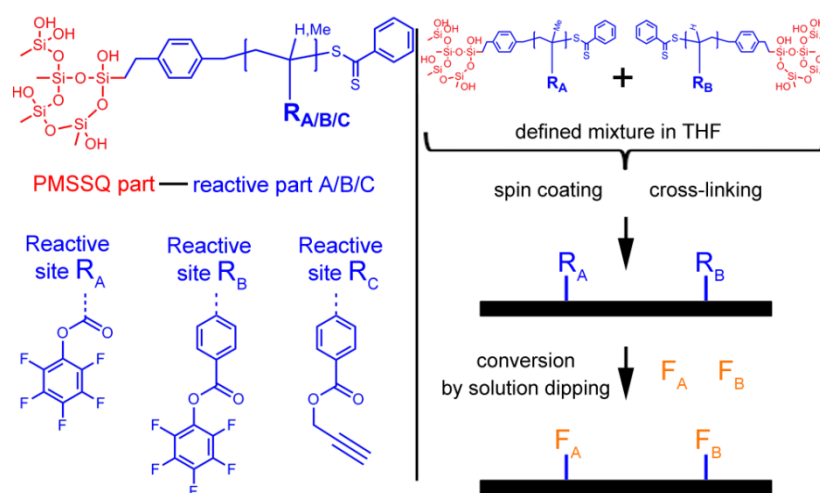


Figure 3.12. Poly(methylsilsesquioxane)-based reactive hybrid polymers containing either reactive site A, B, or C. Spin-coating defined mixtures of different polymers resulted in defined multi-reactive coatings, which could selectively be converted with different functions (F_A , F_B).

By a sequential surface-analogous reaction different functions could be immobilized in a defined ratio, resulting in dual- or triple-functionalized surfaces. For example, temperature-responsive and pH-responsive functions were immobilized in different ratios, which allowed to adjust the accessible contact angle switching range by temperature and by pH.

4 Publications

All publications contributing to this thesis are given in thematical order in the following chapters:

Synthesis of Hybrid Polymers

- 4.1 "Synthesis of Processable Inorganic-Organic Hybrid Polymers Based on Poly(silsesquioxanes): Grafting from Polymerization Using ATRP"
Kessler, D.; Teutsch, C.; Theato, P. *Macromol. Chem. Phys.* **2008**, *209(14)*, 1437-1446.
- 4.2 "Synthesis of Functional Inorganic-Organic Hybrid Polymers Based on Poly(silsesquioxanes) and Their Thin Film Properties"
Kessler, D.; Theato, P. *Macromolecules* **2008**, *41(14)*, 5237-5244.
- 4.3 "Synthesis of Defined Poly(silsesquioxane)s: Fast Polycondensation of Trialkoxysilanes in a Continuous-Flow Microreactor"
Kessler, D.; Löwe, H.; Theato, P. *Macromol. Chem. Phys.* **2009**, *210(10)*, 807-813.
- 4.4 "Surface Coatings Based on Polysilsesquioxanes: Grafting-from Approach Starting from Organic Polymers"
Kessler, D.; Theato, P. *MRS Proc.* **2009**, *1190*, accepted.

Functional Surface Coatings

- 4.5 "Temperature-Responsive Surface Coatings Based on Poly(methylsilsesquioxane)-Hybrid Polymers"
Kessler, D.; Theato, P. *Macromol. Symp.* **2007**, *249-250*, 424-430.
- 4.6 "Surface Coatings Based on Polysilsesquioxanes: Solution Processible Smooth Hole-Injection-Layers for Optoelectronic Applications"
Kessler, D.; Lechmann, M. C.; Noh, S.; Berger, R.; Lee, C.; Gutmann, J. S.; Theato, P. *Macromol. Rapid Commun.* **2009**, doi: 10.1002/marc.200900196 .

Reactive Surface Coatings

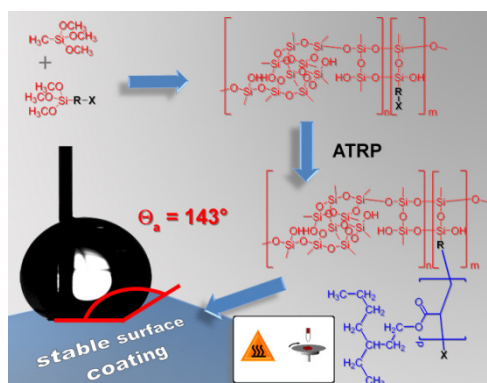
- 4.7 "Substrate-Independent Stable and Adherent Reactive Surface Coatings and Their Conversion with Amines"
Kessler, D.; Metz, N.; Theato, P. *Macromol. Symp.* **2007**, *254*, 34-41.
- 4.8 "Reactive Surface Coatings Based on Polysilsesquioxanes: Defined Adjustment of Surface Wettability"
Kessler, D.; Theato, P. *Langmuir* **2009**, doi: 10.1021/la9005949.

4.9 “Reactive Surface Coatings Based on Polysilsesquioxanes: Controlled Functionalization for Specific Protein Immobilization”

Kessler, D.; Roth, P. J.; Theato, P. *Langmuir* **2009**, doi: 10.1021/la901878h.

4.10 “Modular Approach toward Multi-Functional Surfaces with Adjustable and Dual-Responsive Wettability Using a Hybrid Polymer Toolbox”

Kessler, D.; Nilles, K.; Theato, P. *Chem. Commun.*, submitted.



Abstract

Inorganic-organic hybrid polymers have been synthesized utilizing atom transfer radical polymerization (ATRP) from a functionalized poly(methylsilsesquioxane) (PMSSQ) macro initiator. Different polymeric ATRP initiators were prepared by co-condensation of functionalized trichlorosilanes with methyltrimethoxysilane. Various vinyl monomers have been successfully grafted from these macro initiators, demonstrating a highly variable synthetic concept, which offers the chance to synthesize a wide spectrum of inorganic-organic hybrid polymers. All synthesized polymers were soluble in various organic solvents. Spin-coating these hybrid materials onto various substrates could produce stable and adherent surface coatings. Successful surface functionalization could be achieved on silicon, glass, metals or polymeric materials.

Keywords

Atom transfer radical polymerization (ATRP), coatings, graft copolymers, inorganic/organic hybrid polymers, poly(silsesquioxanes)

Introduction

Combining inorganic and organic materials on a molecular scale offers the possibility not only to combine properties of both material classes but also to obtain new materials with new properties. Materials that consist of inorganic and organic elements are termed hybrid materials and the simplest routes to prepare functional hybrid materials are based on the controlled modification of inorganic solids by various organic and organo-metallic reagents^[1]. Accordingly, the first formation of organic-inorganic compounds was accomplished by intercalation of organic molecules into inorganic solids using phyllosilicates, a clay mineral^[2]. Different mechanisms have been proposed to explain the host-guest interactions, e.g. electrical forces^[3], Van der Waals forces, hydrogen bonding^[4], ion-dipole coordination, and proton transfer. In a similar way polymers have been used successfully to modify clays^[5]. However, essentially all of these hybrid materials have been prepared primarily by functionalization of the inorganic compound by no covalent bonding.

The method of choice to obtain covalently linked inorganic-organic hybrid materials is based on the sol-gel chemistry of alkoxy silanes^[6]. In the last decades, sol-gel chemistry has found applications in many different areas. For example, polysilsesquioxanes and bridged polysilsesquioxanes^[7,8] provide a chemical basis for low dielectric constant materials^[9,10], adsorbent materials^[11], precursors for optical and electronically materials^[12,13] and materials with superior mechanical properties^[14]. ORMOCERs (organic modified ceramics) are well known sol-gel hybrid materials, already commercially available. Their properties can be adjusted with respect to the different applications^[15].

Beside these commercially available but structurally poorly defined silicon-based polymers, many approaches have been introduced to synthesize silicon-oxide or silicon-based hybrid materials, which are ordered or well defined on a nanometer scale. One approach starts from well-defined silica nanoparticles, co-hydrosilated from trichlorophenylsilane and trichloromethylsilane^[16]. Furthermore, well-defined inorganic/organic hybrid materials with pH-induced reversible complexation of weak electrolytes, could be obtained by the sol-gel method^[17,18]. Synthesizing defined architectures of silica can also be realized by using inorganic/organic hybrid polymers. For example, by addition of different additives to a bio-inspired silification process defined silica structures can be obtained^[19,20].

Atom transfer radical polymerization (ATRP) has recently received dramatic attention as a versatile polymerization technique in terms of control over molecular weights, molecular weight distributions and molecular structures^[21]. ATRP offers not only the advantage to be applicable to a broad range of monomers but also the use of well-defined initiating sites, i.e. chemically defining the site of polymer chain growth. Therefore, ATRP has evolved into a method of choice for perfect grafting-from polymerizations, not only from soluble macro initiators^[22] but also from silicon surfaces^[23].

Polyhedral oligomeric silsesquioxanes (POSS; $\text{Si}_8\text{O}_{12}\text{R}_8$)^[24,25,26] can be thought of as the smallest particles of silica possible. POSS functionalized with ATRP initiators can be used to oligomers and polymers graft onto the inorganic POSS core^[27,28,29]. Polysilsesquioxanes, in contrast to POSS, possess free silanol groups (Si-OH), which offer the intrinsic possibility to

undergo a secondary condensation, induced either thermally or catalytically. Thus, polysilsesquioxanes containing free Si-OH groups are expected to find application as suitable materials for stable functional coatings as they exhibit strong adhesion to different substrates by condensing with silanol groups of surfaces.

Herein, we present a synthetic concept that introduces a flexible and versatile strategy to prepare graft copolymers consisting of an inorganic poly(methylsilsesquioxane) block and a block of a broad range of organic polymers. These inorganic-organic hybrid polymers have the potential to be used as convenient surface coatings.

Experimental Part

Materials. All chemicals and solvents were commercially available and used as received unless otherwise stated. All monomers were purified by distillation under reduced pressure prior the polymerization. THF was freshly distilled from sodium/benzophenone under nitrogen. CuBr and CuCl were purified by stirring for 24 h with acetic acid, filtered off, washed with methanol and dried in vacuum, respectively. *p*-Chlormethylphenyl trichlorosilane was purchased from Gelest ABCR. All reactions were performed in Argon atmosphere.

Instrumentation. All ^1H and ^{13}C NMR spectra were recorded on a Bruker 300 MHz FT-NMR spectrometer. ^{29}Si CPMAS NMR spectra were measured on a Bruker DSX 400 MHz FT-NMR spectrometer (Rotation: 5000 Hz, T = RT, 4 mm rotor). Chemical shifts (δ) were given in ppm relative to TMS. Gel permeation chromatography (GPC) was used to determine molecular weights and molecular weight distributions, M_w/M_n , of polymer samples with respect to polystyrene standards (PSS). (THF used as solvent, polymer concentration: 2 mg/mL, column setup: MZ-Gel-SDplus 10^2 \AA^2 , 10^4 \AA^2 and 10^6 \AA^2 , used detectors: refractive index, UV and light scattering). Thermo gravimetric analysis was performed using a Perkin Elmer Pyris 6 TGA in nitrogen (10 mg pure polymer in aluminum fan). FD mass spectra were measured using a Finnigan MAT 95 mass spectrometer. Elemental analyses were done with an Elementar Vario Micro Cube (detecting C, H, N, S).

Film stability and adhesion on substrates was tested using ISO 2409:1992(E) – Cross-cut test as explained therein.

Synthesis of 2-bromoisobutyroic acid pent-4-enylate (1). 160 mmol (13.9 g) penten-4-ol and 50 mL chloroform were placed in a 100 mL two-necked flask equipped with stirring rod and cooled to 0 °C. Slowly 160 mmol (36.8 g) 2-bromoisobutyroic acid bromide in 20 mL chloroform were added under cooling and the resulting solution was stirred magnetically for 4 h at room temperature. The reaction solution was then washed three times with water, dried over MgSO_4 and the solvent was evaporated. The crude product was distilled in high vacuum. Bp. 50 °C at $3.3 \cdot 10^{-2}$ mbar. Yield: 34,79 g (148 mmol, 92.5%)

$^1\text{H-NMR}$ (CDCl_3): δ (ppm) = 5.74 (m, 1H), 4.96 (m, 2H), 4.12 (t, $^3J = 6.6$ Hz, 2H), 2.10 (m, 2H), 1.87 (s, 6H), 1.72 (quin., $3J = 6.3$ Hz, 2H)

$^{13}\text{C-NMR}$ (CDCl_3): δ (ppm) = 171.34, 137.05, 115.35, 65.05, 55.66, 30.58, 29.73, 27.37

FD mass spectra: 234.0 (27.8%); 235.0 (100%)

EA (%): calculated: C = 45.98; H = 6.43; measured: C = 45.87; H = 6.43

Synthesis of 2-bromoisobutyroic acid 5-(trichlorosilanyl)-pentyl ester (2). 50 mg platinum on charcoal and 100 mL toluene were placed in a 200 mL flask equipped with a stirring rod, 75 mmol (10.8 g) trichlorosilane and 50 mmol (11.75 g) 2-bromoisobutyroic acid pent-4-enylat were added. The solution was stirred magnetically at 80 °C for 24 h. After filtration and evaporation of the solvent the crude product was distilled in high vacuum. Bp. 104 °C at $7 \cdot 10^{-3}$ mbar. Yield: 16.12 g (44 mmol, 88.0%)

$^1\text{H-NMR}$ (CDCl_3): $\delta(\text{ppm}) = 4.11$ (t, $^3J = 6.6$ Hz, 2H), 1.86 (s, 6H), 1.66 (m, 2H), 1.57 (d, $^3J = 6.9$ Hz, 2H), 1.47 (d, $^3J = 6.6$ Hz, 2H), 1.38 (m, 2H)

$^{13}\text{C-NMR}$ (CDCl_3): $\delta(\text{ppm}) = 171.35, 65.41, 55.67, 30.60, 27.97, 27.67, 24.20, 21.86$

FD mass spectra: 369.9 (15.6%); 370.8 (17.38%); 121,0 (100%)

EA (%): calculated: C = 29.17; H = 4.35; measured: C = 30.39; H = 4.45

Synthesis of *p*-(chloromethyl)-phenylethyltrichlorosilane (3). *p*-(chloromethyl)-phenylethyltrichlorosilane was prepared via a hydrosilylation reaction of *p*-chloromethylstyrene with trichloromethylsilane. 100 mg platinum on charcoal and 100 mL toluene were placed in a 250 mL flask equipped with stirring rod, 75 mmol trichloromethylsilane and 50 mmol *p*-chloromethylstyrene were added. The reaction mixture was stirred magnetically for 48 h at 110 °C. After filtering over celite the solvent was removed and the crude product was distilled at $2.5 \cdot 10^{-3}$ mbar. Yield: 11.07 g (39 mmol, 77.1 %)

$^1\text{H-NMR}$ (CDCl_3): $\delta(\text{ppm}) = 7.34$ (d, $^3J = 8.1$ Hz, 2H); 7.22 (d, $^3J = 7.8$ Hz, 2H); 4.58 (s, 2H); 2.90 (m, 2H); 1.74 (m, 2H)

$^{13}\text{C-NMR}$ (CDCl_3): $\delta(\text{ppm}) = 141.61; 135.71; 128.91; 128.24; 45.94; 27.91; 25.90$

EA (%): calculated: C = 37.52; H = 3.50; measured: C = 38.70; H = 3.73

General synthesis of PMSSQ macro initiators. Methyltrimethoxysilane (MTMS) and the respective functionalized ATRP initiator were added in different ratios in a 500 mL flask. Then 20 mL THF, 1000 mol% water and 3 mol% HCl were injected. The solution was stirred magnetically at 0 °C or room temperature for 3 h, dissolved in diethyl ether, washed with water and dried over MgSO_4 . The solvent was evaporated and the product was dried at high vacuum ($1 \cdot 10^{-3}$ mbar).

Synthesis of PMSSQ macro initiator 1 (PMSSQ-MI-1). According to the above procedure MTMS and 2-bromoisobutyroic acid 5-(trichlorosilanyl)pentyl ester (2) were co-condensed in the molecular ratios 20:1, 40:1 and 80:1.

$^1\text{H-NMR}$ (CDCl_3): $\delta(\text{ppm}) = 5.55$ (br); 4.14 (br, 2H); 3.44 (s); 1.91 (br, 6H); 1.77 (br, 2H); 1.60 (br, 2H); 1.42 (br, 2H); 0.63 (br, 2H); 0.13 (br)

^{29}Si CPMAS NMR: $\delta(\text{ppm}) = -48.26$ (T1); -57.23 (T2); -65.87 (T3)

Synthesis of PMSSQ macro initiator 2 (PMSSQ-MI-2). According to the above procedure MTMS and *p*-chloromethylphenyl trichlorosilane were co-condensed in the molecular ratios 20:1, 40:1 and 80:1.

$^1\text{H-NMR}$ (CDCl_3): $\delta(\text{ppm}) = 7.73$ (br, 2H); 7.40 (br, 2H); 5.72 (br); 4.64 (br, 2H); 3.45 (br); 0.11 (br)

^{29}Si CPMAS NMR: $\delta(\text{ppm}) = -47.00$ (T1); -59.39 (T2); -67.88 (T3)

Synthesis of PMSSQ macro initiator 3 (PMSSQ-MI-3). According to the above procedure MTMS and *p*-(chloromethyl)-phenylethyltrichlorosilane (3) were co-condensed in the molecular ratios 20:1, 40:1 and 80:1.

$^1\text{H-NMR}$ (CDCl_3): $\delta(\text{ppm}) = 7.28$ (br, 2H); 7.22 (br, 2H); 5.74 (br); 4.61 (br, 2H); 3.47 (br); 2.70 (br, 2H); 0.93 (br, 2H); 0.10 (br)

$^{29}\text{Si CPMAS NMR}$: $\delta(\text{ppm}) = -48.57$ (T1); -58.10 (T2); -66.21 (T3)

Atom transfer radical polymerization. In a 20 mL Schlenk-flask the macro initiator (0.5 g), CuBr or CuCl, 2,2'-bipyridine, monomer (2 g) and 4 mL dioxane were placed and degassed for three times. The solution was then stirred in Ar atmosphere at 55 °C for 8 h and precipitated in heptane. The polymer was re-precipitated twice from THF into heptane and dried in high vacuum ($1 \cdot 10^{-3}$ mbar).

PMSSQ-PMA. $^1\text{H-NMR}$ (CDCl_3): $\delta(\text{ppm}) = 5.02$ (br); 3.64 (br); 2.32 (br); 1.73 (br); 0.16 (br)

PMSSQ-PEHA. $^1\text{H-NMR}$ (CDCl_3): $\delta(\text{ppm}) = 4.98$ (br); 3.94 (br); 2.33 (br); 1.89 (br); 1.57 (br); 1.27 (br); 0.91 (br); 0.14 (br)

PMSSQ-PMMA. $^1\text{H-NMR}$ (CDCl_3): $\delta(\text{ppm}) = 4.92$ (br); 3.57 (br); 1.72 (br); 1.03 (br); 0.15 (br)

PMSSQ-PDMA. $^1\text{H-NMR}$ (CDCl_3): $\delta(\text{ppm}) = 5.00$ (br); 3.91 (br); 1.92 (br); 1.58 (br); 1.25 (br); 0.89 (br); 0.15 (br)

PMSSQ-PS. $^1\text{H-NMR}$ (CDCl_3): $\delta(\text{ppm}) = 6.98$ (br); 5.00 (br); 2.35 (br); 1.44 (br); 0.15 (br)

(Signals originating from the ATRP initiating units in the macro initiator and integrations are not considered here, because of the variation due to the used macro initiator)

Results and discussion

Atom transfer radical polymerization (ATRP) is a versatile method of preparing defined polymers as it not only allows control of molecular weights and polydispersities but also offers the possibility to initiate the polymerization from defined species^[30,31]. Therefore, synthetic pathways towards inorganic-organic hybrid polymers based on PMSSQ can be divided into two steps. The first step is the synthesis of functionalized PMSSQs^[32,33] capable of initiating ATRP of different vinyl monomers under controlled conditions as presented in scheme 1.

Co-condensation. Three different functionalized ATRP initiators (2-bromoisobutyroic acid 5-(trichlorosilanyl)pentyl ester (2), *p*-chloromethylphenyl trichlorosilane, *p*-(chloromethyl)-phenylethyltrichlorosilane) (3) were co-condensed with methyltrimethoxysilane (MTMS) to yield a series macro initiators PMSSQ-MI-1, PMSSQ-MI-2, and PMSSQ-MI-3, respectively (see scheme 1 and table 1), which provide a high functionality of unreacted silanol groups and initiating groups for the atom transfer radical polymerization. The synthesis of different macro initiators allows us to investigate differences between three PMSSQ matrices as well as differences during ATRP polymerization.

The successful incorporation of the initiating moiety into the PMSSQ polymer was determined by $^1\text{H NMR}$ spectroscopy and compared with the initial molecular ratios (see table 1). No significant differences between the three classes of initiators could be found. The initiator ratio after co-condensation varies slightly from the initial molecular ratio, but none of the initiating groups is preferentially incorporated into the network. It seems that the linking

Table 1. Properties of the different initiators prepared by co-condensation at 0 °C and at 25 °C.

macro initiator	reaction temperature	initial molecular ratio	M _n [g/mol]	PDI	initiator ratio after co-condensation	m/n ¹	IPM ²
PMSSQ-MI-1a	0°C	20 : 1	3600	1.71	19 : 1	9	3.9
PMSSQ-MI-1b	0°C	40 : 1	4150	1.62	47 : 1	23	2.0
PMSSQ-MI-1c	0°C	80 : 1	3870	1.81	61 : 1	30	3.4
PMSSQ-MI-2a	0°C	20 : 1	4860	1.59	17 : 1	8	5.9
PMSSQ-MI-2b	0°C	40 : 1	3830	1.77	44 : 1	22	2.2
PMSSQ-MI-2c	0°C	80 : 1	4200	1.98	57 : 1	28	2.1
PMSSQ-MI-3a	0°C	20 : 1	3090	1.44	18 : 1	8	3.2
PMSSQ-MI-3b	0°C	40 : 1	5500	1.50	48 : 1	24	2.4
PMSSQ-MI-3c	0°C	80 : 1	5030	1.62	57 : 1	28	1.9
PMSSQ-MI-1d	25°C	20 : 1	4300	1.92	20 : 1	9	5.1
PMSSQ-MI-1e	25°C	40 : 1	9510	1.88	45 : 1	22	5.4
PMSSQ-MI-1f	25°C	80 : 1	7890	2.01	66 : 1	33	3.4
PMSSQ-MI-2d	25°C	20 : 1	11550	2.12	18 : 1	9	17.7
PMSSQ-MI-2e	25°C	40 : 1	13200	1.65	51 : 1	25	6.1
PMSSQ-MI-2f	25°C	80 : 1	15900	1.93	57 : 1	28	2.1
PMSSQ-MI-3d	25°C	20 : 1	12450	1.54	24 : 1	11	10.7
PMSSQ-MI-3e	25°C	40 : 1	10020	1.78	50 : 1	25	5.0
PMSSQ-MI-3f	25°C	80 : 1	14900	1.62	70 : 1	35	4.9

¹ ratio between pure PMSSQ rungs and initiator rungs in an assumed ladder like structure of the macro initiator, ² IPM (initiating groups per molecule): calculated average number of initiating groups per PMSSQ macro initiator derived from integral ratio of ¹H NMR spectra.

Polymerization. Using common ATRP conditions ^[34,35], each PMSSQ based macro initiator was used to initiate the polymerization of methyl acrylate (MA), ethyl hexyl acrylate (EHA), methyl methacrylate (MMA), decyl methacrylate (DMA) and styrene (S). PMSSQ-MI-1 was activated using CuBr where as PMSSQ-MI-2 and PMSSQ-MI-3 were activated using CuCl, all other reaction conditions were kept identical for all polymerizations. The estimated weight ratio for all hybrid polymers was 80 : 20 (org.:inorg.) as summarized in Table 2 and 3.

Each macro initiator was able to initiate polymerization of acrylates, methacrylates and styrene. For PMSSQ-MI-1, the molecular weights of the obtained hybrid polymers were slightly lower than those of the hybrid polymers obtained from PMSSQ-MI-2 or PMSSQ-MI-3. The weight ratios between organic and inorganic block matched very well the estimated ratios of 80 : 20.

Table 2. Results of ATRP of various monomers initiated by the three different macro initiators PMSSQ-MI-1, PMSSQ-MI-2 and PMSSQ-MI-3, which were previously co-condensated at 0 °C.

Hybrid polymer	Initial ratio of initiator species	macro initiator	M _n [g/mol]	PDI	org. : inorg. molecular ratio ¹	org. : inorg. weight ratio ²
PMSSQ-PMA_MI-1a	20:1	PMSSQ-MI-1a	16900	2.2	87 : 13	81 : 19
PMSSQ-PMA_MI-2a	20:1	PMSSQ-MI-2a	19900	2.0	88 : 12	82 : 18
PMSSQ-PMA_MI-3a	20:1	PMSSQ-MI-3a	18300	1.9	90 : 10	85 : 15
PMSSQ-PEHA_MI-1a	20:1	PMSSQ-MI-1a	20300	1.9	75 : 25	80 : 20
PMSSQ-PEHA_MI-2a	20:1	PMSSQ-MI-2a	22900	2.1	77 : 23	82 : 18
PMSSQ-PEHA_MI-3a	20:1	PMSSQ-MI-3a	25000	2.4	75 : 25	80 : 20
PMSSQ-PMMA_MI-1a	20:1	PMSSQ-MI-1a	19990	2.0	83 : 17	78 : 22
PMSSQ-PMMA_MI-2a	20:1	PMSSQ-MI-2a	22920	2.1	86 : 14	82 : 18
PMSSQ-PMMA_MI-3a	20:1	PMSSQ-MI-3a	20560	1.8	84 : 16	79 : 21
PMSSQ-PDMA_MI-1a	20:1	PMSSQ-MI-1a	18200	1.8	75 : 25	83 : 17
PMSSQ-PDMA_MI-2a	20:1	PMSSQ-MI-2a	24300	2.6	71 : 29	80 : 20
PMSSQ-PDMA_MI-3a	20:1	PMSSQ-MI-3a	27300	2.2	69 : 31	78 : 22
PMSSQ-PMA_MI-1b	40:1	PMSSQ-MI-1b	19340	2.0	85 : 15	78 : 22
PMSSQ-PMA_MI-2b	40:1	PMSSQ-MI-2b	25830	1.9	89 : 11	84 : 16
PMSSQ-PMA_MI-3b	40:1	PMSSQ-MI-3b	26700	2.2	85 : 15	78 : 22
PMSSQ-PEHA_MI-1b	40:1	PMSSQ-MI-1b	22300	2.6	78 : 22	83 : 17
PMSSQ-PEHA_MI-2b	40:1	PMSSQ-MI-2b	26850	2.0	75 : 25	80 : 20
PMSSQ-PEHA_MI-3b	40:1	PMSSQ-MI-3b	25500	2.7	74 : 26	79 : 21
PMSSQ-PDMA_MI-1b	40:1	PMSSQ-MI-1b	21400	2.6	70 : 30	79 : 21
PMSSQ-PDMA_MI-2b	40:1	PMSSQ-MI-2b	25970	2.3	72 : 28	81 : 19
PMSSQ-PDMA_MI-3b	40:1	PMSSQ-MI-3b	24300	2.2	70 : 30	79 : 21
PMSSQ-PS_MI-1b	40:1	PMSSQ-MI-1b	23930	2.8	85 : 15	81 : 19
PMSSQ-PS_MI-2b	40:1	PMSSQ-MI-2b	25290	2.5	83 : 17	79 : 21
PMSSQ-PS_MI-3b	40:1	PMSSQ-MI-3b	27950	2.2	87 : 13	83 : 17
PMSSQ-PMA_MI-1c	80:1	PMSSQ-MI-1c	17900	1.8	89 : 11	83 : 17
PMSSQ-PMA_MI-2c	80:1	PMSSQ-MI-2c	19300	1.9	86 : 14	79 : 21
PMSSQ-PMA_MI-3c	80:1	PMSSQ-MI-3c	22900	2.2	86 : 14	80 : 20
PMSSQ-PMMA_MI-1c	80:1	PMSSQ-MI-1c	20030	2.0	85 : 15	80 : 20
PMSSQ-PMMA_MI-2c	80:1	PMSSQ-MI-2c	21450	2.5	81 : 19	76 : 24
PMSSQ-PMMA_MI-3c	80:1	PMSSQ-MI-3c	26390	2.7	86 : 14	81 : 19
PMSSQ-PDMA_MI-1c	80:1	PMSSQ-MI-1c	20900	2.1	72 : 28	81 : 19
PMSSQ-PDMA_MI-2c	80:1	PMSSQ-MI-2c	22400	2.3	71 : 29	80 : 20
PMSSQ-PDMA_MI-3c	80:1	PMSSQ-MI-3c	25490	2.9	72 : 28	81 : 20
PMSSQ-PS_MI-1c	80:1	PMSSQ-MI-1c	18340	1.8	82 : 18	78 : 22
PMSSQ-PS_MI-2c	80:1	PMSSQ-MI-2c	22300	2.1	84 : 16	79 : 21
PMSSQ-PS_MI-3c	80:1	PMSSQ-MI-3c	26700	2.3	84 : 16	80 : 20

¹determined by ¹H-NMR spectroscopy, ²calculated from the molecular ratio.

Table 3. Results of ATRP of various monomers initiated by the three different macro initiators PMSSQ-MI-1, PMSSQ-MI-2 and PMSSQ-MI-3, which were previously co-condensated at 25 °C.

hybrid polymer	Initial ratio of initiator species	macro initiator	M _n [g/mol]	PDI	org. : inorg. molecular ratio ¹	org. : inorg. weight ratio ²
PMSSQ-PMA_MI-1d	20:1	PMSSQ-MI-1d	32700	2.6	87 : 13	80 : 20
PMSSQ-PMA_MI-2d	20:1	PMSSQ-MI-2d	39840	2.9	84 : 16	77 : 23
PMSSQ-PMA_MI-3d	20:1	PMSSQ-MI-3d	34500	3.5	87 : 13	80 : 20
PMSSQ-PS_MI-1d	20:1	PMSSQ-MI-1d	38450	3.0	83 : 17	79 : 21
PMSSQ-PS_MI-2d	20:1	PMSSQ-MI-2d	31850	2.9	78 : 22	73 : 27
PMSSQ-PS_MI-3d	20:1	PMSSQ-MI-3d	35450	2.8	85 : 15	81 : 19
PMSSQ-PMA_MI-1e	40:1	PMSSQ-MI-1e	31780	2.7	85 : 15	78 : 22
PMSSQ-PMA_MI-2e	40:1	PMSSQ-MI-2e	39010	3.1	86 : 14	79 : 21
PMSSQ-PMA_MI-3e	40:1	PMSSQ-MI-3e	33045	3.2	87 : 13	80 : 20
PMSSQ-PS_MI-1e	40:1	PMSSQ-MI-1e	22450	2.7	80 : 20	76 : 24
PMSSQ-PS_MI-2e	40:1	PMSSQ-MI-2e	30280	3.0	86 : 14	83 : 17
PMSSQ-PS_MI-3e	40:1	PMSSQ-MI-3e	32200	3.0	86 : 14	82 : 18
PMSSQ-PMA_MI-1f	80:1	PMSSQ-MI-1f	29200	2.8	87 : 13	81 : 19
PMSSQ-PMA_MI-2f	80:1	PMSSQ-MI-2f	31220	2.9	86 : 14	81 : 19
PMSSQ-PMA_MI-3f	80:1	PMSSQ-MI-3f	30780	2.6	88 : 12	82 : 18
PMSSQ-PS_MI-1f	80:1	PMSSQ-MI-1f	34500	3.0	85 : 15	80 : 20
PMSSQ-PS_MI-2f	80:1	PMSSQ-MI-2f	37000	3.1	84 : 16	80 : 20
PMSSQ-PS_MI-3f	80:1	PMSSQ-MI-3f	38940	2.9	85 : 15	81 : 19

¹ determined by ¹H-NMR spectroscopy, ² calculated from the molecular ratio.

Composition analysis. The similar polymers obtained by different macro initiators were compared by ¹H NMR analysis. Figure 1 shows the representative NMR spectra of PMSSQ-PMA prepared by the three different initiators PMSSQ-MI-1a, PMSSQ-MI-2a and PMSSQ-MI-3a. All three spectra show the CH₃ signal of the inorganic block at $\delta = 0.15$ ppm as well as the signals from the organic polymer backbone ($\delta = 1.0 - 2.2$ ppm) and the methyl ester ($\delta = 3.55$ ppm). Differences due to the different initiating groups are very small but detectable, e.g. hybrid polymers produced via grafting from PMSSQ-MI-2 or PMSSQ-MI-3 show small signals between 6.5 and 7 ppm due to the aromatic initiating species. Hybrid polymers descending from PMSSQ-MI-1 show a signal at 4.1 ppm arising from the methylene group in α -position to the ester group. Hybrid copolymers consisting of PEHA, PMMA, PDMA or PS initiated by different macro initiators also showed no differences in the signals assigned to the organic or inorganic block. As expected hybrid polymers obtained from a low molecular weight PMSSQ macro initiator gave lower molecular weights compared with hybrid polymers obtained by initiation from a PMSSQ co-condensed at room temperature. Table 2 lists the hybrid polymers initiated from a low molecular weight PMSSQ, condensed at 0°C, while table 3 lists the hybrid polymers initiated by different PMSSQ-MI-1, PMSSQ-MI-2, and PMSSQ-MI-3, condensed at room

temperature. The block ratios were not affected by the molecular weights of the initiating species. Block ratios were determined by NMR and not by GPC because a slight condensation of the inorganic blocks during polymerization cannot fully be excluded.

However, after decomposition of the inorganic block using hydrofluoro acid, organic homopolymers with narrow molecular weight distributions were obtained, e.g. PMSSQ-PS_MI-3f (initiator ratio 80:1, $M_n = 38940$ g/mol) showed after decomposition of the inorganic block a M_n of 21500 g/mol and a M_w/M_n of 1.29.

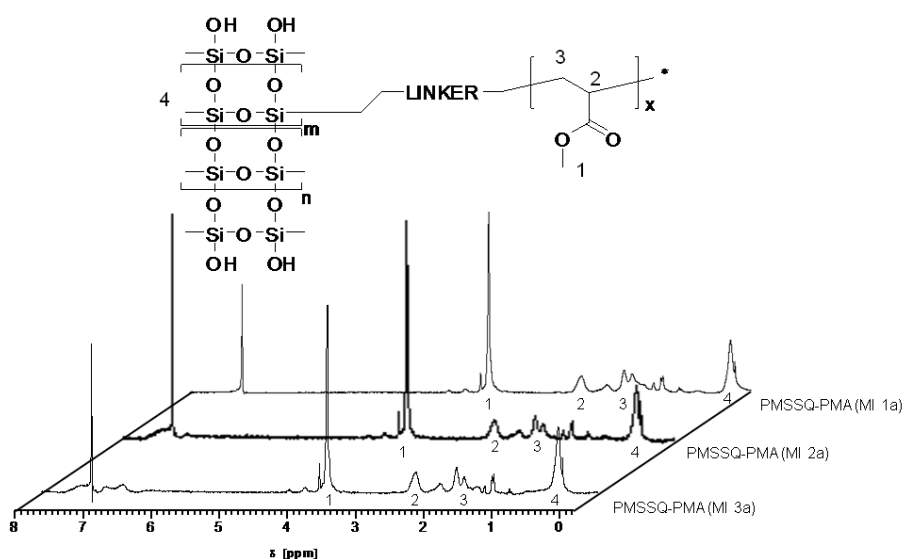


Figure 1. ^1H NMR spectra of PMSSQ-PMA, synthesized using different macro initiators. (peak at 7.24 ppm due to residual CHCl_3 in CDCl_3)

Thermal behavior. The thermal behavior of the hybrid polymers was analyzed using TGA. As expected the inorganic block showed a mass loss (< 8%) due to a secondary condensation processes between residual Si-OH and Si-OCH₃ groups within a temperature range of 110 °C to 200 °C.

This thermally induced condensation offers the chance to cross-link the polymers using an external thermal trigger and thereby leading to the production of insoluble surface coatings or thin films. At higher temperatures ($T > 300$ °C), the decomposition of the organic block could be detected. As an example, the thermal behavior of the PMSSQ-PMMA hybrid polymers, initiated from the different PMSSQ macro initiators PMSSQ-MI-1a, PMSSQ-MI-2a and PMSSQ-MI-3a, is shown in figure S1 (Supplementary information). Clearly, the temperature window for condensation (115 °C < T < 200 °C) and decomposition (300 < T < 400 °C) were separated. The thermal behavior didn't show any difference with respect to the three different hybrid copolymers, indicating that the hybrid polymer synthesis does not depend on the macro initiator used. All hybrid polymers showed a clear secondary condensation and a separated

thermal decomposition of its organic block. Table 4 summarizes the respective condensation and decomposition temperatures of all synthesized polymers.

Table 4. Condensation and decomposition temperatures of hybrid polymers.

polymer	condensation	decomposition
	temperature*	temperature*
	[°C]	[°C]
PMSSQ-PMA_MI-1a	187	412
PMSSQ-PMA_MI-2a	190	403
PMSSQ-PMA_MI-3a	168	428
PMSSQ-PEHA_MI-1a	220	419
PMSSQ-PEHA_MI-2a	216	431
PMSSQ-PEHA_MI-3a	233	420
PMSSQ-PMMA_MI-1a	161	365
PMSSQ-PMMA_MI-2a	178	354
PMSSQ-PMMA_MI-3a	175	369
PMSSQ-PDMA_MI-1a	255	408
PMSSQ-PS_MI-1a	243	431

* peak values of the first derivative, error range $\pm 5^\circ\text{C}$

The internal structure and reactivity of the inorganic block can be followed by ^{29}Si CPMAS NMR spectroscopy. Due to the degree of condensation, three different signals can be observed for a silicon atom, marked as T1-, T2 or T3-peak, respectively. T1 indicates only one oxygen bridge to another silicon, T2-branches are connected to two other silicons, T3 indicates a fully cross-linked silyl group. The structural alteration of the inorganic block during the polymerization and condensation was monitored for the hybrid polymer PMSSQ-PMMA. As example the spectra of PMSSQ-PMMA prepared from macro initiator PMSSQ-MI-1a is given in figure 2 and the integration ratios are summarized in table 5.

Before polymerization the pure macro initiator showed a high reactivity, meaning that a T1 peak and a T2 peak could be observed in the ^{29}Si CPMAS NMR. After polymerization the hybrid polymer showed a small sign of condensation but the T1- and T2-branches still dominate. After a complete secondary condensation, induced by thermal annealing of the polymer, all T1- and the majority of T2-branches were condensed to T3-branches. The residual T2 peak is due to the structural hindrance during condensation. Thus, a fully cross-linked material could be obtained.

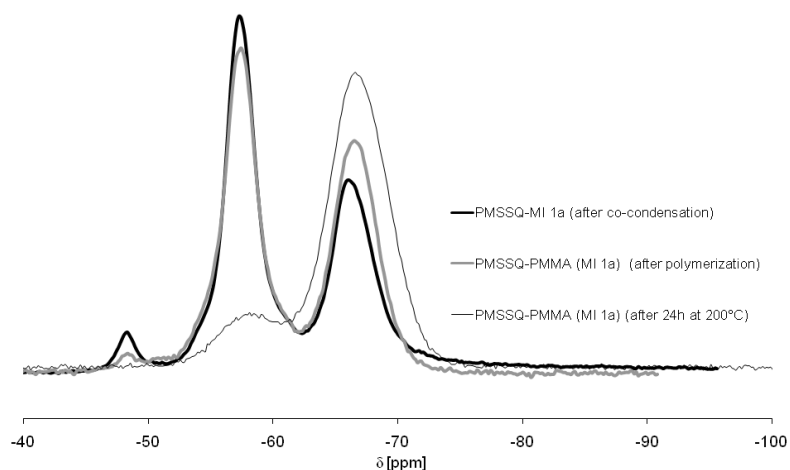


Figure 2. ^{29}Si CPMAS NMR spectra of PMSSQ-MI-1a before polymerization (thick black line), PMSSQ-PMMA_MI-1a after polymerization (thick grey line) and after curing for 24 h at 200 °C (thin black line).

All analyzed macro initiators and the corresponding hybrid polymers showed similar thermal behaviors. After co-condensation, a highly reactive inorganic macro initiator is obtained. After the controlled radical polymerization under equivalent conditions, the inorganic blocks still show reactive T1 and T2 branches. As a consequence thereof, the hybrid polymers can be cross-linked by thermal annealing. After heating to 200 °C for 24 h, fully condensed materials were obtained, which were completely insoluble in *n*-hexane, chloroform, methylene chloride, THF, dioxane, acetone and ethyl acetate.

Table 5. Integration ratios of the ^{29}Si CPMAS NMR spectra for various PMSSQ-PMMA hybrid polymers.

polymer and macro initiator	macro initiator			hybrid polymer			cured polymer		
	T1	T2	T3	T1	T2	T3	T1	T2	T3
PMSSQ-PMMA_MI-1a	0,05	0,54	0,41	0,03	0,51	0,41	0,00	0,18	0,82
PMSSQ-PMMA_MI-2a	0,07	0,49	0,44	0,01	0,49	0,50	0,00	0,13	0,87
PMSSQ-PMMA_MI-3a	0,06	0,51	0,43	0,01	0,44	0,55	0,00	0,16	0,84

Surface coating. The opportunity to cross-link these hybrid polymers via a thermally induced secondary condensation of the inorganic block offers the chance to obtain highly stable surface coating materials. To check whether these materials are applicable as coatings two main properties had to be investigated: First surface functionalization, meaning a successful change in surface properties in comparison to the substrate, had to be screened on different materials. Second the film stability and adhesion on these different substrates had to be determined.

Thin films of the hybrid polymers were prepared on silicon, glass, steel, copper, polycarbonate and PMMA surfaces via spin-coating (4000 rpm, 15 s) from a solution of 10 wt%

in THF. After coating the substrates were annealed at 130 °C for 1 h. Obtained film thicknesses on silicon wafers were measured by ellipsometry. All measured film thicknesses were close to 450 nm ranging from PMSSQ-PEHA with 417 ± 5 nm to PMSSQ-PS with 472 ± 5 nm.

To check the expected change of surface properties on all substrates, the advancing contact angle of water was measured in comparison to the uncoated clean substrate. The results of the coatings obtained from PMSSQ-MI-1 are summarized in table 6, polymers obtained from PMSSQ-MI-2 or PMSSQ-MI-3 showed the same results in the range of measuring accuracy. All materials showed a successful surface functionalization, which is not influenced by the substrate. Especially PEHA and PDMA coatings exhibit a high contact angle when coated onto the surface. The reason of this behavior is not fully understood, but currently under investigation.

Table 6. Contact angle measurements of different surfaces before and after coating with different hybrid polymers.

hybrid polymer (after curing)	advancing contact angle [°]*					
	Si	glass	steel	copper	PC	PMMA
without coating	42	9	92	114	98	70
PMSSQ-PMA_MI-1a	107	102	99	97	106	103
PMSSQ-PEHA_MI-1a	143	139	131	128	129	129
PMSSQ-PMMA_MI-1a	103	104	104	95	102	104
PMSSQ-PDMA_MI-1a	141	138	131	133	128	126
PMSSQ-PS_MI-1a	101	101	98	104	101	103

* Average value of 20 individual measurements, error range $\pm 3^\circ$.

To determine the film stabilization and adhesion on these substrates the ISO 2409:1992(E) – Cross-cut test ^[36] was carried out with all surface coatings. The coating and the underlying surface of the substrate was cross-cut with a knife and covered with a tape. After taking of the tape with a defined power the attachment or detachment of the coating was determined under an optical microscope. Results were classified as stated in the standard procedure. 0 indicates a complete attachment on the surface after the test, 5 indicates a detachment of more than 50% coating material. Tape test results of the coatings are summarized in table 7, no significant differences due to the different macro initiator could be found. As expected uncured coatings are not very stable on the surface and could be detached very easy from the surface by the tape. After curing (130 °C, 1 h), the coating became very stable and adherent. No coating material on any substrate could be detached. Stable films could be prepared on silicon, glass, metals like steel or copper as well as polymeric materials like PC or PMMA, proving the potential use of the prepared hybrid polymers as coating materials.

Table 7. Tape test results of the surface coatings on different substrates, before curing (left number) and after curing (right number) with the ISO classification: 0 = very good adhesion, 5 = easy detachment).

hybrid polymer	tape test results											
	Si		glass		steel		copper		PC		PMMA	
PMSSQ-PMA_MI-1a	3	0	4	0	5	0	5	0	3	0	3	1
PMSSQ-PEHA_MI-1a	3	0	4	0	5	0	5	1	3	0	3	0
PMSSQ-PMMA_MI-1a	4	0	4	0	4	0	5	0	4	0	4	0
PMSSQ-PDMA_MI-1a	3	0	4	0	5	0	5	1	4	0	4	0
PMSSQ-PS_MI-1a	5	0	4	0	5	0	5	0	4	0	4	0

Conclusions

Overall, a variable synthetic concept to prepare inorganic-organic hybrid polymers via the combination of sol-gel chemistry with controlled radical polymerization using ATRP conditions has been presented. Different trichlorosilyl functionalized ATRP initiators were prepared and co-condensed with methyl trimethoxysilanes. No significant differences during co-condensation between the different initiators were observed. Inorganic macro initiators for the ATRP could be prepared with different concentrations of initiating species. Acrylates, methacrylates and styrene could successfully be grafted from all three inorganic macro initiators. These different inorganic-organic hybrid polymers showed a very similar thermal behavior. A thermally induced cross-linking of the inorganic block and a well-separated decomposition of the organic block could be detected. The structural composition of the inorganic block was monitored by ^{29}Si solid state NMR spectroscopy. Thereby, we could show that the synthesized hybrid polymers still maintained highly reactive silanol groups. A thermally induced secondary condensation behavior of the inorganic/organic hybrid polymers to produce stable and adherent surface coating materials was investigated. After spin-coating on silicon, glass, metals or polymeric materials, the hybrid polymer coatings were cross-linked by curing. Accordingly, functional and adherent coatings could be achieved in a very convenient way.

Acknowledgement

The authors thank Young Joo Lee (Max Planck Institute for Polymer Research, Mainz) and Bernd Mathiasch (Institute of Inorganic Chemistry, University of Mainz) for measuring ^{29}Si CPMAS NMR spectra and for valuable discussions. Initial financial support from University of Mainz and FCI is gratefully acknowledged. Bayer MaterialScience AG, Leverkusen, is acknowledged for financial and scientific support.

References

- [1] P. Gomez-Romero, C. Sanchez, (Editors) *Functional Hybrid Materials*, Wiley-VCH 2004, 15-44.
- [²] W.F. Bradley, *J. Am. Chem. Soc.*, **1945**, 67, 975.
- [3] S.B. Hendricks, *J. Phys. Chem.*, **1941**, 45, 65.
- [4] E. Ruiz-Hizky, B. Casal, *Nature*, **1978**, 276, 596.
- [5] A. Blumstein, *Bull. Soc. Chim. Fr.*, **1961**, 899.
- [6] S.J. Clarson, J.J. Fitzgerald, M.J. Owen, S.D. Smith, Ed.: ACS Symp. Ser. 944, *Silicones and Silicone-modified materials*, 2000.
- [7] D.A. Loy, K.J. Shea, *Chem. Rev.*, **1995**, 95, 1431.
- [8] P.P. Pescarmona, T. Maschmeyer, *Aust. J. Chem.*, **2001**, 54, 583.
- [9] R.D. Miller, *Science*, **1999**, 286, 421.
- [10] H.W. Ro, K.J. Kim, P. Theato, D.W. Gidley, D.Y. Yoon, *Macromolecules*, **2005**, 38, 1031.
- [11] T.J. Barton, *Chem. Mater.*, **1999**, 11, 2633.
- [12] W. Li, Q. Wang, J. Cui, H. Chou, S.E. Shaheen, E. Jabbour, J. Anderson, P. Lee, B. Kippelen, N. Peyghambarian, N.R. Armstrong, T.J. Marks, *Adv. Mater.*, **1999**, 11, 730.
- [13] C. Carbonneau, R. Frantz, J.-O. Durand, G.F. Lanneau, R.J.P. Corriu, *Tetrahedron Lett.*, **1999**, 40, 5855.
- [14] J.F. Brown, L. Vogt, A. Katchman, K. Euslance, K. Kriser, *J. Am. Chem. Soc.*, **1960**, 82, 6294.
- [15] J. Kron, S. Amberg-Schwab, G. Schottner, *J. Sol-Gel Sci. Tech.*, **1994**, 2, 189.
- [16] C. Ma, I. Taniguchi, M. Miyamoto, Y. Kimura, *Polym. J.*, **2003**, 35, 270.
- [17] H. Mori, M.G. Lanzendörfer, A.H.E. Müller, *Macromolecules*, **2004**, 37, 5228.
- [18] H. Mori, A.H.E. Müller, J.E. Klee, *J. Am. Chem. Soc.*, **2003**, 125, 3712.
- [19] S.V. Patwardhan, S.J. Clarson, C.C. Perry, *Chem. Commun.*, **2005**, 1113.
- [20] S.V. Patwardhan, N. Mukherjee, S.J. Clarson, *J. Inorg. Organomet. Polym.*, **2001**, 11, 193.
- [21] K. Matyjaszewski, Ed.: ACS Symp. Ser. 944, *Controlled/Living Radical Polymerization*, 2006.
- [22] S.C. Hong, D. Neugebauer, Y. Inoue, J.-F. Lutz, K. Matyjaszewski, *Macromolecules*, **2003**, 36, 27.
- [23] S. Muthukrishan, D.P. Erhard, H. Mori, A.H.E. Müller, *Macromolecules*, **2006**, 39, 2743.
- [24] L. Zhang, H.C.L. Abbenhuis, Q. Yang, Y.-M. Wang, P.C.M.M. Magusin, B. Mezari, R.A. van Santen, C. Li, *Angew. Chem. Int. Ed.*, **2007**, 46, 5003.
- [25] H. Xu, S.-W. Kuo, J.-S. Lee, F.-C. Chang, *Macromolecules*, **2002**, 35, 8788.
- [26] C. Zhang, R.M. Laine, *J. Am. Chem. Soc.*, **2000**, 122, 6979.
- [27] J. Pyun, P.J. Miller, G. Kickelbick, K. Matyjaszewski, J. Schwab, J. Lichtenhahn, *Polymer Preprints*, **1999**, 40, 454.
- [28] C.-F. Huang, S.-W. Kuo, F.-J. Lin, W.-J. Huang, C.-F. Wang, W.-Y. Chen, F.-C. Chang, *Macromolecules*, **2006**, 39, 300.
- [29] R.O.R. Costa, W.L. Vasconcelos, R. Tamaki, R.M. Laine, *Macromolecules*, **2001**, 34, 5398.
- [30] K. Matyjaszewski, T.E. Patten, *Acc. Chem. Res.*, **1999**, 32, 895.
- [31] K. Matyjaszewski, T.E. Patten, *Adv. Mater.*, **1998**, 10, 12.

- [32] P. Theato, K.J. Kim, D.Y. Yoon, *Phys. Chem. Chem. Phys.*, **2004**, *6*, 1458.
[33] J.K. Lee, K. Char, H.-W. Rhee, D.Y. Yoo, D.Y. Yoon, *Polymer*, **2001**, *42*, 9085.
[34] K. Matyjaszewski, *Chem. Eur. J.*, **1999**, *5*, 3095.
[35] K. Matyjaszewski, J.J. Xia, *Chem. Rev.*, **2001**, *101*, 2921.
[36] ISO 2409:1992(E).

Supporting information

Figure S1:

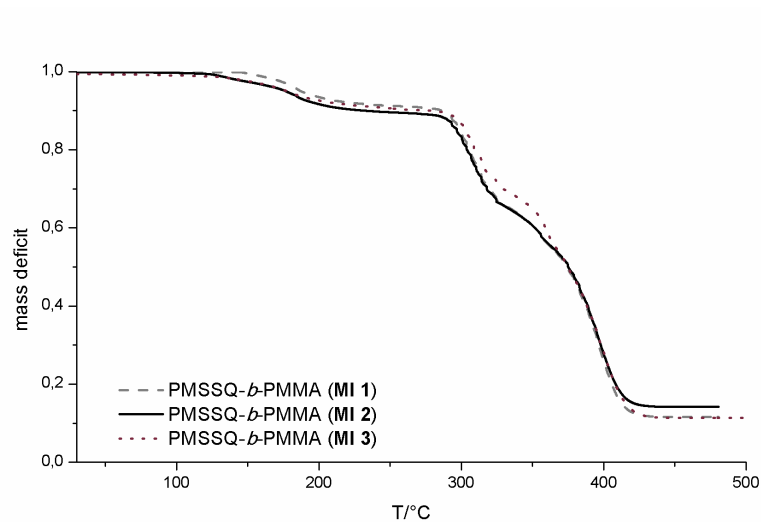


Figure S1. Thermal behavior of PMSSQ-PMMA, synthesized using different macro initiators.

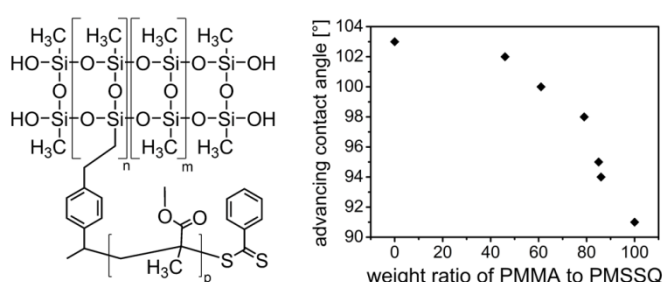
4.2

Synthesis of Functional Inorganic-Organic Hybrid Polymers Based on Poly(silsesquioxanes) and Their Thin Film Properties

Daniel Kessler¹, Patrick Theato^{1*}

Institute of Organic Chemistry, University of Mainz, Duesbergweg 10-14, 55099 Mainz, Germany

Macromolecules **2008**, *41*(14), 5237-5244.



Abstract

New stable and adherent coating materials have been synthesized on the basis of inorganic/organic hybrid polymers. As the inorganic part, different poly(silsesquioxanes) (PSSQ) have been functionalized to act as polymeric chain transfer agents (CTAs) for a reversible addition fragmentation chain transfer polymerization, thereby determining the starting point of a controlled radical polymerization of vinyl-type monomers. Using two different CTAs acrylates, methacrylates and styrene have successfully been polymerized under RAFT polymerization conditions. Different monomers were co-polymerized in such an organic block to incorporate multiple functionalities. The variation of the block ratios and the secondary condensation behavior of the inorganic block were investigated.

Finally, these materials were used as surface coating materials on silicon, glass, metal and polymeric substrates. Successful surface functionalization was demonstrated by contact angle measurements. The stability of the film and the adhesion on the substrate were tested in an ISO tape test.

Keywords

Reversible addition fragmentation chain transfer (RAFT), graft copolymers, coatings, inorganic/organic hybrid polymers, poly(silsesquioxanes)

Introduction

Precise control of surface properties is becoming ever more important recently. For example, interfacial interactions have found applications in synthetic systems,¹⁻⁶ biological systems⁷ or surface responsive materials.⁸ In order to precisely adjust surface properties, different approaches have been explored, all depending on the desired application. Unfortunately, most approaches are not general. Rather they are often adapted only to one specific substrate and one desired property. For example, trichlorosilylalkanes are used to prepare hydrophobic glass surfaces.⁹ But they cannot be used to modify for example gold or polymer surfaces. In 2005 Russell and Hawker introduced a first simple strategy to create coatings for a versatile modification of surfaces.¹⁰ Their method is based on cross-linking random organic copolymers. The desired surface properties can be tuned by employing different monomers during the copolymer synthesis. The surface stability is then achieved by cross-linking cyclobutyl groups, resulting in stable and insoluble polymer coatings on surfaces.

Besides organic cross-linkers, inorganic compounds like trifunctional silanes, such as trichlorosilanes, have found broad application in sol-gel chemistry. In addition to the cross-linking ability of trichlorosilanes, they also bind directly to hydroxylated metal oxide surfaces or glass substrates.¹¹

Inorganic-organic hybrid materials have received tremendous attention for various applications due to their favorable and often unique combination of properties within one material, which can be used in surface science and other applications. For example, the combination of dyes with triethoxysilanes results in thermally and mechanically stable materials used as waveguides,¹² lasers,¹² sensors¹² or light emitting diodes.¹³ Nano-structured hybrid materials with promising properties, such as low dielectric constant materials for applications in microelectronics¹⁴⁻¹⁶ or superior mechanical properties,¹⁷ have been described. However, to design new materials with desirable and predictable properties, a detailed understanding of structure-property relationships is required.

There are many successful approaches to preparing inorganic/organic hybrid materials containing silica precursors, for example polymers containing tri-alkoxysilyl side groups as precursors for sol-gel processing were prepared using RAFT polymerization.¹⁸ Diblock copolymers can be obtained using polymeric PMMA RAFT agents.¹⁹ Polymer-ceramic hybrid materials can also be prepared using appropriate block copolymer and ceramic precursors (ormocers²⁰). Based on this unique polymer-ceramic interface unprecedented morphology control on the nanoscale has been obtained. Polyhedral oligomeric silsesquioxanes (POSS, $\text{Si}_8\text{O}_{12}\text{R}_8$) as the smallest molecular silica finds broad application within hybrid materials.²¹⁻²³ Polymers can be either grafted to or from POSS.²⁴⁻²⁷ Also POSS cubes can be incorporated as side chains.²⁸ In the work of Wiesner et al., hydrophilic parts of a diblock copolymer were integrated into silica networks²⁹, while Clarson et al. investigated the influence of different additives to a bio-inspired silification process.^{30,31}

Despite the importance of poly(silsesquioxanes) (PSSQs) as emerging materials for low dielectric constant materials in microelectronic devices^{14,15} because of their excellent thermal and electrical properties, their use as coating materials has not been well investigated as yet.

The chemical modification of metal oxide surfaces with various organosilanes (R_nSi_{x-4}) has been investigated intensively. In this context, infrared spectroscopy and ^{29}Si -NMR spectroscopy proved to be useful analytical techniques to study the molecular structure. Especially the binding of organosilanols with surface Si-OH groups and the tendency of mono-, di- and trifunctional silanols towards surface binding or internal cross-linking were examined.³⁵⁻³⁸ Polysilsesquioxanes consist of T1, T2 and T3 branches, which are comparable to mono-, di- and trifunctional silanols. Thus, they combine the tendency to bind to surface silanols as well as to form networks. To the best of our knowledge polysilsesquioxanes have not found broad application in the modification of surfaces. However, in conjunction with the versatility of the organic R group, polysilsesquioxanes seem to be ideal candidates to be used as coating materials.³⁹

In this paper, we report a versatile surface coating procedure. It is based on a new synthetic concept; applying the RAFT polymerization process to prepare inorganic-organic hybrid polymers, consisting of a poly(silsesquioxane) (PSSQ) inorganic block, which should serve as an adhesion promoter for the substrate as well as a cross-linking unit, and an organic block, which should provide the desired surface properties.

Experimental Part

Materials. All chemicals and solvents were commercially available (Acros Chemicals, ABCR) and used as received unless otherwise stated. All used monomers were distilled under reduced pressure. THF was distilled from sodium/benzophenone under nitrogen.

Instrumentation. All 1H and ^{13}C NMR spectra were recorded on a Bruker 300 MHz FT-NMR spectrometer. ^{29}Si CPMAS NMR spectra were measured on a Bruker DSX 400 MHz FT-NMR spectrometer (Rotation: 5000 Hz, T = RT, 4 mm rotor). Chemical shifts (δ) were given in ppm relative to TMS. Gel permeation chromatography (GPC) was used to determine molecular weights and molecular weight distributions, M_w/M_n , of polymer samples with respect to polystyrene standards (PSS). (THF used as solvent, polymer concentration: 2 mg/mL, column setup: MZ-Gel-SDplus 10^2 \AA^2 , 10^4 \AA^2 and 10^6 \AA^2 , used detectors: refractive index, UV and light scattering). Thermo gravimetric analysis was performed using a Perkin Elmer Pyris 6 TGA in nitrogen (10 mg pure polymer in aluminum fan). FD mass spectra were measured using a Finnigan MAT 95 mass spectrometer. Elemental analyses were done with an Elementar Vario Micro Cube (detecting C, H, N, S). All reactions were performed in Argon atmosphere.

Synthesis of *p*-(chloromethyl)-phenylethyltrichlorosilane (1). *p*-(chloromethyl)-phenylethyltrichlorosilane was prepared by hydrosilylation reaction of *p*-chloromethylstyrene with trichlorosilane. 100 mg platinum on charcoal and 100 mL toluene were placed in a 250 mL round-bottomed flask equipped with a stirring rod, 75 mmol (10.16 g) trichlorosilane and 50 mmol (7.63 g) *p*-chloromethylstyrene were added. The reaction mixture was stirred magnetically at 110 °C for 48 h. After filtering over celite, the solvent was removed and the crude product was distilled at $2.5 \cdot 10^{-3}$ mbar.

Yield: 11.07 g (39 mmol, 77.1 %)

$^1\text{H-NMR}$ (CDCl_3): $\delta(\text{ppm}) = 7.34$ (d, $^3J = 8.1$ Hz, 2H); 7.22 (d, $^3J = 7.8$ Hz, 2H); 4.58 (s, 2H); 2.90 (m, 2H); 1.74 (m, 2H)

$^{13}\text{C-NMR}$ (CDCl_3): $\delta(\text{ppm}) = 141.61$; 135.71 ; 128.91 ; 128.24 ; 45.94 ; 27.91 ; 25.90

EA (%): calculated: C = 37.52; H = 3.50; measured: C = 38.70; H = 3.73

Synthesis of *p*-(chloromethyl)-phenylethyltrimethoxysilane (2). 35 mmol (9.98 g) *p*-(chloromethyl)-phenylethyltrichlorosilane (1) was dropped in 100 mL methanol (freshly distilled over sodium) in a 200 mL round-bottomed flask equipped with a stirring bar. The mixture was stirred over night and the solvent was removed afterwards on a rotary evaporator.

Yield: 8.44 g (31 mmol, 87.8 %)

$^1\text{H-NMR}$ (CDCl_3): $\delta(\text{ppm}) = 7.29$ (d, $^3J = 8.1$ Hz, 2H); 7.20 (d, $^3J = 8.1$ Hz, 2H); 4.55 (2, 2H); 3.56 (s, 9H); 2.73 (m, 2H); 0.99 (m, 2H)

$^{13}\text{C-NMR}$ (CDCl_3): $\delta(\text{ppm}) = 144.61$; 134.81 ; 128.54 ; 128.04 ; 50.38 ; 28.35 ; 11.09

FD mass spectra: 273.9 (100.0%); 274.9 (15.6%); 275.9 (38.9%)

EA (%): calculated: C = 52.45; H = 6.97; measured: C = 53.38; H = 7.22

Synthesis of dithiobenzoic acid benzyl-(4-ethyltrimethoxysilyl) ester (3). To a solution of 31.6 mmol phenyl magnesium bromide in THF in a 250 mL round-bottomed flask 49.7 mmol (3.78 g) of carbon disulfide was added and stirred magnetically for 15 min at 40 °C. Afterwards 31.7 mmol (8.71 g) of *p*-(chloromethyl)-phenylethyl-trimethoxysilane (2) was added and the solution was stirred at 50 °C for 1 h. The reaction mixture was poured onto ice and the product was extracted with diethyl ether. The ether phase was washed three times with water, dried over MgSO_4 and the solvent was removed on a rotary evaporator.

Yield: 9.91 g (25.3 mmol, 79.7 %)

$^1\text{H-NMR}$ (CDCl_3): $\delta(\text{ppm}) = 8.01$ (m, 1H); 7.27 (m, 8H); 4.53 (d, $^3J = 2.4$ Hz, 2H); 3.59 (s, 9H); 2.76 (m, 2H); 1.04 (m, 2H)

$^{13}\text{C-NMR}$ (CDCl_3): $\delta(\text{ppm}) = 213.79$; 144.61 ; 137.37 ; 132.26 ; 129.16 ; 128.62 ; 128.21 ; 128.06 ; 126.76 ; 50.41 ; 42.31 ; 28.44 ; 11.10

FD mass spectra: 391.9 (100.0%); 392.9 (26.9%); 393.9 (15.4%); 274.0 (64.6%); 275.9 (38.9)

EA (%): calculated: C = 58.13; H = 6.16; S = 16.33; measured: C = 56.20; H = 6.32; S = 16.51

Synthesis of *p*-(1-chloroethyl)-styrene (4). Hydrogen chloride was bubbled through 100 mmol 1,4-divinyl benzene in a three neck 250 mL flask during 5 h (approx. 1 bubble per second). The crude product was purified by distillation in vacuum ($p = 20$ mbar).

Yield: 7.89 g (47 mmol, 47.0 %)

$^1\text{H-NMR}$ (CDCl_3): $\delta(\text{ppm}) = 7.52 - 7.26$ (m, 4H); 6.78 (dd, $^3J_1 = 10.8$ Hz, $^3J_2 = 6.6$ Hz, 1H); 5.83 (dd, $^3J_1 = 17.7$ Hz, $^3J_2 = 6.3$ Hz, 1H); 5.35 (dd, $^3J_1 = 11.1$ Hz, $^3J_2 = 5.5$ Hz, 1H); 5.14 (quad, $^3J = 6.6$ Hz, 1H); 1.90 (d, $^3J = 6.9$ Hz, 3H)

$^{13}\text{C-NMR}$ (CDCl_3): $\delta(\text{ppm}) = 139.31$; 137.69 ; 134.95 ; 127.24 ; 125.91 ; 113.99 ; 59.07 ; 25.31

FD mass spectra: 165.9 (100.0%); 166.9 (35.5%); 167.9 (11.8%)

EA (%): calculated: C = 72.07; H = 6.65; measured: C = 72.56; H = 6.89

Synthesis of *p*-(1-chloroethyl)-phenylethyltrichlorosilane (5). 50 mg platinum on charcoal and 100 mL toluene were placed in a 250 mL round-bottomed flask, 75 mmol (10.12 g) trichlorosilane and 47 mmol (7.83 g) *p*-(1-chloroethyl)-styrene (4) was added. The solution was

stirred magnetically at 80 °C for 24 h. After filtration and evaporation of the solvent the crude product was distilled in high vacuum. Bp. 119 °C at 6*10⁻³ mbar.

Yield: 5.88 g (19.5 mmol, 41.4 %)

¹H-NMR (CDCl₃): δ(ppm) = 7.42 – 7.15 (m, 4H); 5.08 (quad, ³J = 6.9 Hz, 1H); 2.91 (t, ³J = 6.4 Hz, 2H); 1.85 (d, ³J = 6.8 Hz, 3H); 1.77 (m, 2H)

¹³C-NMR (CDCl₃): δ(ppm) = 141.02; 138.23; 129.08; 128.37; 59.11; 28.71; 25.73; 21.94

FD mass spectra: 301.9 (100.0%); 300.9 (55.1%); 299.9 (27.9%)

EA (%): calculated: C = 39.76; H = 4.00; measured: C = 41.28; H = 4.11

Synthesis of *p*-(1-chloroethyl)-phenylethyltrimethoxysilane (6). 19.55 mmol (5.91 g) *p*-(1-chloroethyl)-phenylethyltrichlorosilane (5) was added to 100 mL methanol (distilled over sodium) in a 200 mL flask equipped with stirring rod and stirred over night. The solvent was removed by rotary evaporator.

Yield: 5.28 g (18.3 mmol, 96.3 %)

¹H-NMR (CDCl₃): δ(ppm) = 7.31 – 7.19 (m, 4H); 4.97 (quad, ³J = 6.8 Hz, 1H); 3.54 (s, 9H); 2.69 (m, 2H); 1.86 (d, ³J = 6.6 Hz, 3H); 0.96 (m, 2H)

¹³C-NMR (CDCl₃): δ(ppm) = 143.88; 136.26; 128.33; 128.09; 58.04; 51.13; 28.72; 25.50; 11.89

FD mass spectra: 287.9 (100.0%); 288.9 (17.9%); 290.9 (34.0%)

EA (%):calculated: C = 54.06; H = 7.33; measured: C = 55.01; H = 7.46

Synthesis of dithio benzoic acid 1-ethylphenyl-4-(ethyltrimethoxysilyl) ester (7). To a solution of 25 mmol phenyl magnesium bromide in THF in a 200 mL flask 35 mmol (2.66 g) carbon disulfide was added and stirred magnetically at 40 °C. After 15 min 18.3 mmol (5.29 g) *p*-(1-chloroethyl)-phenylethyltrimethoxysilane (6) was added and stirred at 50 °C for 1 h. The reaction mixture was poured onto ice and extracted with diethyl ether. The organic phase was washed with water, dried over MgSO₄ and the solvent was removed by rotary evaporator.

Yield: 5.13 g (12.63 mmol, 69,0 %)

¹H-NMR (CDCl₃): δ(ppm) = 8.08 (m, 1H); 7.31 – 7.19 (m, 8H); 4.41 (quad, ³J = 6.5 Hz, 1H); 3.54 (s, 9H); 2.80 (m, 2H); 1.74 (d, ³J = 6.6 Hz, 3H); 0.92 (m, 2H)

¹³C-NMR (CDCl₃): δ(ppm) = 217.02; 142.44; 139.12; 135.55; 131,01; 129.04; 128.99; 127.85; 127.00; 52.11; 43.24; 27.16; 20.37; 12.40

FD mass spectra: 405.9 (100.0%); 406.9 (34.5%); 404.9 (20.3%); 289.9 (60.8%)

EA (%):calculated: C = 59.07; H = 6.44; S = 15.77; measured: C = 58.79; H = 6.81; S = 13.29

Synthesis of *p*-hydroxy benzophenone acrylate (8). 50 mmol (9.91 g) *p*-hydroxy benzophenone and 30 mL chloroform were placed in a 100 mL round bottomed flask, first 50 mmol (5.06 g) triethyl amine was added and afterwards 100 mmol (9.05 g) acryloyl chloride. The reaction mixture was stirred at room temperature for 2 h, washed with water and dried over MgSO₄. After removing the solvent, the crystalline product was recrystallized from hexane.

Yield: 9.87 g (39.16 mmol, 78.3 %)

¹H-NMR (CDCl₃): δ(ppm) = 7.84 (d, ³J = 8.4 Hz, 2H); 7.78 (d, ³J = 7.2 Hz, 2H); 7.46 (t, ³J = 17.4 Hz, 1H); 7.44 (t, ³J = 7.2 Hz, 2H); 7.25 (d, ³J = 8.4 Hz, 2H); 6.61 (d, ³J = 17.4 Hz, 1H); 6.32 (dd, ³J₁ = 17.4 Hz, ³J₂ = 10.4 Hz, 1H); 6.04 (d, ³J = 10.5 Hz, 1H)

^{13}C -NMR (CDCl_3): $\delta(\text{ppm}) = 195.42; 163.92; 153.82; 137.46; 135.06; 133.28; 132.46; 131.64; 129.92; 128.33; 127.54; 121.49$

FD mass spectra: 252.2 (100.0%); 253.2 (16.23%)

EA (%): calculated: C = 76.18; H = 4.76; measured: C = 75.95; H = 4.74

Synthesis of *p*-hydroxy benzophenone methacrylate (9). Preparation similar to (8).

Yield: 9.48 g (35.61 mmol, 71.2 %)

^1H -NMR (CDCl_3): $\delta(\text{ppm}) = 7.84$ (d, $^3J = 8.4$ Hz, 2H); 7.76 (d, $^3J = 7.2$ Hz, 2H); 7.53 (t, $^3J = 7.2$ Hz, 1H); 7.45 (t, $^3J = 7.2$ Hz, 2H); 7.23 (d, $^3J = 8.4$ Hz, 2H); 6.35 (s, 1H); 5.77 (s, 1H); 2.04 (s, 3H)

^{13}C -NMR (CDCl_3): $\delta(\text{ppm}) = 195.53; 165.29; 154.21; 137.51; 135.54; 134.95; 132.55; 131.66; 129.93; 128.32; 127.89; 121.57; 18.31$

FD mass spectra: 266.2 (100.0%); 267.2 (18.2%)

EA (%): calculated: C = 76.68; H = 5.30; measured: C = 75.99; H = 5.12

Synthesis of PSSQ macro RAFT agents. The PSSQ macro initiators have been synthesized following a general procedure: The desired trifunctional silane and the functionalized RAFT agent were added in the molar ratio 20 : 1 in a 200 mL flask. Then 20 mL THF, 1000 mol% Water and 3 mol% HCl were injected. The solution was stirred magnetically at 0 °C for 3 h, then diluted with diethyl ether, washed with water and dried over MgSO_4 . The solvent was evaporated and the product was dried in high vacuum ($1 \cdot 10^{-3}$ mbar).

PMSSQ macro RAFT agent 1 (MI-1) by reaction of methyltrimethoxy silane with (3). ^1H -

NMR (THF-d_8): $\delta(\text{ppm}) = 7.99$ (br, 5H); 7.36 (br, 2H); 7.20 (br, 2H); 5.80 (br, 1.9H); 4.55 (br, 2H); 3.48 (br, 1.1H); 2.71 (br, 2H); 0.99 (br, 2H); 0.17 (br, 69.1H)

^{29}Si CPMAS NMR: $\delta(\text{ppm}) = -48.27$ (T1); -57.41 (T2); -66.47 (T3)

$M_n = 4990$ g/mol, PDI = 1.63

PMSSQ macro RAFT agent 2 (MI-2) by reaction of methyltrimethoxy silane with (7). ^1H -

NMR (acetone-d_6): $\delta(\text{ppm}) = 7.63 - 7.15$ (br, 9H); 5.26 (br, 2.1H); 3.61 (br, 1H); 2.88 (br, 2H); 1.77 (br, 3H); 1.07 (br, 2H); 0.16 (br, 69.1H)

^{29}Si CPMAS NMR: $\delta(\text{ppm}) = -48.88$ (T1); -57.90 (T2); -65.29 (T3)

$M_n = 3210$ g/mol, PDI = 1.78

PODSSQ macro RAFT agent (MI-3) by reaction of octadecyltrichloro silane with (3). ^1H -

NMR (THF-d_8): $\delta(\text{ppm}) = 7.20$ (br, 9H); 4.98 (br); 4.10 (br, 2H); 3.53 (br); 2.50 (br, 2H); 1.65 (br, 2H); 1.30 (br); 0.95 (br); 0.63 (br)

$M_n = 4213$ g/mol, PDI = 1.73

PFOSSQ macro RAFT agent (MI-4) by reaction of 1H,1H,2H,2H-perfluorooctyltrichloro silane with (3). ^1H -NMR (THF-d_8): $\delta(\text{ppm}) = 7.21$ (br, 9H); 4.60 (br); 4.03 (br, 2H); 3.60 (br, 2H); 2.75 (br, 2H); 2.30 (br); 1.74 (br, 2H); 0.95 (br)

$M_n = 9339$ g/mol, PDI = 3.00

PPSSQ macro RAFT agent (MI-5) by reaction of phenyltrimethoxy silane with (3). ^1H -

NMR (CDCl_3): $\delta(\text{ppm}) = 7.65 - 7.01$ (br); 5.18 (br); 4.47 (br, 2H); 3.50 (br); 1.77 (br, 2H); 1.19 (br, 2H)

$M_n = 4600$ g/mol, PDI = 2.00

POSSQ macro RAFT agent (MI-6) by reaction of octyltrichloro silane with (3).

$^1\text{H-NMR}$ (CDCl_3): $\delta(\text{ppm}) = 8.04 - 7.46$ (br, 9H); 4.68 (br, 2H); 3.61 (br); 1.50 – 0.63 (br)

$M_n = 5070$ g/mol, PDI = 1.80

RAFT Polymerization. Inorganic-organic hybrid polymers have been prepared by a RAFT polymerization. A general procedure was as follows: 0.5 g of the macro RAFT agent, 10 mg AIBN, 4 mL dioxane and a defined amount of monomer (usually 2 g unless otherwise stated) were placed in a 20 mL Schlenk flask, degassed and stirred magnetically at 80 °C for 4 h in Ar atmosphere. The resulting polymer was precipitated in *n*-hexane and dried in high vacuum ($1 \cdot 10^{-3}$ mbar).

PMSSQ-PMA using MI-1.

$^1\text{H-NMR}$ (CDCl_3): $\delta(\text{ppm}) = 3.63$ (br, 3H); 2.29 (br, 1H); 1.66 (br, 2H); 0.16 (br, 0.55 H)

^{29}Si CPMAS NMR: $\delta(\text{ppm}) = -57.80$ (T2); -66.92 (T3)

$M_n = 28100$ g/mol, PDI = 2.2, Yield: 1.97 g

PMSSQ-PEHA using MI-1.

$^1\text{H-NMR}$ (CDCl_3): $\delta(\text{ppm}) = 4.81$ (br, 0.1H); 3.93 (br, 2H); 2.32 (br, 1H); 1.85 (br, 1H); 1.58 (br, 2H); 1.29 (br, 8H); 0.99 (br, 6H); 0.17 (br, 0.7H)

$M_n = 33500$ g/mol, PDI = 1.9, Yield: 1.35 g

PMSSQ-PMMA using MI-2.

$^1\text{H-NMR}$ (CDCl_3): $\delta(\text{ppm}) = 5.02$ (br, 0.1H); 3.59 (br, 3H); 1.81 (br, 2H); 1.34 (br, 3H); 0.16 (br, 0.8H)

^{29}Si CPMAS NMR: $\delta(\text{ppm}) = -58.23$ (T2); -67.10 (T3)

$M_n = 28930$ g/mol, PDI = 1.5, Yield: 1.96 g

PMSSQ-PDMA using by MI-2.

$^1\text{H-NMR}$ (CDCl_3): $\delta(\text{ppm}) = 5.06$ (br, 0.1H); 4.00 (br, 2H); 1.90 – 1.72 (br, 16H); 1.27 (br, 3H); 1.10 – 1.01 (br, 3H); 0.15 (br, 1.3H)

$M_n = 25520$ g/mol, PDI = 2.4, Yield: 2.19 g

PMSSQ-PS using MI-1.

$^1\text{H-NMR}$ (CDCl_3): $\delta(\text{ppm}) = 7.10$ (br, 5H); 4.55 (br, 0.1H); 2.34 (br, 1H); 1.25 (br, 2H); 0.16 (br, 1.2H)

$M_n = 29840$ g/mol, PDI = 2.9, Yield: 2.11 g

PMSSQ-PS using MI-2.

$^1\text{H-NMR}$ (CDCl_3): $\delta(\text{ppm}) = 7.10$ (br, 5H); 5.10 (br, 0.1H); 2.40 (br, 1H); 1.33 (br, 2H); 0.17 (br, 1.4H)

$M_n = 23000$ g/mol, PDI = 2.7, Yield: 2.30 g

PPSSQ-PMA using MI-5.

$^1\text{H-NMR}$ (CDCl_3): $\delta(\text{ppm}) = 7.22$ (br, 1.7H); 3.66 (br, 3H); 2.29 (br, 1H); 1.68 (br, 2H)

$M_n = 35890$ g/mol, PDI = 1.98, Yield: 1.77 g

PPSSQ-PEHA using MI-5.

$^1\text{H-NMR}$ (CDCl_3): $\delta(\text{ppm}) = 7.25$ (br, 1.6H); 3.89 (br, 2H); 2.26 (br, 1H); 1.92 (br, 1H); 1.55 (br, 2H); 1.33 (br, 8H); 0.95 (br, 6H)

$M_n = 33200$ g/mol, PDI = 1.68, Yield: 1.57 g

POSSQ-PMA using MI-6.

$^1\text{H-NMR}$ (CDCl_3): $\delta(\text{ppm}) = 3.68$ (br, 3H); 2.28 (br, 1H); 1.65 (br, 2H); 1.45 – 0.60 (br, 6H)

$M_n = 32900$ g/mol, PDI = 1.99, Yield: 1.40 g

POSSQ-PEHA using MI-6.

$^1\text{H-NMR}$ (CDCl_3): $\delta(\text{ppm}) = 3.69$ (br, 2H); 2.28 (br, 1H); 1.95 (br, 1H); 1.60 (br, 2H); 1.45 – 0.60 (br, 5.2H)

$M_n = 27000$ g/mol, PDI = 1.82, Yield: 1.52 g

PODSSQ-PMA using MI-3.

$^1\text{H-NMR}$ (CDCl_3): $\delta(\text{ppm}) = 3.70$ (br, 3H); 2.30 (br, 1H); 1.64 (br, 2H); 1.31 (br, 18H); 0.90 (br, 1.6H); 0.60 (br, 1H)

$M_n = 37090$ g/mol, PDI = 1.92, Yield: 1.44 g

PODSSQ-PEHA using MI-3.

$^1\text{H-NMR}$ (CDCl_3): $\delta(\text{ppm}) = 3.70$ (br, 2H); 2.20 (br, 1H); 1.97 (br, 1H); 1.60 (br, 2H); 1.31 (br, 18H); 0.97 – 0.90 (br, 1.6H); 0.60 (br, 1H)

$M_n = 35200$ g/mol, PDI = 1.74, Yield: 1.30 g

PFOSSQ-PMA using MI-4.

$^1\text{H-NMR}$ (CDCl_3): $\delta(\text{ppm}) = 3.68$ (br, 3H); 2.28 (br, 1H); 2.20 (br, 1.4H); 1.65 (br, 2H); 0.90 (br, 1.4H)

$M_n = 22000$ g/mol, PDI = 1.74, Yield: 1.48 g

PFOSSQ-PEHA using MI-4.

$^1\text{H-NMR}$ (CDCl_3): $\delta(\text{ppm}) = 3.69$ (br, 3H); 2.20 (br, 2.1H); 1.95 (br, 1H); 1.60 (br, 2H); 0.97 – 0.90 (br, 1.1H)

$M_n = 24560$ g/mol, PDI = 1.60, Yield: 1.20 g

PMSSQ-PMA containing 5 mol% (8).

$^1\text{H-NMR}$ (CDCl_3): $\delta(\text{ppm}) = 7,80 - 7,24$ (m, H1, 0,3H), 3,67 (br, H2, 3H), 2,30 (br, H3, 2H), 1,67 (br, H4, 1H), 0,13 (br, H5, 1,2H)

$M_n = 37480$ g/mol, PDI = 1,22

PMSSQ-PMMA containing 5 mol% (9).

$^1\text{H-NMR}$ (CDCl_3): $\delta(\text{ppm}) = 7,85- 7,17$ (m, H1, 0,35H), 3,68 (br, H2, 3H), 1,79 (br, H3, 2H), 1,24 – 0,81 (br, H4, 3H), 0,14 (br, H5, 1,2H)

$M_n = 22310$ g/mol, PDI = 1,65

(signals coming from the initiating units and integrations are not considered here, because of the small values comparing to the polymer signals)

Results and discussion

A polymeric precursor for a versatile surface coating material must fulfill a number of different requirements. Basically, general coating systems must satisfy two main requirements: film stability and adhesion to the substrate of choice must be effective and second, a simple method for surface functionalization and modification is highly desirable. An inorganic-organic hybrid polymer based on poly(silsesquioxanes) (PSSQ) as an inorganic block and an organic

block composed of simple vinyl monomers should offer potential to develop a variety of surface coating materials with well-defined but tailorable properties.

The synthetic concept presented here consists mainly of two parts. First, a PSSQ ($\text{RSiO}_{1.5}$) macro chain transfer agent (CTA) is synthesized, consisting of the desired silsesquioxane [e.g. methyltrimethoxy silane to synthesize poly(methyltrimethoxysilane) (PMSSQ)] and a functional moiety that follows control of RAFT polymerization of vinyl monomers yielding an organic polymer block. The method of choice, for preparing inorganic/organic hybrid materials is a controlled radical polymerization, not only due to the possibility to obtain low polydispersities but mostly due to the fact that the polymer chain grows only from a defined site (grafting-from).

Atom transfer radical polymerization (ATRP) of methyl methacrylate initiated by functionalized PMSSQ macro initiators using usual ATRP conditions has been described previously^{16,32}. Further the reversible addition-fragmentation chain transfer (RAFT) polymerization offers an excellent opportunity to control radical polymerization and to initiate the radical polymerization from a defined site, in our case from PSSQ macro chain transfer agents. In sum, the synthetic pathway begins with the synthesis of trimethoxysilyl-functionalized dithioesters as the CTA for the RAFT process. Second, these CTAs are co-condensed with methyl trimethoxysilane (MTMS) or other trialkoxy silanes to build up PSSQ macro CTAs.

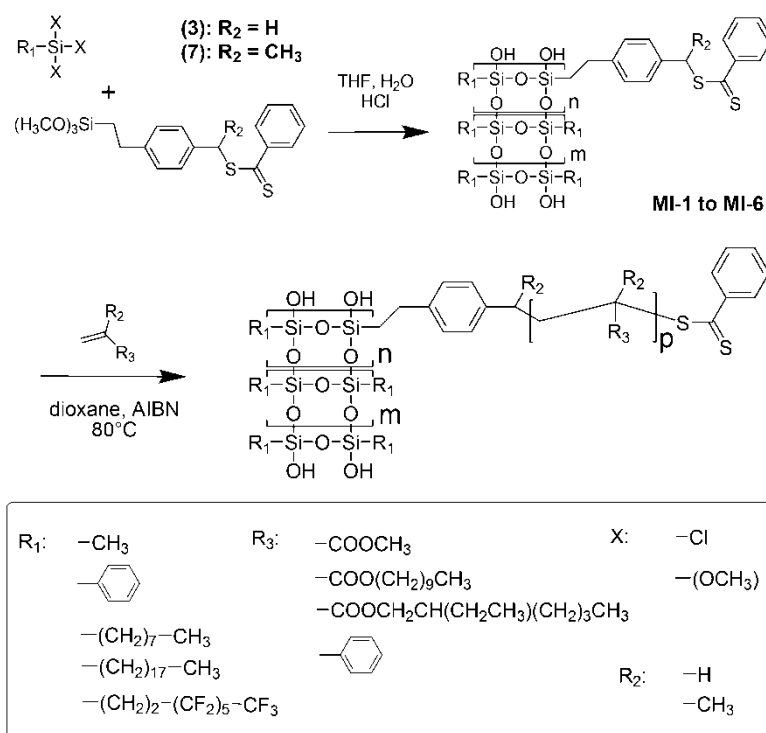
In the last step, the polymerization of the desired monomer controlled by the macro CTA results in the formation of the organic polymer chains attached onto the PMSSQ block. Scheme 1 visualizes the synthetic concept, which features a high variability: easy modification of the inorganic block or the organic block, adjustability of the block ratio and the variable amount of initiating sites in the PSSQ macro CTA resulting in different numbers of organic chains on one inorganic block. In the following the resulting flexibility of the synthesis will be discussed in detail.

Synthesis of PMSSQ macro CTA. The CTA must be able to be co-condensed into a PSSQ and to regulate the controlled radical polymerization. Co-condensation is achieved by hydrolysis of a trimethoxy silyl group. To keep the variability as high as possible it is desired to polymerize acrylates, methacrylate and styrene based monomers. Thus, two different CTAs were synthesized to mimic the growing chain end of acrylates and methacrylates, respectively. The obtained CTAs dithiobenzoic acid benzyl-(4-ethyltrimethoxysilyl) ester (3) and dithiobenzoic acid 1-ethylphenyl-4-(ethyltrimethoxysilyl) ester (7) are shown in scheme 1. The overall yield to (3) was 54 %, in case of (7) the yield was 13 %. The low overall yield resulted from the low yield of the purification after the first step. It was expected that (3) can be used in the polymerization of acrylates and styrene, while (7) should be applicable for methacrylates. Overall, this should cover a wide spectrum of vinyl-type monomers to be used for the synthesis of hybrid polymers.

A co-condensation step is then used to generate soluble PSSQ macro CTAs, which can be used in a subsequent polymerization. To show the versatility of the concept, different polymeric CTAs were synthesized based on PSSQ. Dithiobenzoic acid benzyl-(4-

ethyltrimethoxysilyl) ester (3) and dithio benzoic acid 1-ethylphenyl-4-(ethyltrimethoxysilyl) ester (7) were co-condensed with MTMS to yield the macro CTAs MI-1 and MI-2, respectively. With both macro CTAs in hands it should be possible to investigate the different chain transfer behavior during the polymerization leading to the polymerization of either acrylates or methacrylates and styrenes.

Scheme 1. Synthetic pathway towards PSSQ based hybrid polymers. The first steps shows the co-condensation of the macro-CTA, the second step shows the grafting from polymerization via RAFT to yield in an inorganic/organic hybrid polymer.



To demonstrate the flexibility of the PSSQ system, other trialkoxy silanes or trichlorosilanes were also used in the synthesis of macro CTAs, yielding MI-3 to MI-6, possessing the same CTA site (dithiobenzoic acid benzyl-(4-ethyltrimethoxysilyl) ester (3)) but different organic moieties on the PSSQ. To compare the effect of different substituted PSSQs octyl- and octadecyl-trichloro silanes (MI-6 and MI-3, respectively) were used during the co-condensation. Phenyl trimethoxy silane and 1H,1H,2H,2H-perfluorooctyltrichloro silane (yielding MI-4 and MI-5, respectively) were used to investigate the influence of aromatic or fluorinated sidechains and also to show potential to incorporate functional groups in the inorganic block. All mentioned tri-alkoxy- or trichloro-silanes could be converted in PSSQ macro CTAs. The molecular weights of all different macro CTAs varied between 3000 and 10000 g/mol (see table 1) and all of them were soluble in common organic solvents, such as dioxane, THF, acetone and ethylacetate. Dioxane was then used as the solvent in the following controlled radical polymerization.

Table 1. Properties of the different macro-CTA in dependence of co-condensation conditions.

macro initiator	initial molecular ratio	M _n [g/mol]	PDI	initiator ratio after co-condensation	m/n ¹	IPM ²
MI-1	20 : 1	4990	1.63	23 : 1	11	4.4
MI-2	20 : 1	3210	1.78	23 : 1	11	3.0
MI-3	20 : 1	4213	1.73	16 : 1	8	1.2
MI-4	20 : 1	9339	3.00	16 : 1	8	4.1
MI-5	20 : 1	4600	2.00	15 : 1	7	3.4
MI-6	20 : 1	5070	1.80	13 : 1	6	3.4

¹ ratio between pure PSSQ rungs and initiator rungs in an assumed ladder like structure of the macro initiator,

² IPM (initiating groups per molecule): calculated average number of initiating groups per PMSSQ macro initiator derived from integral ratio of ¹H NMR spectra.

The incorporation of the CTA sites in the PSSQ polymers was determined by ¹H NMR spectroscopy and compared with the initial molecular ratios (see table 1). The initial molecular ratio was determined by the ratio of CTA sites to the number of regular side groups. The remaining reactivity in the form of silanol groups (Si-OH) of the inorganic block was determined by ²⁹Si solid state NMR spectroscopy for MI-1 and MI-2. The spectra are shown in the supplementary figure S1. Both of them show T1- and T2- branches, indicating a highly reactive polysilsesquioxanes.

Table 2. Thermo gravimetrical analysis of PMSSQ-PEHA (grafted from MI-1) and PMSSQ-PMMA (grafted from MI-2).

hybrid polymer	macro - CTA	amount macro-CTA [g]	amount monomer [g]	expected weight ratio Org.: Inorg.	weight ratio by TGA Org.: Inorg.
PMSSQ-PEHA-1	MI-1		0.50	50 : 50	60 : 40
PMSSQ-PEHA-2	MI-1		1.00	67 : 33	75 : 25
PMSSQ-PEHA-3	MI-1	0.5	1.50	75 : 25	88 : 12
PMSSQ-PEHA-4	MI-1		2.00	80 : 20	92 : 8
PMSSQ-PEHA-5	MI-1		2.50	83 : 17	94 : 6
PMSSQ-PMMA-1	MI-2		0.50	50 : 50	46 : 54
PMSSQ-PMMA-2	MI-2		1.00	67 : 33	61 : 39
PMSSQ-PMMA-3	MI-2	0.5	1.50	75 : 25	79 : 21
PMSSQ-PMMA-4	MI-2		2.00	80 : 20	85 : 15
PMSSQ-PMMA-5	MI-2		2.50	83 : 17	86 : 14

Polymerization. In the next step, the macro CTAs were used as starting points for radical polymerization under RAFT conditions resulting in hybrid organic/inorganic copolymers. First, the polymerization behavior of the different CTA species was determined: Due to the different chemical architectures of the polymeric CTAs (3) and (7), MI-1 is expected to polymerize acrylates while MI-2 should polymerize methacrylates. No influence should be detected on the polymerization of styrene. Both macro CTAs were used in the polymerization of methyl

acrylate (MA), ethyl hexyl acrylate (EHA), methyl methacrylate (MMA), decyl methacrylate (DMA) and styrene (S). The obtained polymers were characterized using ^1H NMR spectroscopy and gel permeation chromatography (GPC) (see table S1, supplementary information). For MI-1 inorganic/organic hybrid polymers were obtained with MA, EHA and S. MI-2 yielded inorganic/inorganic hybrid polymers using MMA, DMA and styrene. In all other cases no hybrid polymer could be obtained after work up. The different macro CTAs were able to yield inorganic/organic hybrid polymers consisting of PMSSQ as an inorganic block and polyacrylate, polymethacrylate or polystyrene as an organic block. Both, MI-1 and MI-2 could be used to initiate the polymerization of styrene. No advantage of one of these CTAs over the other in regard to the polymerization of styrene could be found. Both, yields and molecular weights were in comparable range.

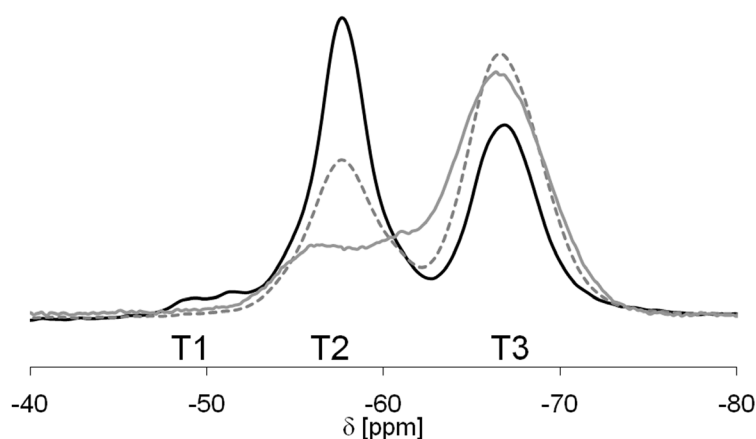
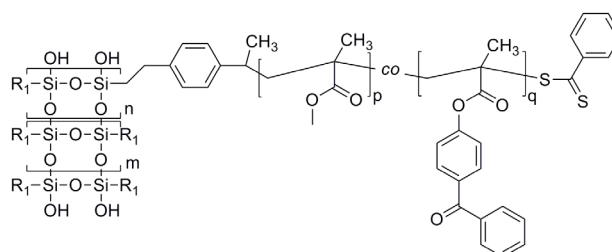


Figure 1: ^{29}Si CPMAS NMR spectra of a) MI-2 (black solid line), b) PMSSQ-PMMA after polymerization (grey dashed line) and c) PMSSQ-PMMA after curing (130 °C, 3 h) (grey solid line).

The other PSSQ macro CTAs, carrying octadecyl- (MI-3), 1H,1H,2H,2H-perfluorooctyl- (MI-4), phenyl- (MI-5) or octyl- (MI-6) sidegroups, were tested in analogous polymerization reactions. As MI-3 – MI-6 are based on the CTA site (3) only the polymerization of acrylates was considered. POSSQ, PODSSQ, PFOSSQ and PPSSQ based macro CTAs initiated the polymerization of MA and EHA, proving that the concept of synthesizing inorganic/organic hybrid polymers can easily be varied in the inorganic part as well as in the organic part. In all cases, GPC measurements showed a monomodal peak for the hybrid polymers with reasonable PDIs between 1.2 and 3, considering the step growth process of trifunctional monomers in the inorganic block (table S1, supplementary information). Achieved molecular weights were in the range between 22000 and 40000 g/mol, very similar to the corresponding PMSSQ based hybrid polymers. Again a significant difference in the polymerization behavior of the different macro CTAs was not found. A collection of all synthesized hybrid polymers can be found in the supplementary information.

To compare the ratios of the inorganic and the organic blocks with the initial ratios of macro CTA to organic monomer, the obtained PMSSQ-PEHA and PMSSQ-PMMA hybrid polymers were analyzed by TGA. An exemplary TGA for both polymers is given in the supporting information figure S3. For both polymers, the secondary condensation of the inorganic block occurred between 100 and 150 °C, indicating cross-linking, while around 400 °C the decomposition of the organic block could be detected. The ratio of decomposed mass to remaining mass was compared with the initial molecular ratio and the results are summarized in Table 2. In all cases the block ratio could to be adjusted by tuning the desired ratio between inorganic macro CTA and organic monomer.

Scheme 2. Structure of the hybrid polymer PMSSQ-PMMA, which contained 5 mol% of a photo cross-linkable benzophenone moiety.



For a material to cross-link and form a stable film or bind to hydroxylated surfaces, the inorganic block must possess sufficient reactive groups in the form of silanol functionalities after the polymerization of the organic monomer. Again, the remaining reactivity of the inorganic block was investigated by ^{29}Si CPMAS NMR spectroscopy. In figure 1, the ^{29}Si CPMAS NMR spectra of PMSSQ-PMMA after co-condensation, after polymerization and after curing at 130 °C for 3 h are compared. The decrease of T1- and T2- branches after polymerization are most likely due to the 80°C polymerization temperature, inducing slight condensation. Nevertheless, after polymerization of the organic monomer, the inorganic block still retained reactive silanol groups, which guarantee cross-linking or binding by secondary condensation afterwards. In the case of PMSSQ-PMA and PMSSQ-PMMA around 40 % of all silicon branches were T1 or T2 branches, ensuring enough reactive silanol groups.

The presented synthetic concept offers many possibilities to tune the desired properties of an inorganic/organic coating material by allowing the incorporation of different functions or monomers in the inorganic as well as the organic block and by adjusting the block ratio between both blocks. However, for some applications it is desired to incorporate more than one function in the organic block. This can be achieved by a statistical copolymerization of two monomers during the polymerization step. As an example, a second monomer, *p*-hydroxy benzophenone (meth)acrylate (8/9), was copolymerized with MA or MMA in the presence of polymeric CTA MI-1 or MI-2. Exemplary the chemical structure of the hybrid polymer PMSSQ-PMMA, which contained 5 mol% of a photo cross-linkable benzophenone moiety, is shown in scheme 2. Using the approach described above, 5 mol% of (8) or (9) were added in the

monomer feed, respectively. Again, ^1H NMR spectroscopy and GPC were used to characterize the obtained hybrid polymers. The ^1H NMR spectrum of PMSSQ-PMMA containing 5 mol% of (9) is shown in figure 2. Clearly, the expected peaks for the benzophenone moiety between 7 and 8 ppm can be assigned. The incorporation of the benzophenone groups was also proved by irradiation with UV light (UV-A). Benzophenone is known to react as a UV cross-linker.³³

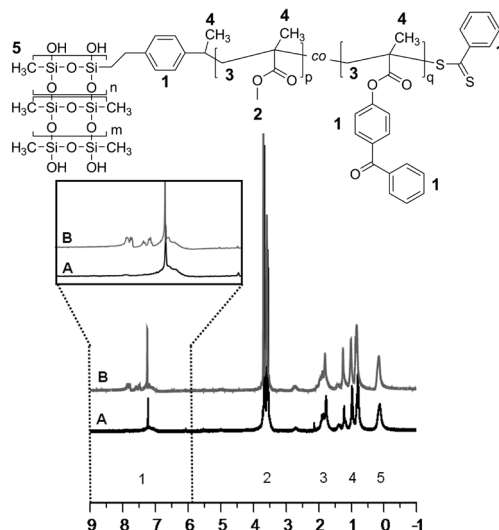


Figure 2. ^1H NMR spectra of PMSSQ-PMMA (A), $\gamma = 0$; PMSSQ-PMMA containing 5 % of (9) (B), $\gamma = 0.05$.

After 20 min irradiation of a 10 wt% solution of the PMA or PMMA hybrid polymers containing 5 wt% (8) or (9) with UV-A light, gelation occurred. Figure S2 in the supplementary information shows a GPC of a PMSSQ - PMMA hybrid polymer with 5 mol% (9) before and after 5 min irradiation (sample in THF solution, 2 mg/mL). Further irradiation resulted in an insoluble polymer (Solubility checked in chloroform, THF and ethylacetate).

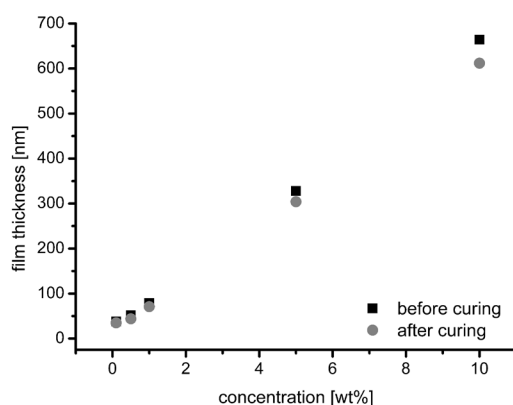


Figure 3. Film thicknesses of PMSSQ-PMMA hybrid films on silicon wafers measured by ellipsometry before and after curing (error range ± 5 nm).

These experiments indicate that by random co-polymerization of different monomers additional functions or properties can be incorporated in the organic block. In this case organic/inorganic hybrid materials were obtained which provide a cross-linking either by the secondary condensation of the inorganic block by heating or by photo cross-linking of the organic block. These materials are supposed to lead to an understanding of film forming properties of inorganic/organic hybrid polymers, because the inorganic secondary condensation of a film can be initiated either in the presence of a flexible organic moiety or a rigid UV-cross-linked organic matrix, which may yield in a different molecular structure within the film. Beside this academic approach, the possibility of photo cross-linking can also be used to pattern the film or to attach other materials on top of surface coatings by UV irradiation.

Surface coatings. To determine the utility of these hybrid materials as surface coatings, thin films on different substrates were prepared via spin-coating from a solution in THF with 4000 rpm for 15 s resulted in stable and transparent films (spin coated from 0.1 - 10wt% solution in THF). The dependence of the film thickness from the concentration of PMSSQ-PMMA in THF is shown in figure 3. As expected, a linear behavior between concentration and thickness was found. Thinner film thicknesses were obtained for cured films compared to uncured films most likely due to the loss of mass in the secondary condensation step.

Table 3. Contact angles of different surface coatings on different substrates (hybrid polymers were spin coated from 10 wt% THF solution and cured at 130 °c for 1h).

hybrid polymer	advancing contact angle [°]					
	Si	glas	steel	copper	PC	PMMA
without coating	42	9	92	114	98	70
PMSSQ-PMA	108	104	102	104	107	106
PPSSQ-PMA	92	91	92	96	91	91
POSSQ-PMA	112	110	111	110	117	123
PODSSQ-PMA	120	115	110	116	119	118
PFOSSQ-PMA	129	130	127	125	128	123

* Average value of 20 individual measurements, error range $\pm 3^\circ$.

As described in the introduction, ideal coating materials should be applicable on a wide range of substrates, i.e. stable and adherent films should be formed on any surface type. Different hybrid polymers were spin coated from a 10 wt% solution in THF as described above on silicon, glass, steel, copper, polycarbonate and poly(methyl methacrylate) surfaces. The successful surface coating of the substrate was analyzed by contact angle measurement and the results are summarized in table 3. While the advancing contact angles of water on different substances vary dramatically, depending on the nature of the material, all surfaces showed after coating with the respective hybrid polymers similar advancing contact angles. In other words, the contact angle is determined only by the hybrid coating agent used and not by the substrate, indicating not only a successful surface modification but also the potential of hybrid polymers as coating materials. Depending on the chemical compositions of the hybrid polymer, the obtained contact angles change. The highest contact angles could be measured for PSOSSQ-PMA, with contact angles well above 120°. Clearly, this high contact angle is due to

the influence of the perfluorinated chains. The lowest contact angles were found for PPSSQ-PMA with contact angles above 90°, which can be assigned to the nature of the phenyl substituents.

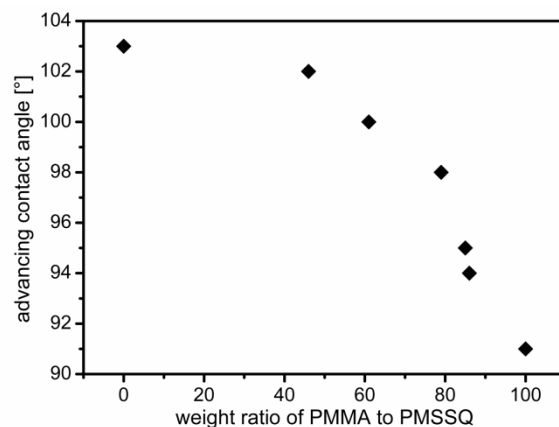


Figure 4. Influence of the variation of the organic to inorganic weight ratio on the observed contact angle after spin coating on a silicon substrate (spin-coated from 10 wt% solution in THF).

The influence of the inorganic/organic ratio of the hybrid polymer on the observed contact angle was measured using the different PMSSQ-PMMA hybrids as summarized in table 2. The weight ratio of the PMMA fraction was varied from 46% to 86%. As shown in figure 4, the observed contact angle showed a nonlinear transition from 103° (pure PMSSQ) to 91° (pure PMMA). This nonlinear behavior indicated that the composition on the surface does not necessarily match with the bulk composition of the hybrid polymer and is rather dominated by the fraction of lower surface energy, in this case PMSSQ. A similar trend was also found for POSSQ-PMA coatings.

The stability of the film and the adhesion on the substrate was tested using an ISO tape test³⁴. The tested surfaces were classified using the classification given in ISO standard procedure, i.e. 0 indicates absolute no tearing, 5 indicates a detachment of more than 50% coating material (see table S2, supplementary information). Before curing, all surface coatings could easily be detached from the surface. After the thermal crosslinking of the hybrid polymer thin films, all coatings showed a complete adhesion independent of the tested substrate, thereby proving their potential use as robust coating materials.

Conclusions

New organic/inorganic hybrid polymers were prepared using RAFT polymerization as a key process to link organic polymers with an inorganic precursor polymer. Two different RAFT agents were prepared. Both of them could be incorporated in a soluble silsesquioxane macro CTA. A wide spectrum of vinyl-type monomers could be polymerized into the organic block by tuning the molecular architecture of the polymeric CTAs. To enlarge the functionality of the organic block random co-polymerization was also investigated. As an example, UV cross-linkable monomers could be incorporated in the hybrid polymer. It is possible to control the block ratios between inorganic and organic blocks by adjusting the initial ratio of macro

initiator and organic monomer before polymerization. The flexibility in the synthesis of the inorganic block was shown by using different tri-functionalized monomers in the co-condensation step to build up different macro initiators. The inorganic block can be tuned towards many properties by condensing the desired monomers. The used silsesquioxane has no significant influence on the following polymerization. PMA and PEHA hybrid polymers could be obtained from alkyl-, aryl- or fluorinated alky-substituted macro initiators. These experiments prove the high variability of the synthetic concept to build up hybrid materials. The properties in the inorganic and the organic block can be adjusted easily. An easy control of the block ratio could be proved by thermo gravimetric measurements. As these materials are supposed to be used as coating materials their ability to crosslink was determined by silicon solid state NMR techniques. After the polymerization usually more than 30 % of the silicon branches are still able to undergo a secondary condensation and so guarantee a crosslinking or bonding to metal or metal oxide substrates. Surface coatings could be processed on a wide range of different substrates. A successful surface functionalization could be determined via contact angle measurements. Beside silicon and glass wafers metals like steel and copper as well as polymeric surfaces like PMMA or PC could be coated very stable. The presented concept to produce highly variable hybrid polymers still having enough reactivity to fully crosslink, seems to fulfill the requirements on an ideal coating material.

Acknowledgement

The authors thank Young Joo Lee (Max Planck Institute for Polymer Research) and Bernd Mathiasch (Institute of Inorganic Chemistry, University of Mainz) for ^{29}Si CPMAS NMR measurements and for valuable discussions. Initial financial support from University of Mainz and FCI is gratefully acknowledged. Bayer MaterialScience AG, Leverkusen, is acknowledged for financial and scientific support.

Supporting Information Available

^{29}Si CPMAS NMR spectra of macro initiator 1 (MI-1) and macro initiator 2 (MI-2), molecular weight distributions of PMSSQ-PMMA containing 5% of (9), a list of synthesized polymers and the tape test results can be found in the supporting information. This information is available free of charge via the Internet at <http://pubs.acs.org>.

References

- (1) Mansky, P.; Liu, Y.; Huang, E.; Russell, T. P.; Hawker, C. J. *Science* **1997**, *275*, 1458-1460.
- (2) Wiltzikus, P.; Cumming, A. *Phys. Rev. Lett.* **1991**, *66*, 3000-3003.
- (3) Coulon, G.; Russell, T. P.; Deline, V. R.; Green, P. F. *Macromolecules* **1989**, *22*, 2581-2589.
- (4) Anastasiadis, S. H.; Russell, T. P.; Satija, S. K.; Majkrzak, C. F. *Phys. Rev. Lett.* **1989**, *62*, 1852-1855.
- (5) Genzer, J.; Efimenko, K. *Science* **2000**, *290*, 2130-2133.
- (6) Chaudhury, M. K.; Whitesides, G. M. *Science* **1992**, *256*, 1539-1451.

- (7) Chen, C. S.; Mrksich, M.; Huang, S.; Whitesides, G. M.; Ingber, D. E. *Science* **1997**, 276, 1425-1428.
- (8) Russell, T. P. *Science* **2002**, 297, 964-967.
- (9) Luten, H. A.; Bohland, J. R. *U.S. Pat. Appl. Publ.* **2006**, US 2006228566 A1 20061012.
- (10) Ryu, D. Y.; Shin, K.; Drockenmuller, E.; Hawker, C. J.; Russell, T. P. *Science* **2005**, 308, 236-239.
- (11) de Boer, B.; Simon, H. K.; Werts, M. P. L.; van der Vegte, E. W.; Hadziioannou, G. *Macromolecules* **2000**, 33, 349-356.
- (12) Choi, M.; Shea, K. J. *Plast. Eng. (N.Y.)* **1998**, 49, 437.
- (13) Kraus, A.; Schneider, M.; Gugel, A.; Mullen, K. *Journal of Materials Chemistry* **1997**, 7, 763-766.
- (14) Miller, R. D. *Science* **1999**, 286, 421-423.
- (15) Singer, P. *Semicond. Int.* **1998**, June, 90.
- (16) Ro, H. W.; Kim, K. J.; Theato, P.; Gidley, D. W.; Yoon, D. Y. *Macromolecules* **2005**, 38 (3), 1031-1034.
- (17) Brown, J. F.; Vogt, L.; Katchman, A.; Euslance, K.; Kriser, K. *J. Am. Chem. Soc.* **1960**, 6294-6195.
- (18) Zhang, Y.; Luo, S.; Liu, S. *Macromolecules* **2005**, 38, 9813-9820.
- (19) Mellon, V.; Rinaldi, D.; Bourgeat-Lami, E.; D'Agosto, F. *Macromolecules* **2005**, 38, 1591-1598.
- (20) Kron, J.; Amberg-Schwab, S.; Schottner, G. *Journal of Sol-Gel Science and Technology* **1994**, 2(1/2/3), 189-192.
- (21) Zhang, L.; Abbenhuis, H. C. L.; Yang, Q.; Wang, Y.-M.; Magusin, P. C. M. M.; Mezari, B.; van Santen, R. A.; Li, C. *Angew. Chem. Int. Ed.* **2007**, 46, 5003-5006.
- (22) Xu, H.; Kuo, S.-W.; Lee, J.-S.; Chang, F.-C. *Macromolecules* **2002**, 35, 8788-8798.
- (23) Zhang, C.; Laine, R. M. *J. Am. Chem. Soc.* **2000**, 122, 6979-6988.
- (24) Pyun, J.; Miller, P. J.; Kickelbick, G.; Matyjaszewski, K.; Schwab, J.; Lichtenhahn, J. *Polymer Preprints* **1999**, 40, 454-455.
- (25) Huang, C.-F.; Kuo, S.-W.; Lin, F.-J.; Huang, W.-J.; Wang, C.-F.; Chen, W.-Y.; Chang, F.-C. *Macromolecules* **2006**, 39, 300-308.
- (26) Costa, R. O. R.; Vasconcelos, W. L.; Tamaki, R.; Laine, R. M. *Macromolecules* **2001**, 34, 5398-5407.
- (27) Cardoen, G.; Coughlin, E. B. *Macromolecules* **2004**, 37, 5123-5126.
- (28) Zheng, L.; Hong, S.; Cardoen, G.; Burgaz, E.; Gido, S. P.; Coughlin, E. B. *Macromolecules* **2004**, 37, 8606-8611.
- (29) Simon, P. F.; Ulrich, R.; Spiess, H. W.; Wiesner, U. *Chem. Mater.* **2001**, 13, 3464-3486.
- (30) Patwardhan, S. V.; Clarson, S. J.; Perry, C. C. *Chem. Commun.*, **2005**, 1113-1121.
- (31) Patwardhan, S. V.; Mukherjee, N.; Clarson, S. J. *J. Inorg. Organomet. Polym.*, **2001**, 11, 193-198.
- (32) Theato, P.; Kim, K. J.; Yoon, D. Y. *Phys. Chem. Chem. Phys.* **2004**, 6, 1458-1462.

- (33) Prucker, O.; Naumann, C. A.; Ruehe, J.; Knoll, W.; Frank, C. W. *J. Am. Chem. Soc.* **1999**, *121*, 8766-8770.
- (34) Paints and varnishes – Cross-cut test (ISO 2409:2007).
- (35) Tripp, C. P.; Hair, M. L. *Langmuir* **1991**, *7*, 923-927.
- (36) Tripp, C. P.; Hair, M. L. *Langmuir* **1992**, *8*, 1961-1967.
- (37) Tripp, C. P.; Hair, M. L. *J. Phys. Chem.* **1993**, *97*, 5693-5698.
- (38) Combes, J. R.; White, L. D.; Tripp, C. P. *Langmuir* **1999**, *15*, 7870-7875.
- (39) Gunji, T.; Iizuka, Y.; Arimitsu, K.; Abe, Y. *J. Poly. Sci. A* **2004**, *42*, 3676-3684.

Supporting information

Figure S1:

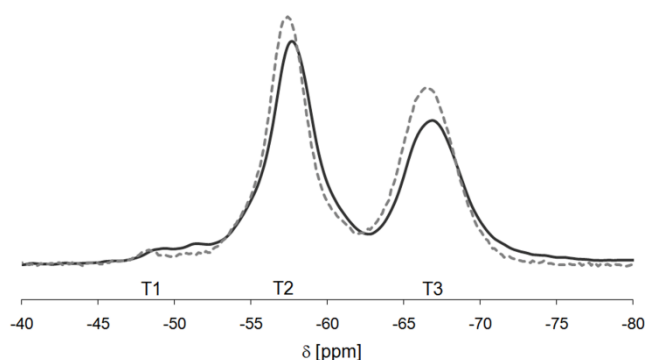


Figure S1. ^{29}Si solid state NMR spectra of MI 1 (dashed line) and MI 2 (solid line).

Figure S2:

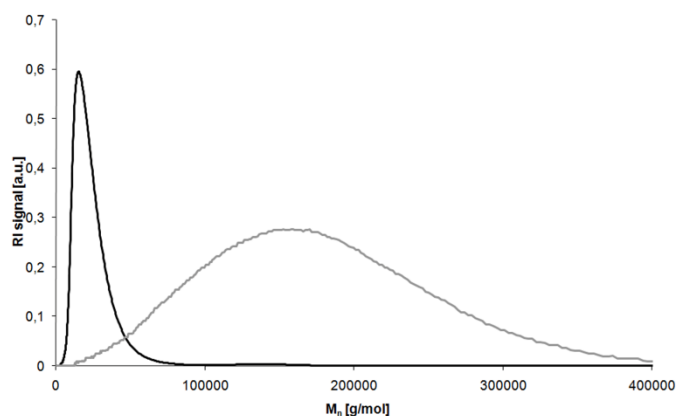


Figure S2. Molecular weight distribution of PMSSQ-PMMA containing 5% of (9). The black curve was measured directly after polymerization, the grey curve was observed after 5 min irradiation with UV light.

4.3

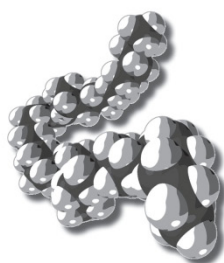
Synthesis of Defined Poly(silsesquioxane)s: Fast Polycondensation of Trialkoxysilanes in a Continuous-Flow Microreactor*Daniel Kessler, Holger Löwe, Patrick Theato**

Institute of Organic Chemistry, University of Mainz, Duesbergweg 10-14, 55099 Mainz, Germany

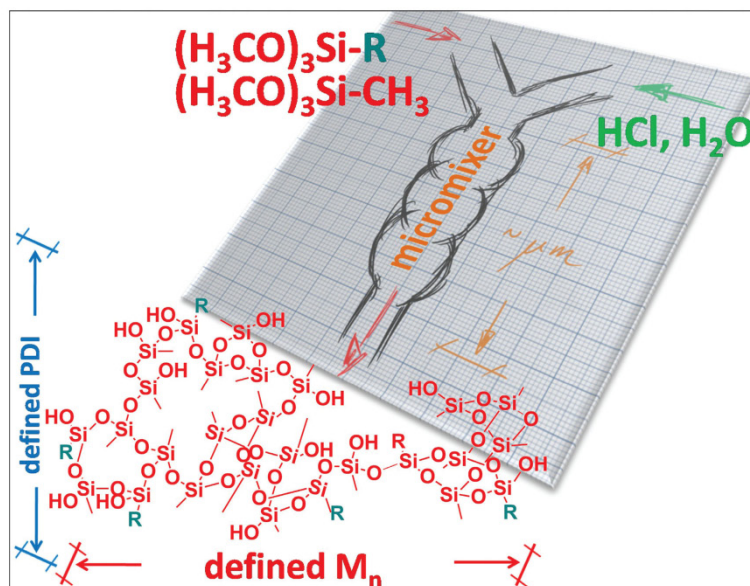
Macromol. Chem. Phys. **2009**, *210*(10), 807-813.Coverage *Macromol. Chem. Phys.* **2009**, *210*(10):

ISSN 1022-1352 · MCHPES 210 (10) 801-892 (2009) · Vol. 210 · No. 10 · May 22, 2009

D 51046

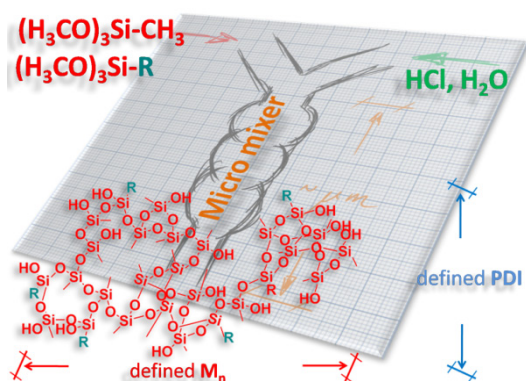


Macromolecular Chemistry and Physics

Founded by
Hermann Staudinger

10/2009

WILEY-VCH



Abstract

Continuous flow processes involving microreactors found various applications in chain growth polymerization whereas its influence on step growth polymerization is less explored and especially the polycondensation of multifunctional monomers has not been investigated in detail yet. We could now successfully perform the polycondensation of trialkoxy silanes to poly(silsesquioxanes) in a micro-reactor setup. Yields were significantly increased, whereas the polydispersity of the obtained polymers decreased in comparison to the batch process. By residence time variation molecular weights could be adjusted reproducibly ranging from $M_n=1900$ g/mol to $M_n=11000$ g/mol. Thus, the microreactor setup offers for the first time the possibility to synthesize poly(silsesquioxane) with adjustable properties.

Keywords

polycondensation, poly(silsesquioxanes), inorganic polymers, microreactor, continuous flow

Introduction

Micro fluidic devices offer an interesting potential for a wide range of organic syntheses due to superior heat exchange, fast effective mixing, wide tolerance towards reaction conditions and facile control of important parameters, affording higher yields and better product quality in a continuous process.^[1,2] Recently, continuous flow processes involving microreactors are used in various polymer syntheses. Capillary microreactors equipped with T-shaped micromixers and different flow sections can significantly improve the control of molecular weight and molecular weight distributions in free radical polymerizations of various acrylates and methacrylates.^[3,4]

Also controlled radical polymerization methods, like atom transfer radical polymerization (ATRP), nitroxide-mediated polymerization (NMP) and reversible addition-fragmentation chain transfer (RAFT) polymerization, could successfully be carried out in micro fluidic continuous flow set-ups.^[5,6,7,8] Those methods intrinsically offer the chance to produce well defined block copolymers, which has been also realized by connecting two microreactors in series.^[9,10] Ionic polymerizations performed in microreactors benefit from the fact that a microreactor provides a closed setup and accordingly prevents any influx of water or other impurities. Wurm et al. recently presented a versatile process for living carbanionic polymerization with subsequent functional termination or diblock synthesis.^[11]

Reviews by Hessel et al.^[12] and Wilms et al.^[13] give an excellent overview concerning various polymerization methods in micro fluidic devices. The synthesis of polymer particles with an improved control over their sizes, size distributions, morphologies, and compositions using microreactors was summarized in a review published by Serra and Chang.^[14]

Micro fluidic devices found various applications in chain growth polymerization whereas its influence on step growth polymerizations is less explored. Even though, Wilms et al. could successfully apply microreactors in the synthesis of hyperbranched polyglycerol with reduced reaction times and experimental effort compared to classical batch methods,^[15] classical step growth polymerization of multifunctional monomers has not been investigated in detail yet. Poly(silsesquioxane), prepared by polycondensation of trifunctional silanols, are emerging materials for various applications ranging from low dielectric constant materials in microelectronic devices^[16,17] to flame retardant materials.^[18]

We recently demonstrated a synthetic pathway to produce inorganic-organic hybrid polymers consisting of poly(silsesquioxane) (PSSQ) and various organic polymers and their ability to produce stable and adherent surface coatings.^[19,20] The challenge in the synthesis of soluble PSSQ is to allow polycondensation, but to avoid macroscopic gelation, which would lead to insoluble materials due to extended reaction times or imperfect temperature control. Thus, the reaction seems to be a promising candidate to benefit from a continuous flow process in micromixer devices.

Within this paper, the polycondensation of trialkoxysilanes will be conducted in a microreactor device and the influence of residence time variation on the polymer properties will be studied.

Experimental Part

Materials. All chemicals and solvents were commercially available and used as received unless otherwise stated. THF was freshly distilled from sodium/benzophenone under nitrogen. All batch reactions were performed in argon atmosphere.

p-(Chlormethyl)-phenylethyltrimethoxysilane (1), dithiobenzoic acid benzyl-(4-ethyltrimethoxysilyl) ester (2) and dithio benzoic acid 1-ethylphenyl-4-(ethyltrimethoxysilyl) ester (3) were synthesized as published in reference [20].

Instrumentation. All ^1H spectra and ^{13}C NMR were recorded on a Bruker 300 MHz FT-NMR spectrometer. ^{29}Si CPMAS NMR spectra were measured on a Bruker DSX 400 MHz FT-NMR spectrometer (Rotation: 5000 Hz, T = RT, 4 mm rotor). Chemical shifts (δ) were given in ppm relative to TMS. Gel permeation chromatography (GPC) was used to determine molecular weights and molecular weight distributions, M_w/M_n , of polymer samples with respect to polystyrene standards (PSS). (THF used as solvent, polymer concentration: 2 mg/mL, column setup: MZ-Gel-SDplus 10^2 \AA^2 , 10^4 \AA^2 and 10^6 \AA^2 , used detectors: refractive index, UV and light scattering).

***N,N*-Diethyl-dithiocarbamoyl-ethylphenyl-(trimethoxy)-silane (4).**

7 g (25.5 mmol) of sodium *N,N*-diethyl-dithiocarbamate in 10 mL THF were added to a solution of 4.37 g (25.5 mmol) of (1) in 10 mL THF and magnetically stirred for 5 h at room temperature. The solution was filtered and the solvent was removed under reduced pressure. The crude product was purified by Kugelrohr distillation at 250°C and $3 \cdot 10^{-3}$ mbar.

Yield 7.12 g (18.4 mmol; 72.1%). ^1H NMR (CDCl_3 , δ): 7,27 (d, 3J = 7,8 Hz, 2H); 7,14 (d, 3J = 7,8 Hz, 2H); 4,47 (s, 2H); 4,01 (quad., 3J = 7,2 Hz, 2H); 3,70 (quad., 3J = 7,2 Hz, 2H); 3,54 (s, 9H); 2,67 (t, 3J = 8,7 Hz, 2H); 1,26 (m, 6H); 0,96 (t, 3J = 8,7 Hz, 2H). ^{13}C NMR (CDCl_3 , δ): 195,32; 143,60; 133,11; 129,35; 127,95; 50,48; 49,31; 46,63; 41,98; 28,28; 12,40; 11,53; 11,12.

Poly(methylsilsesquioxane) (PMSSQ). Polycondensation reactions of methyltrimethoxysilane (MTMS) in batch reactions were carried out as explained in references [19] and [20].

^1H NMR (CDCl_3 , δ): 6.2 – 5.4 (br, Si-OH); 3.5 (br, Si-O-CH₃); 0.13 (br, Si-CH₃). ^{13}C NMR (CDCl_3 , δ): 69.05 (Si-O-CH₃); -2.11 (Si-CH₃). ^{29}Si CPMAS NMR (δ): -47.00 (T1); -59.39 (T2); -67.88 (T3).

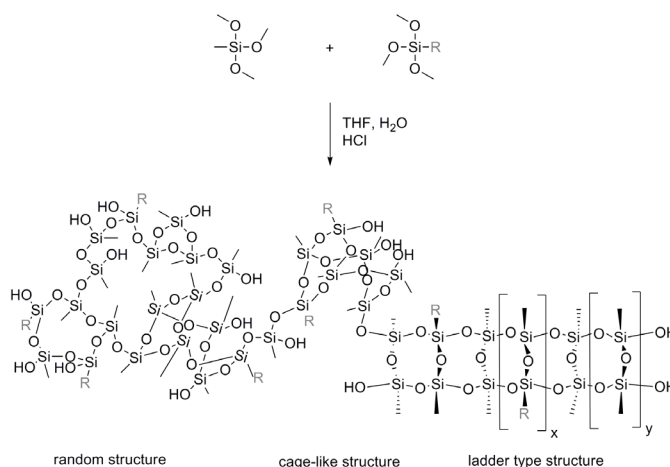
Polycondensation in microreactor. The co-condensation reaction was performed in a bench scale plant. It consisted of two syringe pumps (Braun Perfusor Secura), two preheating loops (3 m) a caterpillar split-recombine micromixer (IMM CPMM-R300/12-PEEK) provided by the Institut für Mikrotechnik (IMM, Mainz, Germany) and tubes of different lengths (1m, 3m, 6m, 9m or 12m, respectively) to adjust certain residence times. The whole setup was kept at constant temperature using a cryostat (Julabo FP 50). As loop material Mecanyl tubes (Mecano Bundy GmbH, inner diameter 0.5 mm, outer diameter 1.5mm) were used. A 20 mL syringe was filled with 28.6 mmol MTMS (3.9 g), 1.43 mmol trifunctional Initiator and 7.25 g THF. A second 20 mL syringe was filled with 286 mmol water (5.15 g), 2.3 mmol HCl (0.285 mL, 2N) and 3.5 mL THF. The feed rate was kept constant at 53.64 mL/h. After passing the delay loop the reaction was quenched by dropping the solution in a liquid nitrogen cooled flask. Immediately

after the run was completed, a GPC sample was prepared by dilution with THF to prevent further condensation.

Results and discussion

The condensation of trialkoxysilanes under very specific conditions yields in molecules with perfect cubic symmetry (T_8 , $(RSiO_{1.5})_8$), offering various applications as nano building blocks.^[21,22,23] But those fully condensed silsesquioxane T_8 -cages lost their ability to undergo further condensation or cross-linking. The synthesis of “random” poly(methyltrimethoxysilanes) (PMSSQ) with free silanol groups starting from methyltrimethoxysilane (MTMS) under acidic catalysis would usually yield in highly cross-linked, completely insoluble materials. To avoid macroscopic gelation, the synthesis has to be performed in dilute solution, the amount of catalyst has to be adjusted and the reaction has to be quenched before reaching macroscopic gelation.^[24] Polycondensation kinetics of trimethoxy/triethoxy functionalized organosilanes concerning acceleration and cyclization processes were intensively studied by Macosko and coworkers,^[25-28] demonstrating that the microstructure of the obtained Poly(silsesquioxanes) depend strongly on the procedure and on the trialkoxysilane used.

Scheme 1. Co-condensation of MTMS and a trimethoxysilyl functionalized initiator, offering the possibility of further PMSSQ modification.



We recently demonstrated a synthetic concept to graft vinyl monomers from a soluble PMSSQ-ATRP-Initiator^[19] or from a PMSSQ-RAFT chain transfer agent.^[20] In the first step a condensation of MTMS with a functional trialkoxysilane – capable of initiating a grafting-from polymerization afterwards – was performed. The co-condensation of MTMS and the functional trialkoxysilane has to produce soluble PMSSQ, possessing enough free silanol groups, which can be cross-linked in a secondary condensation step afterwards to create stable and insoluble materials on demand (i.e. to create very stable and adherent surface coatings as explained in the references given).

Especially the co-condensation step of MTMS with a functional trialkoxysilane (see scheme 1) is crucial and thus a reproducible control of molecular weight is highly desired, however, very difficult to obtain by a classical batch synthesis in a round bottom flask. Even though the ratio of MTMS and the functionalized trialkoxysilane could be adjusted very well and controlled in the batch synthesis, we observed a not satisfying control over molecular weight and PDI.

Therefore, the co-condensation step has been studied using microreactors in order to achieve a better thermal control and to reduce mass transfer effects during the polycondensation, which should result in improved control over molecular weight. Both, the synthesis in a batch process and the synthesis in a microreactor will be compared in respect to reaction temperature and residence time/reaction time.

Batch process. First, we performed 20 identical batch reactions using 28.6 mmol MTMS, 1.43 mmol (1), 10.75 g THF, 286 mmol water and 0.285 mL 2N HCl (same amounts as used in microreactor synthesis) at 0°C and at 20°C for 3 h each. The obtained molecular weights (M_n) were measured using GPC without any further workup.

When the synthesis was done at 0°C in a flask, the obtained molecular weights varied between 1100 g/mol and 9220 g/mol, with an average molecular weight of 4450 g/mol and the standard deviation 2888 g/mol. In comparison the synthesis conducted at 20 °C resulted in molecular weights varying between 1050 g/mol and 10900 g/mol, with an average molecular weight of 6300 g/mol, standard deviation 3184 g/mol. The molecular weight distribution was found to be usually between 2.2 and 3.

The residual amount of free silanol groups in the PMSSQ network, which is a first indication of the internal microstructure of the obtained PMSSQ, was determined by ^{29}Si CPMAS NMR spectroscopy. In all synthesized PMSSQs the amount of T1 branches (two free OH groups per Si) was in average 5% ($\pm 2\%$), the amount of T2 branches (one free OH group per Si) was in average 50% ($\pm 12\%$) and the amount of fully condensed T3 branches (no free OH group per Si) was in average 45% ($\pm 10\%$).

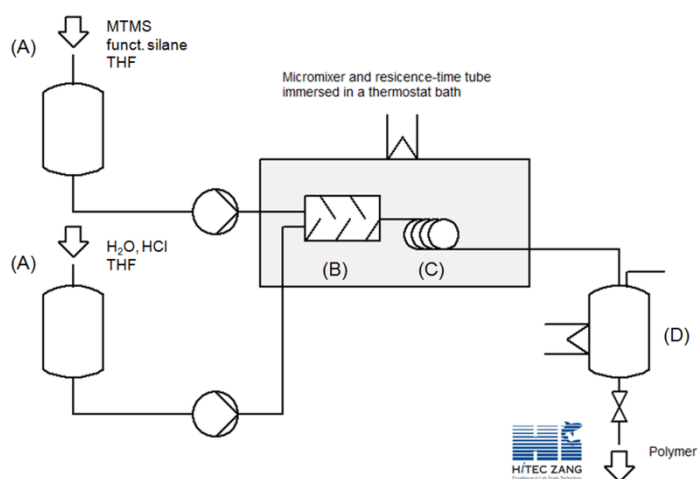
The batch reaction was able to produce soluble PMSSQ with a large amount of free silanol groups, i.e. T1 and T2 branches together account for more than 50%. But almost no control of molecular weight had been possible; molecular weights varied between 1000 and 10000 g/mol, even though the synthesis was always carried out in exactly the same way. Beside the large variation in molecular weights or molecular weight distribution, also the yields varied between 0.7 g and 2.0 g (31 - 90%).

Microreactor process. To overcome those disadvantages, we used a microreactor setup, as shown in scheme 2, in order to keep most reaction parameters constant, to guarantee a very effective mixing of monomer and catalyst and to study the influence of the residence time after mixing.

The co-condensation process was performed using different trimethoxysilyl functionalized initiating species: *p*-(chloromethyl)-phenylethyltrimethoxysilane (1) to act as PMSSQ-ATRP macroinitiator, dithiobenzoic acid benzyl-(4-ethyltrimethoxysilyl) ester (2) and dithio benzoic acid 1-ethylphenyl-4-(ethyltrimethoxysilyl) ester (3), which have been shown to act as PMSSQ-

RAFT chain transfer agents in grafting from polymerization, and *N,N*-diethyl-dithiocarbamoyl-ethylphenyl-(trimethoxy)-silane (4), which can initiate a grafting from polymerization using the inifiter method.^[29]

Scheme 2. Microreactor setup:
(A) syringe pumps; (B) IMM micromixer; (C) delay loops; (D) cooled flask.



The first pump was filled with MTMS, the functionalized initiator and THF, while the second pump was filled with water, 2N HCl and THF. A constant feed rate was set at 53.64 mL/h. After passing the preheating loops, all reactants were mixed using a caterpillar split-recombine micromixer. The delay loop was varied between 1 m and 12 m, which is equivalent to a residence time between 0.22 min and 2.64 min. After passing the delay loop, the reaction was quenched by dropping into a collecting flask, cooled in a liquid nitrogen bath. The molecular weights (M_n) were measured by GPC after dilution with THF in order to prevent further polycondensation.

The obtained molecular weights are summarized in Table 1. The dependence of the molecular weight on the residence time for the co-condensation of MTMS with (4) conducted at 0 °C and 20 °C is exemplarily shown in figure 1. In all cases soluble poly(methylsilsesquioxanes) were obtained. Regardless of the chemical nature of the trialkoxysilanes used in the co-condensation, the molecular weight was always linearly dependent on the residence time. With longer residence times higher molecular weights were obtained. In all cases the molecular weight distribution was found to be below 2. The yields varied only between 1.69 g and 2.29 g, and were significantly higher than in the batch process.

To demonstrate the reproducibility of the microreactor synthesis, three individual runs of a polycondensation reaction at 0 °C and at 20 °C were performed with 0.22 min, 1.32 min and 2.64 min residence time, respectively, and the results are given in Table 2. The standard deviation of all obtained molecular weights was 3.4%, while the standard deviation of the obtained molecular weight distribution was 2.4%. Also the standard deviation of the yields was found to be extremely small with 4.2%. In comparison to the batch process, which showed a

standard deviation of the molecular weight larger than 50%, the microreactor setup offers the possibility to obtain in very reproducible way PMSSQ with precisely adjustable molecular weights.

Table 1. Obtained molecular weights, PDI and yields in microreactor synthesis.

used initiator	T [°C]	residence time [min]	M _n [g/mol]	PDI	Yield [g]
(1)	0	0.22	1900	1.47	1.91
(1)	0	0.66	3450	1.49	1.82
(1)	0	1.32	4350	1.50	2.02
(1)	0	1.98	6250	1.54	2.19
(1)	0	2.64	8400	1.59	2.01
(1)	20	0.22	2700	1.71	2.02
(1)	20	0.66	4650	1.63	2.25
(1)	20	1.32	7000	1.79	2.05
(1)	20	1.98	8200	1.89	2.12
(1)	20	2.64	9550	1.93	2.21
(2)	0	0.22	2100	1.46	1.89
(2)	0	0.66	3400	1.59	1.95
(2)	0	1.32	4250	1.61	1.92
(2)	0	1.98	5800	1.62	1.91
(2)	0	2.64	8200	1.69	2.02
(2)	20	0.22	3200	1.79	2.15
(2)	20	0.66	4500	1.77	2.13
(2)	20	1.32	6050	1.81	2.05
(2)	20	1.98	7800	1.82	2.21
(2)	20	2.64	9700	1.87	2.25
(3)	0	0.22	2200	1.53	1.71
(3)	0	0.66	3950	1.59	1.85
(3)	0	1.32	4900	1.58	1.79
(3)	0	1.98	7050	1.68	1.92
(3)	0	2.64	8900	1.65	1.99
(3)	20	0.22	3400	1.71	2.11
(3)	20	0.66	5200	1.78	2.07
(3)	20	1.32	7200	1.82	2.29
(3)	20	1.98	9200	1.83	1.98
(3)	20	2.64	10100	1.92	2.20
(4)	0	0.22	2250	1.39	1.69
(4)	0	0.66	3900	1.48	1.82
(4)	0	1.32	5050	1.47	1.93
(4)	0	1.98	6750	1.55	1.88
(4)	0	2.64	8100	1.61	1.79
(4)	20	0.22	3700	1.87	2.09
(4)	20	0.66	4550	1.92	2.22
(4)	20	1.32	7600	1.92	2.25
(4)	20	1.98	8900	1.98	2.13
(4)	20	2.64	11000	1.95	1.97

Table 2. Reproducibility experiments for 0.22 min, 1.32 min and 2.64 min residence time (3 individual runs each).

used initiator	T [°C]	residence time [min]	average M_n [g/mol]	standard deviation M_n [g/mol]	average PDI	standard deviation PDI	average Yield [g]	standard deviation Yield [g/mol]
(1)	0	0.22	1933	104	1.50	0.03	1.96	0.04
(1)	0	1.32	4317	104	1.52	0.02	1.99	0.03
(1)	0	2.64	8533	126	1.56	0.05	2.10	0.10
(1)	20	0.22	3183	176	1.70	0.02	2.09	0.07
(1)	20	1.32	7150	304	1.81	0.02	2.04	0.06
(1)	20	2.64	9633	104	1.91	0.02	2.13	0.07
(2)	0	0.22	2183	236	1.45	0.05	1.93	0.05
(2)	0	1.32	4250	150	1.64	0.03	1.97	0.05
(2)	0	2.64	8183	126	1.70	0.08	2.00	0.11
(2)	20	0.22	3150	50	1.75	0.04	2.03	0.10
(2)	20	1.32	6083	104	1.78	0.05	2.00	0.13
(2)	20	2.64	9617	76	1.83	0.04	2.14	0.13
(3)	0	0.22	2150	50	1.54	0.04	1.78	0.13
(3)	0	1.32	4867	104	1.60	0.05	1.87	0.11
(3)	0	2.64	8900	200	1.66	0.03	2.05	0.06
(3)	20	0.22	3583	161	1.81	0.09	2.01	0.10
(3)	20	1.32	7317	340	1.85	0.04	2.18	0.11
(3)	20	2.64	10000	100	1.97	0.05	2.20	0.11
(4)	0	0.22	2250	150	1.43	0.05	1.73	0.05
(4)	0	1.32	5083	104	1.47	0.03	1.90	0.11
(4)	0	2.64	8133	202	1.66	0.06	1.77	0.05
(4)	20	0.22	3750	229	1.92	0.05	1.99	0.09
(4)	20	1.32	7533	208	1.92	0.04	2.18	0.08
(4)	20	2.64	10667	416	1.93	0.02	2.09	0.12

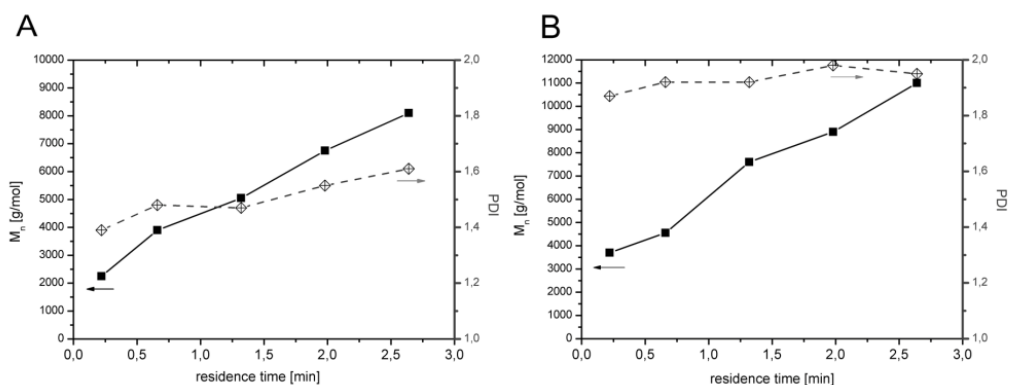


Figure 1. Dependence of the molecular weight on the residence time of the co-condensation of MTMS and (4). (A): T = 0°C; (B): T = 20°C (Black solid line: molecular weight, grey dashed line: M_w/M_n).

Similar to the polymers obtained in the batch process, the amount of free silanol groups was checked by ²⁹Si CPMAS NMR spectroscopy. The solid black line in figure 2 shows exemplarily the ²⁹Si NMR spectrum of the PMSSQ obtained via co-condensation of MTMS and (4) at 20°C and 2.64 min residence time. In comparison the dashed grey line in figure 2 shows the ²⁹Si NMR spectrum of PMSSQ, which was obtained after batch synthesis using the same conditions. Integration of peaks in the ²⁹Si NMR spectrum of the PMSSQ obtained via co-condensation of MTMS and (4) at 20°C yields 8% T1 branches, 67% T2 branches and 25% T3 branches. This is slightly higher than the values measured for the same PMSSQ prepared in the respective batch process (batch process: 6% T1; 62% T2; 32% T3).

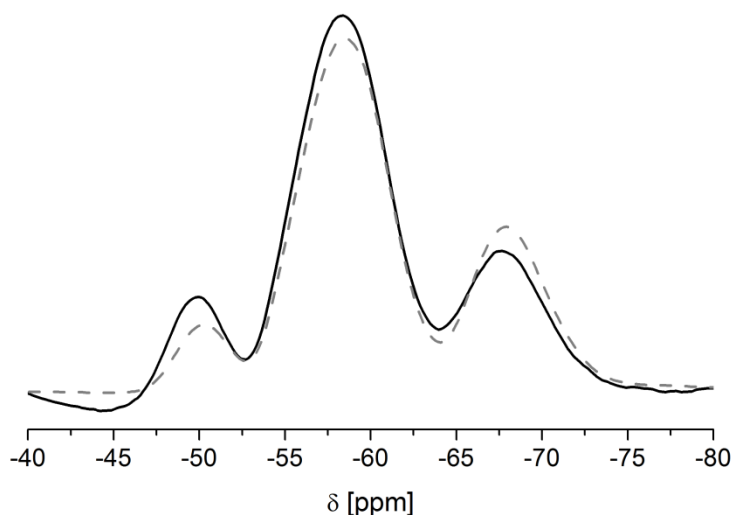


Figure 2. Solid black line: ²⁹Si CPMAS NMR spectra of the polymer obtained by the co-condensation of MTMS and (4) at 20°C and 2.64 min residence time. Dashed grey line: ²⁹Si CPMAS NMR spectra of the polymer obtained by co-condensation and (4) in batch synthesis.

Conclusions

The polycondensation reaction of trimethoxysilanes could successfully be performed in a microreactor setup. Taking advantage of the fast mixing and the well adjustable reaction parameters, well-defined polymers of those trifunctional monomers with adjustable molecular weight could be obtained. Molecular weight distributions could be decreased whereas at the same time yields could be reproducibly increased. The very precise adjustment of the residence time in the micromixer enabled the synthesis of poly(methylsilsequioxanes) with defined molecular weights for the first time.

Acknowledgments

D.K. gratefully acknowledges financial support from the FCI.

References

- [1] K. Jähnisch, V. Hessel, H. Löwe, M. Baerns, *Angew. Chem. Int. Ed.* **2004**, *43*, 406.
- [2] T.-H. Yoon, S.-H. Park, K.-I. Min, X. Zhang, S. J. Haswell, D.-P. Kim, *Lab on a Chip* **2008**, *8*, 1454.
- [3] T. Iwasaki, J. Yoshida, *Macromolecules* **2005**, *38*, 1159.
- [4] C. Serra, G. Schlatter, N. Sary, F. Schonfeld, G. Hadziioannou, *Microfluidics and Nonfluidics* **2007**, *3*, 451.
- [5] Y.Q. Shen, S. P. Zhu, R. Pelton, *Macromol. Rapid Commun.* **2000**, *21*, 956.
- [6] T. E. Enright, M. F. Cunningham, B. Keoshkerian, *Macromol. Rapid Commun.* **2005**, *26*, 221.
- [7] C. Rosenfeld, C. Serra, C. Brochon, G. Hadziioannou, *Chemical Engineering Science* **2007**, *62*, 5245.
- [8] J. P. Russum, C. W. Jones, F. J. Schork, *Macromol. Rapid Commun.* **2004**, *25*, 1064.
- [9] Y.O. Shen, S. P. Zhu, *AIChE J.* **2002**, *48*, 2609.
- [10] C. Rosenfeld, C. Serra, C. Brochon, G. Hadziioannou, *Lab on chip* **2008**, *8*, 1682.
- [11] F. Wurm, D. Wilms, J. Klos, H. Löwe, H. Frey, *Macromol. Chem. Phys.* **2008**, *209*, 1106.
- [12] V. Hessel, C. Serra, H. Löwe, G. Hadziioannou, *Chemie Ingenieur Technik* **2005**, *77*, 1693.
- [13] D. Wilms, J. Klos, H. Frey, *Macromol. Chem. Phys.* **2008**, *209*, 343.
- [14] C. A. Serra, Z. Chang, *Chem. Eng. Technol.* **2008**, *31*, 1099.
- [15] D. Wilms, J. Nieberle, J. Klos, H. Löwe, H. Frey, *Chem. Eng. Technol.* **2007**, *30*, 1519.
- [16] R. D. Miller, *Science* **1999**, *286*, 421.
- [17] A. Kraus, M. Schneider, A. Gügel, K. Müllen, *J. Mater. Chem.* **1997**, *7*, 763.
- [18] C.L. Chiang, C.C.M. Ma, *J. Polym. Sci. Part A: Polym. Chem.* **2003**, *41*, 1371.
- [19] D. Kessler, C. Teutsch, P. Theato, *Macromol. Chem. Phys.* **2008**, *209*, 1437.
- [20] D. Kessler, P. Theato, *Macromolecules* **2008**, *41*, 5237.
- [21] M. Z. Asuncion, R. M. Laine, *Macromolecules* **2007**, *40*, 555.
- [22] M. Z. Asuncion, M. F. Roll, R. M. Laine, *Macromolecules* **2008**, *41*, 8047.
- [23] S. Sulaiman, A. Bhaskar, J. Zhang, R. Guda, T. Goodson III, R. M. Laine, *Chemistry of Materials* **2008**, *20*, 5563.

-
- [24] D. A. Loy, B. M. Baugher, C. R. Baugher, D. A. Schneider, K. Rahimian *Chem. Mater.* **2000**, 12, 3624.
- [25] S. E. Rankin, C. W. Macosko, A. V. McCormick *J. Polym. Sci., Part A: Polym. Sci.* **1997**, 35, 1293.
- [26] S. E. Rankin, C. W. Macosko, A. V. McCormick *AIChE Journal* **1998**, 44, 1141.
- [27] S. E. Rankin, C. W. Macosko, A. V. McCormick *Chem. Mater.* **1998**, 10, 2037.
- [28] S. E. Rankin, L. J. Kasehagen, A. V. McCormick, C. W. Macosko *Macromolecules* **2000**, 33, 7639.
- [29] B. de Boer, H. K. Simon, M. P. L. Werts, E. W. van der Vegte, G. Hadziioannou, *Macromolecules* **2000**, 33, 349.

4.4**Surface Coatings Based on Polysilsesquioxanes: Grafting-from Approach Starting from Organic Polymers**

Daniel Kessler, Patrick Theato

Institute of Organic Chemistry, Johannes Gutenberg University Mainz, Duesbergweg 10-14, 55099 Mainz

in *Active Polymers*, edited by A. Lendlein, V. Prasad Shastri, K. Gall (Mater. Res. Soc. Symp. Proc. **Volume 1190**, Warrendale, PA, 2009), NN10-02 (accepted).

Abstract

Poly(methylsilsesquioxane) (PMSSQ) based hybrid materials are promising candidates to produce substrate-independent stable and adherent surface coatings. Usually these materials are synthesized by controlled radical polymerization from inorganic precursors. The presented synthetic pathway in here demonstrates how to graft PMSSQ networks from an endgroup-functionalized organic polymer and thus enlarges the range of accessible inorganic/organic hybrid coating materials.

Introduction

The quality of adhesion between solids, e.g. between a film and its substrate, depends to a large extent on the microstructure of the interface layer that is being formed [1]. Usually four types of interface layers can be formed during the coating process of polymers onto different substrates: 1. mechanically interlocked interfaces; 2. chemical bonding interface layers; 3. electric double layers; 4. diffusion interface layers [2,3].

Many different approaches have been explored recently to coat various substrates with polymers for various applications: The technique of grafting polymers from or onto surfaces [4-6] relies on chemical bonding interface layers and therefore depends on corresponding functional groups on the surface. Sol-Gel based coatings require free hydroxyl groups on the surface to form chemical bonds. For example on glass, silicon or metals hydroxyl groups are usually present [7], while on other substrates an additional plasma procedure may be necessary [8]. Polymer coatings on plastic substrates adhere due to a diffusion interface layer, if the polymers are miscible [9], requiring fine tuning between film and surface material. Electric double layer interfaces were formed in polyelectrolyte coatings [10]. Cross-linkable random copolymers as coating materials [11] exhibit a mechanically interlocked interface on rough surfaces. After cross-linking the former substrate topography is filled with rigid and stable polymer networks.

The disadvantage of almost all reported procedures is their limitation towards the natured substrate to be coated, which is due to the utilization of only one interface layer phenomenon to guarantee adhesion.

Recently, we introduced inorganic/organic hybrid polymers, consisting of poly(methylsilsesquioxane) (PMSSQ) and radically polymerized organic polymers [12,13]. After curing, stable and adherent films on various substrates have been achieved. On hydroxylated surfaces chemical bonding interfaces causes adherence, on polymeric substrates diffusion interfaces improve adherence and due to cross-linking of the PMSSQ moieties rigid polymer networks at the interface create mechanical interlocking.

Usually those hybrid polymers were synthesized in a controlled radical polymerization of the organic monomer from a PMSSQ precursor (ATRP in ref.[12] and RAFT in ref. [13]), which limits this class of materials to (meth)acrylate or styrene based polymers. Within these studies we want to enlarge the range of accessible PMSSQ hybrid coating materials by grafting PMSSQ from the pre-formed organic polymer.

Experiment

Materials. All chemicals and solvents were commercially available (Acros Chemicals, ABCR) and used as received unless otherwise stated. THF was distilled from sodium/benzophenone under nitrogen.

Instrumentation. ^1H -NMR spectra were recorded on a Bruker 300 MHz FT-NMR spectrometer, ^{29}Si CPMAS NMR spectra were measured on a Bruker DSX 400 MHz FT-NMR spectrometer (Rotation: 5000 Hz, T = RT, 4 mm rotor). Chemical shifts (δ) were given in ppm relative to TMS. Gel permeation chromatography (GPC) was used to determine molecular

weights and molecular weight distributions, Mw/Mn, of polymer samples. (THF used as solvent, polymer concentration: 2 mg/mL, column setup: MZ-Gel-SDplus 10^2 \AA^2 , 10^4 \AA^2 and 10^6 \AA^2 , used detectors: refractive index, UV and light scattering). Thermo gravimetric analysis was performed using a Perkin Elmer Pyris 6 TGA in nitrogen (10 mg pure polymer in aluminum pan). Atomic force microscopy (AFM) measurements were performed using a Veeco Dimension 3100 in tapping mode. IR spectra were recorded using a Nicolet 5 DXC FT-IR-spectrometer on ATR crystal. Advancing and receding CA of water were measured using a Dataphysics Contact Angle System OCA 20 and fitted by SCA 20 software. Given CA are average values of 10 individual measurements with an accuracy of 3°. All chemical reactions were performed in Argon atmosphere.

Allylphenyl-terminated Polycarbonate (1) was synthesized as explained in [14].

Yield: 44.2 g. $^1\text{H-NMR}$ (CDCl_3) δ (ppm): 7.25 (d, 60H); 7.17 (d, 60H); 5.93 (m, 2H); 5.12 (m, 4H); 3.43 (d, 4H); 1.68 (s, 77H). Mn = 4912 g/mol; PDI = 1.38. Tg = 180 °C.

Trichlorosilyl-propylphenyl-terminated Polycarbonate (2). 15 g of (1) was dissolved in 100 mL THF and 15 mg platinum on charcoal and 10 mL silicochloroform were added. The solution was refluxed at 80 °C for 12 h. Afterwards the solution was filtered over celite and the solvent was removed under reduced pressure. Yield: 14.7 g. $^1\text{H-NMR}$ (CDCl_3) δ (ppm): 7.26 (m, 60H); 7.17 (d, 60H); 2.77 (t, 4H); 1.67 (s, 81H); 0.92 (m, 4H).

Poly(methylsilsesquioxane)-functionalized Polycarbonate (3). 4 g of (2) and 4.42 g methyl trimethoxysilane were dissolved in 250 mL THF and 2.93 mL water and 0.24 mL 2N HCl were added. The solution was stirred at room temperature for 8 h. 300 ml chloroform was added, the solution was washed three times with water, dried over MgSO_4 and the solvents were removed. The polymer was dried in high vacuum. Yield: 5.8 g. $^1\text{H-NMR}$ (CDCl_3) δ (ppm): 7.27-7.09 (m); 5.02 (br); 2.78 (t, 4H); 1.67 (s, 81H); 0.91 (m, 4H); 0.16 (br, 29H). ^{29}Si CPMAS NMR δ (ppm): -48.61 (T1, 4%); -57.20 (T2, 58%); -66.08 (T3, 38%). Mn = 47200 g/mol; PDI = 2.15.

Di-(trichlorosilyl)-functionalized Polyethyleneglycol (4). 5 g polyethyleneglycol (2000 g/mol, water removal by azeotrope distillation with toluene) was dissolved in 100 mL THF and 1 g isocyanatopropyltriethoxysilane and 0.5 mL triethylamine were added. The mixture was stirred at room temperature for 12 h. After removing the solvent at low pressure, the polymer was dried in high vacuum. Yield: 4.55 g. $^1\text{H-NMR}$ (CDCl_3) δ (ppm): 6.30 (s, 2H); 4.12 (m, 4H); 3.79 (quad., 12H); 3.61 (br, 240H); 3.11 (quad., 4H); 1.61 (m, 4H); 1.18 (t, 18H); 0.60 (t, 4H).

Poly(methylsilsesquioxane)-functionalized Polyethyleneglycol (5). 4 g of (4) and 4.42 g methyl trimethoxysilane were dissolved in 250 mL THF and 2.93 mL water and 0.24 mL 2N HCl were added. The solution was stirred at room temperature for 8 h. 300 ml chloroform was added, the solution was washed three times with water, dried over MgSO_4 and the solvents were removed. The polymer was dried in high vacuum. Yield: 5.2 g. $^1\text{H-NMR}$ (CDCl_3) δ (ppm): 6.34 (s); 4.12 (m); 3.61 (br, 240H); 3.11 (quad.); 1.61 (m); 0.61 (t); 0.15 (br, 186H). ^{29}Si CPMAS NMR δ (ppm): -47.98 (T1, 6%); -58.01 (T2, 54%); -65.55 (T3, 40%). Mn = 38800 g/mol; PDI = 2.44.

Surface coating. The hybrid polymer solution was spin-coated onto clean substrates (15 s, 4000 rpm, 10 wt% solution in THF). To induce the secondary cross-linking of the inorganic

block, the samples were annealed at 130 °C for 2 h and afterwards washed with THF for 30 minutes to remove any non-bonded material.

Discussion

PMSSQ-based hybrid polymers obtained in an ATRP or RAFT process show an excellent adherence on various substrates (e.g. Si, glass, copper, steel, gold, PMMA and PDMS) [12,13]. This method gives convenient access to defined surface properties on different substrates (e.g. to coat gold with PMMA using a PMSSQ-PMMA hybrid polymer). Stable and adherent polymeric coatings of non-radically formed polymers like polycarbonate (PC) (produced via polycondensation) or polyethyleneglycole (PEG) (produced via anionic polymerization) could not be produced by covalent attachment of those polymers to PMSSQ.

Synthesis of PMSSQ-PC and PMSSQ-PEG hybrid materials

Our synthetic concept to attach pre-formed polymers to a PMSSQ network consists of a trichlorosilyl-endgroup functionalization of PC or PEG and further co-condensation with methyl trimethoxysilane (MTMS) to yield a PMSSQ network (synthetic scheme for PMSSQ-PC hybrid materials: figure 1).

To synthesize endgroup-functionalized PC (2), we quenched the polycondensation reaction of bisphenol A and diposgene with *o*-allylphenol and the successful introduction of the allyl-endgroups was confirmed by ¹H NMR spectroscopy (figure 1, upper spectrum). Hydrosilylation with silicochloroform and further co-condensation with MTMS yielded in the desired PMSSQ-PC hybrid polymer (3). ¹H NMR spectroscopy of (3) shows the additional Si-CH₃ signal at 0.16 ppm, whereas the allyl signals vanished (figure 1, lower spectrum). The molecular weight increased from 5 kg/mol to 47 kg/mol and showed a monomodal distribution, indicating that PC segments were incorporated in a PMSSQ network. The ability of this hybrid material to undergo further cross-linking was checked by ²⁹Si CPMAS NMR spectroscopy, 62% of all silicon atoms still carry two or one free OH group (T1 and T2 branches). Cross-linking occurred, similar to other PMSSQ systems, between 100 °C and 130 °C and took less than 70 min at 130 °C (measured by TGA). The ratio between silicon moieties and organic repeating units, calculated by NMR integration, was 50:50. Taking molecular weights into account the weight ratio between inorganic and organic part was calculated as 27% : 73 %.

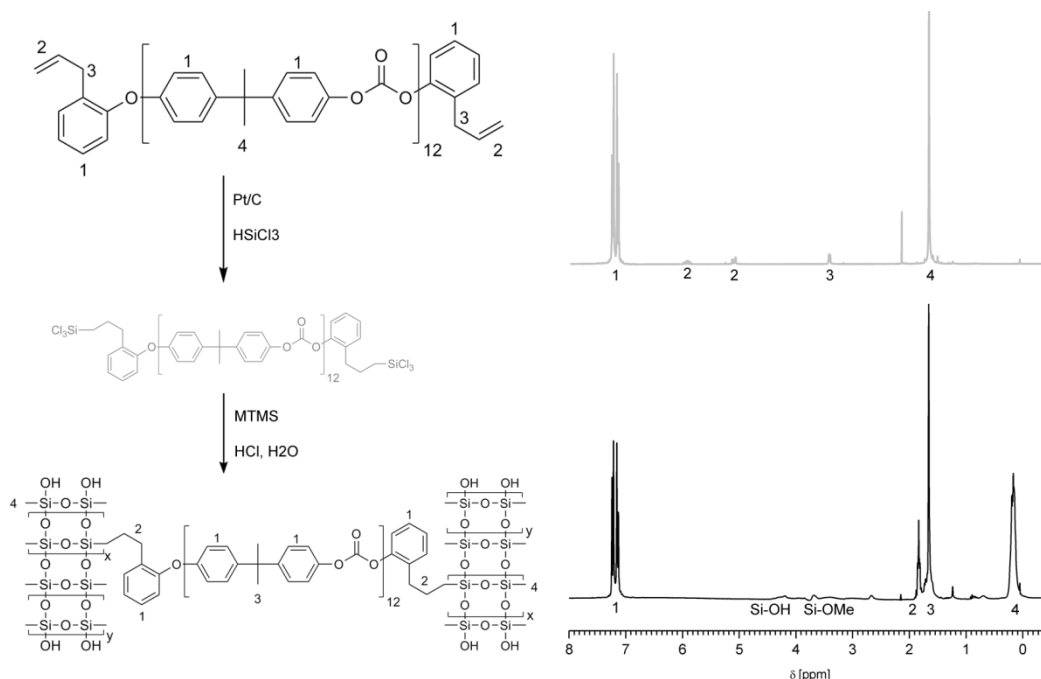


Figure 1. Synthetic pathway toward PMSSQ-PC hybrid polymers, including ^1H NMR spectra.

A PMSSQ-PEG hybrid polymer was synthesized by endgroup-functionalization of PEG-diol (2 kg/mol) with isocyanatopropyltriethoxysilane, yielding - similar to the functionalization of PC - a di-(trichlorosilyl)-functionalized PEG (4). Further co-condensation with MTMS led to the PMSSQ-PEG hybrid polymer (5). GPC showed a monomodal molecular weight distribution with $M_n = 39$ kg/mol. ^{29}Si CPMAS NMR spectroscopy showed 60% T1 and T2 branches, cross-linking occurred under similar conditions as explained above. The ratio between silicon moieties to PEG repeating units was calculated to 50:50. Weight ratio between inorganic and organic block was calculated as 72% : 28%.

PMSSQ-PC (3) as well as PMSSQ-PEG (5) showed the desired features to produce stable and adherent surface coatings after spin-coating and annealing.

Preparation of PMSSQ-PC and PMSSQ-PEG coatings on various substrates

10 wt% solutions of PMSSQ-PC (3) and PMSSQ-PEG (5) in THF were spin-coated at 4000 rpm onto Si, glass, copper, steel, gold, PMMA, PC and PDMS substrates, respectively. The coated substrates were cured at 130 °C for 2 h to thermally induce cross-linking of the PMSSQ part.

To characterize the surface topography and film thickness, AFM measurements were performed on coatings on silicon wafers. The PMSSQ-PC coating showed an image RMS value of 0.523 nm, indicating a smooth coating. The film thickness was 420 nm. The PMSSQ-PEG coating resulted in smooth surfaces (image RMS: 0.492 nm), film thickness was 375 nm.

The successful surface modification was tested by measuring advancing (Θ_a) and receding (Θ_r) contact angles on all different substrates. After coating with PMSSQ-PC the advancing contact angle was $78^\circ \pm 5^\circ$, on all coated materials (see table I). To demonstrate the long-term stability of the coating, the wafers were kept in boiling water for 4 h and the contact angle was checked every hour; the surface properties were not affected, indicating a substrate-independent permanent surface modification (table I). The adhesion and stability of the coatings on the underlying material was tested using the ISO tape test [15] directly after annealing and in a similar long-term stability experiment as explained above. Classification 0 indicates a perfect adherence (no detachment), classification 5 indicates more than 50 % detachment of the coating. The observed stabilities on all substrates are summarized in table I, even after 4 h in boiling water the tape test result did not drop below classification 1, indicating the desired high stability on a wide range of materials.

Table I. Contact angles and tape test results of PMSSQ-PC coatings on various substrates.

	Θ_a/Θ_r [°]					tape test results				
	0 h	1 h	2 h	3 h	4 h	0 h	1 h	2 h	3 h	4 h
Si	79/69	78/69	79/70	77/70	78/70	C	0	0	0	0
Glass	77/69	78/67	78/65	77/69	77/70	0	0	0	0	0
Copper	82/71	81/71	82/74	82/70	81/70	0	0	0	1	1
Steel	83/70	82/70	80/70	81/70	80/71	0	0	0	1	1
Gold	80/74	79/72	78/70	79/71	77/69	0	0	1	1	1
PMMA	74/68	75/68	74/70	73/70	74/69	0	0	0	0	1
PC	73/69	74/69	75/73	73/68	74/68	0	0	0	0	1
PDMS	73/70	75/68	77/70	77/69	77/70	0	0	1	1	1

Similar experiments were performed to determine the successful surface coating using PMMSQ-PEG hybrid materials. Advancing contact angles on all tested underlying materials were $39^\circ \pm 5^\circ$, which did not change significantly after 4 h in boiling water independent from the substrate. Tape test results also support the high long-term stability of the PMSSQ-PEG coating (for detailed information see table II).

Both coating materials, PMSSQ-PC as well as PMSSQ-PEG, showed comparable abilities to produce substrate-independent adherent surface coatings with high long-term stabilities.

Table II. Contact angles and tape test results of PMSSQ-PEG coatings on various substrates.

	Θ_a/Θ_r [°]					tape test results				
	0 h	1 h	2 h	3 h	4 h	0 h	1 h	2 h	3 h	4 h
Si	41/32	40/35	42/37	40/36	40/35	0	0	0	0	0
Glass	39/34	40/34	38/34	38/32	38/33	0	0	0	0	0
Copper	34/29	35/29	36/31	35/30	35/30	0	0	1	1	1
Steel	34/27	34/28	35/28	34/27	34/27	0	0	0	1	1
Gold	35/29	35/31	34/31	35/31	36/30	0	1	1	1	1
PMMA	42/35	41/34	40/36	41/36	39/36	0	1	1	1	1
PC	41/36	43/36	40/35	39/33	40/34	0	0	0	1	1
PDMS	40/31	39/34	38/32	39/33	38/33	0	0	0	0	1

Conclusions

PMSSQ-activated hybrid materials successfully combine several interlayer phenomena in one coating material and thus form stable and adherent coatings on a wide range of substrates. The presented synthetic scheme allows preparing PMSSQ-based inorganic/organic hybrid materials starting from pre-formed organic polymers, using first a trichlorosilyl-functionalization of both polymer endgroups and a polycondensation with MTMS yielding the desired hybrid PMSSQ network. PMSSQ-PC and PMSSQ-PEG could be used to produce surface coatings on a wide range of substrates. Successful surface modification and high long-term stability of the coatings could be demonstrated by contact angle measurements and ISO tape test.

Acknowledgement

D.K. gratefully acknowledges financial support from the FCI, POLYMAT (Graduate School of Excellence “Polymers in Advanced Materials”) and the IRTG 1404 (“Self-Organized Materials for Optoelectronic Applications”).

References

1. H. K. Pulker, A. J. Perry, *Surface Technology* **14**, 25 (1981).
2. W. Possart (Ed.), “Adhesion. Current Research and Applications” 2005, Wiley-VCH (Weinheim).
3. D. E. Packham (Ed.), “Handbook of Adhesion” 2nd Ed. 2005; John Wiley & Sons (New York).
4. P. Mansky, Y. Liu, E. Huang, T. P. Russell, C. J. Hawker, *Science* **275**, 1458 (1997).
5. R. C. Advincula, W. J. Brittain, K. C. Caster, J. R uhe, (Eds.) “Polymer Brushes” 2004, Wiley-VCH (Weinheim).
6. L. Gao, T. J. McCarthy, *J. Am. Chem. Soc.* **128** (28), 9052 (2006).
7. J. den Toonder, J. Malzbender, G. de With, R. Balkenende, *J. Mater. Res.* **17** (1), 224 (2002).

8. C. M. Chan, G. Z. Cao, H. Fong, M. Sarikaya, T. Robinson, L. Nelson, *J. Mater. Res.* **15** (1), 148 (2000).
9. A. R. Marrion (Ed.), “The Chemistry and Physics of Coatings” 2004, RSC (Cambridge).
10. N. Benkirane-Jessel, P. Lavallo, V. Ball, J. Ogier, B. Senger, C. Picart, P. Schaaf, J.-C. Voegel, G. Decher, *Macromol. Eng.* **2**, 1249 (2007).
11. D. Y. Ryu, K. Shin, E. Drockenmuller, C. J. Hawker, T. P. Russell, *Science* **308**, 236 (2005).
12. D. Kessler, C. Teutsch, P. Theato, *Macromol. Chem. Phys.* **209** (14), 1437 (2008).
13. D. Kessler, P. Theato, *Macromolecules* **41** (14), 5237 (2008).
14. S. H. Kim, H. G. Woo, S. H. Kim, H. G. Kang, W. G. Kim, *Macromolecules* **32**, 6363 (1999)
15. *Paints and Varnishes – Cross-cut test (ISO 2409:2007)*

4.5

Temperature-Responsive Surface Coatings Based on Poly(methylsilsesquioxane)-Hybrid Polymers

*Daniel Kessler, Patrick Theato**

Institute of Organic Chemistry, University of Mainz, Duesbergweg 10-14, 55099 Mainz, Germany

Macromol. Symp. **2007**, 249-250, 424-430.

Summary

The present paper presents a new method to build up temperature-responsive surfaces. First a poly(silsesquioxane)-block-poly(N-isopropyl-acrylamide) (PMSSQ-b-PNIPAM) was successfully synthesized using RAFT polymerization. Spin-coating or dip-coating of PMSSQ-b-PNIPAM onto glass surfaces resulted in temperature-responsive surfaces. Surface ATR FT-IR measurements proofed the successful surface modification using PMSSQ-b-PNIPAM. IR fine structures of PNIPAM and PMSSQ could be assigned, respectively. In capillary rise experiments a change of the meniscus height measured at temperatures below or above LCST was observed, indicating a different wetting behavior. Thus, a simple spin- or dip-coating step results in a clean and temperature-responsive surface.

Keywords

stimuli-responsive polymers, reversible addition fragmentation chain transfer (RAFT), atom transfer radical polymerization (ATRP), surfaces, inorganic-organic hybrid polymers, block copolymers, lower critical solution temperature (LCST)

Introduction

Poly(*N*-isopropylacrylamide) (PNIPAM) exhibits a reversible, temperature-dependent soluble/insoluble transition at its lower critical temperature in aqueous media. The lower critical solution temperature (LCST) of PNIPAM in water was found to be around 32°C^[1-5]. It is known, that the phase transition of PNIPAM accompanies not only a drastic conformation change from a coil to a globule, but also a rapid change in interfacial properties^[8-10]. Recently, there have been many reports on grafting of PNIPAM onto solid surfaces for both scientific and engineering purposes^[6-10].

Below the LCST a PNIPAM coated surface shows a hydrophilic behavior, when heated above the LCST the behavior changes to hydrophobic^[6]. This effect on substrates offers the ability to control important interfacial phenomena such as wetting^[11-12], fluid flows^[13] and adhesion^[14-15]. Further, the reversible adsorption of biomolecules on surfaces is of special interest^[16].

Two main routes of preparing covalent linked PNIPAM surfaces are well known. End group functionalized PNIPAM is bonded directly to an oxidized silicon surface in a polymer analogues esterification^[17] or ATRP initiators are directly linked to the surface and PNIPAM is grafted from the surface^[6]. In both cases several surface preparation steps have to be performed.

Within the present study, we introduce a new surface functionalization method which allows the preparation of the coating material in solution and attach it covalently to the surface in one single coating step. In order to combine the linkage part and the temperature-sensitive part in one block copolymer, inorganic-organic hybrid polymers were used. A poly(methylsilsesquioxane) (PMSSQ) block enabled the attachment on glass surfaces, a PNIPAM block provided the temperature-responsive behavior.

Experimental

Materials. All reagents, solvents, and substances used were of reagent grade quality and were obtained from commercial sources. NIPAM was recrystallized from *n*-hexane. CuBr was stirred over acetic acid, filtered off, washed with methanol and dried in vacuum.

Instrumentations. The synthesized compounds were characterized by NMR-spectroscopy, mass spectroscopy and elemental analysis. Molecular weights of the polymers were determined by gel permeation chromatography using a PSS standard column, UV-, refractive index- and light scattering-detector. NMR-spectra were recorded on a 300 MHz Bruker FT-NMR-spectrometer using CDCl₃ as a solvent. Chemical shifts (δ) were given in ppm relative to TMS. IR spectra were recorded on a Nicolet 5 DXC FT-IR-spectrometer. FD mass spectra were measured using a Finnigan MAT 95 mass spectrometer. Elemental analyses were done with an Elementar Vario Micro Cube (detecting C, H, N, S).

***p*-(Chloromethyl)-phenylethyltrichlorosilane (1)**

1 was synthesized in a hydrosilylation reaction of *p*-chloromethylstyrene with Silicochloroform. 100 mg of platinum on charcoal and 100 ml toluene were placed in a round bottomed flask, 75 mmol trichlorosilane and 50 mmol *p*-chloromethylstyrene were added. The reaction mixture was stirred for 48 h at 110 °C. After filtering over celite the solvent was removed and the crude

product was distilled at 2.5×10^{-3} mbar. The yield of **1** was 39 mmol (77.1 %). $^1\text{H-NMR}$ (CDCl_3) δ : 7.34 (d, $^3J = 8.1$ Hz, 2H); 7.22 (d, $^3J = 7.8$ Hz, 2H); 4.58 (s, 2H); 2.90 (m, 2H); 1.74 (m, 2H). EA (%): C = 38.70; H = 3.73.

***p*-(Chloromethyl)-phenylethyltrimethoxysilane (2)**

To 100 ml methanol 35 mmol of **1** was added. After stirring over night the solvent was removed and the product was dried in vacuum (Yield: 31 mmol, 87.8 %). $^1\text{H-NMR}$ (CDCl_3) δ : 7.29 (d, $^3J = 8.1$ Hz, 2H); 7.20 (d, $^3J = 8.1$ Hz, 2H); 4.55 (s, 2H); 3.56 (s, 9H); 2.73 (m, 2H), 0.99 (m, 2H). EA (%): C = 53.38, H = 7.22. FD mass spectra: 273.9 (100%); 274.9 (15.6%); 275.9 (38.9%).

Dithiobenzoic acid 4-ethyltrimethoxysilylester (RAFT-Si)

31.6 mmol phenyl magnesium bromide was placed with 50 ml THF in a round bottomed flask. After heating to 40 °C 49.7 mmol CS_2 was added. After 15 minutes 31.7 mmol **2** was injected and the reaction mixture was stirred for 1 h at 50 °C. The mixture was dissolved in ether and washed with water, the ether phase was dried over magnesium sulfate, filtered and ether was removed. The product was dried in vacuum. (Yield: 25.3 mmol, 79.7 %). $^1\text{H-NMR}$ (CDCl_3) δ : 8.01 (m, 1H); 7.27 (m, 8H); 4.58 (d, $^3J = 2.4$ Hz, 2H); 3.59 (s, 9H); 2.76 (m, 2H); 1.04 (m, 2H). EA (%): C = 56.20; H = 6.32; S = 10.51. FD mass spectra: 391.9 (100%); 392.9 (26.9%); 393.9 (15.4%).

PMSSQ RAFT macro initiator

50 mmol methyltrimethoxysilane (MTMS), 2.5 mmol **RAFT-Si**, 20 ml THF, 500 mmol water and 10 mmol HCl were stirred for 3 h at 0 °C. The reaction mixture was dissolved in ether, washed with water. After drying the ether was removed and the product was dried in high vacuum. $^1\text{H-NMR}$ (CDCl_3) δ : 7.99 (br, 5H); 7.36 (br, 2H); 5.80 (br, 1.9H); 4.55 (br, 2H); 3.48 (br, 1.1H); 2.71 (br, 2H); 0.99 (br, 2H); 0.17 (br, 69.1H). $M_n = 4990$ g/mol, PDI = 1.63.

PMSSQ-*b*-PNIPAM

0.5 g PMSSQ RAFT macro initiator, 10 mg AIBN, 4 mL dioxane and 2 g NIPAM were placed in a Schlenk flask. The reaction mixture was stirred 4h at 80 °C and afterwards two times precipitated in *n*-hexane. (Yield: 1.9 g). $^1\text{H-NMR}$ (CDCl_3) δ : 7.91 (br); 7.30 (br); 6.52 (br); 4.50 (br); 3.62 (br); 2.88 (br); 2.25 (br); 1.21 (br); 1.14 (br); 0.83 (br); 0.13 (br). $M_n = 23430$ g/mol, PDI = 3.2.

2-Bromoisobutyric acid 5-(trichlorosilyl)pentyl ester (ATRP-Si)

Synthesis analog [18]. Bp. 104 °C at 7×10^{-3} mbar. Yield: 44 mmol, 88.0%. $^1\text{H-NMR}$ (300 MHz, CDCl_3): δ : 4.11 (t, $^3J = 6.6$ Hz, 2H); 1.86 (s, 6H); 1.66 (m, 2H), 1.57 (d, $^3J = 6.9$ Hz, 2H); 1.47 (d, $^3J = 6.6$ Hz, 2H); 1.38 (m, 2H)

PMSSQ ATRP macro initiator

Synthesis analog [18]. $^1\text{H-NMR}$ (CDCl_3) δ : 5.55 (br); 4.14 (br, 2H); 3.44 (br); 1.91 (br, 6H); 1.77 (br, 2H); 1.42 (br, 2H); 0.63 (br, 2H); 0.13 (br, 57.2H).

Surface coating

Standard glass plates and glass tubes were used as surfaces. The glass tubes had an inner diameter of approximately 0.6 mm and a length of 80 mm. Both were cleaned with acetone and methanol and dried with nitrogen. Solutions of PMSSQ-*b*-PNIPAM, **ATRP-Si** and ATRP macro

initiator (10 wt% in THF) were prepared. These polymer solutions were either spin-coated onto the clean glass plates (15 s, 4000 rpm) or glass tubes were dip-coated into the polymer solution for 20 minutes.

Preparation of PNIPAM coating A

A reference PNIPAM coating A was prepared using grafting-from polymerization of NIPAM from the glass surface (Figure 1). After **ATRP-Si** was coated onto the glass surface, the glass plates or tubes were washed five times with THF to remove unattached molecules. ATRP was then carried out in a degassed aqueous solution consisting of 30 mL millipore water and 2 g NIPAM. 50 mg CuBr were added and the solution was kept at room temperature for 1 hour. To remove free material the glass plates and tubes were taken out and washed several times with THF and water.

Preparation of PNIPAM coating B

Similar to the preparation of PNIPAM coating A, the PMSSQ ATRP macro initiator was coated onto the glass surfaces. After washing with THF the samples were cured for 2 h at 130 °C. The grafting-from polymerization of NIPAM was accomplished in the procedure described above.

Preparation of PNIPAM coating C

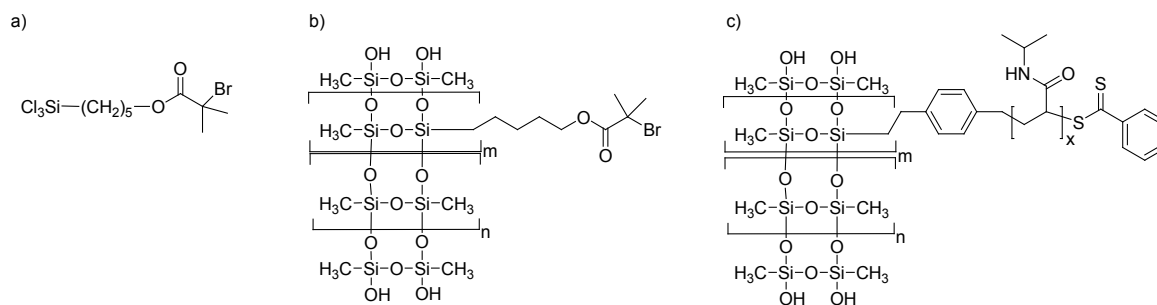
A 10 wt% solution of PMSSQ-*b*-PNIPAM in THF was coated onto the glass surface as described above. To fix the polymer onto the surface, the surfaces were heated in THF solution for 30 minutes to 50 °C and washed several times with THF.

Results and Discussion

It is the intention of the present study to compare different coating procedures in order to receive temperature-responsive surfaces. Temperature-responsive behavior can be achieved using poly(*N*-isopropylacrylamide) (PNIPAM), known for its LCST at 32°C in water. Three different approaches have been performed to prepare PNIPAM coated surfaces: a) grafting-from atom transfer radical polymerization (ATRP) of NIPAM using a low-molecular weight initiator, b) grafting-from ATRP of NIPAM using a high-molecular weight PMSSQ based initiator, and c) coating of a PMSSQ-*b*-PNIPAM polymer. The respective structures are shown in scheme 1.

Scheme 1. Different coating materials:

a) ATRP-Si initiator, b) PMSSQ ATRP initiator and c) PMSSQ-*b*-PNIPAM.



Synthesis

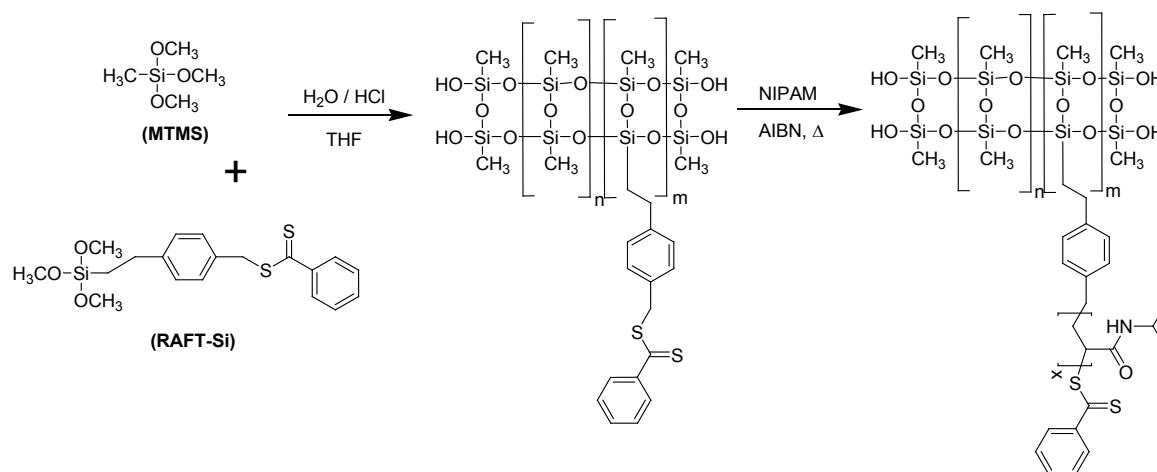
In the first step, three different coating materials have been synthesized. **ATRP-Si** was prepared as described previously in a two-step synthesis by esterification of 4-pentenol with 2-bromo-isobutyric acid bromide, followed by a hydrosilylation with trichlorosilane.[18]

The corresponding PMSSQ based ATRP initiator was then synthesized using **ATRP-Si** by co-condensation with MTMS under acidic catalysis.[18]

As a third route, RAFT polymerization using a PMSSQ based RAFT agent was investigated. Thus, dithiobenzoic acid 4-ethyltrimethoxysilylester (**RAFT-Si**) was prepared in a three-step synthesis. First, *p*-chloromethylstyrene was hydrosilylated with trichlorosilane using a Pt/C catalyst. The resulting trichlorosilane was then transformed into the corresponding trimethoxy compound by reaction with methanol. In the final step, the dithiobenzoic acid group was introduced by nucleophilic substitution of the chlorine yielding **RAFT-Si**.

The trimethoxysilyl RAFT agent (**RAFT-Si**) was then co-condensated with methyltrimethoxysilane (MTMS) to give a PMSSQ RAFT macro initiator, as shown in scheme 2.

Scheme 2. Synthesis of PMSSQ-*b*-PNIPAM via RAFT polymerization.

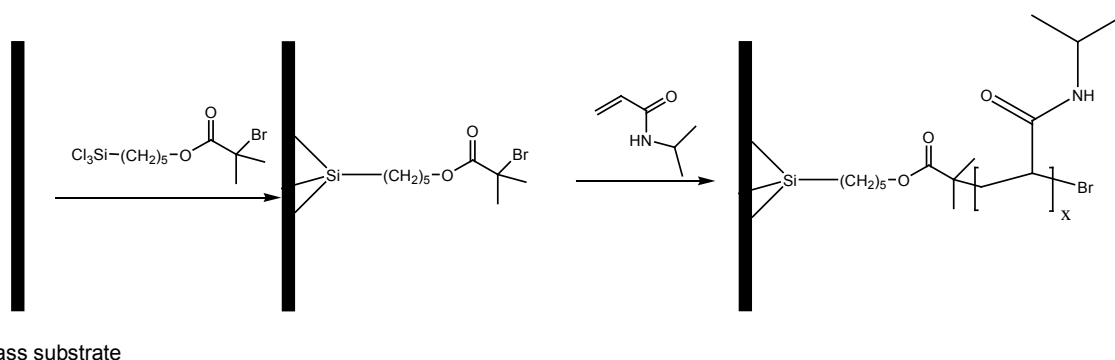


In a second step *N*-isopropylacrylamide (NIPAM) was grafted-from the prepared PMSSQ RAFT macro initiator using typical RAFT polymerization conditions in solution to yield a PMSSQ-PNIPAM block copolymer as shown in scheme 2.

Surface coating

All prepared coating compounds were then coated onto glass surfaces. A reference PNIPAM coating A was prepared using grafting-from polymerization of NIPAM from the glass surface, as shown in Figure 1. The analogue PMSSQ macro initiator for ATRP was also coated onto glass surfaces and PNIPAM was grafted-from its initiating species under ATRP conditions in water resulting in a thin PNIPAM film on the surface.

At last, the PMSSQ-*b*-PNIPAM hybrid polymer was coated onto glass surfaces from a THF solution via spin- or dip-coating and fixed by slight temperature curing (50 °C, 20 min). All described methods resulted in PNIPAM coated surfaces.



glass substrate

Figure 1. Preparation of PNIPAM coating by grafting-from polymerization of NIPAM from functionalized glass surfaces.

The three different PNIPAM surfaces were characterized via ATR FT-IR spectroscopy. All samples show PNIPAM at the surface, indicated by the amide bands. Figure 2 shows the IR spectra in comparison to usual PNIPAM (not attached to a surface).

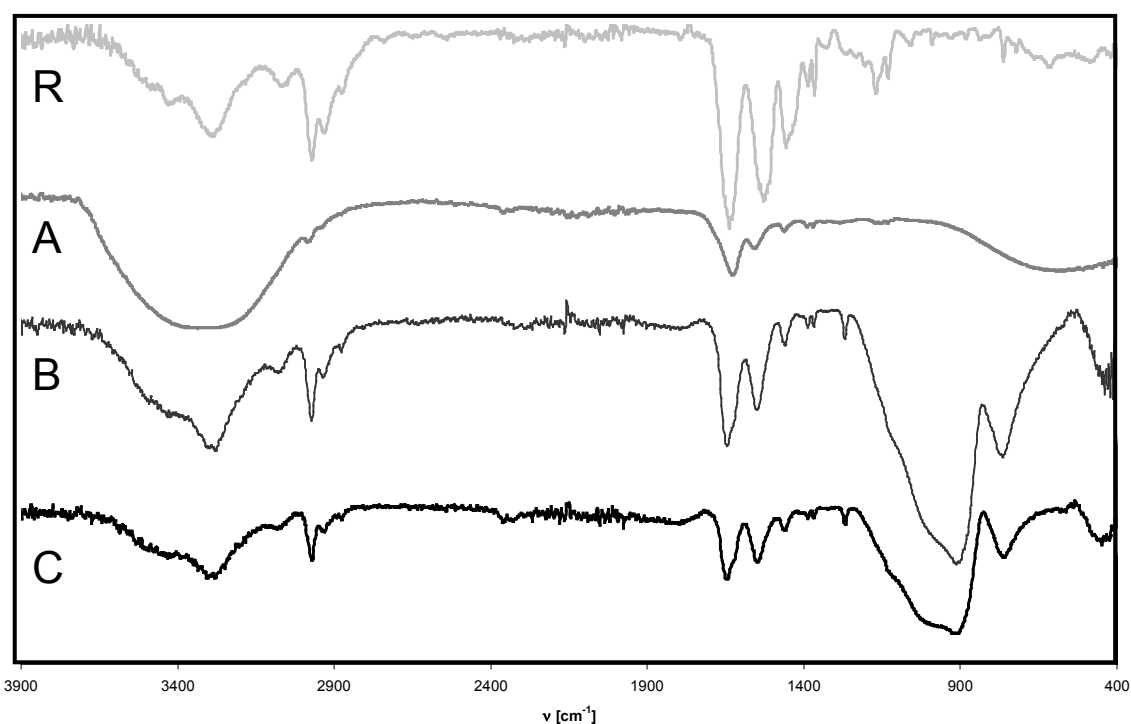


Figure 2. R: PNIPAM reference spectra; A: PNIPAM coating (A) on glass surface; B: PNIPAM coating (B) on glass surface; C: PNIPAM coating (C) on glass surface.

All surface coatings show the NH-band around 3300 cm^{-1} and the amide band at 1640 cm^{-1} and 1530 cm^{-1} . The fine structures of the PNIPAM spectra correspond precisely to the spectra of coating (B) and (C), giving evidence that method (B) and (C) are appropriate methods to prepare PNIPAM coated surfaces. Additionally to the PNIPAM bands the spectra of

coating (B) and (C) show Si-CH₃ and Si-O-Si bands between 1200 cm⁻¹ and 900 cm⁻¹. Especially the IR spectra of C approves that the one step coating process with PMSSQ-*b*-PNIPAM is a convenient route to prepare temperature-responsive surfaces. Coating C is comparable to the established grafting-from methods. A difference induced by the PMSSQ block could be found neither in coating (B) nor in coating (C).

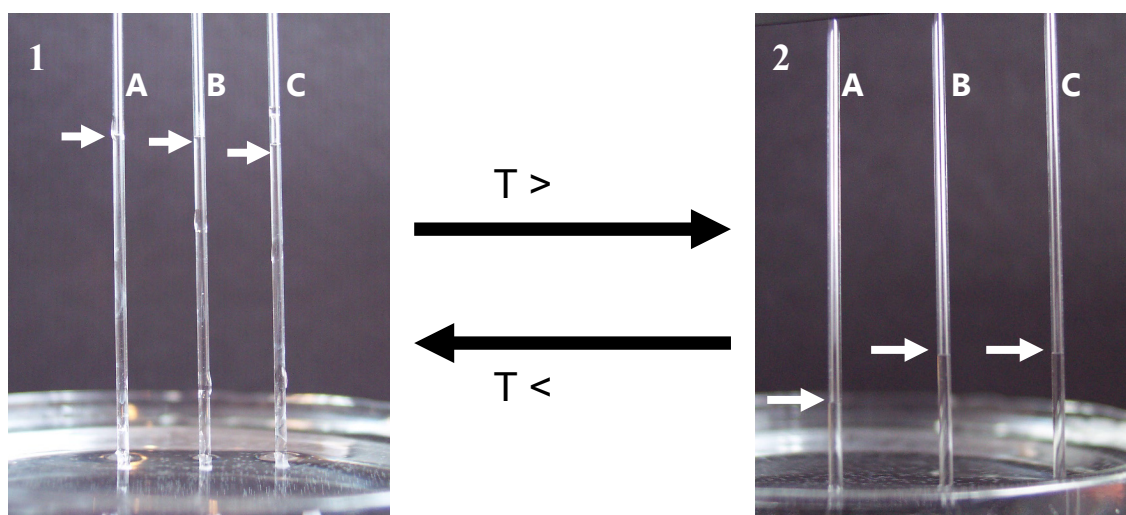


Figure 3. Capillary rise experiment of PNIPAM coated glass tubes, picture 1: water temperature 15 °C, picture 2: water temperature 40 °C. Tubes A, B and C correspond to the different surface coatings A, B and C.

To check the temperature-responsive behavior of the surfaces, capillary rise experiments with water of different temperatures have been carried out. The coated glass tubes were placed over a water surface just touching it. The meniscus height was measured as an indication of the surface hydrophobicity. In capillary rise experiments carried out with water at a temperature of 15 °C (below LCST of PNIPAM) the meniscus height in all three samples was measured to be 3.8 cm, indicating a hydrophilic surface. The error of the measurement was ± 0.2 cm. Thus, the values of three independent measurements were averaged. When the water was heated at 40 °C (above the LCST of PNIPAM) the meniscus height was found to be 1.1 cm in the case of coating (A) and 1.4 cm in the case of coating (B) and (C). Exemplary snapshots of the capillary rise experiments are shown in Figure 3. As a comparison, the meniscus height of an uncoated capillary did not change while changing the water temperature to 40 °C.

The experiment was repeated several times by cooling/heating cycles of the water bath resulting in a rise and fall of the meniscus. In every cycle the previously measured heights of the meniscus were observed without a significant change. For all three surface coatings (A, B and C) a very similar temperature-responsive behavior of the surface was found. Only for surface coating procedure A, a lower meniscus height above LCST was found, which may correspond to a higher population density of PNIPAM chains at the surface due to the higher initiator density during the surface coating procedure.

Overall, using PMSSQ-*b*-PNIPAM polymers as coating materials offers a variety of advantages compared to classical grafting-from techniques. A simple spin- or dip-coating step results in a clean and temperature-responsive surface, avoiding contact of catalysts or other compounds with the surface.

Conclusions

A new method to build up temperature-responsive surfaces was introduced. The successful synthesis of PMSSQ-*b*-PNIPAM gives the possibility to simplify the coating process dramatically. By simple spin-coating or dip-coating procedures a PNIPAM modified surface could be obtained in one step. The synthetic concept to build up functionalized hybrid polymers using the RAFT polymerization carries the potential to incorporate other vinyl monomers in the organic block. For example by using the well known active ester monomers^[19] a micro-structured surface pattern could be prepared by μ -contact printing. An analogous surface coating consisting of a active ester layer can be converted by polymer analogues reaction to PNIPAM (with isopropyl amine) but also to other surface modifications are considerable.

References

- [1] E.I. Tiktopulo, V.E. Bychkova, J. Ricka, O.B. Ptitsyn, *Macromolecules* **1994**, 27, 2879
- [2] S. Fujishige, K. Kubota, I. Ando, *J. Phys. Chem.* **1989**, 93, 3311
- [3] K. Otake, H. Inomata, M. Konno, S. Saito, *Macromolecules* **1990**, 23, 283
- [4] H. Feil, Y.H. Bae, J. Feijen, S.W. Kim, *Macromolecules* **1993**, 26, 2496
- [5] V.Y. Grinberg, A.S. Dubovik, D.V. Kuznetsov, N.V. Grinberg, A.Y. Groberg, T. Tanaka, *Macromolecules* **2000**, 33, 8685
- [6] D.M. Jones, J.R. Smith, W.T.S. Huck, C. Alexander, *Adv. Mater.* **2002**, 14, 1130
- [7] Y.V. Pan, R.A. Wesley, R. Luginbuhl, D.D. Denton, B.D. Ratner, *Biomacromolecules* **2001**, 2, 32
- [8] S. Kidoaki, S. Ohya, Y. Nakayama, T. Matsuda, *Langmuir* **2001**, 17, 2552
- [9] F.-J. Schmitt, C. Park, J. Simon, H. Ringsdorf, J. Israelachivilli, *Langmuir* **1998**, 14, 2838
- [10] L. Liang, X. Feng, J.L. Peter, P.C. Rieke, G.E. Fryxell, *Macromolecules* **1998**, 31, 7845
- [11] Y. Xia, D. Qin, Y.D. Yin, *Curr. Opin. Colloid Interface Sci.* **2001**, 6,54
- [12] P. Lenz, *Adv. Mater.* **1999**, 11, 1531
- [13] D.E. Kataoka, S.M. Troian, *Nature* **1999**, 402, 794
- [14] M.E. Callow, J.A. Callow, L.K. Ista, S.E. Coleman, A.C. Nolasco, G.P. Lopez, *Appl. Environ. Microbiol.* **2000**, 66, 3249
- [15] M. Fujihira, Y. Tani, M. Furugori, U. Akiba, Y. Okabe, *Ultamicroscopy* **2001**, 86, 633
- [16] D. Gan, L.A. Lyon, *Macromolecules* **2002**, 35, 9634
- [17] E.C. Cho, Y.D. Kim, K. Cho, *Journal of Colloid and Interface Science* **2005**, 2, 479
- [18] P. Theato, K.J. Kim, D.Y. Yoon, *Phys. Chem. Chem. Phys.* **2004**, 6, 1458
- [19] M. Eberhard, P. Theato, *Macromolecular Rapid Communications* **2005**, 26, 1488

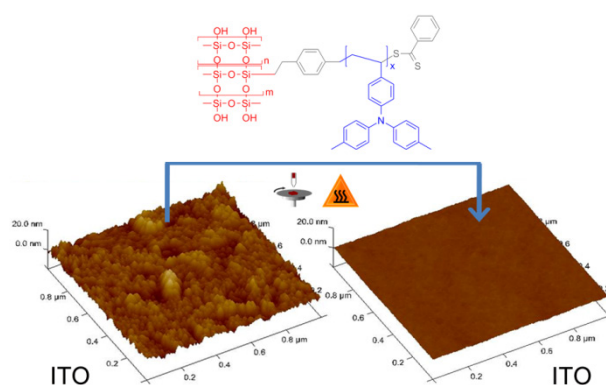
4.6

Surface Coatings Based on Polysilsesquioxanes:**Solution Processible Smooth Hole-Injection-Layers for Optoelectronic Applications**

Daniel Kessler,^{1,2} Maria C. Lechmann,² Seunguk Noh,³ Rüdiger Berger,² Changhee Lee,³ Jochen S. Gutmann,^{2,4} Patrick Theato^{1,5*}

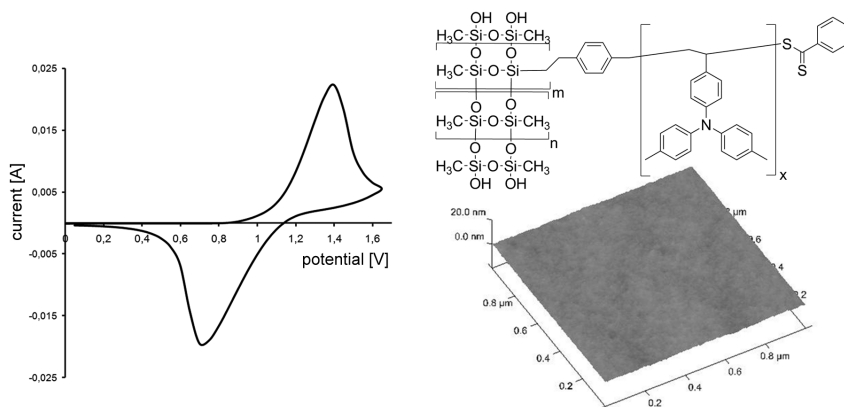
- 1 Institute of Organic Chemistry, Johannes Gutenberg University Mainz, Duesbergweg 10-14, 55099 Mainz, Germany
- 2 Max Planck Institute for Polymer Research Ackermannweg 10, 55128 Mainz, Germany
- 3 Organic Semiconductor Laboratory School of Electrical Engineering and Computer Science Seoul National University, Seoul, Korea
- 4 Institute of Physical Chemistry, Johannes Gutenberg University Mainz
- 5 World Class University (WCU) program of Chemical Convergence for Energy & Environment (C₂E₂) School of Chemical and Biological Engineering, College of Engineering Seoul National University (SNU), Seoul, Korea

Macromol. Rapid Commun. **2009**, published online June 30,
<http://dx.doi.org/10.1002/marc.200900196> .



Keywords

adhesion, coatings, interfaces, light-emitting diodes, reversible addition fragmentation chain transfer (RAFT)

Summary

Optoelectronic devices usually consist of a transparent conductive oxide (TCO) as one electrode. Interfacial engineering between the TCO electrode and the overlying organic layers is an important method for tuning device performance. We introduce poly(methylsilsesquioxane)-poly(*N,N*-di-4-methylphenylamino styrene) (PMSSQ-PTPA) as a potential hole-injection layer forming material. Spin-coating and thermally induced cross-linking resulted in an effective planarization of the anode interface. HOMO level (-5.6 eV) and hole mobility ($1 \cdot 10^{-6} \text{ cm}^2/\text{Vs}$) of the film on ITO substrates were measured by cyclovoltammetry and time-of-flight measurement demonstrating the hole injection capability of the layer. Adhesion and stability for further multilayer built-up could be demonstrated. Contact angle measurements and tape tests after several solvent treatments proved the outstanding film stability.

Introduction

Transparent conducting oxides (TCOs), such as indium tin oxide, are optically transparent and electrically conductive. TCOs find increasing application in many optoelectronic devices, such as organic light-emitting diodes (OLED),^[1,2] organic photovoltaics (OPV),^[3,4,5] or electrochemical sensors.^[6,7]

Interfacial engineering of electrical devices between the anode surface and the overlying organic layer is an important method for tuning electronic properties. In particular, the need for precise control of the electrode/organic semiconductor interface is apparent in the area of polymer light-emitting diodes (PLED).^[8-11] Several approaches have been employed in decreasing the hole-injection barrier in order to lower the turn-on voltage, to increase the brightness or to increase the efficiency of the devices. Typically, physical surface treatments like oxygen plasma treatment,^[12,13] ultraviolet-ozone cleaning,^[14,15] or argon ion bombardment^[4] have to be applied. The typical chemical approach is to deposit an intermediate layer of an organic semiconductor as a hole-injection layer (HIL) or hole-transport layer (HTL), which features a HOMO level between that of the ITO work function and the desired organic emitting layer.^[16-18] For example, a HIL enhances hole injection from indium tin oxide anode into the light-emitting layer (EML), which results in balanced charge-injection/charge-transport and better device performance. Besides the electronic properties of an effective HIL, there are further important requirements on a high-quality thin film: minimum number of defects, such as aggregates or pinholes, good adhesion of the organic layer on top of the hydrophilic oxide anode to prevent physical delamination or decohesion,^[19,20] and a smooth amorphous film-forming morphology^[21-26] to achieve an effective planarization of the ITO surface.^[27] Furthermore, for an efficient use of HILs in multilayer PLEDs, the material needs to possess very good solvent resistance in order to facilitate a multilayer processing. The commonly employed approaches use either a suitable solvent combination to avoid dissolution of the bottom layer or cross-linkable hole-transporting materials.^[27] Casting different layers from two different solvents is limited to only a small number of suitable materials, e. g. poly(3,4-ethylenedioxythiophene)/(poly(styrene sulfonate) (PEDOT:PSS), which is processed from aqueous dispersion. The main drawbacks are the poor control of film quality and the hygroscopicity of the resulting film.^[28] A hole-injection material that is soluble in an organic solvent would avoid these issues.

Recently, different approaches for cross-linkable hole-injection/hole-transport interlayers for improved charge injection were introduced. Marks and coworkers investigated in detail the utilization of trialkoxysilane-^[29-32] or trichlorosilane-^[33-36] functionalized electroactive small molecules, which were applied via spin-coating or by self-assembly from solution, forming silsesquioxane-like networks on the ITO surface. They could show that the OLED performance improved significantly. Other approaches use phosphonic acid-^[37] or styryl-^[38] functionalized electroactive small molecules to create cross-linkable HILs on ITO, or copolymers containing perfluorocyclobutane^[39,40] or benzocyclobutene^[41] as thermal cross-linkers and hole-conducting moieties. Surface-initiated polymerization of semi-conductive polymers was also used to prepare a conjugated polymer network as a HIL.^[42]

Poly(methylsilsesquioxane) (PMSSQ) based hybrid polymers are able to create very stable and adherent smooth homogenous films on a wide range of substrates, independent of the organic moiety.^[43,44] Within this manuscript, we describe the synthesis of triphenylamine containing PMSSQ hybrid polymers and their use as promising hole-injection materials.

Experimental Part

Materials. All chemicals and solvents were commercially available and used as received unless otherwise stated. THF was freshly distilled from sodium/benzophenone under nitrogen. All reactions were performed in argon atmosphere.

Instrumentation. All ¹H- and ¹³C-NMR spectra were recorded on a Bruker 300 MHz FT-NMR spectrometer. ²⁹Si CPMAS NMR spectra were measured on a Bruker DSX 400 MHz FT-NMR spectrometer (Rotation: 5000 Hz, T = RT, 4 mm rotor). Chemical shifts (δ) were given in ppm relative to TMS. Gel permeation chromatography (GPC) was used to determine molecular weights and molecular weight distributions, M_w/M_n , of polymer samples with respect to polystyrene standards (PSS). Cyclovoltammetry (CV) data were obtained using a three electrode cell in an electrolyte of 0.1 M (C₄H₉)₄N BF₄ in acetonitrile, using ferrocene as internal standard and Ag/Ag⁺ as reference electrode. The CV scans were performed anodically, proceeding from 0 V to 1.65 V (10 mV/s). Samples were coated onto ITO substrate, used as one electrode; a Pt-net was used as counter electrode. Advancing and receding contact angles (Θ_a , Θ_r) of water were measured using a Dataphysics Contact Angle System OCA 20 and fitted by SCA 20 software. Given values are averaged of 10 individual measurements with an accuracy of 3°. Film stability and adhesion on substrates was tested using ISO 2409:1992(E) – Cross-cut test as explained therein. Atomic Force Microscopy (AFM) measurements were performed using a Multimode operated in non-contact mode (Veeco Instruments; Cantilever: OMCL 160 TS).

***N,N*-di-4-methylphenylamino styrene (TPA)** was synthesized from *p*-iodotoluene and aniline in an Ullmann reaction, followed by Vilsmeier formylation and Wittig reaction as explained in detail in [45]. ¹H-NMR (CDCl₃) δ : 7.23 (m, 2H); 6.98 (m, 10H); 6.64 (dd, 1H); 6.60 (d, 1H); 5.12 (d, 1H), 2.31 (s, 6H). ¹³C-NMR (CDCl₃) δ : 147.92; 145.17; 136.31; 132.56; 130.96; 129.85; 126.89; 124.63; 122.38; 111.57; 20.79.

PMSSQ RAFT macro chain transfer agent (PMSSQ-mCTA). The macro initiator was synthesized as described in reference [44]. ¹H-NMR (CDCl₃) δ : 7.99 (br, 5H); 7.36 (br, 2H); 5.80 (br, 1.9H); 4.55 (br, 2H); 3.48 (br, 1.1H); 2.71 (br, 2H); 0.99 (br, 2H); 0.17 (br, 69.1H). M_n = 4990 g/mol, PDI = 1.63.

PMSSQ-PTPA. 0.5 g PMSSQ-mCTA, 10 mg AIBN, 4 mL dioxane and 2 g *N,N*-di-4-methylphenylamino styrene were placed in a 20 mL Schlenk flask and degassed for three times. The reaction mixture was stirred magnetically at 80 °C for 4 h and afterwards precipitated into *n*-hexane twice. (Yield: 1.92g). ¹H-NMR (CDCl₃) δ : 7.98 (br); 7.58-6.78 (br); 4.46 (br); 2.73 (br); 2.31 (br); 2.25 (br); 1.28 (br); 0.89 (br); 0.17 (br). ²⁹Si CPMAS NMR δ : -49.02 (T1, 7 %); -58.11 (T2, 45 %); -66.34 (T3, 48 %). M_n = 37400 g/mol, PDI = 1.81. TGA results: cross-linking PMSSQ part between 50 °C and 150 °C, organic decomposition between 300 °C and

500 °C, weight ratio org.:inorg.: 90 : 10.

ITO preparation and surface coating. ITO covered glass slides (CEC010S, ≤ 10 Ohm/sq.; from pgo, Germany) were cleaned with THF, dried in nitrogen stream and O₂ plasma treated (1 W, 5 min). PMSSQ-PTPA was spin-coated from 0.2 wt.-% solution for AFM and contact angle investigations. An 8 wt.-% solution was used to spin-coat samples for TOF, CV and tape test investigations. Coatings were annealed at 160 °C for 2 h to induce cross-linking.

Results and discussion

Poly(methylsilsesquioxane) (PMSSQ) hybrid polymers could successfully be applied as thin films onto various underlying substrates via spin-coating.^[43,44] After temperature-induced cross-linking of the residual immanent Si-OH and Si-OCH₃ groups, stable and adherent smooth surface coatings were obtained, independent of the incorporated organic polymer and independent of the substrate.

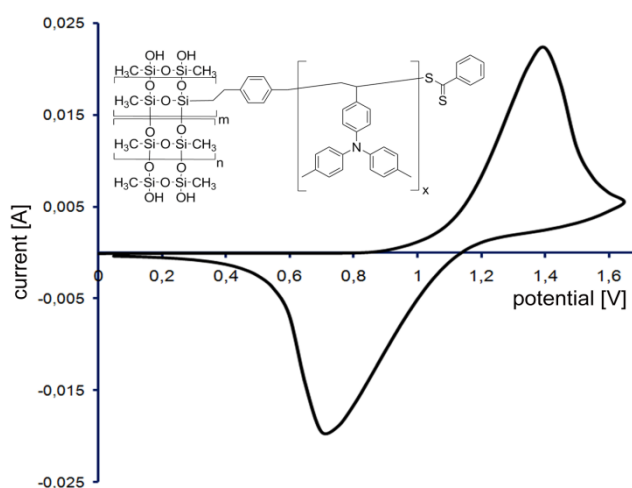


Figure 1. Cyclic voltammogram of PMSSQ-PTPA coated ITO covered glass slide ($P_{ox} = 1.35$ V; HOMO level = -5.60 eV).

Synthesis consists of (i) preparation of soluble PMSSQ that is capable to act as a chain transfer agent in the grafting-from polymerization, (ii) RAFT polymerization of organic vinyl monomers to yield the desired PMSSQ hybrid structure. Thus, the only requirement toward the organic moiety is the polymerizability of the monomer by the RAFT technique.^[44] For example, *N,N*-di-4-methylphenylamino styrene (TPA) is known as a monomer yielding hole-conductive polymers,^[45] which are used as promising HIL materials. Thus, grafting TPA from PMSSQ should result in hybrid polymers that feature strong adhesion to ITO and planarization of the immanent surface roughness, while at the same time attaching the hole-conductive polymer covalently onto the substrate. By incorporation of cross-linked PMSSQ (usually 10 – 20 wt.-%) into the HIL, in situ electrode passivation would be possible; as already shown for thin dielectric layers produced by self-assembly processes, enhancing external quantum efficiency and luminous efficiency.^[46]

PMSSQ-PTPA could successfully be prepared by grafting TPA from a soluble PMSSQ macro chain transfer agent (structure shown in figure 1). Molecular weight, determined by GPC was $M_n = 37400$ g/mol; ^{29}Si CPMAS NMR spectra showed 52 % of all Si still have free OH groups, indicating a high cross-linking ability. The cross-linking temperature was found to be between 50 °C and 150 °C, as determined by TGA. The hybrid polymer contained 10 wt.-% PMSSQ (calculated from TGA results). Spin-coating the polymer and annealing the films at 160 °C for 2 h resulted in polymer covered ITO glass slides. Film stability and adhesion on ITO was tested by ISO tape test^[47] and excellent adhesion of PMSSQ-PTPA on ITO was found (results summarized in table 1). The oxidation potential (P_{ox}) and HOMO level were determined by cyclovoltammetry (CV) of PMSSQ-PTPA on ITO (see figure 1), P_{ox} was 1.35 V, the corresponding HOMO level was -5.60 eV. To characterize the hole transport in the film and to quantify their mobility, we used time-of-flight (TOF) photoconductivity technique to measure the charge carrier mobility.^[48] PMSSQ-PTPA films were spin-coated on ITO, annealed at 160 °C for 2 h, 100 nm Al was evaporated as back electrode and then the devices were encapsulated. A dispersive transport behavior with a hole mobility of $\sim 1 \cdot 10^{-6}$ cm²/Vs was found (see figure 2), which is in the range of other amorphous TPA-based HIL, obtained by evaporation of small molecules.^[49-51]

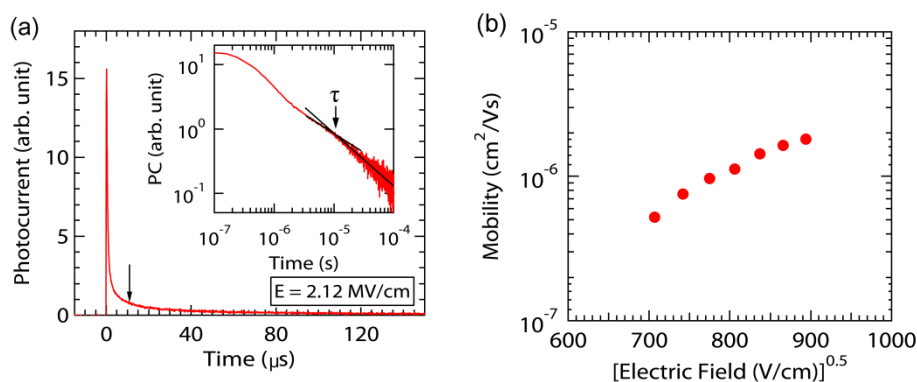


Figure 2. Time of flight photoconductivity data to determine the hole mobility inside the PMSSQ-PTPA film. (a) Photocurrent signal in a linear and log-log (inset) scale measured under the bias field of 2.12 MV/cm. The transit time τ , determined at the crossing point of two slopes in the inset, is marked with an arrow. (b) The hole mobility, calculated from the transit times at various electric fields, as a function of the square root of the electric field.

As planarization of ITO surface roughness is an important feature of HIL, we compared the surface roughness of bare ITO-covered glass slides (as received, cleaned as explained above) with PMSSQ-PTPA coated ITO substrates. Coatings were applied from a 0.2 wt.-% solutions, equivalent to 25 nm film thickness (measured by ellipsometry on silicon wafer). The topography of bare ITO revealed a root mean square (RMS) roughness of 2.33 nm on an area of 1 μm^2 (figure 3A). After coating with PMSSQ-PTPA, an effective planarization was observed. The respective AFM topography is shown in figure 3B. The RMS roughness was estimated to be 0.36 nm (on 1 μm^2), showing a decrease of surface roughness by nearly a factor of 10.

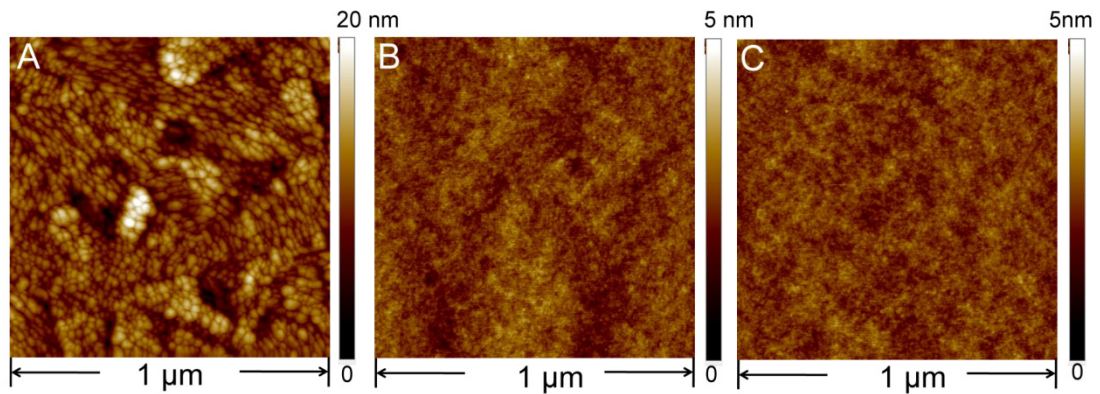


Figure 3. Left image: AFM topography of bare ITO (RMS roughness 2.33 nm), middle image: AFM topography of PMSSQ-PTPA coated ITO (RMS roughness 0.36 nm), right image: PMSSQ-PTPA coated ITO after 1 h toluene treatment (RMS roughness 0.31 nm).

Table 1. Contact angle, cyclic voltammetry and tape test results of PMSSQ-PTPA coated ITO, right after coating and after 1h solvent treatment. Tape test classification: 0 indicates no detachment, 5 indicates more than 50 % detachment of the coating (DCB: dichlorobenzene).

	Θ_a [°]	Θ_r [°]	tape test	P_{ox}
bare ITO	21 ± 3	15 ± 3	n/a	n/a
after coating	88 ± 3	79 ± 3	0	1.35
1 h in toluene	87 ± 3	79 ± 3	0	1.35
1 h in DCB	88 ± 3	78 ± 3	0	1.33
1 h in THF	87 ± 3	76 ± 3	0	1.35

To investigate if a further multilayer fabrication on top of the PMSSQ-PTPA HIL is in principle possible, coated ITO substrates were placed in toluene, dichlorobenzene and THF for 1 h. After drying, the coating properties were determined by contact angle measurements, CV and tape test; the results were summarized in table 1. The advancing contact angle (Θ_a) on plasma-cleaned ITO was 21 °, on the coated substrate Θ_a was 88 ° and did not change significantly after any solvent treatment. Similar results were obtained by CV measurements, the oxidation potential P_{ox} remained at 1.35 eV. Adhesion on ITO after solvent treatment was also not affected (Tape test results remained 0). After 1 h in toluene, the topography of the coated ITO substrate was visualized by AFM, shown in figure 3C, and no change in RMS roughness was detected (RMS: 0.31 nm). Overall, no influence of the solvent treatment on the PMSSQ-PTPA coating could be observed, indicating the possibility for a further multilayer device fabrication.

Conclusions

Poly(methylsilsesquioxane)-poly(*N,N*-di-4-methylphenylamino styrene) (PMSSQ-PTPA) was synthesized by grafting the electroactive monomer TPA from a PMSSQ macro chain transfer agent. In principle, this synthetic process can be applied to various monomers, and thus gives easy accesses for further improvement of the electronic properties. The obtained hole injection material (HIM) features a HOMO level of -5.6 eV and a hole mobility of $1 \cdot 10^{-6} \text{ cm}^2/\text{Vs}$.

PMMSQ-PTPA is an ideal coating material, achieving an effective planarization of the ITO substrate. By spin-coating and annealing of the HIM, surface roughness was decreased from 2.33 nm to 0.357 nm (image RMS $1 \times 1 \mu\text{m}^2$). High stability, adhesion and surface functionalization was preserved even after solvent treatment, thus the described HIL fabrication strategy is capable for a further spin-on multilayer device fabrication.

Acknowledgments

The authors acknowledge financial support from the IRTG 1404 / 2006-IRTG-001 (Self-Assembled Materials for Optoelectronic Applications), jointly funded by the Deutsche Forschungsgemeinschaft (DFG) of Germany and by the Korean Science Foundation (KOSEF) of Korea. This research was supported by WCU (World Class University) program through the Korea science and Engineering Foundation funded by the Ministry Of Education, Science and Technology (400-2008-0230).

References

- [1] C. W. Tang, S. A. VanSlyke, *Appl. Phys. Lett.* **1987**, *51*, 913.
- [2] M. Schat, W. Helfrich, *Appl. Phys. Lett.* **1971**, *18*, 127.
- [3] Y. Cao, G. Yu, C. Zhang, R. Menon, A. J. Heeger, *J. Synth. Met.* **1997**, *87*, 171.
- [4] J. S. Kim, M. Granstrom, R. H. Friend, N. Johansson, W. R. Salaneck, R. Daik, W. Feast, F. Calcioli, *J. Appl. Phys.* **1998**, *84*, 6859.
- [5] H. Hoppe, N. S. Sariciftci, *J. Mater. Res.* **2004**, *19*, 1924.
- [6] T. W. McBee, L. Y. Wang, C. H. Ge, B. M. Beam, A. L. Moore, D. Gust, T. A. Moore, N. R. Armstrong, S. S. Saavedra, *J. Am. Chem. Soc.* **2006**, *18*, 2184.
- [7] C. H. Ge, W. J. Doherty, S. B. Mendes, N. R. Armstrong, S. S. Saavedra, *Talanta* **2005**, *65*, 1126.
- [8] C. C. Wu, C. I. Wu, J. C. Sturm, A. Kahn, *Appl. Phys. Lett.* **1997**, *70*, 1348.
- [9] F. Li, H. Tang, J. Shinar, O. Resto, S. Z. Weisz, *Appl. Phys. Lett.* **1997**, *70*, 2741.
- [10] T. Kugler, M. Lögdlund, W. R. Salaneck, *IEEE Trans. Electron. Devices* **1998**, *4*, 14.
- [11] A. R. Schlatmann, D. Wilms Floet, A. Hilberer, F. Garten, P. J. M. Smulders, *Appl. Phys. Lett.* **1996**, *69*, 1764.
- [12] Z. Z. You, J. Y. Dong, *Appl. Surf. Sci.* **2005**, *249*, 271.
- [13] D. J. Milliron, I. G. Hill, C. Shen, A. Kahn, J. Schwartz, *J. Appl. Phys.* **2000**, *87*, 572.
- [14] C. N. Li, C. Y. Kwong, A. B. Djuricic, P. T. Lai, P. C. Chui, W. K. Chan, S. Y. Liu, *Thin Solid Films* **2005**, *477*, 57.
- [15] M. G. Mason, L. S. Hung, C. W. Tang, S. T. Lee, K. W. Wong, M. Wang, *J. Appl. Phys.* **1999**, *86*, 1688.
- [16] Y. H. Niu, M. S. Liu, J. W. Ka, A. K. Y. Jen, *Appl. Phys. Lett.* **2006**, *88*, 93505.
- [17] G. E. Jabbour, J.-F. Wang, N. Peyghambarian, *Appl. Phys. Lett.* **2002**, *80*, 2026.
- [18] P. Strohriegel, J. V. Grazulevicius, *Adv. Mater.* **2002**, *14*, 1439.
- [19] J. Cui, Q. Huang, J. C. G. Veinot, H. Yan, Q. Wang, G. R. Hutchison, A. G. Richter, G. Evmenenko, P. Dutta, T. J. Marks, *Langmuir* **2002**, *18*, 9958.

- [20] W. Yu, J. Pei, Y. Cao, W. Huang, *J. Appl. Phys.* **2001**, *89*, 2343.
- [21] X. Ren, B. D. Alleyne, P. I. Djurovich, C. Adachi, I. Tsyba, R. Bau, M. E. Thompson, *Inorg. Chem.* **2004**, *43*, 1697.
- [22] R. D. Hreha, C. P. George, A. Haldi, B. Domercq, M. Malagoli, S. Barlow, J.-I. Bredas, B. Kippelen, S. R. Marder, *Adv. Funct. Mater.* **2003**, *13*, 967.
- [23] X. Gong, D. Moses, A. J. Heeger, S. Liu, A. K. Y. Jen, *Appl. Phys. Lett.* **2003**, *83*, 183.
- [24] S. Liu, X. Jiang, H. Ma, M. S. Liu, A. K. Y. Jen, *Macromolecules* **2000**, *33*, 3514.
- [25] B. E. Koene, D. E. Loy, M. E. Thompson, *Chem. Mater.* **1998**, *10*, 2235.
- [26] S. Thayumanavan, S. Barlow, S. R. Marder, *Chem. Mater.* **1997**, *9*, 3231.
- [27] M. S. Liu, Y.-H. Niu, J.-W. Ka, H.-L. Yip, F. Huang, J. Luo, T.-D. Kim, A. K. Y. Jen, *Macromolecules* **2008**, *41*, 9570.
- [28] T.-W. Lee, Y. Kwon, J.-J. Park, L. Pu, T. Hayakawa, M. Kakimoto, *Macromol. Rapid Commun.* **2007**, *28*, 1657.
- [29] W. Li, Q. Wang, J. Cui, H. Chou, S. E. Shaheen, G. E. Jabbour, J. Anderson, P. Lee, B. Kippelen, N. Peyghambarian, N. R. Armstrong, T. J. Marks, *Adv. Mater.* **1999**, *11*, 730.
- [30] J. Cui, A. Wang, N. L. Edleman, J. Ni, P. Lee, N. R. Armstrong, T. J. Marks, *Adv. Mater.* **2001**, *13*, 1476.
- [31] Q. Huang, G. A. Evmenenko, P. Dutta, P. Lee, N. R. Armstrong, T. J. Marks, *J. Am. Chem. Soc.* **2005**, *127*, 10227.
- [32] J. Li, T. J. Marks, *Chem. Mater.* **2008**, *20*, 4873.
- [33] J. Cui, Q. Huang, Q. Wang, T. J. Marks, *Langmuir* **2001**, *17*, 2051.
- [34] Q. Huang, G. A. Evmenenko, P. Dutta, T. J. Marks, *J. Am. Chem. Soc.* **2003**, *125*, 14704.
- [35] Q. Huang, J. Li, G. A. Evmenenko, P. Dutta, T. J. Marks, *Chem. Mater.* **2006**, *18*, 2431.
- [36] J. Li, L. Wang, J. Liu, G. A. Evmenenko, P. Dutta, T. J. Marks, *Langmuir* **2008**, *24*, 5755.
- [37] J. A. Bardecker, H. Ma, T. Kim, F. Huang, M. S. Liu, Y.-J. Cheng, G. Ting, A. K. Y. Jen, *Adv. Funct. Mater.* **2008**, *18*, 3964.
- [38] Y.-J. Cheng, M. S. Liu, Y. Zhang, Y. Niu, F. Huang, J.-W. Ka, H.-L. Yip, Y. Tian, A. K. Y. Jen, *Chem. Mater.* **2008**, *20*, 413.
- [39] B. Lim, J. T. Hwang, J. Y. Kim, J. Ghim, D. Vak, Y. Y. Noh, S. H. Lee, K. Lee, A. J. Heeger, D. Y. Kim, *Org. Lett.* **2006**, *8*, 4703.
- [40] J. L. Zhao, J. A. Bardecker, A. M. Munro, M. S. Liu, Y. H. Niu, I. K. Ding, J. D. Luo, B. Q. Chen, A. K. Y. Jen, D. S. Ginger, *Nano. Lett.* **2006**, *6*, 463.
- [41] B. Ma, F. Lauterwasser, L. Deng, C. S. Zonte, B. J. Kim, J. M. J. Fréchet, *Chem. Mater.* **2007**, *19*, 4827.
- [42] T. M. Fulghum, P. Taranekar, R. C. Advincula, *Macromolecules* **2008**, *41*, 5681.
- [43] D. Kessler, C. Teutsch, P. Theato, *Macromol. Chem. Phys.* **2008**, *209*, 1437.
- [44] D. Kessler, P. Theato, *Macromolecules* **2008**, *41*, 5237.
- [45] M. Behl, E. Hattemer, M. Brehmer, R. Zentel, *Macromol. Chem. Phys.* **2002**, *203*, 503.
- [46] J. E. Malinsky, G. E. Jabbour, S. E. Shaheen, J. D. Anderson, A. G. Richter, T. J. Marks, N. R. Anderson, B. Kippelen, P. Dutta, N. Peyghambarian, *Adv. Mater.* **1999**, *11*, 227.
- [47] Paints and Varnishes – Cross-cut test (ISO 2409:2007)

- [48] C.-Y. Lin, Y.-M. Chen, H.-F. Chen, F.-C. Fang, Y.-C. Lin, W.-Y. Hung, K.-T. Wong, R. C. Kwong, S. C. Xia, *Organic Electronics* **2009**, *10*, 181.
- [49] Y. Shirota, H. Kageyama, *Chem. Rev.* **2007**, *107*, 953.
- [50] Q. Zhang, J. Chen, Y. Cheng, L. Wang, D. Ma, X. Jing, F. Wang, *J. Mater. Chem.* **2004**, *14*, 895.
- [51] Y. Shirota, S. Nomura, H. Kageyama, *Proc. SPIE – Int. Soc. Opt. Eng.* **1998**, *3476*, 132.

4.7

Substrate-Independent Stable and Adherent Reactive Surface Coatings and Their Conversion with Amines

Daniel Kessler,^{1,2} Nadine Metz,¹ Patrick Theato*¹

1 Institute of Organic Chemistry, University of Mainz, Duesbergweg 10-14, 55099 Mainz, Germany

2 Max Planck Institute for Polymer Research, Ackermannweg 10, 55128 Mainz, Germany

Macromol. Symp. **2007**, *254*, 34-41.

Summary

To create stable, adherent and reactive surface coatings, a hybrid polymer composed of poly(methylsilsesquioxane) (PMSSQ) and poly(pentafluorophenyl acrylate) PFPA with a Mn of 32000 g/mol was prepared by a RAFT polymerization procedure. These hybrid polymer has been used for coating experiments. The PFPA part enabled a variable functionalization of the coating afterwards. The stability on various substrates (e.g. glass, PMMA, steel) was tested in an ISO tape test. These reactive surface coatings were modified using different amines, such as amino-terminated PEG, dodecyl amine and N-isopropyl amine. The conversion was analyzed by FT-IR and contact angle measurements.

Keywords

surfaces; RAFT polymerization; graft copolymers; active esters; films; adhesion; atomic force microscopy (AFM); inorganic-organic hybrid polymers; PNIPAM

Introduction

In various applications for research or industry hydrophilic, hydrophobic or stimuli-responsive surface coatings are of special interest^[1-8]. Reactive coatings could be a precursor for simple tunable surface properties. Just using a simple modification step should convert the surface towards the desired properties or structures.

Active ester polymers are ideal candidates which can be converted by a simple polymer analogues reaction into the desired functional polymer. Just by the reaction with nucleophiles, such as amines, many functionalized polymers can be synthesized as shown in reference [9] and references therein. Attached onto a substrate the conversion could be induced by dipping it in an amine solution or by micro contact printing of amines onto the surface.

Typical methods to prepare polymeric films on a surface are grafting from polymerization or the chemical vapor deposition polymerization. Both methods were already used to prepare reactive coatings consisting of active ester monomers. Jerome et al. reported the electrografting of *N*-succinimidyl acrylate, a well known reactive ester monomer, from glassy carbon^[10-11]. Lahann et al. demonstrated the chemical vapor deposition polymerization of [2.2]paracyclophane pentafluorophenol ester on silicon wafers and its conversion with amines to obtain structuralized surfaces^[12-13]. Both methods yielded in reactive surface coatings but the procedures are hardly convertible to any scientific or industrial application.

Within the present study, we analyzed a reactive inorganic/organic hybrid polymer as a versatile coating material.

Experimental Part

Materials. All reagents, solvents, and substances used were of reagent grade quality and were obtained from commercial sources.

Instrumentations. The synthesized compounds were characterized by NMR-spectroscopy, mass spectroscopy, FT-IR spectroscopy and elemental analysis. Molecular weights of the polymers were determined by gel permeation chromatography using a PSS standard column, UV-, refractive index- and light scattering-detector. NMR-spectra were recorded on a 300 MHz Bruker FT-NMR-spectrometer using CDCl₃ as a solvent. Chemical shifts (δ) are given in ppm relative to TMS. IR spectra were recorded on a Nicolet 5 DXC FT-IR-spectrometer. FD mass spectra were measured using a Finnigan MAT 95 mass spectrometer. Elemental analyses were done with an Elementar Vario Micro Cube (detecting C, H, N, S). Film thicknesses were measured on an EL X-02C ellipsometer. Thermo gravimetric analysis was performed using a Perkin Elmer Pyris 6 TGA. Atomic force microscopy (AFM) measurements were observed on a Veeco Dimension 3100.

Dithio benzoic acid 4-ethyltrimethoxysilylester (RAFT-Si). 31.6 mmol phenyl magnesium bromide was placed with 50 mL THF in a round bottomed flask. After heating to 40 °C 49.7 mmol CS₂ was added. After 15 minutes 31.7 mmol *p*-(Chloromethyl)-phenylethyltrimethoxysilane was injected and the reaction mixture was stirred at 50 °C for 1 h. The mixture was dissolved in diethyl ether and washed with water, the ether phase was dried over magnesium sulfate, filtered and the ether was removed. The product was dried in

vacuum. Yield: 25.3 mmol (79.7 %). $^1\text{H-NMR}$ (CDCl_3) δ : 8.01 (m, 1H); 7.27 (m, 8H); 4.58 (d, 3J = 2.4 Hz, 2H); 3.59 (s, 9H); 2.76 (m, 2H); 1.04 (m, 2H). EA (%): C = 56.20; H = 6.32; S = 10.51. FD mass spectra: 391.9 (100%); 392.9 (26.9%); 393.9 (15.4%).

PMSSQ RAFT macro initiator. 50 mmol methyltrimethoxysilane (MTMS), 2.5 mmol RAFT-Si, 20 mL THF, 500 mmol water and 10 mmol HCl were stirred at 0 °C for 3 h. The reaction mixture was dissolved in diethyl ether, washed with water. After drying, the ether was removed and the product was dried in high vacuum. $^1\text{H-NMR}$ (CDCl_3) δ : 7.99 (br, 5H); 7.36 (br, 2H); 5.80 (br, 1.9H); 4.55 (br, 2H); 3.48 (br, 1.1H); 2.71 (br, 2H); 0.99 (br, 2H); 0.17 (br, 69.1H). M_n = 4990 g/mol, PDI = 1.63.

PMSSQ-*b*-PFPA. 0.5 g PMSSQ RAFT macro initiator, 10 mg AIBN, 4 mL dioxane and 2 g pentafluorophenyl acrylate ester were placed in a Schlenk flask. The reaction mixture was stirred at 80 °C for 4 h and afterwards precipitated into *n*-hexane twice. (Yield: 1.1 g). $^1\text{H-NMR}$ (CDCl_3) δ : 7.40 – 6.85 (br); 3.05 (br, 1H); 2.81 (br); 2.32 – 2.10 (br, 2H); 1.50 – 1.20 (br); 0.15 (br, 1H). M_n = 32000 g/mol, PDI = 1.7.

Amino-terminated poly(ethyleneglycol) ($\text{H}_2\text{N-PEG500}$). Amino-terminated PEG was synthesized as described in [14].

ESI mass spectra: 550 g/mol

Surface coating and modification. The polymer solution was spin-coated onto clean substrates (15 s, 4000 rpm). To cross-link the inorganic block, the samples were annealed at 130 °C for 2 h and afterwards washed with THF for 30 minutes to remove any non-bonded material.

To functionalize the surface afterwards in a polymer analogous reaction the samples were placed in a 10 wt% solution of the desired amine in THF at room temperature for 1 h. To remove the excess of the amine the surface was washed several times with THF. The surface reaction was detected by FT-IR measurements using an ATR setup.

Results and Discussion

A new concept to prepare reactive surface coatings should imply reactivity, stability and adhesion on various substrates and easy application and processability.

To combine all these challenges in one material inorganic/organic hybrid polymers seems to be a promising approach. The hybridization of inorganic and organic materials on a nanometer scale offers the chance not even to combine their advantages in one material but also to achieve new, unique properties^[15].

As inorganic component poly(methylsilsesquioxane)s (PMSSQ) are known to be able to crosslink thermally and stabilize films but also as adhesion promoters on metal or metal oxide surfaces^[16]. Beside these important characteristics soluble silsesquioxanes can be easily synthesized in a sol-gel process^[17]. Their reactivity towards a secondary condensation in the film can be monitored using thermo gravimetric analysis.

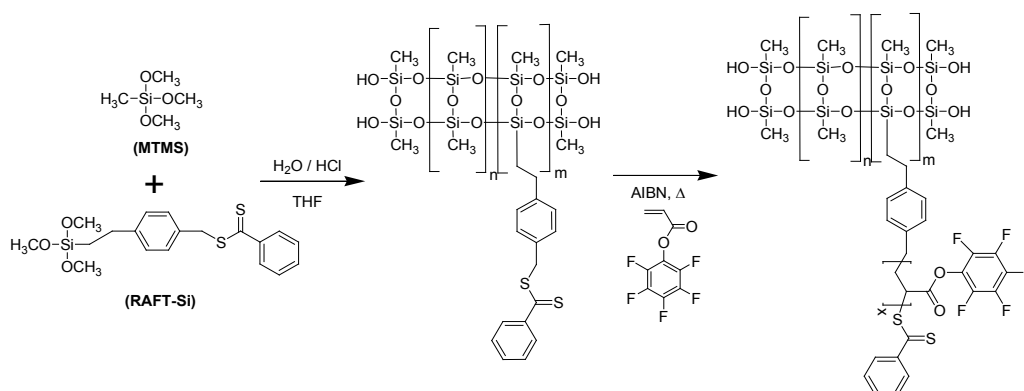
Connecting these fundamental properties with the reactivity of reactive ester polymers would result in a reactive coating material with high stability and easy processability.

As reactive ester monomer pentafluorophenyl acrylate emerges as a perfect candidate to

build up reactive polymers, which can be converted in a polymer analogues reaction to yield a wide spectrum of functionalized polymers. One example is the conversion of poly(pentafluorophenyl acrylate) (PFPA) with isopropyl amine to yield poly(*N*-isopropyl acrylamide) (PNIPAM) [18-20], known for its stimuli-responsive behavior in water.

First, an inorganic/organic hybrid polymer, consisting of PMSSQ and PFPA, was synthesized as shown in scheme 1. In the first step a PMSSQ based macro chain transfer agent is co-condensated using MTMS and the functionalized RAFT agent RAFT-Si. From this controlling agent pentafluorophenyl acrylate is grafted using usual RAFT conditions.

Scheme 1. Synthetic pathway towards reactive PMSSQ-PFPA hybrid polymers.



The obtained polymer had a molecular weight of 32000 g/mol and was soluble in THF. The thermo gravimetrical analysis of the polymer hybrid is shown in figure 1. A secondary condensation occurs between 120 °C and 160 °C. At 400 °C the decomposition of the PFPA block could be observed.

The block ratio between the organic and inorganic block could be calculated from the mass deficits, resulting in the weight ratio of 82 % PFPA and 18 % PMSSQ.

The obtained hybrid polymer was spin-coated from a 10 wt% solution in THF onto silicon, glass, PMMA and steel. Afterwards the films were cured at 130 °C for 2h to stabilize the coating by thermally induced secondary condensation as it was observed in the TGA.

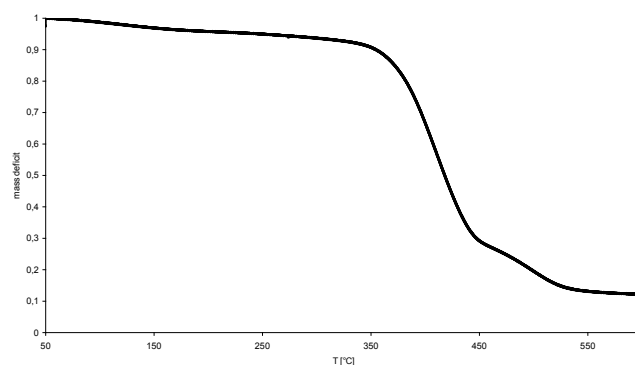


Figure 1. Thermo gravimetrical analysis of PMSSQ-*b*-PFPA.

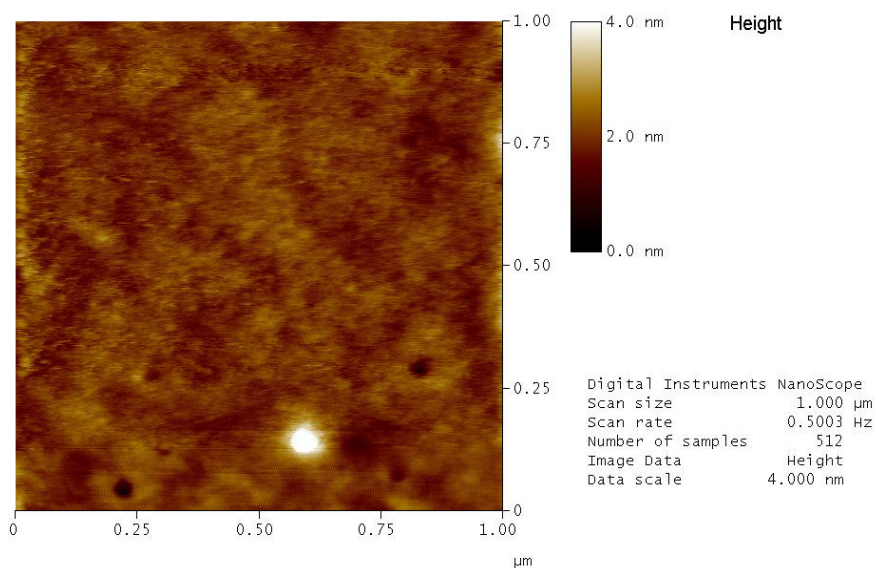


Figure 2. AFM height image of PMSSQ-*b*-PFPA coated on silicon after curing.

The film thickness determined by ellipsometry on silicon wafer was 395 nm before curing, 375 nm after curing. The surface roughness of the films before and after curing were determined by AFM measurement, the height image after curing is shown in figure 2, the corresponding phase images gave no additional information and were not shown in this context. The RMS value before curing is 0.471 nm, after curing 0.305 nm (both are image RMS values, calculated over $1\mu\text{m}^2$). Thus, the prepared surface coating on silicon is very smooth after curing.

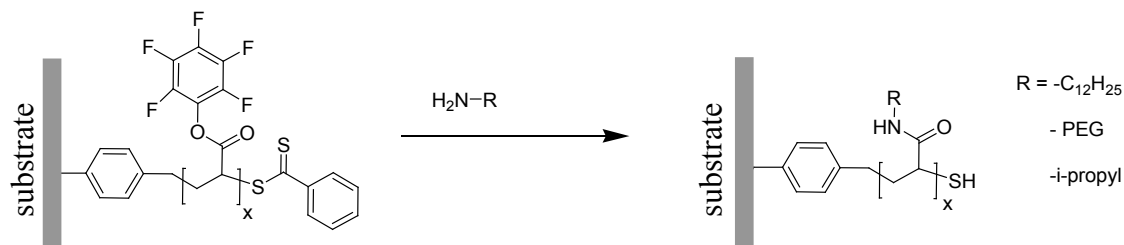
The adhesion and stability of the film was tested using a standard ISO tape test ^[21]. The test mainly focuses on the adhesion of the coating. One half of the surface coating is taped with commercially available tape. After tearing off the tape the condition of the taped and not taped surfaces are compared under microscope.

The Microscopy images of the PMSSQ-*b*-PFPA coatings on glass, PMMA and steel were analyzed. The estimated border between the taped and the not tabbed part of the surface coating is indicated by a dashed line.

The differences before and after curing are apparently on all three substrates. Before curing, the reactive surface coating can easily rupture off the surface. After curing, the secondary condensation results in a stable and adherent film not only on glass or steel but also on polymeric substrates like PMMA (ISO classification 4 before curing, indicating a poor adhesion on the substrate; ISO classification 0 after curing, indicating a completely maintained coating).

After proofing the ability to produce stable coatings the reactivity of the functionalized substrates were investigated. The functionalization of the surface via a polymer analogues reaction is shown in scheme 2.

Scheme 2. Surface modification of a reactive surface by a polymer analogous reaction with different amines.



The reactive character of the obtained surfaces after spin-coating opens the possibility for a flexible functionalization procedure. As example, three case studies were conducted by conversion into a hydrophilic, a hydrophobic and a temperature-responsive surface.

For the preparation of a hydrophilic surface amino-terminated PEG was used as a nucleophile in the polymer analogous reaction with the exposed active ester. Dodecyl amine was employed to create a hydrophobic surface coating, while isopropyl amine converted the reactive coating into a poly(*N*-isopropyl acryl amide) (PNIPAM) coating, which should show a temperature-sensitive behavior.

In case of *N*-isopropyl amine the conversion of the reactive coating on glass, monitored using FT-IR spectroscopy, is shown in figure 3. The surface properties after conversion with amino-PEG, dodecyl amine and *N*-isopropyl amine on all substrates were investigated by means of contact angle measurements.

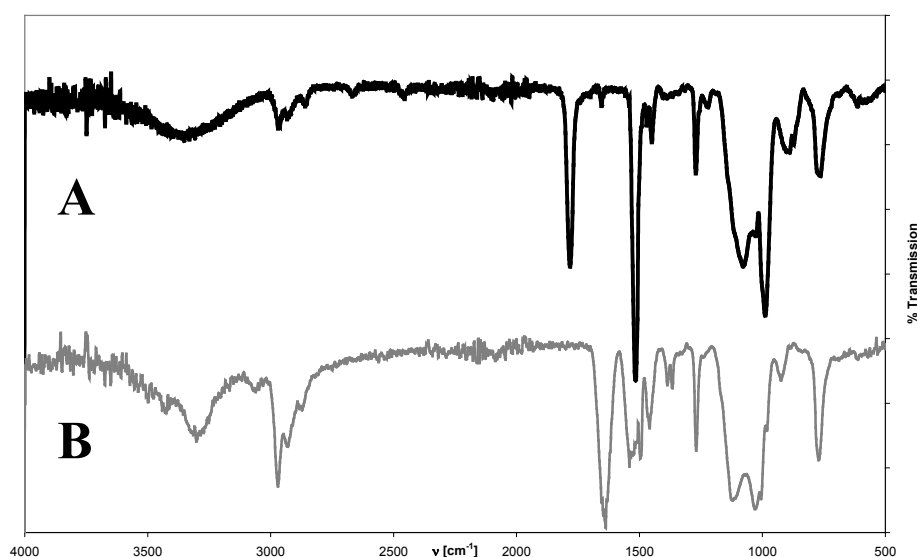


Figure 3. FT-IR spectra proving the conversion of PFPA surface to PNIPAM surface, A: PMSSQ -PFPA coated glass after curing; B: after modification with isopropyl amine.

Spectrum A in figure 6 shows the FT-IR of the reactive coating, which is characterized by the band at 1772 cm^{-1} , a unique signal for the activated ester bond. After the polymer analogous reaction with isopropyl amine the characteristic band at 1772 cm^{-1} disappeared completely (see figure 3B) and the characteristic bands for an amide at 1638 cm^{-1} and 1530 cm^{-1} were found, proving a complete conversion of all active ester groups. Additionally a band at 3300 cm^{-1} , characteristic for a NH-bond appeared. Both spectra showed the characteristic bands of the PMSSQ block between 1270 cm^{-1} and 900 cm^{-1} , respectively. FT-IR spectroscopy proved a successful surface modification also with amino-PEG and dodecyl amine.

To investigate the surface behavior of the different coatings contact angles of water were measured on functionalized glass and silicon substrates. The advancing and the receding contact angles of a drop of water on the surface using an image processing software were determined. Averaged values of six independent measurements for each film are summarized in table 1.

In principle the conversion of the reactive coating works on all tested substrates. The resulted contact angles are almost equal and seem not to be influenced by the nature of the substrate. The reaction with amino-PEG resulted in a hydrophilic surface (Θ_a between 30° and 37°). Dodecyl amine converts the reactive coating to a hydrophobic coating ($\Theta_a > 90^\circ$).

Table 1. Contact angles measured on silicon, glass, PMMA and steel substrates. (If not mentioned $T = 25^\circ\text{C}$)

	silicon		glass		PMMA		steel	
	Θ_a	Θ_r	Θ_a	Θ_r	Θ_a	Θ_r	Θ_a	Θ_r
reactive surface after curing	93.3°	64.3°	94.2°	70.1°	93.0°	72.1°	92.1°	69.1°
after amino-PEG treatment	33.2°	14.9°	32.6°	12.6°	30.1°	17.9°	36.6°	16.9°
after dodecyl amine treatment	101.9°	60.1°	102.1°	60.6°	100.2°	71.1°	94.1°	63.2°
after isopropyl amine treatment	79.2°	45.0°	80.1°	52.2°	77.3°	49.0°	71.1°	49.7°
after isopropyl amine treatment (50°C)	100.0°	68.0°	102.9°	70.2°	96.7°	72.5°	104.3°	70.2°

The conversion with *N*-isopropyl amine to a PNIPAM surface resulted in a stimuli-responsive surface behavior. At a temperature below the lower critical solution temperature (LCST) the surface shows a more hydrophilic behavior. When heated above the LCST the surface behavior turns hydrophobic. The values correspond well with the literature values of PNIPAM functionalized surfaces, produced by other methods^[22-23].

The switching of contact angles by temperature on a silicon substrate is shown in figure 4.

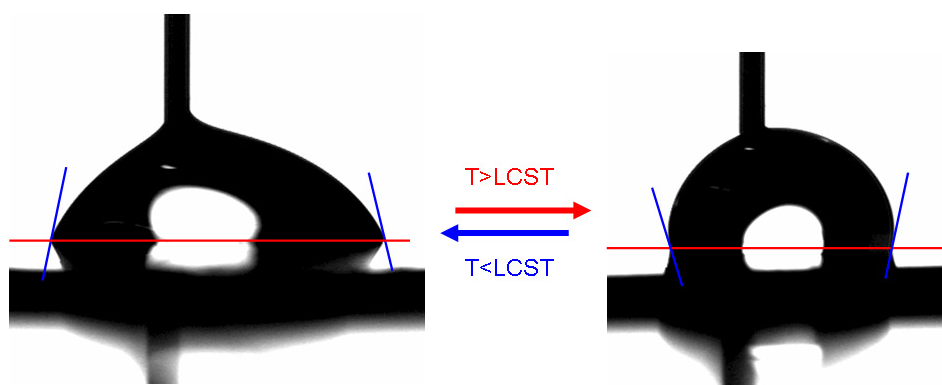


Figure 4. Contact angle images of the stimuli-responsive coating on silicon, obtained by the conversion of the reactive coating with *N*-isopropyl amine. The left picture is taken at $T = 25^{\circ}\text{C}$, the right picture at $T = 50^{\circ}\text{C}$.

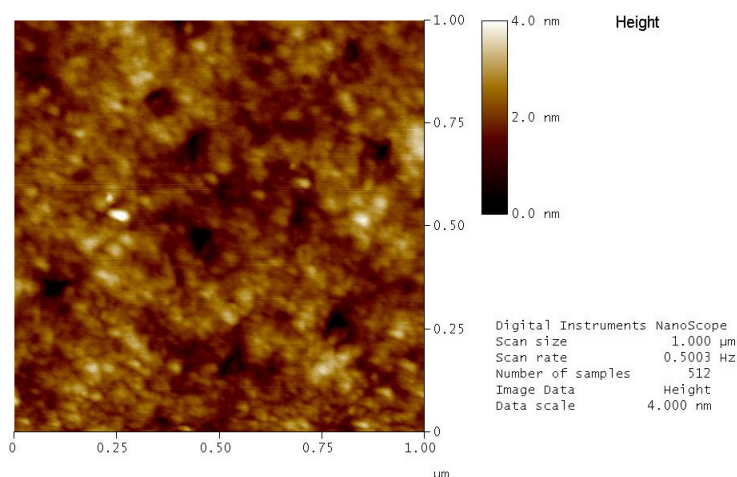


Figure 5. AFM height image of PMSSQ-*b*-PFPA coated on silicon after curing after conversion with *N*-isopropyl amine.

The surface roughness after conversion to a PNIPAM surface was determined using AFM. The image RMS value is 0.479 nm (calculated over $1\mu\text{m}^2$). Compared with the reactive coating the surface roughness does not change due to the functionalization.

Conclusion

Preparing reactive surface coatings from a PMSSQ-based precursor just by spin-coating and curing seems to be an easy processable and applicable method.

Obtained reactive surfaces can be converted completely just by dipping in amine solutions at room temperature. Hydrophilic, hydrophobic and also stimuli-responsive surfaces could be prepared on different kinds of substrates. The most important issue on surface coatings is the stability and adhesion on the substrate. Using the tape-test the stability of the thermally cross-

linked coating could be proved on silicon, glass and steel, which can be explained by covalent bonds from the PMSSQ part to the substrate. In addition the stability of the coated film itself is high enough to obtain stable reactive coatings also on polymeric substrates. Beside the reactivity and stability of the surface coatings prepared by PMSSQ-PFPA hybrid materials, the films are before as well as after conversion very smooth.

Acknowledgement

The authors of this paper would like to thank Ruediger Berger, Max Planck Institute for Polymer Research, for AFM assistance.

References

- [1] P. Mansky, Y. Liu, E. Huang, T.P. Russell, C.J. Hawker, *Science* **1997**, *275*, 1458
- [2] P. Wiltzikus, A. Cumming, *Phys. Rev. Lett.* **1991**, *66*, 3000
- [3] G. Coulon, T.P. Russell, V.R. Deline, P.F. Green, *Macromolecules* **1989**, *22*, 2581
- [4] S.H. Anastasiadis, T.P. Russell, S.K. Satija, C.F. Majkrzak, *Phys. Rev. Lett.* **1989**, *62*, 1852
- [5] J. Genzer, K. Efimenko, *Science* **1992**, *256*, 1539
- [6] M.K. Chaudhury, G.M. Whitesides, *Science* **1992**, *256*, 1539
- [7] C.S. Chen, M. Mrksich, S. Huang, G.M. Whitesides, G.E. Ingber, *Science* **1997**, *276*, 1425
- [8] T.P. Russell, *Science* **2002**, *297*, 964
- [9] N. Metz, P. Theato, *European Polymer Journal* **2006**, accepted
- [10] C. Jerome, S. Gabriel, S. Voccia, C. Detrembleur, M. Ignatova, R. Gouttebaron, R. Jerome, *Chem. Commun.* **2003**, 2500
- [11] S. Cuenot, S. Gabriel, R. Jerome, C. Jerome, C.-A. Fustin, A. M. Jonas, A.-S. Duwez, *Macromolecules* **2006**, *39*, 8428
- [12] J. Lahann, M. Balcells, T. Rodon, J. Lee, I. Choi, K.F. Jensen, R. Langer, *Langmuir* **2002**, *18*, 3632
- [13] J. Lahann, M. Balcells, H. Lu, T. Rodon, K.F. Jensen, R. Langer, *Anal. Chem.* **2003**, *75*, 2117
- [14] P. Mongondry, C. Bonnans-Plaisance, M. Jean, J.F. Tassin, *Macromol. Rapid Commun.* **2003**, *24*, 681
- [15] T. Ogoshi, Y. Chujo, *Composite Interfaces* **2005**, *11(8-9)*, 539
- [16] G.L. Witucki, *J. Coat. Technol.* **1993**, *65*, 57
- [17] D.A. Loy, K.J. Shea, *Chem. Rev.* **1995**, *95*, 1431
- [18] M. Eberhardt, P. Theato, *Macromol. Rapid Commun.* **2005**, *26*, 1488
- [19] M. Eberhardt, R. Mruk, R. Zentel, P. Theato, *European Polymer Journal* **2005**, *41*, 1569
- [20] P. Theato, J.-K. Kim, J.-C. Lee, *Macromolecules* **2004**, *37*, 5475
- [21] ISO 2409:1992(E) (Tape-Test)
- [22] V.P. Gilcreest, W.M. Carroll, Y.A. Rochev, I. Blute, K.A. Dawson, A.V. Gorelov, *Langmuir* **2004**, *20*, 10138
- [23] D.L. Hubert, R.P. Manginell, P.M. Samara, B.-M. Kim, B.C. Bunker, *Science* **2003**, *301*, 352

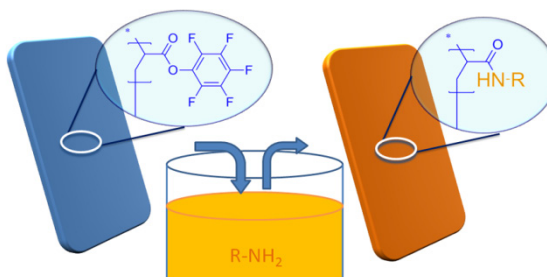
4.8

Reactive Surface Coatings Based on Polysilsesquioxanes: Defined Adjustment of Surface Wettability**(Part of the “Langmuir 25th year: Wetting and superhydrophobicity” special issue)***Daniel Kessler^{1,2}, Patrick Theato^{1*}*

1 Institute of Organic Chemistry, University of Mainz, Duesbergweg 10-14, 55099 Mainz, Germany

2 Max Planck Institute for Polymer Research, Ackermannweg 10, 55128 Mainz, Germany

Langmuir **2009**, published online April 16, <http://dx.doi.org/10.1021/la9005949>.

**Abstract**

We have investigated a generally applicable protocol for a substrate-independent reactive polymer coating that offers interesting possibilities for further molecular tailoring via simple wet chemical derivatization reactions. Poly(methylsilsesquioxane)-poly(pentafluorophenyl acrylate) hybrid polymers have been synthesized by RAFT polymerization and stable reactive surface coatings have been prepared by spin-coating on the following substrates: Si, glass, gold, PMMA, PDMS and steel. These coatings have been used for a defined adjustment of surface wettability by surface-analogous reaction with various amines, e.g. glutamic acid to obtain hydrophilic surfaces ($\Theta_a = 18^\circ$) or perfluorinated amines to obtain hydrophobic surfaces ($\Theta_a = 138^\circ$). Besides the successful covalent attachment of small molecules and polymers, also amino-functionalized nanoparticles could be deposited on the surface, resulting in nanostructured coatings, thereby expanding the accessible contact angle of hydrophobic surfaces further to $\Theta_a = 152^\circ$. The surface-analogous conversion of the reactive coating with isopropyl amine produced in situ temperature-responsive coatings. Using the presented simple, generally applicable protocol for substrate-independent reactive polymer coatings, the contact angle of water could be switched reversibly by almost 60° .

Introduction

The manipulation of surface wettability, either towards a hydrophilic or towards a hydrophobic behavior, through a combination of chemical and topological modifications has been of recent interest for a variety of applications.¹ Especially, extreme wetting behaviors, known as superhydrophilic or superhydrophobic surfaces, have been explored. Superhydrophilic surfaces were recently discussed as anti-fog coatings.² If water vapor condenses on a low contact angle surface, it forms a continuous water film and scattering events are mitigated and optical transmission is preserved.³ On the other side, superhydrophobic behavior causes water droplets to freely roll along the surface and may carry dirt away, which is widely known as "Lotus-Effect".^{4,5} Potential applications could be found in microfluidic devices,⁶ self-cleaning windows,⁷ building exteriors,⁸ and fabrics.^{9,10} Beside the mentioned extreme wetting behaviors, a defined adjustment of surface wettability is desired; for example for a controlled adsorption and adhesion of proteins at surfaces.^{11,12} Most recently, also surfaces featuring a stimuli-responsive behavior have found interest for a controlled adsorption and desorption upon an external stimulus.¹³

Over the last few decades an enormous number of literature has been published describing the control of interactions between water and surfaces.¹⁴ The contact angle (CA) is not only affected by the chemical nature of the interface, but also by the surface roughness and the chemical heterogeneity. First empirical laws on the contact angle were described by Wenzel^{15,16} and Cassie, Baxter¹⁷ and were modified and refined during the last decades.¹⁸⁻²⁰ Besides the absolute value of the CA, the difference between advancing CA (Θ_a) and receding CA (Θ_r), the so called CA hysteresis, is important.²¹⁻²³

Various coating materials were investigated to modify the chemical nature toward a desired wetting behavior on a given flat substrate. Widely used in research as well as in industry are alkylsilane monolayers that are covalently attached to silicon or siliconoxide surfaces. However, there are some draw-backs of this method: reaction time, temperature, concentration and additional base concentration have to be optimized precisely in order to achieve a complete and homogenous surface coverage.²⁴ Furthermore, mono-, di- and trialkoxy alkylsilanes either prefer surface binding or internal cross-linking.²⁵⁻²⁸ However, most striking is the limitation to silicon or siliconoxide surfaces. Nevertheless, initiating species for controlled radical polymerizations were immobilized at silicon surfaces using functionalized alkoxy silanes and surface modification was achieved by grafting polymer brushes from those initiators.^{29,30} Other methods to adjust the surface wettability on flat substrates are based on spin casting of polymers without covalent linkage to the surface,^{31,32} self-assembled monolayers³³ or multilayers,³⁴ or on chemical treatment of polymeric surfaces.^{35,36} Usually all of those methods are limited to one unique substrate and/or to the accessible CA scope or the desired CA hysteresis.

Considerable attempts have been made recently to create generally applicable protocols for substrate-independent reactive polymer coatings, offering interesting possibilities for further tailoring surface properties via simple wet chemical functionalization reactions. Reactive polymer interlayers, consisting of alternating copolymers of vinyl isocyanate and

maleic anhydride, have successfully been used to coat metal oxide surfaces maintaining reactive isocyanate and maleic anhydride groups at the surface.³⁷ *N*-Succinimidyl acrylate has been grafted from conducting substrates resulting in a reactive surface for the anchoring of a large variety of molecules.^{38,39} Plasma-polymerized maleic anhydride films showed excellent adhesion on various substrates and have been converted with decylamine to yield hydrophobic surfaces.⁴⁰ Langer and coworkers introduced the CVD polymerization of [2.2]paracyclophane pentafluorophenol ester to create chemically and topologically uniform reactive polymer coatings.^{41,42} Their method could successfully be used to pattern surfaces onto a broad range of different materials. However, this solvent free process is not applicable toward large structured surfaces or devices and the reaction conditions must be controlled very precisely to avoid the decomposition of the reactive groups.^{43,44}

In previous studies, we described the general synthesis of poly(silsesquioxane) hybrid polymers and their adherence on various substrates.⁴⁵⁻⁴⁷ Combining this concept of hybrid polymers as coating materials with poly(pentafluorophenyl acrylates) (PFPA), which are well recognized reactive polymers,⁴⁸ may yield in stable and adherent reactive coatings, that offer possibilities to be functionalized afterwards. In the present study we describe the synthesis of poly(methylsilsesquioxane)-poly(pentafluorophenyl acrylate) (PMSSQ-PFPA) hybrid polymers to be used as reactive coating materials, which can be applied via spin-coating from solution and converted afterwards to adjust surface wettability or surface functionalization.

Experimental Section

Materials. All chemicals and solvents were commercially available (Acros Chemicals, ABCR) and used as received unless otherwise stated. 1,4-Dioxane and THF were distilled from sodium/benzophenone under nitrogen.

Instrumentation. ¹H-NMR spectra were recorded on a Bruker 300 MHz FT-NMR spectrometer, ¹⁹F-NMR spectra on a Bruker DRX 400 FT-NMR spectrometer. ²⁹Si CPMAS NMR spectra were measured on a Bruker DSX 400 MHz FT-NMR spectrometer (Rotation: 5000 Hz, T = RT, 4 mm rotor). Chemical shifts (δ) were given in ppm relative to TMS. Gel permeation chromatography (GPC) was used to determine molecular weights and molecular weight distributions, M_w/M_n , of polymer samples. (THF used as solvent, polymer concentration: 2 mg/mL, column setup: MZ-Gel-SDplus 10² Å², 10⁴ Å² and 10⁶ Å², used detectors: refractive index, UV and light scattering). Thermo gravimetric analysis was performed using a Perkin Elmer Pyris 6 TGA in nitrogen (10 mg pure polymer in aluminum pan). Surface Plasmon Resonance (SPR) was measured on a home built system, using a $\Theta/2\Theta$ setup, a 632 nm laser and a photodiode. Glass slides were coated with 1.5 nm chromium and 50 nm gold by evaporation. SPR scans were fitted using WINSPALL.⁴⁹ Atomic force microscopy (AFM) measurements were performed using a Veeco Dimension 3100 in tapping mode. IR spectra were recorded using a Nicolet 5 DXC FT-IR-spectrometer on ATR crystal. Film thicknesses were measured using an EL X-02C ellipsometer. XPS measurements were done using an ESCALAB-II apparatus (VG). Advancing and receding CA of water were measured using a Dataphysics Contact Angle System OCA 20 and fitted by SCA 20 software. Given CA are average values of 10

individual measurements with an accuracy of 3°. To measure temperature dependent CA, the substrate temperature was controlled with a peltier element underneath (Accuracy of temperature dependent CA measurements 5°, due to complicate temperature adjustment). All chemical reactions were performed in Argon atmosphere.

PMSSQ RAFT macro chain transfer agent (PMSSQ-mCTA). The macro initiator was synthesized as described in reference [46]. ¹H-NMR (CDCl₃) δ: 7.99 (br, 5H); 7.36 (br, 2H); 5.80 (br, 1.9H); 4.55 (br, 2H); 3.48 (br, 1.1H); 2.71 (br, 2H); 0.99 (br, 2H); 0.17 (br, 69.1H). M_n = 4990 g/mol, PDI = 1.63.

PMSSQ-PFPA.^{46,47} 0.5 g PMSSQ-mCTA, 10 mg AIBN, 4 mL dioxane and 2 g pentafluorophenyl acrylate ester were placed in a 20 mL Schlenk flask and degassed for three times. The reaction mixture was stirred magnetically at 80 °C for 4 h and afterwards precipitated into *n*-hexane twice. (Yield: 1.1g). ¹H-NMR (CDCl₃) δ: 7.40 – 6.85 (br); 3.05 (br, 1H); 2.81 (br); 2.32 – 2.10 (br, 2H); 1.50 – 1.20 (br); 0.15 (br, 1H). ¹⁹F-NMR (CDCl₃) δ: -153.52; -157.11; -162.50. ²⁹Si CPMAS NMR δ: -48.55 (T1); -57.92 (T2); -65.93 (T3). M_n = 32000 g/mol, PDI = 1.72.

Poly(pentafluorophenyl acrylate) (PFPA). 4 mg AIBN, 4 mL dioxane and 2 g pentafluorophenyl acrylate ester were placed in a 20 mL Schlenk flask and degassed for three times. The reaction mixture was stirred magnetically at 80 °C for 4 h and afterwards precipitated into *n*-hexane twice. (Yield: 1.7g). ¹H-NMR (CDCl₃) δ: 7.40 – 6.85 (br); 3.05 (br, 1H); 2.52 – 2.10 (br, 2H). ¹⁹F-NMR (CDCl₃) δ: -153.79; -156.90; -162.43. M_n = 27500 g/mol, PDI = 1.18.

Amino-terminated poly(ethyleneglycol) (H₂N-PEG). Amino-terminated PEG was synthesized as described in reference [50]. M_n = 550 g/mol.

Piperazinyl-NBD (pipNBD). Piperazinyl-functionalized NBD was synthesized according to reference [51].

Amino-functionalized SiO₂ nanoparticles (H₂N-SiO₂-NP). SiO₂ nanoparticles were obtained in a Stoeber process.⁵² To finish the Stoeber process, aminopropyl dimethyl methoxysilane was added to the suspension of nanoparticles in ethanol/water and stirred magnetically for 3 h. Afterwards the nanoparticles were centrifuged, redispersed in THF (three times) and finally dried in high vacuum.

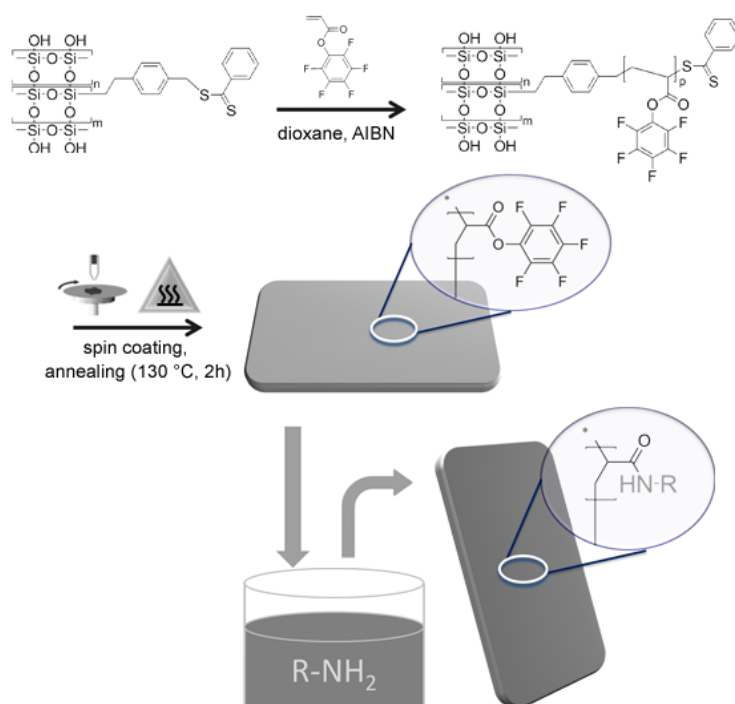
Surface coating and modification. The PMSSQ-PFPA solution was spin-coated onto clean substrates (15 s, 4000 rpm, 10 wt% solution in THF, if not otherwise stated). To induce the secondary cross-linking of the inorganic block, the samples were annealed at 130 °C for 2 h and afterwards washed with THF for 30 minutes to remove any non-bonded material. To functionalize the surface afterwards via a polymer analogous reaction, the samples were placed in a solution of the desired amine in THF (10 wt%) at room temperature for 1 h. To remove the excess of the amine, the surface was washed several times with THF.

Results and Discussion

Our concept to create functional surfaces for a wide range of applications is based on the synthesis of poly(methylsilsesquioxane)-poly(pentafluorophenyl acrylate) hybrid polymers

(PMSSQ-PFPA). These materials can be either spin- or dip-coated onto various substrates, thermally cross-linked and afterwards used for functionalization with different amines via a simple dipping process.

Scheme 1. To build up the PFPA hybrid polymer, pentafluorophenyl acrylate was polymerized under RAFT conditions, using AIBN as initiator and PMSSQ-mCTA as chain transfer agent. Afterwards the PMSSQ-PFPA hybrid polymer is spin coated onto the substrate and annealed at 130°C for 2h, yielding the desired reactive surface. By surface analogues reaction the reactive coating can be converted with various amines in a wet chemical process.



Polymer Synthesis. PMSSQ-PFPA hybrid polymers could be prepared by RAFT polymerization using PMSSQ based polymeric chain transfer agents (PMSSQ-mCTA) as shown in scheme 1. The general protocol is described in detail in reference [46]. The obtained hybrid polymer was soluble in THF, acetonitrile, dioxane, ethyl acetate, CH₂Cl₂ and chloroform. Molecular weight and molecular weight distribution of the polymer as well as the polymeric CTA were determined by GPC. The M_n of the PMSSQ precursor was 4990 g/mol, while the M_n of the hybrid polymer was 32000 g/mol (the GPC elugramms are shown in supporting information, figure S1). Further, analysis by NMR spectroscopy was used to determine the presence of the inorganic part (H₃C-Si signal at 0.15 ppm in ¹H-NMR spectra), the presence of the organic acrylate polymer backbone (broad signals between 1 and 3.5 ppm in ¹H-NMR spectra) and the conservation of the perfluorinated phenol in ¹⁹F-NMR spectra (spectra shown in supporting information, figures S2 and S3).

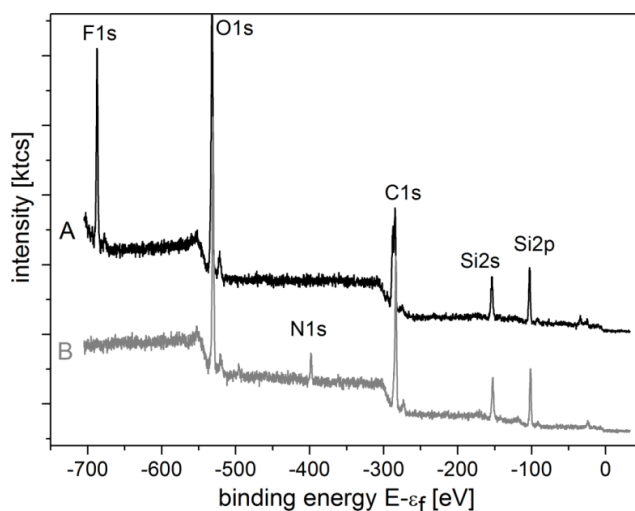


Figure 1. XPS measurements of the reactive coating (black line) and of the coating after conversion with H₂N-PEG (grey line).

The thermal behavior of the hybrid polymer, which is an important aspect to create stable coatings by thermal induced cross-linking, was analyzed using TGA (see SI, figure S4) and ²⁹Si CPMAS NMR spectroscopy. The polymeric CTA, the hybrid polymer after polymerization and after annealing have been analyzed (see SI, figure S5). The secondary condensation of the inorganic block occurred between 100 and 130 °C, while the thermal decomposition of the organic block was observed at temperatures greater than 350°C. ²⁹Si-NMR spectroscopy revealed that after RAFT polymerization enough free silanol groups remained in the inorganic part (T1 and T2 branches: -48.55 and -57.92 ppm), while after annealing for 2 h at 130°C almost all silanol groups were fully condensed as observed by an intense signal at -65.93 ppm, corresponding to T3 branches. However, due to sterical hindrance some T2 branches remained, but the ratio between T2 and T3 did not change if the sample was heated to 200°C for 24 h, thus demonstrating that the annealing conditions of 2h at 130°C were sufficient to induce a quantitative cross-linking.

Coating properties. As shown in scheme 1, the obtained PMSSQ-PFPA hybrid polymer was spin-coated onto various substrates (4000 rpm, 15 s, annealing at 130 °C for 2 h). One challenge was to create stable and adherent coatings onto different solid surfaces, thus the adherence of the coatings was tested using an ISO cross-cut test.⁵³ To check the long-term stability of the coatings, all coated substrates were placed in boiling water and the cross-cut test was performed every 60 min. As substrates Si, glass, gold, PMMA, PDMS and steel were investigated and the results are summarized in the supporting information, Table S1. Excellent adherence of the reactive hybrid polymer coating was found for all substrates and did not change in the long-term test. FT-IR spectroscopy was used to detect the presence of reactive groups at the surface of the coating, which was confirmed by the strong band at 1772 cm⁻¹ assigned to the activated ester (spectra A in figure 3). The conservation of this reactive surface was also checked using a similar long-term experiment as described above. The coatings were

kept in boiling water for 4 h and the intensity of the ester band was checked every 60 min. As no change in the intensity of the activated ester band was found, we concluded that the reactive groups were very stable over time.

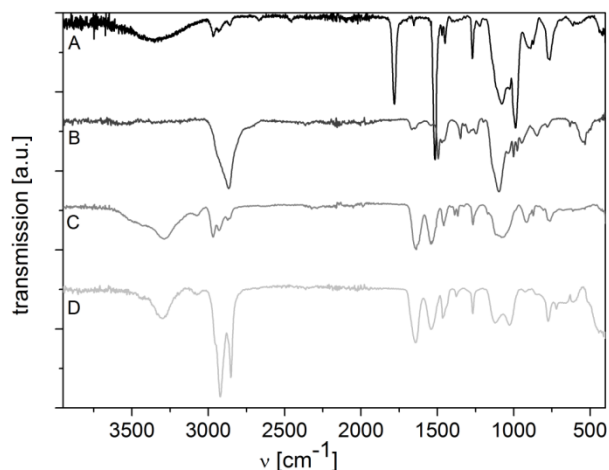


Figure 2. FT-IR spectra of the reactive coating on glass substrate (spin coated from 10 wt% THF solution, annealed at 130°C for 2 h) before surface analogues reaction (A), after conversion with H₂N-PEG (B), after conversion with isopropyl amine (C) and after conversion with dodecyl amine (D).

The film thickness (determined by ellipsometry) of the reactive coating could easily be adjusted using different concentrations during the spin-coating process. For example, spin-coating a 0.1 wt% polymer solution in THF resulted in 18 nm thick films, while using a 10 wt% solution resulted in 340 nm thick films (details in SI, figure S6). The surface roughness of the spin-coated films after annealing was determined by AFM in tapping mode and a RMS (image size 1x1 μm²) of 0.586 nm was calculated on a silicon substrate (see SI Figure S7, left image), indicating that very smooth reactive coatings could be prepared by a spin-coating and annealing process of PMSSQ-PFPA hybrid polymers.

Surface-analogous reaction. Poly(pentafluorophenyl acrylate) is known to react quantitatively with various amines in solution at room temperature yielding the respective polyacrylamide derivatives.⁴⁸ To convert the reactive PMSSQ-PFPA surfaces into the respective functional polyacrylamides, the coated substrates were placed into a 10 wt% solution of the desired functional amine for 60 minutes. Afterwards the substrate was washed several times to remove any unreacted amine from the surface. Dipping a reactive coating into 10 wt% solution of amino-functionalized poly(ethylene glycol) (H₂N-PEG) in THF resulted in a change of the advancing contact angle from 93° to 33°. XPS measurements of the reactive coating before and after the reaction with H₂N-PEG also proved the successful conversion. Before the reaction, the XPS spectrum showed the 1s peak of fluorine, while after the conversion the fluorine peak disappeared and the 1s peak of nitrogen was observed instead (figure 1). Besides XPS, the surface-analogous reaction could also be followed by FT-IR spectroscopy (figure 2a – 2d). Prior conversion, the band at 1772 cm⁻¹ indicated the presence of the activated ester group (A), while after conversion with H₂N-PEG (B), isopropyl amine (C) or dodecyl amine (D),

the ester band vanished and the typical amide bands at 1638 cm^{-1} and 1530 cm^{-1} were found. The adsorption process of H_2N -PEG onto the thin reactive coating could be monitored using surface plasmon resonance (SPR). PMSSQ-PFPA coated gold-covered glass slides (spin coated from 0.04 wt% solution, equivalent to 3.8 nm film thickness, fitted by Winspall) were allowed to react in situ with a solution of 0.1 mg/ml H_2N -PEG in water. The measured SPR kinetics are shown in figure 3 (C). A thickness increase of 0.9 nm was calculated for the binding of amino-PEG onto the reactive coating (fitted using Winspall). The surface-analogous reaction using other water-soluble amines could also be detected by SPR. For example, the conversion with poly(lysine) (figure 3 A) and poly(allyl amine) (figure 3 B) resulted in an increase of the film thickness of 1.3 nm. For all amines that have been investigated, the conversion was always complete in less than 1 h.

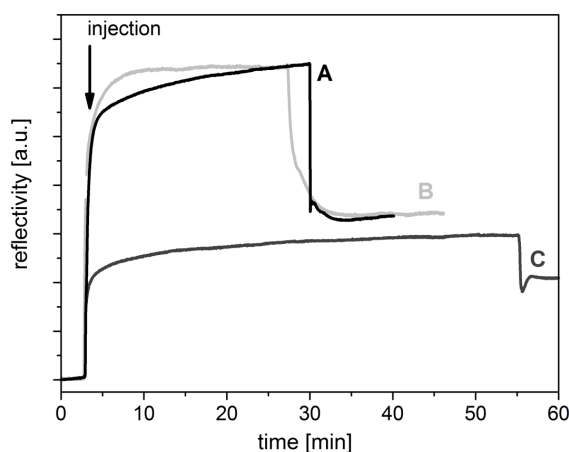


Figure 3. SPR kinetics of the conversion of the PFPA coating (spin coated on gold, 0.04 wt% solution). A: conversion with 0.1 mg/ml poly(lysine) in water (1.3 nm); B: conversion with 0.1 mg/ml poly(allylamine) in water (1.3 nm); C: conversion with 0.1 mg/ml H_2N -PEG in water (0.9 nm).

The surface reactions had no influence on the surface-roughness of the coating. The image RMS value (image size $1 \times 1 \mu\text{m}^2$) after conversion with H_2N -PEG was 0.479 nm (AFM height scan: SI, figure S7, left image before conversion, right image after conversion). Also the stability of the coatings was not affected by the surface-analogous reactions. ISO cross-cut test results remained 0 after conversion, indicating a complete adhesion onto any tested substrate.

A very simple method to show the conversion of reactive polymers is the attachment of amino-functionalized dyes. We could previously show that PFPA covered nanoparticles can be visualized using piperazinyl NBD (pipNBD) dye.⁵⁴ Using the same amino-functionalized piperazinyl NBD dye in a reaction on the PFPA coated glass slides, a strong absorption at 480 nm was found in UV/Vis spectra. Even after several washing steps the absorption did not change in intensity. The reactive coating itself was optically transparent in this region (see SI, figure S9). In conversion experiments of reactive coatings of different thicknesses with pipNBD, we found a linear behavior between film thickness and the resulting absorption up to a film thickness of 670 nm (SI, figure S9). This indicated that the entire reactive film was converted by

the amine. For films thicker than 670 nm, the adsorption did not increase linearly anymore, even for conversion times longer than one day.

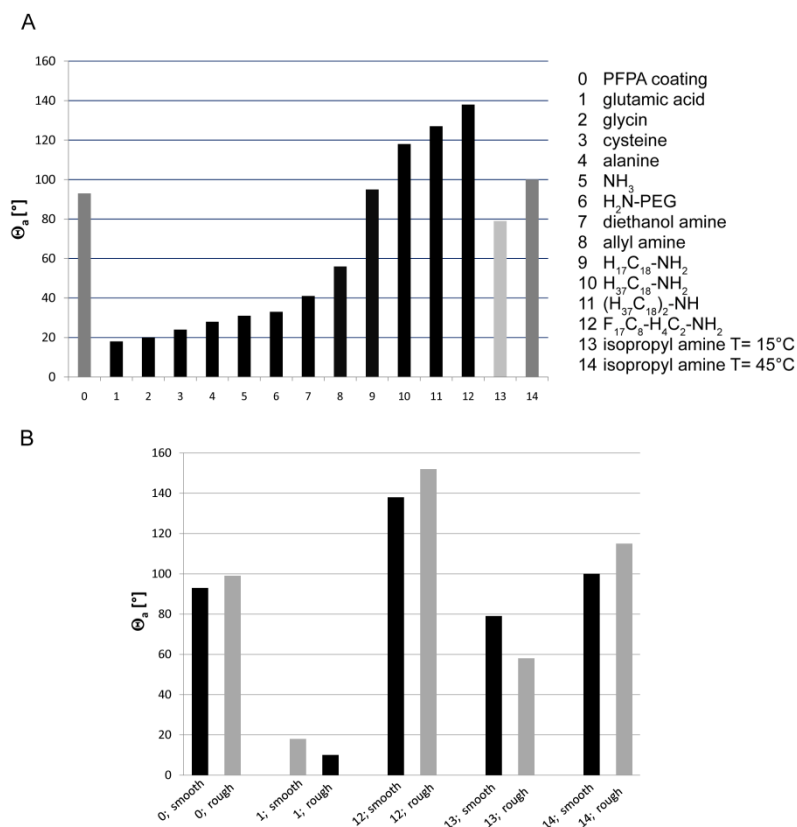


Figure 4. A: Via surface analogues reaction of the reactive coatings, the wetting behavior could be permanently altered (advancing contact angle values given for coatings on silicon, contact angles on other substrates only vary $\pm 3^\circ$). Bar 13 and 14 show the reversible switching behavior after conversion with isopropyl amine at different temperatures.

B: Permanently altered wettability on smooth PMSSQ-PFPA coatings (I-RMS: 0.586 nm, indicated as “smooth”) and after deposition of amino-functionalized silica particles and adsorption of PFPA homopolymer (I-RMS: 20.9 nm, indicated as “rough”) before and after conversion with glutamic acid (1); 1H,1H,2H,2H perfluoro decyl amin (12) and isopropyl amine at 15 °C (13) and at 45°C (14).

Surface functionalization towards permanently altered wettability. As pointed out by Langmuir in 1938, the spatial arrangement of ligands and atoms in the top surface region of the coating defines the surface wettability.⁵⁵ In other words, a functionalization of the top layer would be sufficient for a successful and defined adjustment of the wettability. To modify the surface wettability of a given substrate, a surface-analogous reaction of the reactive coating was performed using a 10wt% solution of the respective amine (1 h dipping at room temperature). By choosing the right amine the CA contact angle could be altered between $\Theta_a = 18^\circ$ ($\Theta_r < 10^\circ$) using glutamic acid and $\Theta_a = 138^\circ$ ($\Theta_r = 129^\circ$) using 1H,1H,2H,2H-perfluoro decyl amine (see figure 4A). Similar to glutamic acid, the conversion with amines, featuring carboxylic acids, such as various amino acids, resulted in a hydrophilic surface behavior (Θ_a

<25°/Θ_r < 20°). Conversion with ammonia, H₂N-PEG or hydroxyl-functionalized amines resulted in contact angles between Θ_a = 25° and Θ_a = 40°, while conversion with alkyl amines at the surface resulted in a hydrophobic wetting behavior with contact angles varying between 95°/83° (Θ_a/Θ_r) and 127°/115° (Θ_a/Θ_r). The attachment of 1H,1H,2H,2H-perfluoro decyl amine (structurally related to Teflon (PTFE)) to the surface resulted in contact angles of Θ_a = 138°, which are even higher than the contact angles found for PTFE on flat surfaces (122°/94°⁵⁶; Θ_a = 110°⁵⁷).

Table 1. Advancing and receding contact angles of water after conversion with various amines on different underlying substrates.

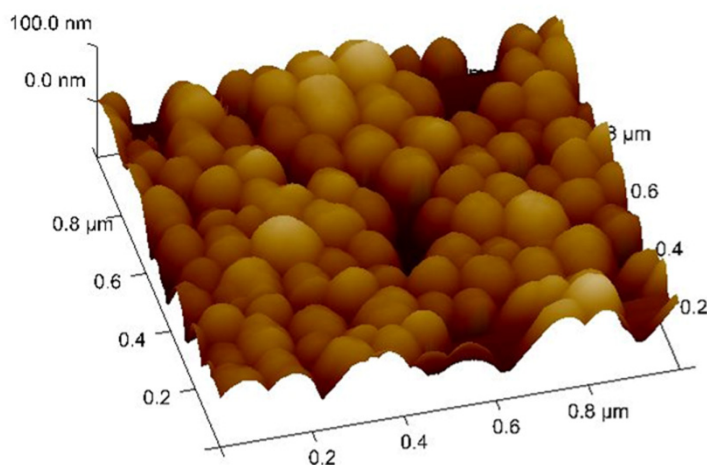
	contact angles Θ _a /Θ _r [°] on different underlying substrates					
	Si	glass	gold	PMMA	PDMS	steel
PFPA coating	93/86	95/88	97/89	94/90	92/83	95/90
glutamic acid	18/<10	20/12	20/10	16/<10	17/<10	20/14
glycine	20/11	22/15	25/15	20/17	21/13	24/16
cysteine	24/15	25/18	27/20	24/18	26/19	28/22
alanine	28/19	30/22	31/25	27/17	28/23	33/24
NH ₃	31/25	33/26	33/23	30/22	32/26	34/27
H ₂ N-PEG	33/25	35/28	34/27	32/26	35/26	36/28
diethanol amine	41/30	40/32	40/30	40/32	43/34	42/35
allyl amine	56/41	59/40	57/44	55/42	52/39	55/43
H ₁₇ C ₈ -NH ₂	95/83	98/88	94/88	93/88	92/79	97/83
H ₃₇ C ₁₈ -NH ₂	118/103	120/108	115/110	117/103	115/100	120/111
(H ₃₇ C ₁₈) ₂ -NH ₂	127/115	131/117	124/110	125/118	122/111	131/120
F ₁₇ C ₈ -H ₄ C ₂ -NH ₂	138/129	139/126	137/125	138/123	133/127	138/128
isopropyl amine (T=25°C)	79/66	78/66	80/67	78/64	76/60	80/68
isopropyl amine (T=50°C)	100/94	102/95	104/95	102/92	98/89	105/99

Noteworthy, the observed contact angles were independent of the nature of the substrate used. Similar contact angles were measured on coated silicon, glass, PMMA, PDMS and steel. The contact angles varied by ± 5°, which was within the error range. All contact angles are summarized in Table 1. It can be noted that the reactive coating material based on PMSSQ-PFPA offers a stable and adherent surface coating on all tested substrates and the surface wettability could be adjusted independent from the substrate.

Improved wetting behavior by nanostructuring of the coating. According to Wenzel's equation, superhydrophilicity or superhydrophobicity can be achieved by nanostructuring of high-surface-energy materials or low-surface-energy materials, respectively.⁵⁸⁻⁶⁰ Micro-, nano-structured surfaces or micronanobinary structures could be obtained using different methods, e.g. deposition of inorganic materials,⁶¹ growth of organosilane nanofibers,⁶² nanoimprinting of polymers,⁶³ or coatings containing silica nanoparticles.⁶⁴ To imply roughness on a smooth substrate coated with the reactive PMSSQ-PFPA coating, we investigated the embedding of

amino-functionalized silica nanoparticles ($\text{H}_2\text{N-SiO}_2\text{-NP}$), which were synthesized in a Stober process. The silica nanoparticles with an average diameter of 140 nm could be suspended in EtOH/water. Dipping a PMSSQ-PFPA coated silicon wafer into the suspension of silica nanoparticles for 1h, followed by several washing steps with different solvents, resulted in a nanoparticle-covered surface. In consequence, the conversion of PMSSQ-PFPA coatings was not only applicable to small molecules and polymers, but also to larger amino-functionalized objects, which could be covalently attached onto the surface, as visualized by AFM (figure 5 and for detailed information SI, figure S10). The density of spheres on the surface was found to be 59.2%, calculated from the AFM height image and accordingly, the surface roughness increased tremendously. The image RMS (image size $1 \times 1 \mu\text{m}^2$) after conversion with $\text{H}_2\text{N-SiO}_2\text{-NP}$ was 22.3 nm. The contact angle of this nanostructured surface, expressing amino groups at the interface was $\Theta_a = 26^\circ$ ($\Theta_r = 19^\circ$). To obtain a reactive surface layer on top of this $\text{H}_2\text{N-SiO}_2\text{-NP}$ covered surface, the substrate was dipped into a solution containing PFPA homopolymer, thereby reacting with the amino groups on the surface of the nanoparticles resulting in pentafluorophenyl esters at the surface (dip coated in 1 wt% PFPA in THF for 3h, washing 3 times with THF). After dip coating, the contact angle changed to $\Theta_a = 99^\circ$ ($\Theta_r = 93^\circ$); indicating the conversion from an amine-functionalized surface to a reactive ester functionalized surface. The surface roughness decreased slightly to an image RMS (image size $1 \times 1 \mu\text{m}^2$) of 20.9 nm, which is still significantly higher than the smooth PMSSQ-PFPA coating, which had an image RMS of 0.586 nm.

Figure 5. Tapping mode AFM height image of PMSSQ-PFPA coating on silicon converted with $\text{H}_2\text{N-SiO}_2\text{-NP}$ after 15 washing steps (5 times THF, 5 times acetone, 5 times ethanol/water). For detailed AFM analysis and TEM images of $\text{H}_2\text{N-SiO}_2\text{-NP}$ see supplementary information figure S10.



After obtaining a reactive surface coating with intrinsic surface roughness, we performed a similar conversion with glutamic acid, which resulted in the most hydrophilic surface after attachment on PMSSQ-PFPA coatings, and with 1H,1H,2H,2H-perfluoro decyl amine, which resulted in the most hydrophobic surface on the PMSSQ-PFPA coating. As expected, the

obtained small contact angle on the glutamic acid functionalized smooth surface decreased even further for the nanostructured surface, with $\Theta_a \approx 10^\circ$ ($\Theta_r \ll 10^\circ$). The receding contact angle on the rough surface was too small to be determined accurately due to an almost complete wetting. After functionalization of the nanostructured reactive surface with 1H,2H,2H-perfluoro decyl amine the contact angle turned out to be $\Theta_a = 152^\circ$ ($\Theta_r = 141^\circ$), which is significantly higher than on smooth surfaces (see figure 4B).

Temperature-induced switching of wettability. Besides the defined adjustment of permanent wetting behavior of surfaces, the reversible control of surface wettability using different stimuli is very desirable. Recently, temperature-responsive surfaces could be realized by surface-initiated atom transfer radical polymerization of *N*-isopropyl acrylamide on either smooth or rough surfaces.^{65,66} In these cases, the temperature-responsive switching of the contact angle is due to the lower critical solution temperature (LCST) at 32 °C of poly(*N*-isopropyl acrylamide) (PNIPAM).⁶⁷⁻⁶⁹ In a surface-analogous reaction of PMSSQ-PFPA coated substrates with isopropyl amine, the corresponding PNIPAM structure is formed in situ at the interface; thereby offering a very convenient and easy method compared to a surface-initiated polymerization. Temperature dependent contact angle measurements have been performed on top of a peltier element, thus measuring the wettability at different temperatures. Below LCST (15 °C) the contact angle was $\Theta_a = 79^\circ$ ($\Theta_r = 66^\circ$) (figure 4A, bar #13). Above LCST (45 °C) PNIPAM switched to a hydrophobic behavior and the contact angle was determined as $\Theta_a = 100^\circ$ ($\Theta_r = 94^\circ$) (figure 4A, bar #14), which is in agreement with grafted PNIPAM on smooth surfaces.⁷⁰ This switching experiment was repeated more than 50 times without significant change in $\Delta\Theta_a \approx 20^\circ$ and $\Delta\Theta_r \approx 30^\circ$.

To imply surface roughness for the thermo-responsive coatings, we used the PMSSQ-PFPA/ H₂N-SiO₂-NP/PFPA procedure described above, which is a convenient substrate-independent method only based on one spin-coat and two dip-coat steps. The obtained nanostructured reactive surface was then converted with isopropyl amine to result in a PNIPAM coating with intrinsic roughness. The switching behavior of this coating was between $\Theta_a = 58^\circ$ ($\Theta_r = 45^\circ$) at $T = 15^\circ\text{C}$ and $\Theta_a = 115^\circ$ ($\Theta_r = 109^\circ$) at $T = 45^\circ\text{C}$ (see figure 4B). Again numerous switching cycles could be performed, indicating a complete reversible behavior. A change of $\Delta\Theta_a = 57^\circ$ and $\Delta\Theta_r = 64^\circ$ is to the best of our knowledge the highest reported reversible change in contact angle obtained in a spin-, or dip-coat procedure. This may still be too low for application, but may be improved by further tuning to a micronanobinary structure at the surface. Amino-functionalized silica nanoparticles with different diameters (reaching from ~ 5 nm up to ~ 500 nm) could offer a convenient method for increasing surface roughness, resulting in further CA increase or decrease, respectively.

Conclusions

Poly(methylsilsesquioxane)-poly(pentafluorophenyl acrylate) hybrid polymer represent a promising coating material, that offers easy access towards adherent reactive surface coatings onto a broad range of substrates. The reactive surface could be converted by a wet chemical surface-analogous functional step with various aliphatic amines. Simple dipping of the coated

substrate into a 10 wt% solution of the desired amine resulted in a complete conversion. By applying this simple functionalization protocol, the surface wettability could be manipulated permanently with contact angles ranging from 18° to 138° on smooth surfaces independent from the underlying material. Roughness on a nanometer scale could be implemented by simple deposition of amino-functionalized silica particles onto PMSSQ-PFPA coatings. After conversion to a reactive interface by dip coating into a solution of PFPA homopolymer, and consecutive reaction with an amine, the contact angle of the surface could be altered between 10° and 152°. Temperature-responsive coatings were produced by surface-analogous reaction with isopropyl amine either on smooth or on silica nanoparticle containing surfaces, resulting in a maximal switching of contact angles of $\Delta\Theta_a = 57^\circ$. In comparison to mostly difficult and expensive surface modification and structuring protocols, our generally applicable protocol of substrate-independent reactive polymer coatings allows the defined adjustment of the surface wettability that may find versatile application.

Acknowledgement

D.K. gratefully acknowledges financial support from the FCI. The authors thank Rüdiger Berger (Max Planck Institute for Polymer Research, Mainz) for AFM support and valuable discussions, Benjamin Balke (Institute of Inorganic Chemistry, University of Mainz) for XPS measurements and Bernd Mathiasch (Institute of Inorganic Chemistry, University of Mainz) for ^{29}Si CPMAS NMR measurements.

Supporting Information Available

A detailed characterization of the synthesized hybrid polymer PMSSQ-PFPA (GPC elugramms, ^1H -NMR, ^{19}F NMR, ^{29}Si CPMAS NMR spectra, TGA), coating characteristics (film thicknesses, detailed AFM images, cross-cut test results), SPR scans and UV/Vis spectra can be found in the supporting information. This information is available free of charge via the Internet at <http://pubs.acs.org>.

References

- (1) De Gennes, P.-G.; Brochard-Wyart, F.; Quéré *Capillarity and Wetting Phenomena – Drops, Bubbles, Pearls, Waves*; Springer: New York, USA, **2002**.
- (2) Howarter, J. A.; Youngblood, J. P. *Macromol. Rapid Commun.* **2008**, *29*, 455-466.
- (3) Zhao, H.; Beysens, D.; *Langmuir* **1995**, *11* (2), 627-634.
- (4) Gao, L.; McCarthy, T. J. *Langmuir* **2006**, *22* (7), 2966-2967.
- (5) Fürstner, R.; Barthlott, W. *Langmuir* **2005**, *21* (3), 956-961.
- (6) Rolland, J. P.; Van Dam, R. M.; Schorzman, D. A.; Quake, S. R.; DeSimone, J. M. *J. Am. Chem. Soc.* **2004**, *126* (8), 2322-2323.
- (7) Marmur, A. *Langmuir* **2004**, *20* (9), 3517-3519.
- (8) Zhang, J.; Sheng, X.; Jiang, L. *Langmuir* **2009**, *25* (3), 1371-1376.
- (9) Sarmadi, A. M.; Kwon, Y. A.; Young, R. A. *Ind. Eng. Chem. Res.* **1993**, *32* (2), 279-287.
- (10) Sarmadi, A. M.; Kwon, Y. A.; Young, R. A. *Ind. Eng. Chem. Res.* **1993**, *32* (2), 287-293.

- (11) Sigal, G. B.; Mrksich, M.; Whitesides, G. M. *J. Am. Chem. Soc.* **1998**, *120* (14), 3464-3473.
- (12) Sethuraman, A.; Han, M.; Kane, R. S.; Belfort, G. *Langmuir* **2004**, *20* (18), 7779-7788.
- (13) Nagel, B.; Warsinke, A.; Katterle, M. *Langmuir* **2007**, *23* (12), 6807-6811.
- (14) Mittal, K. L., Ed. *Contact Angle, Wettability and Adhesion*; VSP: Utrecht, The Netherlands, **1993**.
- (15) Wenzel, R. N. *Ind. and Eng. Chem.* **1936**, *28*, 988-994.
- (16) Wenzel, R. N. *J. Phys. Colloid Chem.* **1949**, *53*, 1466-1470.
- (17) Cassie, A. B. D.; Baxter, S. *Trans. Faraday Soc.* **1944**, *40*, 546-551.
- (18) Toshev, B. V.; Platikanov, D.; Scheludko *Langmuir* **1988**, *4* (3), 489-499.
- (19) Drehlich, J.; Miller, J. D. *Langmuir* **1993**, *9* (2), 619-621.
- (20) Swain, P. S.; Lipowsky, R. *Langmuir* **1998**, *14* (23), 6772-6780.
- (21) Öner, D.; McCarthy, T. J. *Langmuir* **2000**, *16* (20), 7777-7782.
- (22) Schwartz, L. W.; Garoff, S. *Langmuir* **1985**, *1* (2), 219-230.
- (23) Miyama, M.; Yang, Y.; Yasuda, T.; Okuno, T.; Yasuda, H. K. *Langmuir* **1997**, *13* (20), 5494-5503.
- (24) Fadeev, A. Y.; McCarthy, T. J. *Langmuir* **1999**, *15* (11), 3759-3766.
- (25) Tripp, C. P.; Hair, M. L. *Langmuir* **1991**, *7* (5), 923-927.
- (26) Tripp, C. P.; Hair, M. L. *Langmuir* **1992**, *8* (8), 1961-1967.
- (27) Tripp, C. P.; Hair, M. L. *J. Phys. Chem.* **1993**, *97*, 5693-5698.
- (28) Combes, J. R.; White, L. D.; Tripp, C. P. *Langmuir* **1999**, *15* (22), 7870-7875.
- (29) He, X.; Yang, W.; Pei, X. *Macromolecules* **2008**, *41* (13), 4615-4621.
- (30) Advincula, R. C.; Brittain, W. J.; Caster, K. C.; R uhe, J., Eds. *Polymer Brushes*, Wiley VCH: Weinheim **2004**.
- (31) Rioboo, R.; Vou e, M.; Vaillant, A.; Seveno, D.; Conti, J.; Bondar, A. I.; Ivanov, D. A.; De Conick, J. *Langmuir* **2008**, *24* (17), 9508-9514.
- (32) Fadeev, A. Y.; McCarthy, T. J. *Langmuir* **1998**, *14* (19), 5586-5593.
- (33) Ulman, A. *Chem. Rev.* **1996**, *96*, 1533.
- (34) Cho, J.; Char, K. *Langmuir* **2004**, *20* (10), 4011-4016.
- (35) Howarter, J. A.; Youngblood, J. P. *Macromolecules* **2007**, *40* (4), 1128-1132.
- (36) Schmidt, D. L.; DeKoven, B. M.; Coburn, C. E.; Potter, G. E.; Meyers, G. F.; Fischer, D. A. *Langmuir* **1996**, *12* (2), 518-529.
- (37) Beyer, D.; Bohanon, T. M.; Knoll, W.; Ringsdorf, H. *Langmuir* **1996**, *12* (10), 2514-2518.
- (38) Cuenot, S.; Gabriel, S.; Jerome, R.; Jermome, C.; Fustin, C.-A.; Jonas, A. M.; Duwez, A.-S. *Macromolecules* **2006**, *39* (24), 8428-8432.
- (39) Jerome, C.; Gabriel, S.; Voccia, S.; Detrembleur, C.; Ignatova, M.; Gouttebaron, R.; Jerome, R. *Chem. Commun.* **2003**, 2500-2501.
- (40) Schiller, S.; Hu, J.; Jenkins, A. T. A.; Timmons, R. B. Sanchez-Estrada, F. S. Knoll, W.; Foerch, R. *Chem. Mater.* **2002**, *14* (1), 235-242.
- (41) Lahann, J.; Choi, I. S.; Lee, J.; Jensen, K. F.; Langer, R. *Angew. Chem. Int. Ed.* **2001**, *40*, 3166-3169.

- (42) Lahann, J.; Balcells, M.; Lu, H.; Rodon, T.; Jensen, K. F.; Langer, R. *Anal. Chem.* **2003**, *75* (9), 2117-2122.
- (43) Lahann, J.; Balcells, M.; Rodon, T.; Lee, J.; Choi, I. S.; Jensen, K. F.; Langer, R. *Langmuir* **2002**, *18* (9), 3632-3638.
- (44) Chen, H.-Y.; Elkasabi, Y.; Lahann, J. *J. Am. Chem. Soc.* **2006**, *128* (1), 374-380.
- (45) Kessler, D.; Teutsch, C.; Theato, P. *Macromol. Chem. Phys.* **2008**, *209* (14), 1437-1446.
- (46) Kessler, D.; Theato, P. *Macromolecules* **2008**, *41* (14), 5237-5244.
- (47) Kessler, D.; Metz, N.; Theato, P. *Macromol. Symp.* **2007**, *254*, 34-41.
- (48) Eberhardt, M.; Theato, P. *Macromol. Rapid Commun.* **2005**, *26*, 1488-1493.
- (49) Su, X.; Wu, Y.-J.; Robolek, R.; Knoll, W. *Langmuir* **2005**, *21* (1), 348-353.
- (50) Mongondry, P.; Bonnas-Plaisance, C.; Jean, M.; Tassin, J. F. *Macromol. Rapid Commun.* **2003**, *24*, 681-685.
- (51) Banerjee, S.; Kahn, M. G. C.; Wong, S. S. *Chem. Eur. J.* **2003**, *9*, 1898-1908.
- (52) Nozawa, K.; Gailhanou, H.; Raison, L.; Panizza, P.; Ushiki, H.; Sellier, E.; Delville, J. P.; Delville, M. H. *Langmuir* **2005**, *21* (4), 1516-1523.
- (53) Paints and Varnishes – Cross-cut test (ISO 2409:2007)
- (54) Tahir, M. N.; Eberhardt, M.; Theato, P.; Faiss, S.; Janshoff, A.; Gorelik, T.; Kolb, U.; Tremel, W. *Angew. Chem. Int. Ed.* **2006**, *45* (6), 908-912.
- (55) Langmuir, I. *Science* **1938**, *87* (2266), 493-512.
- (56) Lee, S.; Park, J.-S.; Lee, T. R. *Langmuir* **2008**, *24* (9), 4817-4826.
- (57) Chen, W.; Fadeev, A. Y.; Hsieh, M. C.; Öner, D.; Youngblood, J.; McCarthy, T. J. *Langmuir* **1999**, *15* (10), 3395-3399.
- (58) Yoshimitsu, Z.; Nakajima, A.; Watanabe, T.; Hashimoto, K. *Langmuir* **2002**, *18* (15), 5818-5822.
- (59) Fürstner, R.; Barthlott, W. *Langmuir* **2005**, *21* (3), 956-961.
- (60) Extrand, C. W.; Moon, S. I.; Hall, P.; Schmidt, D. *Langmuir* **2007**, *23* (17), 8882-8890.
- (61) Zhang, J.; Huang, W.; Han, Y. *Langmuir* **2006**, *22* (7), 2946-2950.
- (62) Rollings, D. E.; Tsoi, S.; Sit, J. C.; Veinot, J. G. C. *Langmuir* **2007**, *23* (10), 5275-5278.
- (63) Lee, W.; Jin, M.-K.; Yoo, W.-C.; Lee, J.-K. *Langmuir* **2004**, *20* (18), 7665-7669.
- (64) Bravo, J.; Zhai, L.; Wu, Z.; Cohen, R. E.; Rubner, M. F. *Langmuir* **2007**, *23* (13), 7293-7298.
- (65) Fu, Q.; Rao, G. V. R.; Basame, S. B.; Keller, D. J.; Artyushkova, K.; Fulgum, J. E.; López, G. *P. J. Am. Chem. Soc.* **2004**, *126* (29), 8904-8905.
- (66) Xia, F.; Feng, L.; Wang, S.; Sun, T.; Song, W.; Jiang, W.; Jiang, L. *Adv. Mater.* **2006**, *18*, 432-436.
- (67) Tiktopulo, E. I.; Bychkova, V. E.; Ricka, J.; Ptitsyn, O. B. *Macromolecules* **1994**, *27* (10), 2879-2882.
- (68) Fujishige, S.; Kubota, K.; Ando, I. *J. Phys. Chem.* **1989**, *93* (8), 3311-3313.
- (69) Kessler, D.; Theato, P. *Macromol. Symp.* **2007**, *249-250*, 424-430.
- (70) Sun, T.; Wang, G.; Feng, L.; Liu, B.; Ma, Y.; Jiang, L.; Zhu, D. *Angew. Chem. Int. Ed.* **2004**, *43* (3), 357-360.

Supporting information

Table S1. The adherence and stability of the coating was determined using the Paints and Varnishes – Cross-cut test (ISO 2409:2007). 0 indicates a perfect adherence (“the edges of the cuts are completely smooth; none of the squares of the lattice is detached”), the indication goes stepwise from 1 to 4 (4: “the coating has flaked along the edges of the cuts in large ribbons and/or some squares have detached partly or wholly. Across-cut area significantly greater than 35%, but not significantly greater than 65%, is affected”). To test the long-term stability, the coated substrates were kept in boiling water (pH =6.5) and the cross-cut test was performed every 60 min. Influences on the reactive ester group were checked by FT-IR on glass substrates also every 30 min (here no significant change of the ester band could be seen) and by CA measurements (Θ_a/Θ_r [°] given in the table below).

	Cross-Cut test result; Θ_a/Θ_r [°]				
	0h	1h	2h	3h	4h
Si	0; 93/86	0; 94/86	0; 93/86	0; 92/85	0; 92/86
glass	0; 95/88	0; 95/88	0; 94/88	0; 94/86	1; 93/87
gold	0; 97/89	0; 96/89	0; 95/88	1; 95/89	1; 94/89
PMMA	0; 94/90	0; 95/91	0; 94/91	0; 93/89	0; 94/88
PDMS	0; 92/83	0; 91/84	0; 92/83	0; 91/83	0; 92/82
steel	0; 95/90	0; 95/91	0; 94/92	1; 94/89	1; 93/89

Figure S1:

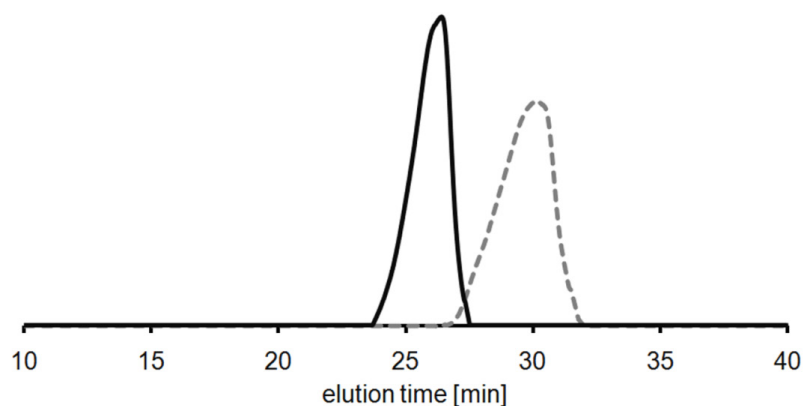


Figure S1. GPC elugramms of PMSSQ-mCTA (grey dashed line, $M_n = 4990$ g/mol, PDI = 1.63), and PMSSQ-PFPA (black solid line, $M_n = 32000$ g/mol, PDI = 1,70).

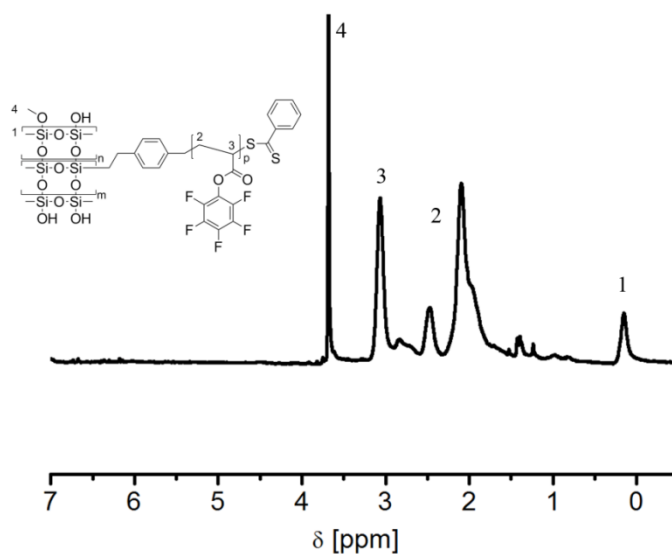
Figure S2:

Figure S2. ^1H NMR spectrum of PMSSQ-PFPA. The peak at 0.15 ppm arises from the methylsilyl-group of the inorganic block, the region between 1 and 3.5 ppm is due to the organic polymer backbone and the sharp peak at 3.6 ppm is due to residual methoxy-groups in the inorganic block.

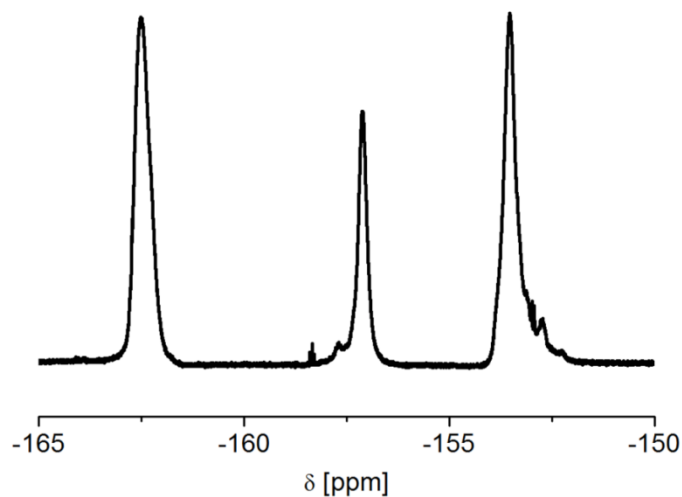
Figure S3:

Figure S3. ^{19}F NMR spectrum of PMSSQ-PFPA, showing the presence of pentafluorophenyl groups in the hybrid polymer.

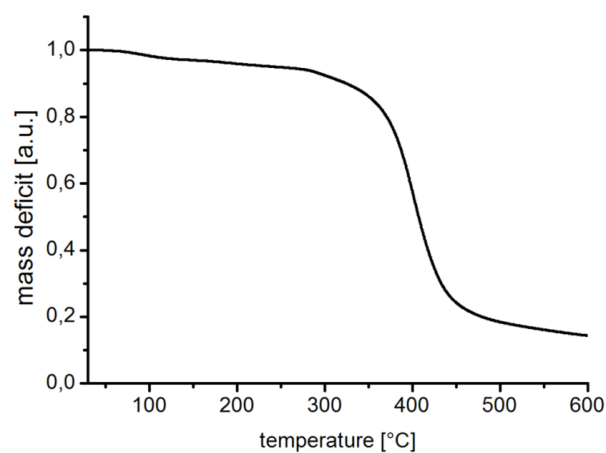
Figure S4:

Figure S4. Thermogravimetric analysis (TGA) of PMSSQ-PFPA. Between 100 and 130°C co-condensation of the inorganic block, between 350 and 400 °C decomposition of the organic block takes place.

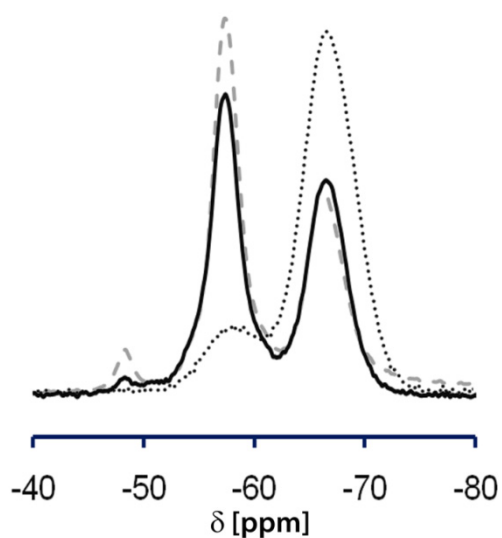
Figure S5:

Figure S5. ²⁹Si CPMAS NMR spectra of PMSSQ-mCTA (grey dashed line), PMSSQ-PFPA after polymerization (black solid line) and PMSSQ-PFPA after 1h at 130°C (black dotted line).

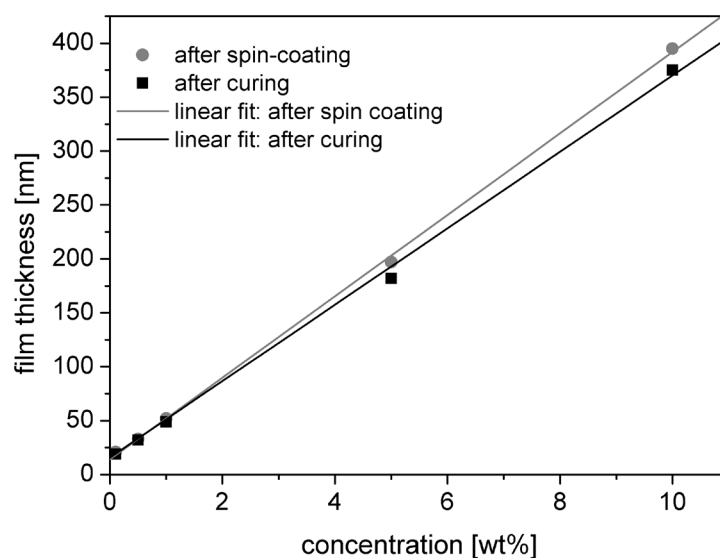
Figure S6:

Figure S6. Film thickness of PMSSQ-PFPA coatings in respect to the polymer concentration in the THF solution used for spin coating (grey: after spin coating; black: after annealing a 130°C for 2h).

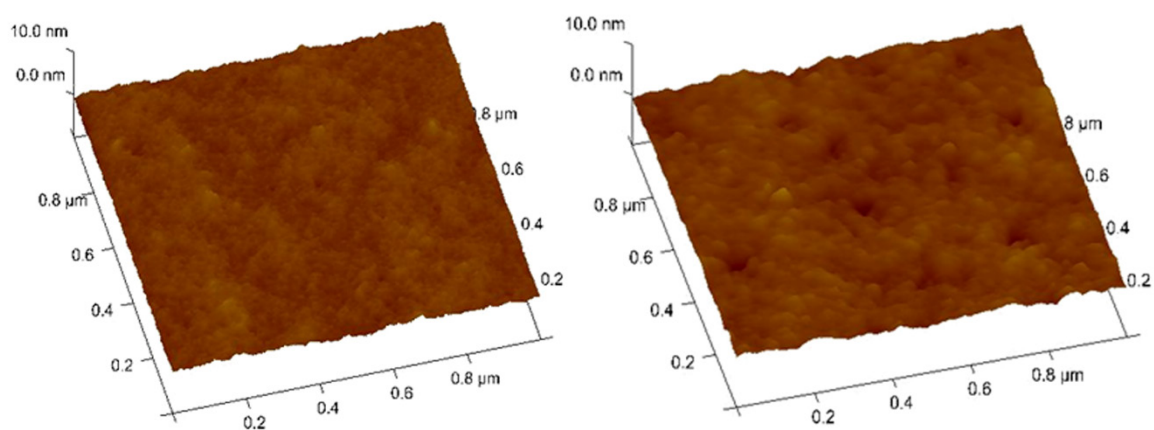
Figure S7:

Figure S7: Left image: tapping mode AFM height image of the PMSSQ-PFPA coating on silicon (image RMS = 0.586 nm). Right image: tapping mode AFM height image after the conversion of the reactive coating with H₂N-PEG (image RMS = 0.479 nm).

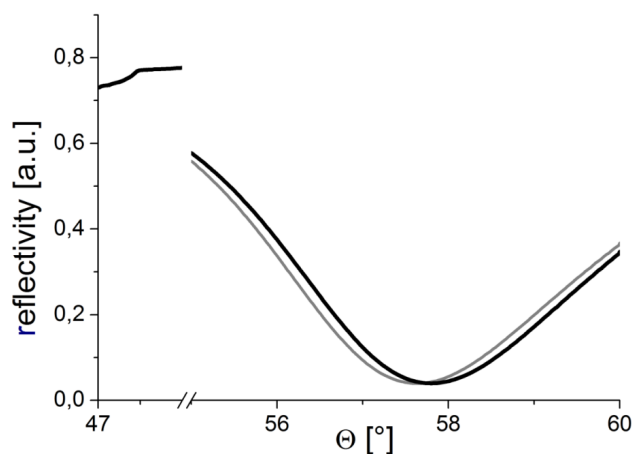
Figure S8:

Figure S8. SPR scans of PMSSQ-PFPA coating (spin coated from 0.04 wt% solution) on gold coated glass slides. Grey line: reactive coating before conversion (4.3 nm), black line: after conversion with $\text{H}_2\text{N-PEG}$ (5.2 nm). See also corresponding SPR kinetic Figure 3c.

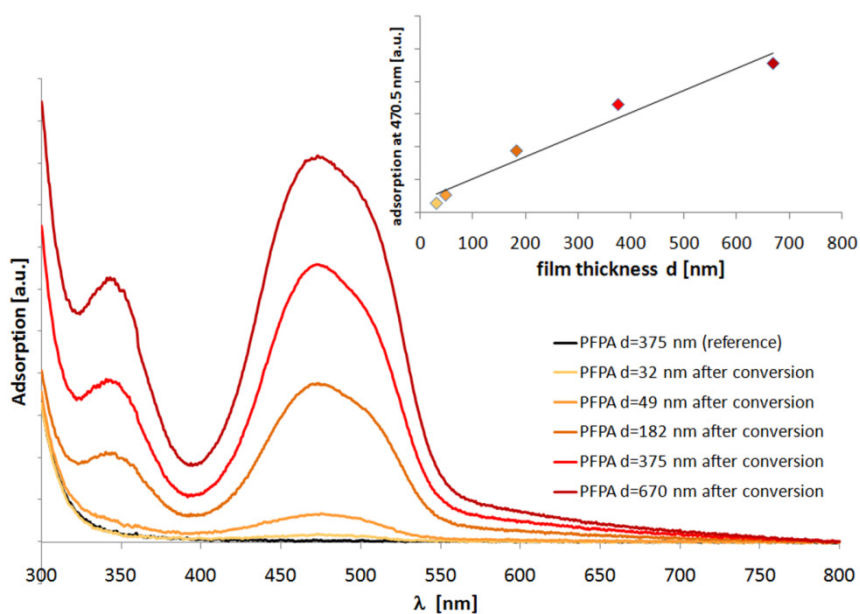
Figure S9:

Figure S9. UV/Vis absorption spectra of PMSSQ-PFPA coatings with different film thicknesses after conversion with pipNBD. Smaller plot: linear dependence of the absorption at $\lambda = 470.5$ nm with the film thickness d .

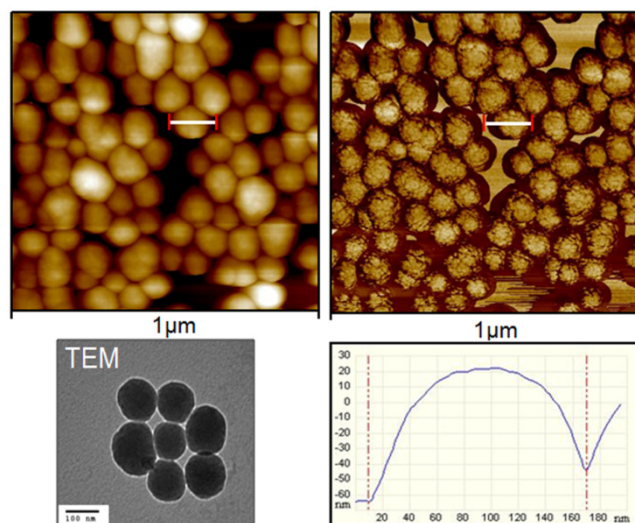
Figure S10:

Figure S10. PMSSQ-PFPA coating on silicon after surface analogues reaction with H₂N-SiO₂-NP. Upper left image: Tapping mode AFM height image; upper right image: Tapping mode AFM phase image; lower left image: TEM of the H₂N-SiO₂ nanoparticles before the surface analogues reaction; lower right image: height scan of one single nanoparticle in the AFM images.

4.9

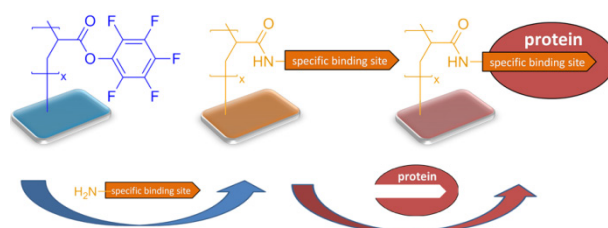
Reactive Surface Coatings Based on Polysilsesquioxanes: Controlled Functionalization for Specific Protein Immobilization

Daniel Kessler^{1,2}, Peter J. Roth¹, Patrick Theato^{1*}

1 Institute of Organic Chemistry, University of Mainz, Duesbergweg 10-14, 55099 Mainz, Germany

2 Max Planck Institute for Polymer Research, Ackermannweg 10, 55128 Mainz, Germany

Langmuir **2009**, published online July 2, <http://dx.doi.org/10.1021/la901878h>.

**Abstract**

The key designing in reliable biosensors is the preparation of thin films in which biomolecular functions may be immobilized and addressed in a controlled and reproducible manner. This requires the controlled preparation of specific binding sites on planar surfaces. Poly(methylsilsesquioxane)-poly(pentafluorophenyl acrylates) (PMSSQ-PFPA) are promising materials to produce stable and adherent thin reactive coatings on various substrates. Those reactive surface coatings could be applied onto various materials, for example, gold, polycarbonate (PC), poly(tetrafluoroethylene) (PTFE), glass. By dipping those substrates in a solution of a desired amine, specific binding sites for protein adsorption could be immobilized on the surface. The versatile strategy allowed the attachment of various linkers, for example, biotin, L-thyroxin, and folic acid. The adsorption processes of streptavidin, pre-albumin, and folate-binding protein could be monitored using surface Plasmon resonance (SPR), Fourier transform infrared (FTIR) spectroscopy, fluorescence spectroscopy, and atomic force microscopy (AFM). The presented protein immobilization strategy, consisting of four steps (a) spin-coating of PMSSQ-PFPA hybrid polymer from tetrahydrofuran (THF) solution, (b) annealing at 130 °C for 2 h to induce thermal cross-linking of the PMSSQ part, (c) surface-analogues reaction with different amino-functionalized specific binding sites for proteins, and (d) controlled assembly of proteins on the surface, may find various applications in future biosensor design.

Introduction

In recent years, there has been remarkable progress in the development of optical affinity biosensors and their applications in various areas.¹⁻⁸ An optical affinity biosensor consists of an optical transducer and a biological recognition element.⁹ Various optical methods have been exploited in biosensors including fluorescent spectroscopy,¹⁰ interferometry,^{11,12} spectroscopy of guided modes in optical waveguides,^{13,14} and surface plasmon resonance (SPR).^{15,16} In the area of biomolecular recognition, SPR, as a surface-oriented method, has shown a great potential for affinity biosensors, allowing real-time analysis of biospecific interactions without the use of labeled molecules.^{17,18}

A common bottleneck in the development of all next generation biosensors is the insufficient stability and reproducibility of their interfacial properties.^{19,20} The selectivity of biosensors is usually obtained by utilizing biomolecular functions such as proteins, antibodies, enzymes, and so on. The key in designing reliable biosensors is the preparation of thin films on which these biomolecular functions may be immobilized and addressed in a controlled and reproducible manner.²¹ This requires the controlled expression of biomolecules on planar surfaces.

Beside the immobilization of various biomolecular functions on thin films, the thin film itself has to adhere onto the desired substrate. For SPR analysis gold or silver surfaces are used, other optical methods require glass or silicon; furthermore, electrochemical detection methods require conductive substrates, such as platinum or carbon.²² Recently, an increased interest in the combination of microfluidics and microarrays has led to the progressive replacement of common inorganic substrates by polymers, especially by PDMS (polydimethylsiloxane) or PC (polycarbonate).²³ Thus, various specific biomolecular functions have to be attached to a variety of underlying materials, covering metals, metal oxides and polymers.

Various concepts have been introduced to covalently immobilize specific biomolecular functions onto surfaces, but most of these methods are limited to the attachment of one chemical function and to one given substrate: Surface-attachment on gold or silicon/silicondioxide substrates is widely realized using self-assembled monolayers (SAM) of thiol- or alkoxysilane-linkers, respectively.^{24,25} Different SAMs can be used to anchor various ligands,²⁶ to anchor initiators capable to graft polymers²⁷ or peptides from the surface,²⁸ or to graft polymers,^{29,30} dendrimers,³¹ or proteins directly to the surface.³² On polymeric substrates, protein immobilization was achieved by grafting-from approach using redox-initiated polymerization,³³ by grafting bio-functionalized polymers to the surface using photocrosslinkers,³⁴ or by utilizing molding and hydrophobic effects at the surface.³⁵ However, all the above mentioned methods are limited to one substrate only and have to be developed for each new substrate.

To overcome limitations towards a specific biomolecular function, various protein immobilization strategies were introduced, using reactive moieties attached to the surface. Those reactive moieties selectively bind to corresponding groups carrying the specific biomolecular function.³⁶ Attachment of epoxides,³⁷ anhydrides,^{38,39} aldehydes,⁴⁰ or reactive

esters (NHS ester,⁴¹⁻⁴³ or pentafluorophenyl ester⁴⁴⁻⁴⁷) on the surface could be used to immobilize amino-functionalized specific binding sites or proteins directly via the N-terminus. Besides amine chemistry to attach biomolecular functions to a surface other methods were successfully used: Michael-addition between maleimide and thiols,^{48,49} Huisgen reaction between acetylene and azide,^{50,51} and Diels-Alder reactions between dienes and dienophiles.^{52,53}

All those methods could successfully be used to immobilize different biomolecular functions onto planar surfaces, but the main drawback is the limitation towards specific substrate materials to attach the reactive moiety and thus limits the applicable biosensor method.

A general approach to immobilize biomolecular functions on surfaces should consist of reactive moieties for later specific immobilization and further more of substrate-independent adhesive moieties.

Recently, we introduced inorganic-organic hybrid polymers, obtained by grafting organic monomers from functionalized poly(methylsilsesquioxanes) (PMSSQ),⁵⁴⁻⁵⁶ The strong substrate-independent adhesion of these materials after spin-coating and curing arises from chemical bonding interfaces on hydroxylated surfaces, polymeric diffusion interlayers on polymeric surfaces and mechanical interlocking interfaces due to high degree of internal cross-linking.^{57,58} By grafting pentafluorophenyl acrylate (PFPA) from PMSSQ, reactive surface coating materials could be synthesized. Stable reactive coatings could be realized on various substrates (e. g. Si, glass, gold, PMMA, PDMS, steel, etc.). Surface-analogous reaction with various amines was used to specifically alter surface properties.⁵⁹

Within the present study, we investigated the use of these PMSSQ-PFPA hybrid polymers as coating materials to attach various biomolecular functions to planar surfaces without applying complex coating techniques or additional surface treatments.

Experimental Section

Materials. All chemicals and solvents were commercially available (Acros Chemicals, ABCR) and used as received unless otherwise stated. All used proteins, fluorescent-labeled proteins and fluorophores were commercially available from Sigma-Aldrich. 1,4-Dioxane and THF were distilled from sodium/benzophenone under nitrogen.

Instrumentation. ¹H-NMR spectra were recorded on a Bruker 300 MHz FT-NMR spectrometer, ¹⁹F-NMR spectra on a Bruker DRX 400 FT-NMR spectrometer. ²⁹Si CPMAS NMR spectra were measured on a Bruker DSX 400 MHz FT-NMR spectrometer (Rotation: 5000 Hz, T = RT, 4 mm rotor). Chemical shifts (δ) were given in ppm relative to TMS. FD mass spectra were measured using a Finnigan MAT 95 mass spectrometer. Gel permeation chromatography (GPC) was used to determine molecular weights and molecular weight distributions, M_w/M_n , of polymer samples. (THF used as solvent, polymer concentration: 2 mg/mL, column setup: MZ-Gel-SDplus 10^2 \AA^2 , 10^4 \AA^2 and 10^6 \AA^2 , used detectors: refractive index, UV and light scattering). Thermo gravimetric analysis was performed using a Perkin Elmer Pyris 6 TGA in nitrogen (10 mg pure polymer in aluminum pan). Surface Plasmon Resonance (SPR) was measured on a

home built system, using a $\Theta/2\Theta$ setup, a 632 nm laser and a photodiode. Glass slides were coated with 1.5 nm chromium and 50 nm gold by evaporation. SPR scans were fitted using WINSPALL.⁶⁰ Atomic force microscopy (AFM) measurements were performed using a Veeco Dimension 3100 in tapping mode. IR spectra were recorded using a Nicolet 5 DXC FT-IR-spectrometer on ATR crystal. Film thicknesses were measured using an EL X-02C ellipsometer. Fluorescence spectra were recorded on a Perkin Elmer Luminescence Spectrometer LS50B. All chemical reactions were performed in Argon atmosphere.

PMSSQ RAFT macro chain transfer agent (PMSSQ-mCTA). The macro initiator was synthesized as described previously.^{55,59} $^1\text{H-NMR}$ (CDCl_3) δ : 7.99 (br, 5H); 7.36 (br, 2H); 5.80 (br, 1.9H); 4.55 (br, 2H); 3.48 (br, 1.1H); 2.71 (br, 2H); 0.99 (br, 2H); 0.17 (br, 69.1H). $M_n = 4990$ g/mol, PDI = 1.63.

PMSSQ-PFPA was synthesized as described previously.⁵⁹ $^1\text{H-NMR}$ (CDCl_3) δ : 7.40 – 6.85 (br); 3.05 (br, 1H); 2.81 (br); 2.32 – 2.10 (br, 2H); 1.50 – 1.20 (br); 0.15 (br, 1H). $^{19}\text{F-NMR}$ (CDCl_3) δ : -153.52; -157.11; -162.50. ^{29}Si CPMAS NMR δ : -48.55 (T1); -57.92 (T2); -65.93 (T3). $M_n = 32000$ g/mol, PDI = 1.72. Cross-linking conditions (determined by TGA): 130 °C, 2h.

Biotin Pentafluorophenyl Ester. 1 g biotin (4.1 mmol) was dissolved in 20 mL DMF and 0.76 mg triethylamine (7.5 mmol). 1.7 g pentafluorophenyl trifluoro acetate (6.15 mmol) was added slowly; afterwards the reaction mixture was stirred for 30 min at room temperature. Residual pentafluorophenyl trifluoro acetate and the solvents were removed by reduced pressure. The crude product was purified by precipitation in diethylether. Yield: 1.51 g (3.66 mmol, 94 %).

$^1\text{H-NMR}$ (DMSO-d_6) δ : 6.44 (s, 1H); 6.36 (s, 1H); 4.28 (t, $^3J = 5.2$ Hz, 1H); 4.14 (t, $^3J = 5.2$ Hz, 1H); 3.05 (m, 1H); 1.71 – 1.40 (m, 8H). $^{19}\text{F-NMR}$ (CDCl_3) δ : -153.02; -156.22; -162.10. FTIR: activated ester band at 1748 cm^{-1} .

FD mass spectra (m/z): 183.5 (100%); 243.0 (99%); 410.1 (90%); 411.1 (15%) (calc. mass: 410.07 g/mol)

Biotin-2-aminoethane Amide ($\text{H}_2\text{N-Biotin}$). 1.5 g biotin pentafluorophenyl ester (3.66 mmol) was slowly added to a solution of 2.2 g ethylene diamine (37 mmol) in 10 mL DMF. The solution was stirred for 2 h at 0 °C. Afterwards the product was precipitated in diethylether, filtered and washed with ether. Yield: 0.90 g (3.1 mmol, 85 %).

$^1\text{H-NMR}$ (DMSO-d_6) δ : 6.50 (s, 1H); 6.36 (s, 1H); 4.29 (t, $^3J = 5.2$ Hz, 1H); 4.12 (t, $^3J = 5.2$ Hz, 1H); 3.07 (m, 2H); 2.58 (m, 2H); 2.48 (t, $^3J = 6.6$ Hz, 2H); 2.06 (t, $^3J = 6.6$ Hz, 2H); 1.46 (m, 2H); 1.29 (m, 2H). FTIR: amide band at 1646 cm^{-1} .

FD mass spectra (m/z): 286.2 (100%); 287.2 (11%); 288.1 (6%) (calc. mass: 286.15 g/mol)

Bis(5-carboxypentyl) Disulfide Bis(pentafluorophenyl) Ester (PFP-Disulfide) was synthesized as previously described.⁶¹

Bis(5-carboxypentyl) Disulfide Dithyroxine Amide (T4-Disulfide). 502 mg (0.646 mmol) of thyroxine were dissolved in 20 mL of dry DMF. 0.4 mL of triethylamine (2.87 mmol) and 175 mg (0.280 mmol) of bis(5-carboxypentyl) disulfide bis(pentafluorophenyl) ester dissolved in 1 mL of dry DMF were added. Upon addition of the activated ester the turbid mixture turned clear within seconds. The reaction was stirred for 7 h at room temperature. The solvent was

removed and the residue dried in high vacuum. Chloroform was added and the mixture was filtered through a 0.2 μ m membrane. After drying with MgSO₄ the solvent was removed.

¹H-NMR (DMSO-d₆) δ : 7.59 (s, 2 H); 7.01 (s, 2 H); 4.70 (m, 1 H); 3.05 (m, 2 H); 2.58 (t, ³J = 6.6 Hz, 2 H); 2.18 (t, ³J = 6.4 Hz, 2 H); 1.57 (m, 4 H); 1.33 (m, 2 H). FTIR (cm⁻¹): 2940 w, 1680 m, 1510 s, 1250 w, 1450 w, 1000 s.

Bis-(2-aminoethane Amide) Folic Acid. 880 mg folic acid (2 mmol) was dissolved in 20 mL DMF and 0.76 mg triethylamine (7.5 mmol). 1.7 g pentafluorophenyl trifluoro acetate (6.15 mmol) was added slowly; afterwards the reaction mixture was stirred for 30 min at room temperature. Residual pentafluorophenyl trifluoro acetate and the solvents were removed by reduced pressure. The crude product was purified by precipitation in diethylether. The obtained pentafluorophenyl ester was slowly added to a solution of 2.2 g ethylene diamine (37 mmol) in 10 mL DMF. The solution was stirred for 2 h at 0 °C. Afterwards the product was precipitated in diethylether, filtered and washed with ether. Yield: 720 mg (1.37 mmol, 68.5 %).

¹H-NMR (DMSO-d₆) δ : 8.51 (s, 1H); 8.42 (s, 1H); 7.5-6.8 (m, 4H); 4.41 (m, 3H); 3.62 (m, 4H); 2.52 (m, 6H); 1.98 (m, 2H). FTIR: amide band at 1648 cm⁻¹.

FD mass spectra (m/z): 527.4 (100%); 528.3 (14%) (calc. mass: 527.27 g/mol)

Perfluorophenyl 4-(2-(chlorodimethylsilyl)ethyl)benzoate. 2 g (6.4 mmol) Pentafluorophenyl 4-vinylbenzoate, 1.21 g (13 mmol) chlorodimethylsilane, 25 mg platinum on charcoal and 20 mL toluene were placed in a 50 mL round-bottomed flask and stirred magnetically at 40°C for 5d. The crude reaction mixture was filtered over Celite and the solvent was removed under reduced pressure. Yield: 2.1 g (5.1 mmol, 79.7 %).

¹H-NMR (CDCl₃) δ : 8.01 (m, 2H); 7.10 (m, 2H); 2.31 (m, 2H); 1.42 (m, 2H); 0.31 (s, 6H). FTIR: activated ester band at 1749 cm⁻¹.

Surface coating and modification. The PMSSQ-PFPA solution was spin-coated onto clean substrates (15 s, 4000 rpm). To induce the secondary cross-linking of the inorganic block, the samples were annealed at 130 °C for 2 h and afterwards washed with THF for 30 minutes to remove any non-bonded material. To functionalize the surface afterwards via a polymer analogous reaction, the samples were placed in a solution of the desired amine in water (10 wt%) at room temperature for 1 h. To remove the excess of the amine, the surface was washed several times with water.

Comparison surfaces / self-assembled monolayers on glass. As comparison surfaces self-assembled monolayers on glass were prepared using either perfluorophenyl 4-(2-(chlorodimethylsilyl)ethyl)benzoate (comparison 1) or 3-aminopropyltriethoxysilane (APTES) (comparison 2). The monolayer preparation was carried out as described in the literature.^{62,63} The freshly cleaned glass substrate was immersed in a 10 mM solution of the adsorbate in dry toluene for 4 h. After the substrate has been removed from the solution, it was rinsed with toluene (three times), dichloromethane (twice), ethanol (twice) and water (twice) to remove any physisorbed material. Advancing contact angle for comparison 1 was 92°, while for comparison 2 an advancing contact angle of 38° was measured.

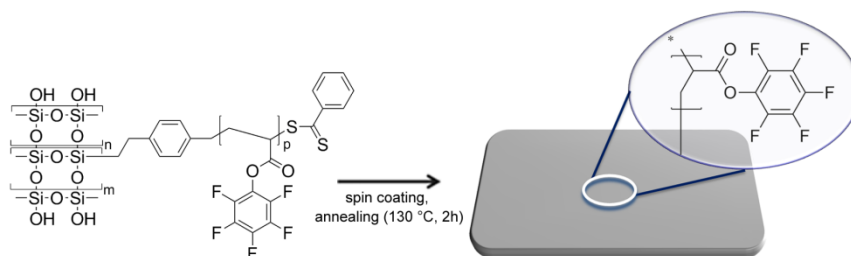
Results and Discussion

Poly(methylsilsesquioxane)-poly(pentafluorophenyl acrylate) (PMSSQ-PFPA) hybrid polymers represent a promising class of coating materials, which offer easy access toward adherent reactive surface coatings onto a broad range of different substrates (e.g. Si, glass, gold, PMMA, PDMS, PC, etc.) (see scheme 1). The quality of adhesion between a film and its substrate, depends to a large extent on the microstructure of the interface layer that is being formed.⁶⁴ Usually four types of interface layers can be formed during the coating process of polymers onto different substrates: 1. mechanically interlocked interfaces; 2. chemical bonding interface layers; 3. electric double layers; 4. diffusion interface layers.^{57,58} The PMSSQ hybrid polymers are able to utilize different interface phenomena to guarantee adhesion on a substrate. On hydroxylated surfaces, e.g. glass or silicon, a chemical bonding interface layer is formed by condensation of surface OH-groups with PMSSQ-OH-groups. On polymeric surfaces, e.g. PDMS, PC, PMMA, diffusion interfaces are involved in the adherence. Gold-covered glass slides or poly(tetrafluoroethylene) (PTFE) surfaces exhibit a micro- to nanometer scale roughness on the surface, due to cross-linking of the PMSSQ parts very rigid regions were formed within the coated film, leading to a mechanical interlocking.

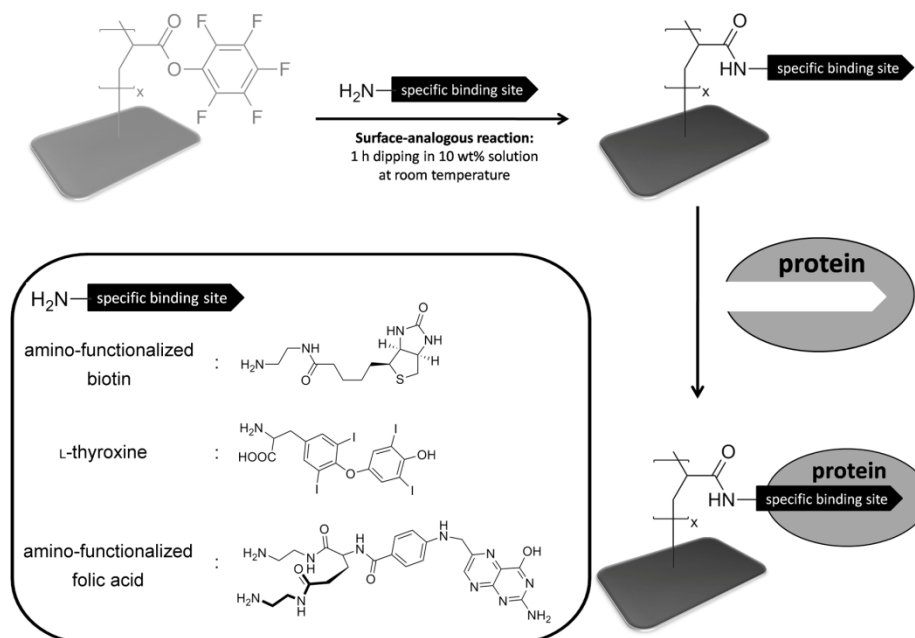
By spin-coating onto a given substrate, annealing at 130 °C for 2 h and conversion by a wet chemical surface-analogous functional step with various amines, surface properties can be controlled precisely, as explained in detail in reference [59].

In the present study, we want to apply PMSSQ-PFPA surface coatings as a powerful tool to attach various proteins to a given planar substrate. The presented protein immobilization strategy consists of four steps: (a) spin-coating of PMSSQ-PFPA hybrid polymer from solution, (b) annealing at 130 °C for 2 h to induce thermal cross-linking of the PMSSQ part, (c) surface-analogous reaction with different amino-functionalized molecules that provide specific binding sites for proteins and (d) controlled assembly of proteins on the surface (see scheme 2). For real-time analysis of bio-specific interactions, especially for the controlled assembly of proteins, we used surface plasmon resonance (SPR). Different binding sites were immobilized to assemble different proteins on the surface, demonstrating that PMSSQ-PFPA surface coatings are useful tools for a versatile protein-immobilization strategy.

Scheme 1. Reactive surface coatings on several substrates were produced by spin coating PMSSQ-PFPA from solution and annealing at 130 °C.



Scheme 2. Spin coating PMSSQ-PFPA hybrid polymers onto a given substrates resulted in thin reactive surface coatings. After surface-analogous reaction with amino-functionalized specific binding sites proteins were assembled on top.



Biotinylated surfaces. As a first example, we choose biotin as specific binding site and streptavidin as protein to immobilize on the surface. Streptavidin is a basic tetrameric protein isolated from *Streptomyces avidinii* with a theoretical diameter of 5.6 nm. It binds tightly to biotin, with a binding constant of $K_d \sim 10^{-15}$ M.⁶⁵ Due to the ability of streptavidin to bind to four biotins, a streptavidin covered surface can be used as immobilization support for further biomolecular functionalization, using for example biotinylated DNA,⁶⁰ biotinylated enzymes,⁶⁶ or biotinylated antibodies.⁶⁷

Amino-functionalized biotin was synthesized by activation of the carboxyl group as a pentafluorophenyl ester using pentafluorophenyl trifluoroacetate, followed by reaction with an excess of ethylene diamine. The PMSSQ-PFPA active ester surface coating on top of a gold-covered glass slide was obtained by spin-coating from 0.04 wt% solution of PMSSQ-PFPA in THF and annealing at 130 °C for 2 h (film thickness: 3.8 nm, SPR scans fitted by Winspall). The surface-analogous reaction of amino-functionalized biotin (H_2N -biotin) with the pentafluorophenyl esters at the surface was carried out by dipping the coated substrate into a 10 wt% solution of H_2N -biotin in water for 60 min (see scheme 2). To determine the conversion of the film, similar experiments were performed after spin-coating PMSSQ-PFPA from a 10 wt% solution on to a glass slide, yielding a comparably thicker film, which could be analyzed by FTIR spectroscopy (see figure 1). Prior conversion, the band at 1772 cm^{-1} indicated the presence of the activated ester group (figure 1A), while after conversion with H_2N -biotin the ester band vanished and the typical amide bands at 1638 cm^{-1} and 1530 cm^{-1} were found (figure 1B). The covalent attachment of H_2N -biotin onto the thin reactive coating could be

monitored using SPR. PMSSQ-PFPA coated gold-covered glass slides were allowed to react in-situ with a solution of 0.1 mg/ml H₂N-biotin in water. The measured SPR kinetic is shown in supporting information figure S2. A thickness increase of 0.5 nm was calculated for the binding of H₂N-biotin onto the reactive coating (fitting using Winspall, assuming constant refractive indices).

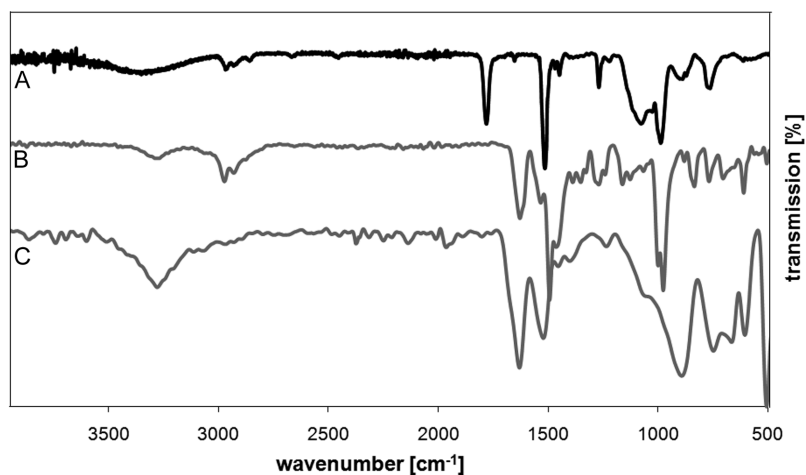


Figure 1. (A) FTIR spectrum of PMSSQ-PFPA coated on glass slides (active ester band at 1772 cm⁻¹). (B) FTIR spectrum of PMSSQ-PFPA coating on glass after conversion in 10 wt% H₂N-biotin solution in water for 1h (amide bands at 1638 cm⁻¹ and 1530 cm⁻¹). (C) FTIR spectrum of Streptavidin in conjugation with the biotinylated surface coating of (B) (additional amine bands at 3300 cm⁻¹, additional amide bands at 1635 and 1530 cm⁻¹ from the polypeptide).

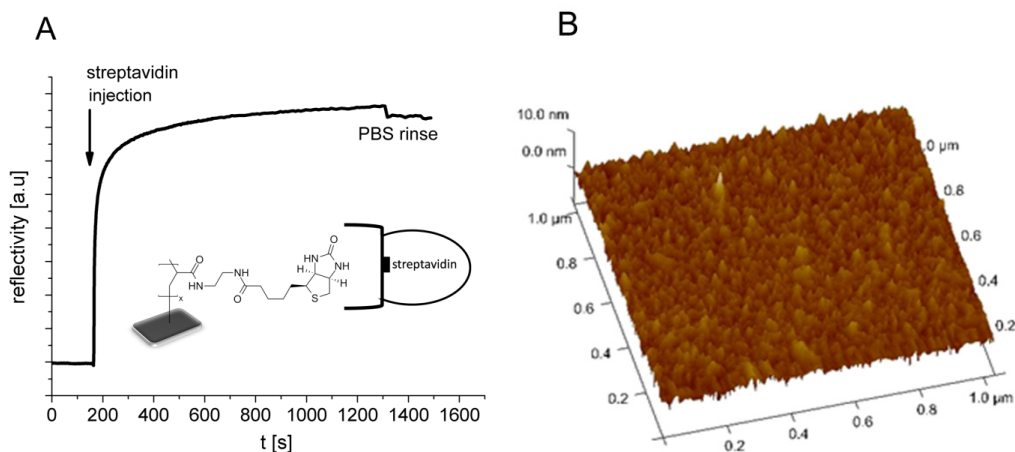


Figure 2. A: SPR kinetic of streptavidin adsorption on a PMSSQ-PFPA coated gold-covered glass slide converted with H₂N-biotin. Calculated thickness increase after several PBS rinsing steps was 5.23 nm. B: AFM height image after streptavidin adsorption on the biotinylated reactive coating on a silicon wafer (image RMS: 0.834).

After successful attachment of the specific binding site, streptavidin was allowed to adsorb onto the biotinylated coating. A solution of 0.1 mg/ml streptavidin in phosphate-buffered saline solution (PBS) was injected into the SPR setup. The measured SPR kinetic is shown in figure 2A. The adsorption was completed in less than 20 min. After complete adsorption, the SPR cell was rinsed with PBS several times to remove any non-specifically bound protein. The thickness increase was fitted from SPR scans before and after protein injection/PBS rinsing and calculated as 5.2 nm (SPR scans in SI, figure S3). This matches with the theoretical diameter of streptavidin of 5.6 nm, indicating the formation of a streptavidin monolayer on top of the biotinylated PMSSQ-PFPA coating.

As the coating procedure is independent of the underlying substrate, different characterization techniques (even if requiring different underlying materials) could be applied. Thus, we also determined the thicknesses by ellipsometry, using exactly the same coating procedure. The obtained thicknesses were 4.1 nm for the biotinylated coating and 9.0 nm in total after streptavidin assembly. Thus, the streptavidin layer thickness of 4.9 nm, determined by ellipsometry, matches very well the thickness of 5.2 nm, obtained from SPR scans, proving the general applicability of PMSSQ-PFPA coatings.

To compare the desired specific adsorption of streptavidin on the biotinylated surface with complete non-specific physisorption of streptavidin on hydrophobic or hydrophilic surfaces, similar adsorption experiments were performed on other surfaces. PMSSQ-PFPA coatings on gold-covered glass slides were functionalized with octylamine, yielding a hydrophobic surface, and amino-functionalized poly(ethylene glycol) ($\text{H}_2\text{N-PEG}$, $M_n = 550$ g/mol), yielding a hydrophilic surface. The SPR kinetics of the streptavidin adsorption on both surfaces in comparison to the biotinylated surface is shown in SI, figure S4. As expected, after rinsing no physisorption could be detected on the PEGylated surface, whereas physisorption was prominent on the octylamine-functionalized coating. The maximum thickness increase was 0.65 nm, after PBS rinsing 0.1 nm thickness remained; indicating that the physisorption on hydrophobic surfaces is only due to the hydrophobic effect of proteins (non-specific denaturation on the surface) and therefore differs dramatically from the controlled specific adsorption on biotinylated surfaces.

Further characterization of the obtained streptavidin surface was performed by AFM. As the PMSSQ-PFPA coating is independent of the nature of the substrate,^{54,55,59} silicon wafers were used for AFM investigations. The same streptavidin immobilization strategy - as explained above - was used. After applying the PMSSQ-PFPA coating, surface-analogous reaction with $\text{H}_2\text{N-biotin}$ was performed and streptavidin was allowed to assemble from solution. The obtained AFM topography image is shown in figure 2B. A smooth streptavidin surface was observed, the root mean square (RMS) roughness was 0.834 nm on an area of $1 \mu\text{m}^2$, indicating again a monolayer formation of streptavidin on top of the coating. These smooth streptavidin layers, obtained in a simple combination of spin-coating and self-assembly, may represent an ideal platform for further biosensor application using biotinylated biomolecules.

The conjugation of streptavidin onto the biotinylated coating on glass could also be identified by surface FTIR spectroscopy (see figure 1C). Additional amine bands at 3300 cm^{-1} and peptide bands at 1635 cm^{-1} , 1530 cm^{-1} appeared. Further, FTIR characterization of the immobilization strategy was also applied on PC and is shown in supporting information figure S5.

To compare the streptavidin binding of the presented surface-biotinylation method with other common glass-biotinylation protocols, we prepared two comparison samples. Well established glass derivatization methods use self-assembled monolayers^{68,69} of either amino-functionalized alkoxysilanes (usually APTES)⁷⁰ or chlorosilanes with activated moieties.^{71,72} Comparison sample 1 was produced by formation of a SAM of perfluorophenyl 4-(2-(chlorodimethylsilyl)ethyl)benzoate on a glass slide, afterwards the activated ester was functionalized with amino-biotin yielding the desired monolayer of biotin moieties on the glass slide. Comparison sample 2 was produced by SAM formation of APTES onto glass, followed by attachment of biotin moieties using biotin pentafluorophenyl ester.

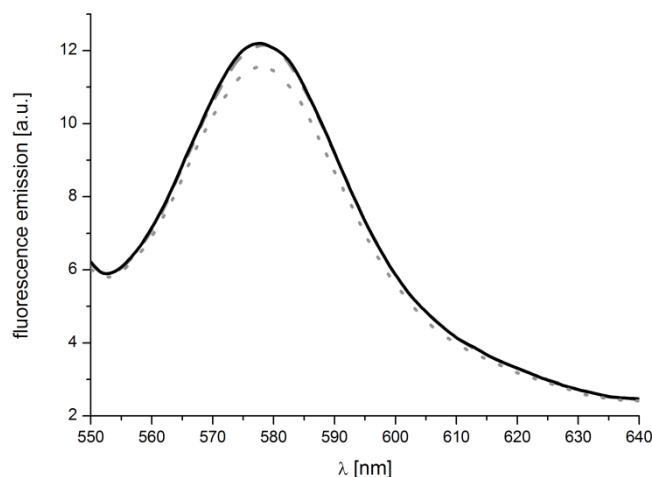


Figure 3. Fluorescence emission spectra of Streptavidin-CY3 immobilized on different glass surfaces (excitation at 520 nm, slits: 15 nm). Black solid line: Streptavidin-CY3 immobilized on a glass slide coated with PMSSQ-PFPA after conversion with biotin-amine. Grey dashed line: Comparison 1, SAM of perfluorophenyl 4-(2-(chlorodimethylsilyl)ethyl)benzoate cfunctionalized with biotin-amine in conjugation with Streptavidin-CY3. Grey dotted line: Comparison 2, SAM of APTES on glass, functionalized with biotin pentafluorophenyl ester after assembly of Streptavidin-CY3.

Comparison samples 1 and 2 and a PMSSQ-PFPA coated glass slide, functionalized with amino-biotin as explained above were incubated in a solution of fluorescent-labeled streptavidin (Streptavidin-CY3, 0.1 mg protein/mL in PBS) for 1h. Fluorescence emission spectra of all three samples were measured and are shown in figure 3. All three biotinylation procedures showed comparable results, as nearly the same fluorescence intensity was observed for all three cases, indicating similar streptavidin conjugation to the biotin-functionalized surfaces with comparable binding capacities on the interface. Further

streptavidin binding experiments were performed using Streptavidin Fluorescent Polymer, Ultrasensitive. The comparison samples 1 and 2 (glass substrate) and PMSSQ-PFPA coated substrates, functionalized with biotin-amine (Si, glass, PDMS, PC, PMMA, PTFE), were incubated in a PBS/BSA solution containing 0.005 mg protein/mL. The fluorescent emission spectra showed similar emission independent from the functionalization method (see supporting information, figure S6). In case of the PMSSQ-PFPA coated substrates, functionalized with amino-biotin, almost no effect of the underlying material was observed, proving again the versatile applicability of the PMSSQ-PFPA coating, independent from the material. Compared to the complicated procedure to obtain defined functional monolayers on glass PMSSQ-PFPA coatings, produced by spin-coating, showed similar ability to immobilize proteins on the surface.

To demonstrate that the remaining binding sites of streptavidin, immobilized by the presented strategy, are available for further binding of biotin-labeled molecules we allowed biotin-5-fluorescein to assemble at the free binding sites. Different streptavidin-functionalized substrates were placed into a solution of 0.5 mg biotin-5-fluorescein/mL PBS for 1 h. The measured fluorescent emission spectra are shown in figure 4. The typical fluorescein emission spectra could be observed on any underlying substrate with again nearly the same intensity, proving the capability of further biotin conjugation to any streptavidin functionalized surface with an equal number of binding site per surface area.

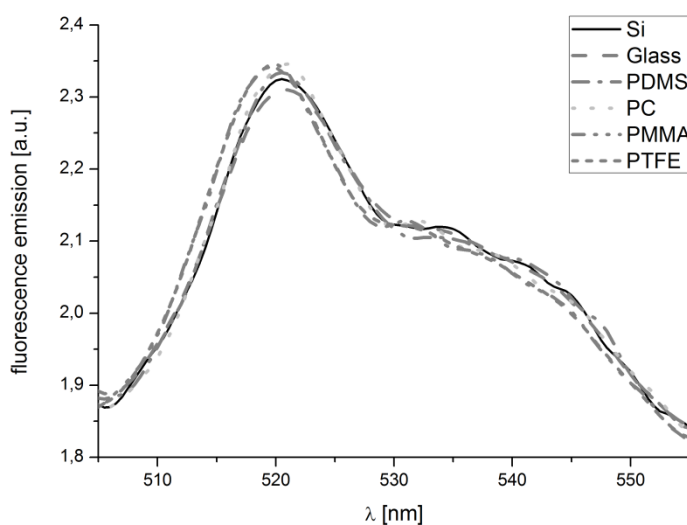


Figure 4. Fluorescence emission spectra of biotin-5-fluorescein conjugate bounded to streptavidin, immobilized on various underlying substrates using the presented reactive coating concept (excitation at 440 nm, slits: 15 nm).

Besides the binding of small biotin-labeled molecules, also biotin-labeled proteins could be attached to the streptavidin functionalized surface. Streptavidin was immobilized on PC using the presented strategy. Afterwards the sample was incubated in a solution of 0.1 mg/ml biotin-labeled albumin in PBS. After several rinsing steps, the immobilized albumin was

detected by adsorption of albumin blue 580, a specific fluorescent dye to determine albumin (functionalization of the well rinsed wafer in 0.5mg/mL solution in PBS, containing isopropanol).^{73,74} The fluorescence emission spectrum is shown in figure 5 (emission max at 600 nm). A similar experiment was performed using non-functionalized albumin. No fluorescence could be detected using the same excitation (excitation wavelength 550 nm), indicating that the attachment is due to the streptavidin-biotin-interaction between the streptavidin functionalized surface and the biotin-labeled albumin.

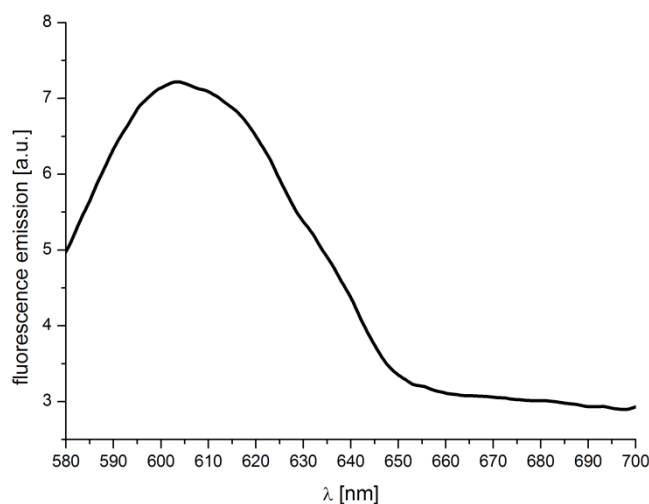


Figure 5. Fluorescence emission spectrum of Albumin blue 580 (excitation at 550 nm, slits: 15 nm). PMSSQ-PFPA was coated onto a PC substrate, converted with biotin-amine, streptavidin was immobilized on top and biotin-functionalized Albumin was allowed to assemble. Afterwards the wafer was placed in a solution of Albumin blue 580 in PBS.

To demonstrate the specific binding of the presented biotinylation process, biotin-functionalized surface coatings were also incubated in a solution of biotin-labeled albumin and pure BSA, respectively. After incubation in the albumin blue 580 solution and rinsing with PBS no fluorescence could be observed in both cases. Further binding experiments on the biotinylated surface coating were performed by SPR. Neither albumin nor pre-albumin showed a binding to the biotin-functionalized gold surface, indicating specific binding of streptavidin to the PMSSQ-PFPA coating after biotin-amine functionalization (SPR kinetics shown in supporting information, figure S7).

Thyroxine-functionalized surfaces. Thyroid hormones, such as L-thyroxine (T4), are essential for the modulation of the cellular metabolic rate and for the development and differentiation of several tissues.^{75,76} The thyroid gland produces and releases T4. Once T4 enters the blood stream, it is bound to transport proteins (thyroxine binding globulin (TBG), transthyretin (TTR), thyroxine binding pre-albumin (PA)).⁷⁷ Due to the interaction of the T4 transport system with polyhalogenated aromatic hydrocarbons (PHAHs), which are used as flame retardants,^{78,79} the demand of biosensors that are selective for T4 transport proteins rises recently.⁸⁰

As T4 consists of an amino acid, well separated from the halogenated aromatic part, an amino-group for attachment to the PMSSQ-PFPA surface is already present. Thus, after surface-analogous reaction of T4 with the reactive polymer coating on a gold substrate (dipping process as explained above, adding 1 equiv. triethylamine to deprotonate the carboxylic acid group), pre-albumin (PA, 0.1 mg/ml) was allowed to adsorb onto the surface *in situ*. The obtained SPR kinetic is shown in figure 6A. After PBS rinsing, a thickness increase of 2.55 nm was found. Complete adsorption took approximately 2 h, indicating that T4-PA binding is less effective than biotin-streptavidin binding, as expected. Again, the same PA-binding strategy was applied to silicon wafers to perform AFM measurements. A smooth and homogenous PA surface could be observed in AFM topography (RMS of 0.492 nm on 1 μm^2 , figure 6B).

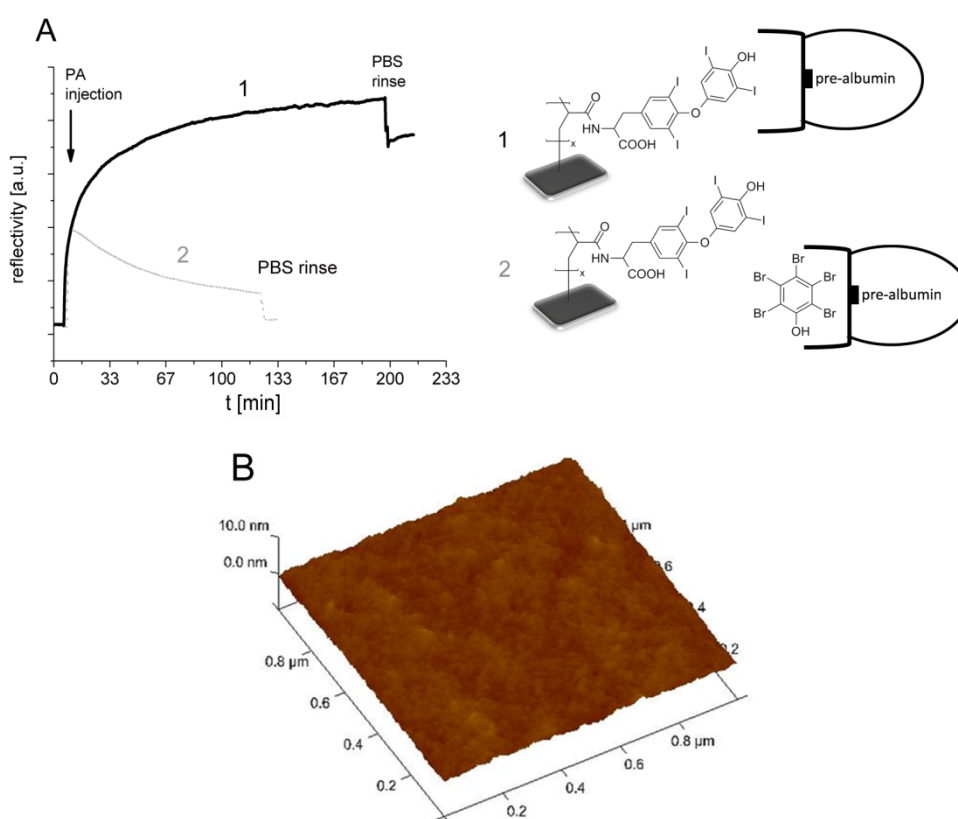


Figure 6. A: After surface-analogous reaction of L-thyroxine (T4) with the reactive coating pre-albumin was adsorbed (SPR kinetic 1). After several PBS rinsing steps the thickness increase was 2.55 nm. SPR kinetic 2: Pre-albumin (PA) adsorption on the L-thyroxine (T4) functionalized PMSSQ-based surface coating after adding pentabromophenol.

B: Pre-albumin adsorbed onto a similarly prepared silicon wafer. AFM topography shows a smooth homogenous surface with image RMS of 0.492 nm.

To compare the obtained SPR kinetic results of the presented PMSSQ-PFPA protein immobilization strategy to the widely used disulfide-attachment⁸¹ of biomolecular functions to

gold surfaces,⁸² we prepared bis(5-carboxypentyl) disulfide dithyroxine amide (T4-disulfide). The SAM formation of T4-disulfide could directly be performed in the SPR setup, using 0.1 mg/ml T4-disulfide in ethanol. After ethanol rinsing a thickness increase of 1.66 nm was observed. Allowing PA to adsorb on top increased the thickness by 2.60 nm (assuming constant refractive index) (see SI, figure S8). Both protein immobilization strategies provide concurrent results of thickness increase and adsorption kinetics.

The determination of the affinity of T4 transport proteins towards other polyhalogenated aromatic hydrocarbons (PHAHs) is an important issue, as explained above. To demonstrate that the presented strategy is applicable as biosensor, comparing binding affinities between PHAHs-PA versus T4-PA we chose pentabromophenol as PHAH example. A PMSSQ-PFPA coated gold-covered glass slide was functionalized with T4 as explained above. We prepared a solution of 0.1 mg/ml PA in PBS and added 0.5 mg pentabromophenol, the solution was allowed to stand for 60 min. Afterwards PA adsorption onto the prepared T4 surface was measured by SPR. The obtained kinetic differed dramatically from the adsorption kinetic of PA without pentabromophenol (figure 6A). No specific binding of PA onto the T4 surface could be detected any more, which can be explained by an effective blocking of the PA binding motive by pentabromophenol. Similar experiments were carried out with other phenols using identical concentrations and setup. Addition of phenol, 4-fluorophenol or bisphenol A showed no effect on the PA adsorption, whereas addition pentachlorophenol eliminated specific adsorption similar to pentabromophenol, which is in agreement with other T4-binding studies.^{80,83-85} Thus, T4 functionalized PMSSQ-PFPA coatings offer a convenient method for further PHAH-PA interaction screenings.

As the T4-functionalized PMSSQ-PFPA coating should be specific for PA adsorption (or other T4 transport proteins) other proteins should not show a stable assembly on this surface. Using the SPR setup we allowed streptavidin and albumin to assemble on the surface from PBS solution. Both proteins showed no specific binding and were completely removed by PBS rinsing steps (see supporting information, figure S9). Furthermore, fluorescence emission spectroscopy was performed after incubating a T4-functionalized PC wafer in albumin solution, rinsing several times with PBS, incubating in albumin blue 580 solution and rinsing again. No fluorescence could be detected (excitation 550 nm).

Folic acid functionalized surfaces. Folic acid is a water soluble vitamin of the B-complex group. It has emerged as an optimal targeting ligand for selective delivery of attached imaging and therapeutical agents to cancer tissues and sites of inflammation. Mammals are incapable of synthesizing folic acid and must obtain it from their dietary intake. Cells use folic acid in the synthesis of the DNA bases thymine and the purines.⁸⁶ The cell internalizes folic acid with the help of folate receptor proteins on the cell surface. To study binding effects between folic acid and folate receptor proteins specific biosensors have been designed, e. g. folic acid was immobilized on cantilever sensors, expressing the pterine end towards folate receptors.⁸⁷ Besides specific binding from folic acid to folate receptors on cell surfaces, folic acid is also known to bind to folate-binding proteins from bovine milk (FBP).⁸⁸⁻⁹⁰ Folic acid functionalized

biosensors were also used to study the interaction between folic acid and FBP, to determine binding affinity between folic acid and its receptors.⁹¹⁻⁹³

To attach folic acid as specific binding site to a PMSSQ-PFPA coating, the carboxylic acid functionalities of the glutamic acid moiety of folic acid were modified with ethylene diamine, similar to the biotin functionalization explained above (the aromatic amino group present is not capable to substitute the pentafluorophenol moiety, due to less nucleophilicity). Like in other folic acid biosensors, mentioned above, the pterine end is expressed at the interface. FBP is adsorbed from 0.1 mg/ml PBS solution. The adsorption process was monitored by SPR and the kinetic is shown in figure 7A. Complete adsorption took less than 30 min, indicating a strong interaction between the pterine end as FBP. The thickness increase was determined from SPR scans to be 1.1 nm (assuming constant refractive index). AFM topography showed a smooth protein layer with an RMS value ($1 \mu\text{m}^2$) of 0.624 nm, indicating a defect-free homogenous immobilization of FBP on the pterine expressing surface (figure 7B).

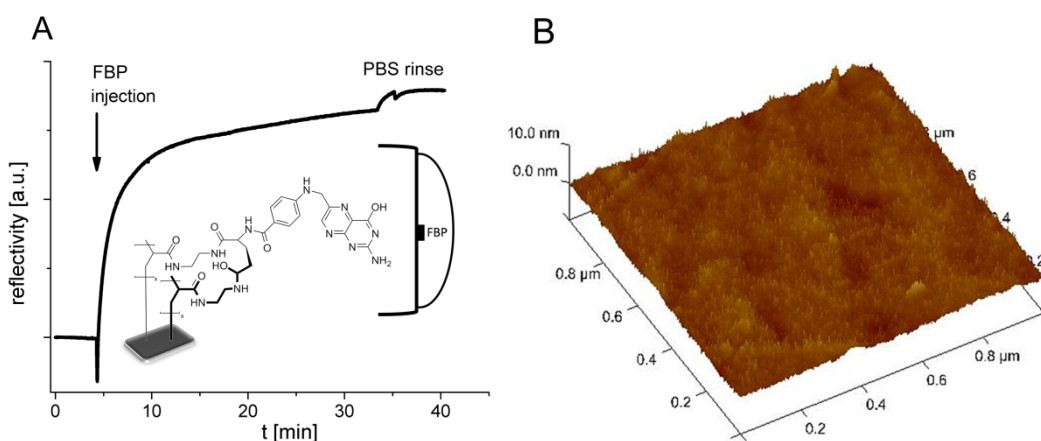


Figure 7. A: After conversion of the reactive coating, either on gold or on silicon surfaces, with amino-functionalized folic acid, folate-binding protein from bovine milk was adsorbed. (thickness increase 1.1 nm), B: AFM topography showed a homogenous protein functionalized surface (image RMS 0.624 nm).

To demonstrate specific binding between the pterine moiety and FBP we performed similar adsorption experiments using albumin and streptavidin. Both did not assemble specifically on to the surface and could be rinsed off using PBS solution (see supporting information, figure S10).

Our approach to functionalize surfaces with different binding motives may be helpful to determine further protein-binding characteristics of FBP and its influence on the protein immobilization mechanism in the future.

Conclusions

Poly(methylsilsesquioxane)-poly(pentafluorophenyl acrylate) hybrid materials could successfully be used to create very thin reactive surface coatings on gold-covered glass slides, capable as immobilization platform for SPR investigations. The strategy to assemble proteins

on top contains a simple surface-analogous conversion step to bind specific binding sites on the surface. Every specific binding site, which carries an aliphatic amine or which can be functionalized with an aliphatic amino group, can be reacted with the thin active ester coating. Using this approach biotin, L-thyroxine and folic acid could successfully be linked to planar surfaces. Streptavidin, pre-albumin and folate-binding protein could be immobilized, respectively. The assembly process could be monitored by SPR insitu.

The variety of attachable specific biolinkers is one main feature of the described PMSSQ-PFPA thin reactive coatings. Another feature is the substrate-independent adherence to the underlying substrate. Thus, the presented protein-immobilization protocol could also be used to functionalize Si, PC, PMMA, PDMS, and PTFE with proteins. The successful protein conjugation could be characterized using AFM, FTIR, fluorescence spectroscopy and ellipsometry. This simple method to obtain smooth homogenous protein layers may be useful for further biosensor applications, especially for streptavidin layers allowing further binding of biotinylated molecules.

In comparison to mostly complex protein immobilization strategies, our generally applicable functionalization method of substrate-independent reactive polymer coatings allows a specific attachment of proteins that may find versatile applications in different biosensor setups.

Acknowledgement

D.K. gratefully acknowledges financial support from the FCI, POLYMAT (Graduate School of Excellence "Polymers in Advanced Materials" GSC 266) and the IRTG 1404 ("Self-Organized Materials for Optoelectronic Applications"). P.J.R. acknowledges the IRTG 1404. The authors thank Rüdiger Berger (Max Planck Institute for Polymer Research, Mainz) for AFM support and valuable discussions, Steffen Seibel for synthetic support and Volker Schmidt and Heiner Detert for support with fluorescence emission spectroscopy.

Supporting Information Available

AFM topographies of PMSSQ-PFPA coatings on Au, PC, PDMS and PMMA, SPR kinetic of H₂N-biotin attachment on the reactive coating, SPR scans of the streptavidin adsorption, SPR kinetic of streptavidin adsorption on different surfaces, FTIR spectrum of streptavidin immobilized on PC, fluorescence spectra of Streptavidin Fluorescent Polymer on various substrates, SPR kinetics of albumin and pre-albumin on a biotinylated surface, the SPR kinetic of T4-disulfide SAM formation and further pre-albumin adsorption, SPR kinetics of streptavidin and albumin on a T4-functionalized surface, and SPR kinetics of albumin and streptavidin on a folic acid functionalized surface can be found in the supporting information. This information is available free of charge via the Internet at <http://pubs.acs.org>.

References

- (1) Rich, R. L.; D. G. Myszka *J. Mol. Recognit.* **2001**, *14*, 273-294.
- (2) Rich, R. L.; D. G. Myszka *J. Mol. Recognit.* **2002**, *15*, 352-376.

- (3) Rich, R. L.; D. G. Myszka *J. Mol. Recognit.* **2003**, *16*, 351-382.
- (4) Rich, R. L.; D. G. Myszka *J. Mol. Recognit.* **2005**, *18*, 1-39.
- (5) Rich, R. L.; D. G. Myszka *J. Mol. Recognit.* **2005**, *18*, 431-4789.
- (6) Rich, R. L.; D. G. Myszka *J. Mol. Recognit.* **2006**, *19*, 478-534.
- (7) Rich, R. L.; D. G. Myszka *J. Mol. Recognit.* **2007**, *20*, 300-366.
- (8) Rich, R. L.; D. G. Myszka *J. Mol. Recognit.* **2008**, *21*, 355-400.
- (9) Homola, J. *Anal. Bioanal. Chem.* **2003**, *377*, 528-539.
- (10) Rowe-Taitt, C. A.; Hazzard, J. W. Hoffman, K. E.; Cras, J. J.; Golden, J. P. Ligler, F. S. *Biosens. Bioelectron* **2000**, *15*, 579-589.
- (11) Piehler, P.; Brecht, A.; Gauglitz, G. *Anal. Chem.* **1996**, *68*, 139-143.
- (12) Heideman, R. G.; Kooyman, R. P. H.; Greve, J. *Sens. Actuators B* **1993**, *10*, 209-217.
- (13) Clerc, D.; Lukosz, W. *Sens. Actuators B* **1994**, *19*, 581-586.
- (14) Cush, R.; Cronin, J. M.; Stewart, W. J.; Maule, C. H.; Molloy, J.; Goddard, N. J. *Biosens. Bioelectron.* **1993**, *8*, 347-353.
- (15) Homola, J. *Chem. Rev.* **2008**, *108* (2), 462-493.
- (16) Liedberg, B.; Nylander, C.; Lundström, I. *Biosens. Bioelectron.* **1995**, *10*, i-ix.
- (17) Rich, R. L.; D. G. Myszka *J. Mol. Recognit.* **2000**, *13*, 388-407.
- (18) Homola, J.; Yee, S. S.; Gauglitz, G. *Sens. Actuators B* **1999**, *54*, 3-15.
- (19) Göpel, W. *Sens. Actuators B* **1991**, *4*, 7-21.
- (20) Göpel, W.; Heiduschka, P. *Biosens. Bioelectron.* **1995**, *10*, 853-883.
- (21) Göpel, W.; Heiduschka, P. *Biosens. Bioelectron.* **1994**, *9*, iii-xiii.
- (22) Mittler-Neher, S.; Spinke, J.; Liley, M.; Nelles, G.; Weisser, M.; Back, R.; Wenz, G.; Knoll, W. *Biosens. Bioelectron.* **1995**, *10*, 903-916.
- (23) Becker, H.; Gärtner, C. *Anal. Bioanal. Chem.* **2008**, *390* (1), 89-111.
- (24) Advincula, R. C.; Brittain, W. J.; Caster, K. C.; Rühle, J. (Eds.), *Polymer Brushes*, Wiley VCH: Weinheim **2004**.
- (25) Senarantne, W.; Andruzzi, L.; Ober, C. K. *Biomacromolecules* **2005**, *6*, 2427-2448.
- (26) Gujraty, K. V.; Ashton, R.; Bethi, S. R.; Kate, S.; Faulkner, C. J.; Jennings, G. K.; Kane, R. S. *Langmuir* **2006**, *22* (24), 10157-10162.
- (27) Lee, B. S.; Chi, Y. S.; Lee, K.-B.; Kim, Y.-G.; Choi, I. S. *Biomacromolecules* **2007**, *8* (12), 3922-3929.
- (28) Mosse, W. K. J.; Koppens, M. L.; Gengenbach, T. R.; Scanlon, D. B.; Gras, S. L.; Ducker, W. A. *Langmuir* **2009**, *25* (3), 1488-1494.
- (29) Lee, Y. W.; Reed-Mundell, J.; Sukenik, C. N.; Zull, J. E. *Langmuir* **1993**, *9* (11), 3009-3014.
- (30) Ducker, R. E.; Janusz, S.; Sun, S.; Leggett, G. J. *J. Am. Chem. Soc.* **2007**, *129* (48), 14842-14843.
- (31) Mark, S. S.; Sandhyarani, N.; Zhu, C.; Campagnolo, C.; Batt, C. A. *Langmuir* **2004**, *20* (16), 6808-6817.
- (32) Veiseh, M.; Zareie, M. H.; Zhang, M. *Langmuir* **2002**, *18* (17), 6671-6678.
- (33) Heyries, K. A.; Blum, L. J.; Marquette, C. A. *Langmuir* **2009**, *25* (2), 661-664.
- (34) Dankbar, D. M.; Gauglitz, G. *Anal. Bioanal. Chem.* **2006**, *386*, 1967.

- (35) Heyries, K. A.; Marquette, C. A.; Blum, L. J. *Langmuir* **2007**, *23* (8), 4523-4527.
- (36) Rusmini, F.; Zhong, Z.; Feijen, J. *Biomacromolecules* **2007**, *8* (6), 1775-1789.
- (37) Chen, B.; Pernodet, N.; Rafailovich, M. H.; Bakhtina, A.; Gross, R. A. *Langmuir* **2008**, *24* (23), 13457-13464.
- (38) Ostuni, E.; Chapman, R. G.; Hollin, R. E.; Takayama, S.; Whitesides, G. M. *Langmuir* **2001**, *17* (18), 5605-5620.
- (39) Schiller, S.; Jenkins, A. T. A.; Timmons, R. B.; Sanchez-Estrada, F. S.; Knoll, W.; Förch, R. *Chem. Mater.* **2002**, *14* (1), 235-242.
- (40) MacBeath, G.; Schreiber, S. L. *Science* **2000**, *289*, 1760-1763.
- (41) Azoune, A.; Slimane, A. B.; Hamou, L. A.; Pleuvy, A.; Chehimi, M. M.; Perruchot, C.; Armes, S. P. *Langmuir* **2004**, *20* (8), 3350-3356.
- (42) Feng, C. L.; Zhang, Z.; Förch, R.; Knoll, W.; Vansco, G. L.; Schönherr, H. *Biomacromolecules* **2005**, *6* (6), 3243-3251.
- (43) Beyer, D.; Bohanon, T. M.; Knoll, W.; Ringsdorf, H. *Langmuir* **1996**, *12* (10), 2514-2518.
- (44) Francesch, L.; Borros, S.; Knoll, W.; Förch, R. *Langmuir* **2007**, *23* (7), 3927-2931.
- (45) Lahann, J. *Polymer International* **2006**, *55* (12), 1361-1370.
- (46) Lahann, J.; Balcells, M.; Rodon, T.; Lee, J.; Choi, I. S.; Jensen, K. F.; Langer, R. *Langmuir* **2002**, *18* (9), 3632-3638.
- (47) Chen, H.-Y.; Elkasabi, Y.; Lahann, J. *J. Am. Chem. Soc.* **2006**, *128* (1), 374-380.
- (48) Viitala, T.; Vikholm, I.; Pelton, J. *Langmuir* **2000**, *16* (11), 4953-4961.
- (49) Drevon, G. F.; Urbanke, C.; Russell, A. J. *Biomacromolecules* **2003**, *4* (3), 675-682.
- (50) Collman, J. P.; Devaraj, N. K.; Eberspacher, T. P. A.; Chidsey, C. E. D. *Langmuir* **2006**, *22* (6), 2457-2464.
- (51) Schlossbauer, A.; Schaffert, D.; Kecht, J.; Wagner, E.; Bein, T. *J. Am. Chem. Soc.* **2008**, *130* (38), 12558-12559.
- (52) Houseman, B. T.; Huh, J. H.; Kron, S. J.; Mrksich, M. *Nat. Biotechnol.* **2002**, *20*, 270-274.
- (53) Sun, X.-L.; Stabler, C. L.; Cazalis, C. S.; Chaikof, E. L. *Bioconjugate Chem.* **2006**, *17* (1), 52-57.
- (54) Kessler, D.; Teutsch, C.; Theato, P. *Macromol. Chem. Phys.* **2008**, *209* (14), 1437-1446.
- (55) Kessler, D.; Theato, P. *Macromolecules* **2008**, *41* (14), 5237-5244.
- (56) Kessler, D.; Löwe, H.; Theato, P. *Macromol. Chem. Phys.* **2009**, doi: 10.1002/macp.200800611.
- (57) Pulker, H. K.; Perry, A. J. *Surface Technology* **1981**, *14*, 25.
- (58) Possart, W. (Ed.), *Adhesion. Current Research and Applications*, Wiley VCH: Weinheim, **2005**.
- (59) Kessler, D.; Theato, P. *Langmuir* **2009**, doi: 10.1021/la9005949.
- (60) Su, X.; Wu, Y.-J.; Robolek, R.; Knoll, W. *Langmuir* **2005**, *21* (1), 348-353.
- (61) Roth, P. J.; Theato, P. *Chem. Mater.* **2008**, *20*, 1614-1621.
- (62) Flink, S.; van Veggel, F. C. J. M.; Reinhoudt, D. N. J. *Phys. Org. Chem.* **2001**, *14*, 407-415.
- (63) Yang, Z.; Galloway, J. A.; Yu, H. *Langmuir* **1999**, *15*, 8405-8411.

- (64) Packham, D. E. (Ed.), *Handbook of Adhesion 2nd Edition*, John Wiley & Sons: New York, **2005**.
- (65) Wilchek, M.; Bayer, E. A. *Anal. Biochem.* **1998**, *171*, 1-6.
- (66) Pantano, P.; Kuhr, W. G. *Anal. Chem.* **1993**, *65*, 623-630.
- (67) De Alwis, U.; Wilson, G. S. *Talanta*, **1989**, *36*, 249-253.
- (68) Ulman, A. *Chem. Rev.* **1996**, *96*, 1533-1554.
- (69) Atanasov, V.; Atanasov, P. P.; Vockenroth, I. K.; Knorr, N.; Köper, I. *Bioconjugate Chem.* **2006**, *17*, 631-637.
- (70) Pirrung, M. C. *Angew. Chem. Int. Ed.* **2002**, *41*, 1276-1289.
- (71) Jung, H.; Kulkarni, R.; Collier, C. P. *J. Am. Chem. Soc.* **2003**, *125*, 12096-12907.
- (72) Basabe-Desmonts, L.; Beld, J.; Zimmerman, R. S.; Hernando, J.; Mela, P.; Garcia Parajo, M. F.; van Hulst, N. F.; van den Berg, A.; Reinhoudt, D. N.; Crego-Calama, M. *J. Am. Chem. Soc.* **2004**, *126*, 7293-7299.
- (73) Kessler, M. A.; Meinitzer, A.; Petek, W.; Wolfbeis, O. S. *Clinical Chemistry* **1997**, *43*, 996-1002.
- (74) Kessler, M. A.; Meinitzer, A.; Wolfbeis, O. S. *Anal. Biochem.* **1997**, *248*, 180-182.
- (75) Yen, P. M. *Physiol. Rev.* **2001**, *81*, 1097-1142.
- (76) Bernal, J.; Guadano-Ferraz, A.; Morte, B. *Thyroid* **2003**, *13*, 1005-1012.
- (77) Schreiber, G. *J. Endocrinol.* **2002**, *175*, 61-73.
- (78) Hakk, H.; Letcher, R. *J. Environ. Int.* **2003**, *29*, 801-828.
- (79) Hallgren, S.; Darnerud, P. O. *Toxicology* **2002**, *177*, 227-243.
- (80) Marchesini, G. R.; Meimaridou, A.; Haasnoot, W.; Meulenberg, E.; Albertus, F.; Mizuguchi, M.; Takeuchi, M.; Irth, H.; Murk, A. *J. Toxicology and Applied Pharmacology* **2008**, *232*, 150-160.
- (81) Schönherr, H.; Ringsdorf, H.; Jaschke, M.; Butt, H.-J.; Bamberg, E.; Allinson, H.; Evans, S. D. *Langmuir* **1996**, *12* (16), 3898-3904.
- (82) Prime, K. L.; Whitesides, G. M. *Science* **1991**, *252*, 1164.
- (83) Meerts, I. A. T. M.; van Zanden, J. J.; Luijckx, E. A. C.; van Leeuwen-Bol, I.; Marsh, G.; Jakobsson, E.; Bergman, A.; Brouwer, A. *Toxicol. Sci.* **2000**, *56*, 95-104.
- (84) den Besten, C.; Vet, J. J. R. M.; Besselink, H. T.; Kiel, G. S.; van Berkel, B. J. M.; Beems, R.; van Bladeren, P. J. *Toxicol. Appl. Pharmacol.* **1991**, *111*, 69.
- (85) van den Berg, K. L. *Chem.-Biol. Interact.* **1990**, *76*, 63-75.
- (86) Low, P. S.; Henne, W. A.; Doorneweerd, D. D. *Accounts of Chemical Research* **2008**, *41* (1), 120-129.
- (87) Bhalerao, K. D.; Lee, S. C.; Soboyejo, W. O.; Soboyejo, A. B. O. *J. Mater. Sci.: Mater. Med.* **2007**, *18*, 3-8.
- (88) Jones, M. L.; Nixon, P. F. *Journal of Nutrition* **2002**, 2690-2694.
- (89) Nixon, P. F.; Jones, M.; Winzor, D. J. *Biochem. J.* **2004**, *382*, 215-221.
- (90) Nygren-Babol, L.; Sternesjö, Å.; Björck, L. *Int. Dairy J.* **2004**, *14*, 761-765.
- (91) Nygren-Babol, L.; Sternesjö, Å.; Björck, L. *Int. Dairy J.* **2003**, *13*, 283-290.

(92) Nygren-Babol, L.; Sternesjö, Å.; Jägerstad, M.; Björck, L. *J. Agric. Food Chem.* **2005**, *53*, 5473-5478.

(93) Colman, N.; Herbert, V. *Ann. Rev. Med.* **1980**, *31*, 433-439.

Supporting information

Figure S1:

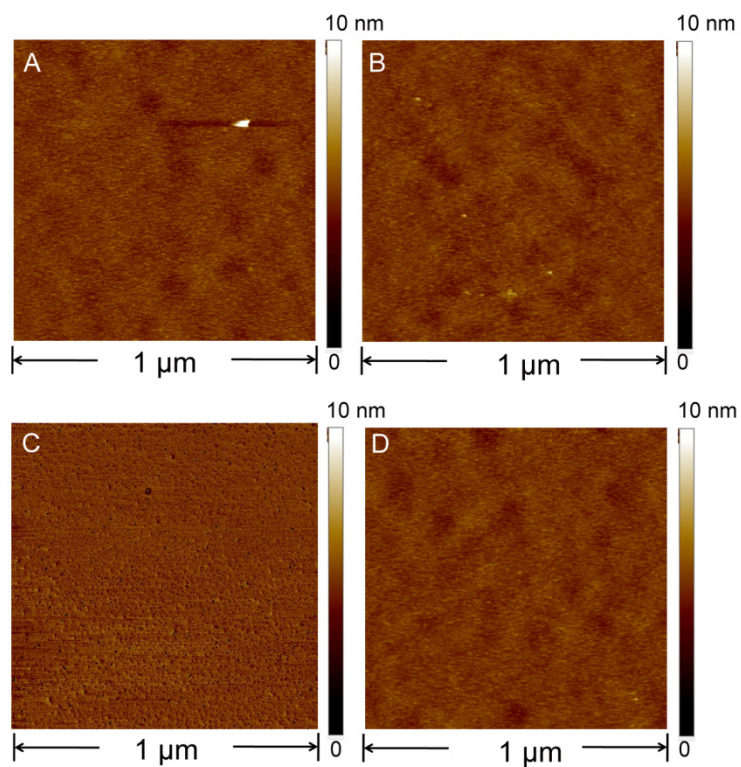


Figure S1. AFM topography of PMSSQ-PFPA on various substrates. (A) gold substrate; (B) PC substrate; (C) PDMS substrate; (D) PMMA.

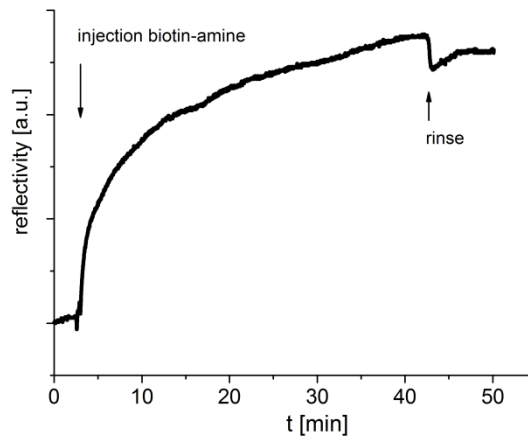
Figure S2:

Figure S2. SPR kinetic of the surface-analogous reaction of H_2N -biotin with the reactive coating on a gold-covered glass slide (thickness increase 0.5 nm).

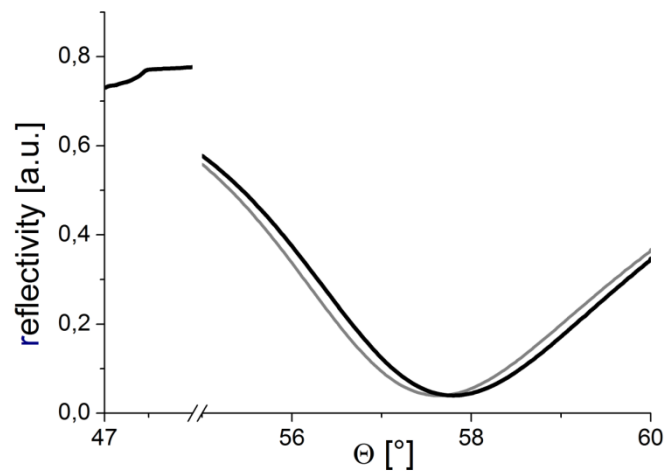
Figure S3:

Figure S3. SPR scan before streptavidin adsorption (grey line) and after complete streptavidin adsorption and PBS rinsing (calculated thickness increase, assuming constant refractive indices: 5.23 nm).

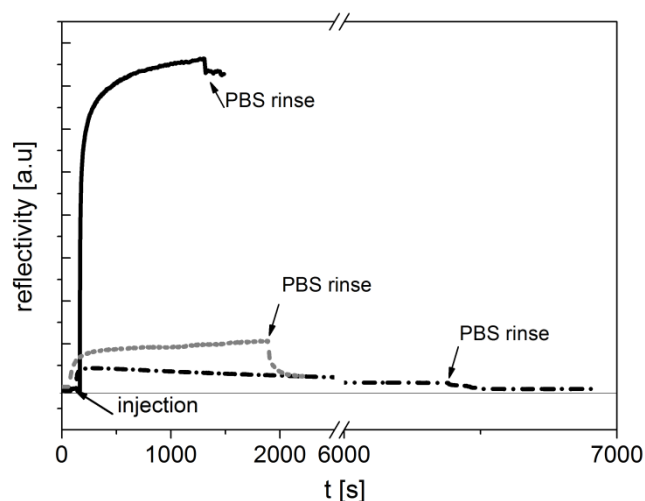
Figure S4:

Figure S4. SPR kinetics of streptavidin adsorption: black solid line: specific adsorption on biotinylated surfaces; grey dotted line: unspecific adsorption on octylamin-functionalized reactive coating on gold; black dashed line: unspecific adsorption on amino-PEG functionalized reactive coating on gold.

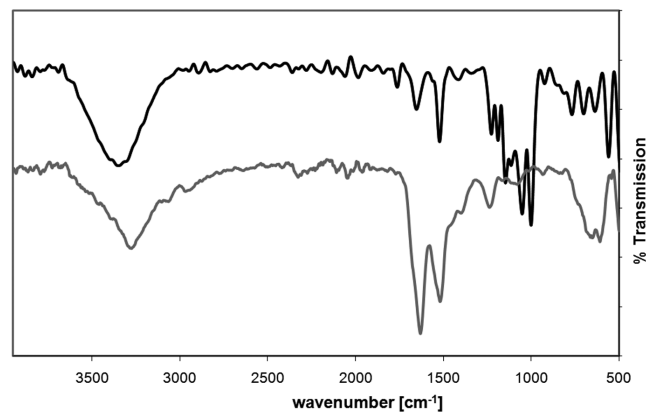
Figure S5:

Figure S5. Upper spectra: FTIR spectra of streptavidin immobilized onto PC using the introduced reactive coating concept (PMSSQ-PFPA coating, conversion with biotin-amine, assembly of streptavidin) measured against blank PC background. Peptide amine and amide bands can be found at 3300 cm⁻¹, 1635 cm⁻¹ and 1530 cm⁻¹, respectively. The Si-O valence bands appear between 1200 cm⁻¹ and 950 cm⁻¹, arising from the intrinsic PMSSQ crosslinker.

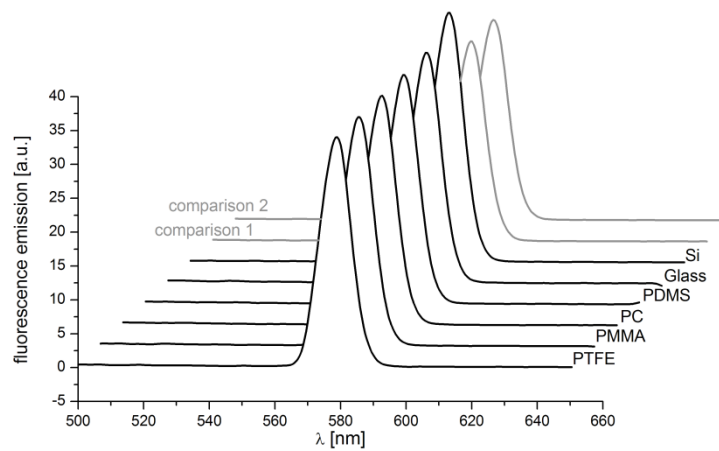
Figure S6:

Figure S6. Fluorescence emission spectra of Streptavidin Fluorescent Polymer Ultrasensitive (Sigma-Aldrich S2313) immobilized on different surfaces. Comparison 1: SAM of perfluorophenyl 4-(2-(chlorodimethylsilyl)ethyl)benzoate on glass, converted with biotin-amine. Comparison 2: APTES SAM on glass, functionalized with Biotin perfluorophenyl ester.

Other spectra: PMSSQ-PFPA coated onto different substrates, converted with biotin-amine. After 1h incubation time of the biotin-functionalized substrate in a PBS/BSA solution containing 0.005 mg protein/ml, the wafers were rinsed several times with PBS/BSA buffer solution and dried in nitrogen stream. (excitation at 295 nm, slits: 5 nm)

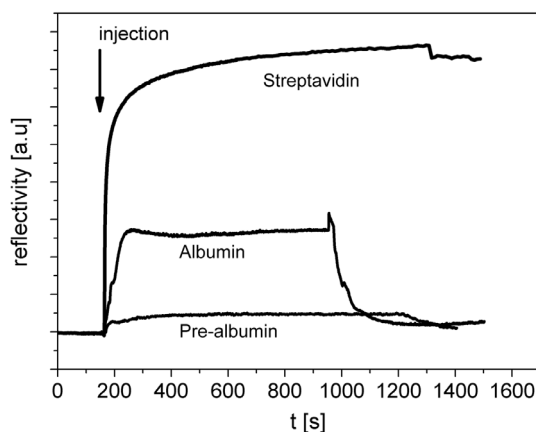
Figure S7:

Figure S7. SPR kinetics of the adsorption of different proteins onto a biotinylated PMSSQ-PFPA coating on gold-covered glass slides. Streptavidin showed the expected strong adsorption whereas albumin and pre-albumin do not assemble on top of the coating.

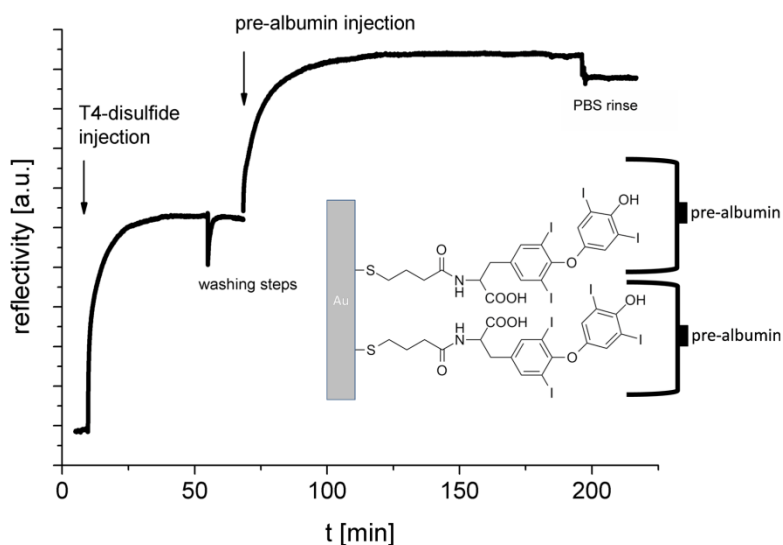
Figure S8:

Figure S8. SPR kinetic of T4-disulfide SAM formation on a gold-covered glass slide (0.1 mg/ml in EtOH), after several washing steps and solvent change pre-albumin was adsorbed (0.1 mg/ml in water). (thickness increase T4-disulfide: 1.66 nm; thickness increase pre-albumin: 2.60 nm; assuming constant refractive indices).

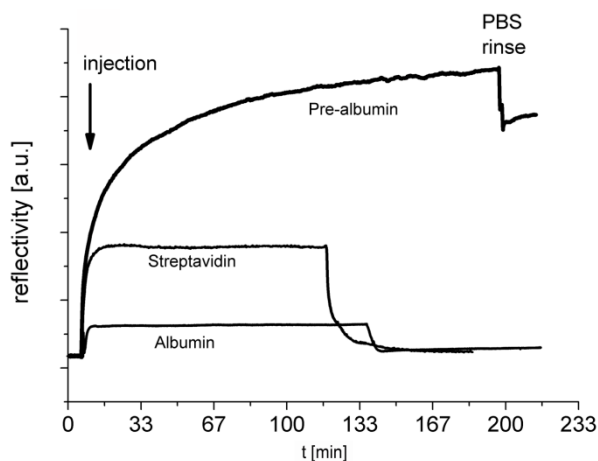
Figure S9:

Figure S9. SPR kinetics of the adsorption of different proteins onto a T4-functionalized PMSSQ-PFPA coating on gold-covered glass slides. Pre-albumin showed the expected strong adsorption whereas albumin and streptavidin do not assemble on top of the coating.

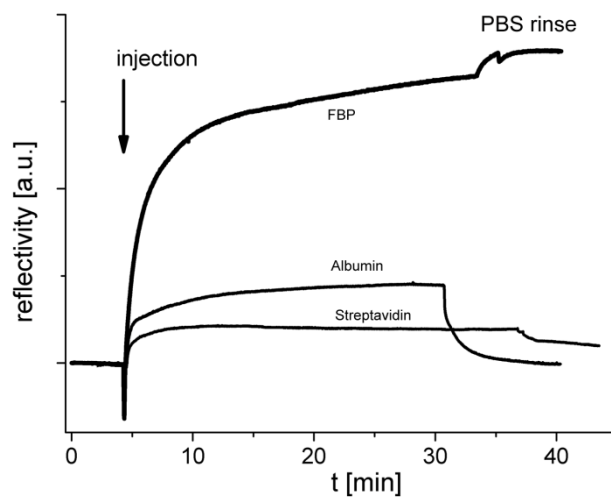
Figure S10:

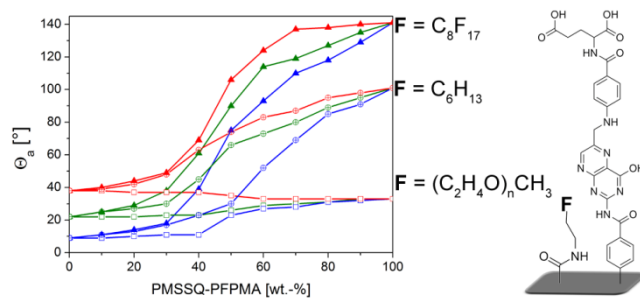
Figure S10. SPR kinetics of the adsorption of different proteins onto a folic acid-functionalized PMSSQ-PFPA coating on gold-covered glass slides. Folate-binding protein (FBP) showed the expected strong adsorption whereas albumin and streptavidin do not assemble on top of the coating.

4.10 Modular Approach toward Multi-Functional Surfaces with Adjustable and Dual-Responsive Wettability Using a Hybrid Polymer Toolbox

Daniel Kessler, Katja Nilles, Patrick Theato

Institute of Organic Chemistry, University of Mainz, Duesbergweg 10-14, 55099 Mainz, Germany

Chem. Commun. **2009**, submitted.



Poly(methylsilsesquioxane)-based hybrid polymers carrying orthogonally reactive moieties demonstrate an effective modular approach to create multi-reactive surface coatings. By a sequential surface-analogous reaction different functions could be immobilized in a defined ratio, resulting in dual- or triple-functionalized surfaces.

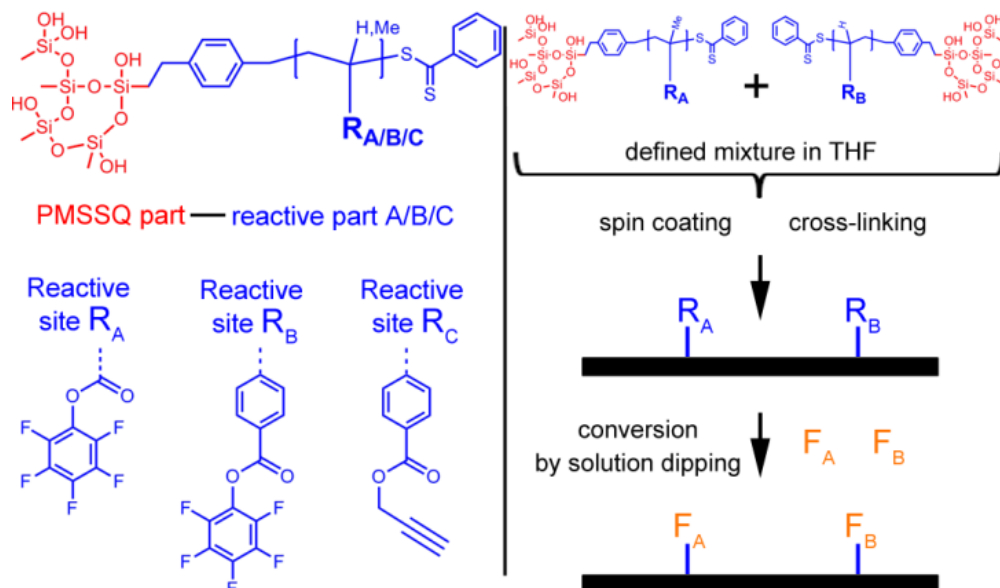
Functional or smart coatings had gained considerable interest recently because of their applications in different fields of natural science: Specific immobilization of bio-active moieties on different surfaces is the basis of state-of-the-art biosensors;¹ control of the interfacial chemistry allows adjustment of surface wettability² and even to fabricate devices featuring switchable surface properties.³

Different generally applicable protocols, such as copolymers containing isocyanates, plasma polymerized maleic anhydride films, or chemical vapour deposition of [2.2]paracyclophane pentafluorophenyl esters were introduced to create reactive surface coatings.⁴ By further surface-analogous reaction various functions could be attached using the same coating material.⁵ Usually these reactive coating materials were limited to one specific reactive moiety and thus allow only the defined immobilization of one specific function. A conversion with two different functions by the same binding mechanism would not allow a defined adjustment of the ratio between both, due to different reaction rates. Expressing different orthogonal reactivities at the interface would allow immobilizing a defined ratio of two or more specific functional moieties on the same surface.

Recently, we introduced poly(methylsilsesquioxane) (PMSSQ) based reactive surface coatings.⁶ The PMSSQ part could be thermally crosslinked to produce stable and adherent films on various underlying materials, whereas a reactive organic part allowed further surface-analogous conversion using various aliphatic amines.⁷ Herein we present a modular approach to produce dual- or triple-reactive surface coatings containing defined ratios of orthogonal reactive sites. We prepared three different PMSSQ-based reactive hybrid polymers consisting of pentafluorophenyl methacrylate (FPMA, R_A), pentafluorophenyl vinylbenzoate (FPVB, R_B), or propargyl vinylbenzoate (PVB, R_C), respectively. R_A can be converted with aliphatic amines to amides,⁸ R_B also reacts with aromatic amines to amides,⁹ whereas R_C undergoes 1,3-dipolar cycloaddition with azides.¹⁰ The obtained PMSSQ-based reactive hybrid polymers are schematically shown in Scheme 1.

Starting from this toolbox of orthogonally convertible hybrid polymers, we prepared defined mixtures of different hybrid polymers in solution. After spin-coating and cross-linking (130 °C, 2h), two or even three reactive sites could be attached to the surface and reacted by two or three surface-analogous conversion steps (conversion by dipping the coated substrate in a 10 wt% solution of corresponding amines or azides).

Scheme 1. Poly(methylsilsesquioxane)-based reactive hybrid polymers containing either reactive site A, B, or C. Spin-coating defined mixtures of different polymers resulted in defined multi-reactive coatings, which could selectively be converted with different functions (F_A , F_B).



As the ratio between two orthogonal reactivities on the surface is adjusted by preparing a defined mixture of the corresponding hybrid polymers in solution, we performed the following experiment to demonstrate that this adjusted ratio is reflected on the surface. Various mixtures of PMSSQ-PFPMA (R_A) and PMSSQ-PPVB (R_C) were spin-coated onto silicon. One series was converted with (1) poly(ethylene glycol)-amine (PEG-NH₂) and (2) with azid-functionalized stearic acid, whereas another series was converted with (1) amino-functionalized stearic acid and (2) PEG-N₃. The change in surface properties was determined by measuring the advancing contact angle of water (Θ_a), which is the ideal parameter to prove a successful conversion on a macroscopic length scale (see figure 1).

As expected in both series, a fully stearic acid functionalized surface exhibits a hydrophobic surface ($\Theta_a = 118^\circ$), a fully PEGylated surface exhibits a hydrophilic surface ($\Theta_a = 33^\circ$). At a 1:1 mixture of PMSSQ-PFPMA and PMSSQ-PPVB a mirror plane can be observed in figure 1, which indicates the preservation of composition between R_A and R_C on the surface. In both series the final surface coatings after conversion consist of alkyl chains from the stearic acid immobilization and of PEG chains from the PEG attachment via amid bond formation or cycloaddition, respectively. The opposite binding concept to attach both moieties in defined ratios showed no influence on the final surface. For example a 1:1 mixture of PMSSQ-PFPMA (R_A) and PMSSQ-PPVB (R_C) exhibits a contact angle of $\sim 70^\circ$, independent of the sequence of the performed functionalization. A surface coating offering 30 % binding sites for PEG-functionalities and 70 % binding sites for stearic acid moieties exhibits a contact angle of $\sim 97^\circ$, independent from the chemical character of the applied binding strategy.

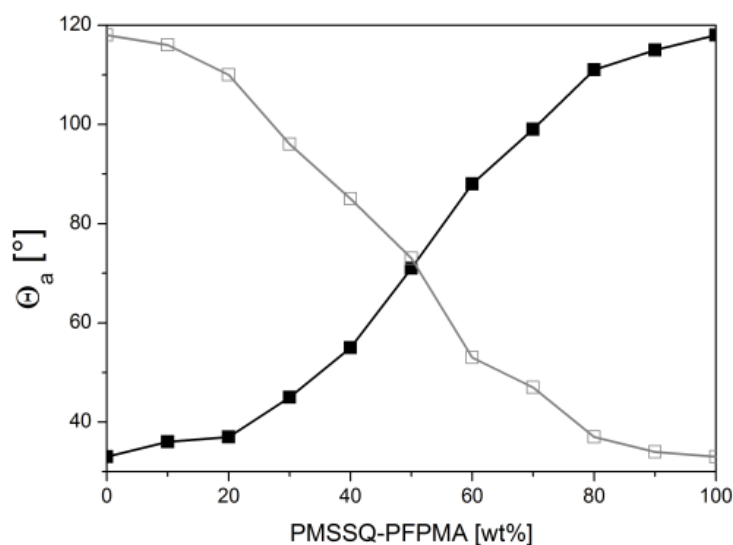


Figure 1. Two series of different mixtures of PMSSQ-PFPMA (R_A) and PMSSQ-PPVB (R_C) were spin-coated on silicon wafers. The black line shows the observed contact angles after conversion with (1) PEG-NH₂, (2) azid-functionalized stearic acid. The grey line shows the observed contact angles after the opposite conversion of similar surfaces: (1) amino-functionalized stearic acid, (2) PEG-N₃.

To create a dual-responsive surface coating by the presented modular approach, similar series of mixtures of R_A and R_C containing hybrid polymers were spin-coated onto silicon wafers.

To demonstrate the individual addressability, R_C was converted with 4-benzoic acid methyl azide and R_A with isopropylamine. As expected, increasing the amount of benzoic acid attached to the surface (by increasing the fraction of polymer with R_C) resulted in a lower contact angle. Whereas a higher fraction of R_A , converted to poly(*N*-isopropyl methacrylamide), resulted in more hydrophobic surfaces.

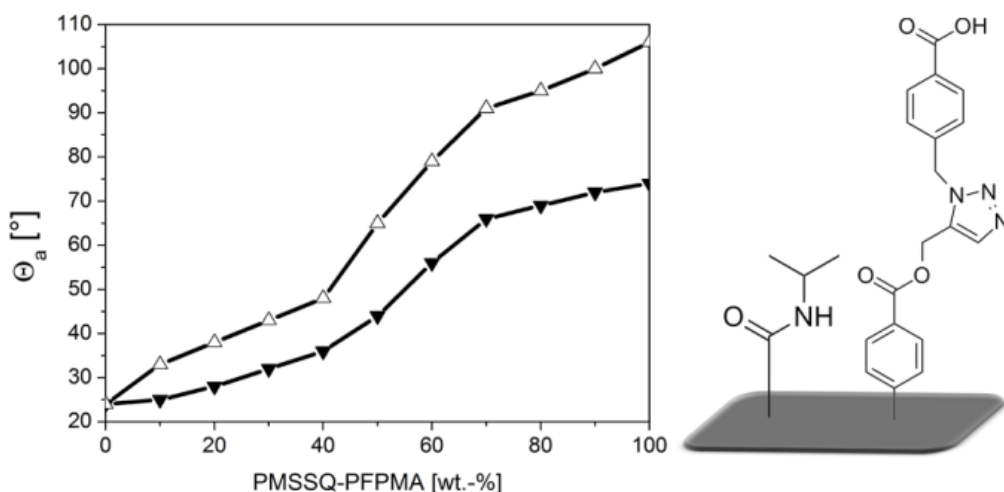


Figure 2. Different mixtures of PMSSQ-PFPMA (R_A) and PMSSQ-PPVB (R_C) were spin-coated onto Si, after conversion with (1) 4-benzoic acid methyl azide and (2) isopropylamine, the advancing contact angles were measured at different temperatures (filled symbols: $T = 15$ °C, free symbols: $T = 60$ °C).

As poly(*N*-isopropyl methacrylamide) exhibits a lower critical solution temperature in water, a temperature-responsiveness was observed on those coatings which allowed attachment of isopropyl amine (figure 2: lower curve measured at 15 °C; upper curve measured at 60 °C). Furthermore, the surface coatings containing benzoic acid showed a pH-responsive behavior (see SI, figure S1). Thus, by conversion of a coating containing reactive sites A and B with isopropyl amine and 4-benzoic acid methyl azide a dual-responsive surface coating was obtained. For example, a coating produced from a solution of 40 % PMSSQ-PFPMA and 60 % PMSSQ-PPVB exhibits after conversion a contact angle of 26° at pH 11 and 15 °C and of 72° at pH 2 and 60 °C.

Similarly, we produced different mixtures of PMSSQ-based polymers, containing either R_A or R_B . After spin coating on Si and cross-linking, R_B was converted with folic acid (folic acid contains one primary aromatic amine and two carboxylic acid moieties, which provide again pH-responsiveness). The reactive site R_A was functionalized using different amines to shift the pH-responsive behaviour over the whole range of wettability. After dipping the substrate in a solution of folic acid (containing 2 equiv. triethylamine) R_A was functionalized either with poly(ethyleneglycol) amine (PEG-NH₂), octylamine, or F₁₇C₈H₂C₂-NH₂, respectively. Depending on the used ratio of hybrid polymers with R_A and R_B , the resulting contact angle can be shifted between those of the homo-functionalized surface coatings, e.g. after functionalization with F₁₇C₈H₂C₂-NH₂ a coating produced by 10 wt% PMSSQ-PFPMA (R_A) exhibits $\Theta_a = 25^\circ$, whereas a coating with 90% PMSSQ-PFPMA exhibits $\Theta_a = 135^\circ$ after conversion (at pH = 7). Similarly, the pH-responsiveness is shifted: 10 wt% PMSSQ-PFPMA (R_A), 90 wt% PMSSQ-PFPVB (R_B) coating after conversion with (1) folic acid (F_B) and (2) F₁₇C₈H₂C₂-NH₂ (F_A) exhibits $\Theta_a = 11^\circ$ at pH = 11 and $\Theta_a = 40^\circ$ at pH = 2. Similar functionalization of a coating produced by a mixture of 90% PMSSQ-PFPMA (R_A) and 10 wt% PMSSQ-PFPVB (R_B) results in $\Theta_a = 129^\circ$ at pH = 11 and $\Theta_a = 140^\circ$ at pH = 2. The whole accessible range of wettability shifts is shown in figure 3.

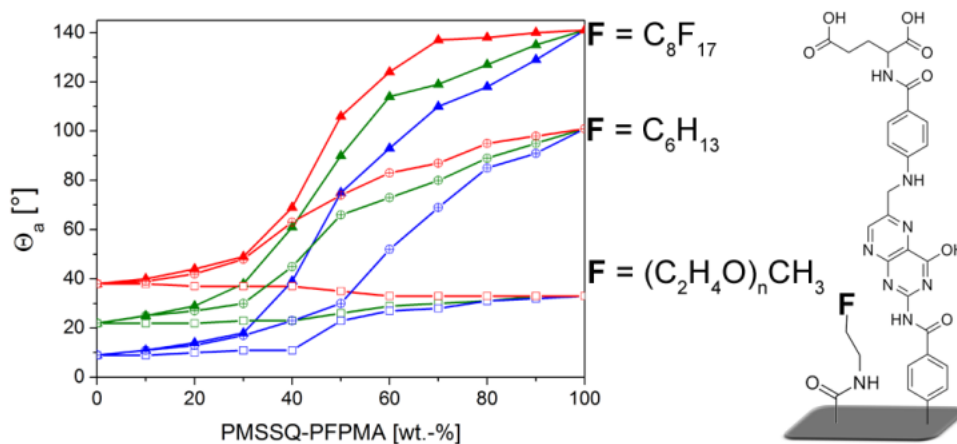


Figure 3. Different mixtures of PMSSQ-PFPMA (R_A) and PMSSQ-PFPVB (R_B) were spin-coated onto silicon, after conversion with (1) folic acid and (2) a perfluorinated amine, an alkyl amine or a PEGylated amine, the advancing contact angles were measured at different pH (blue curves: pH = 11; green curves: pH = 7; red curves: pH = 2).

As the three presented reactive hybrid polymers showed orthogonal reactivity, we prepared a mixture of all three in the ratio 1:1:1. After spin-coating and annealing a triple-reactive surface coating should be obtained. To prove the addressability of all reactive groups present on the surface, we performed the following functionalization procedure: (1) conversion of the pentafluorophenyl vinyl benzoate (R_B) by dipping into a solution of *p*-amino benzoic acid, (2) conversion of the pentafluorophenyl methacrylate (R_A) by dipping the same substrate in a solution of isopropylamine and (3) conversion of the acetylene (R_C) by performing cycloaddition with (a) PEG- N_3 or (b) azide-functionalized stearic acid (see figure 4).

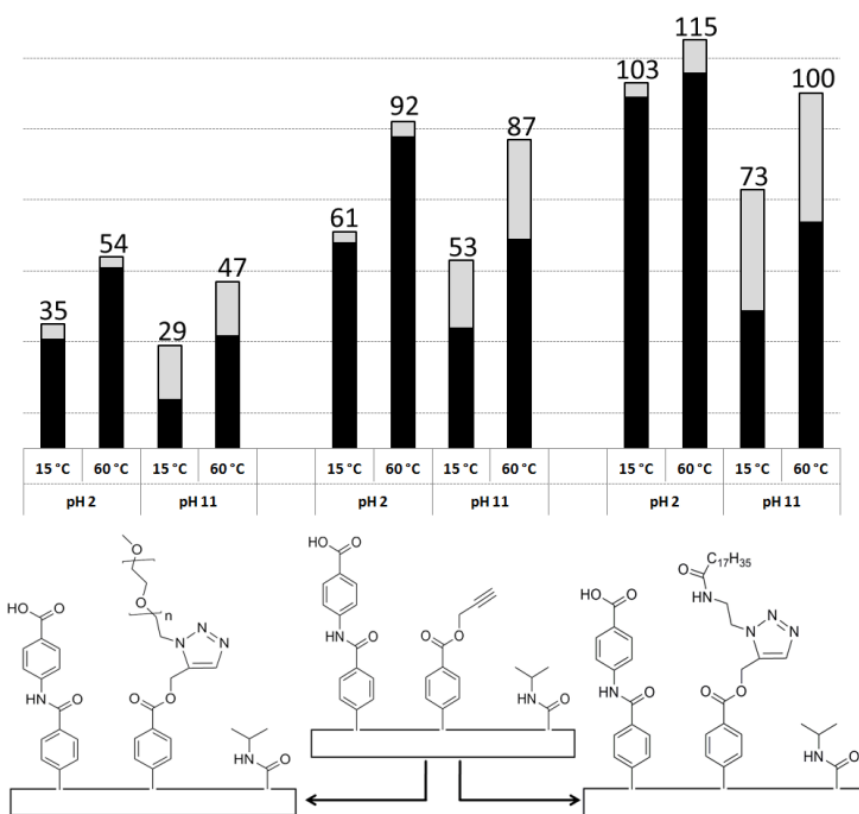


Figure 4. Triple-reactive surface coating, expressing three orthogonal reactivities on the surface. First the R_B groups were converted with *p*-amino benzoic acid, which offers a pH-dependence, a second conversion of the R_A groups with isopropylamine resulted in a temperature-dependant wettability. The third conversion of the acetylene groups (R_C) allowed to adjust the switching range to a hydrophilic or hydrophobic behaviour. Grey bares show the advancing contact angles (values given), the black bars show the corresponding receding contact angles (all values are summarized in ESI, table S1).

Before performing conversion step 3 a dual responsive surface coating was obtained which allows switching of contact angles between 53° and 92° by pH and temperature change. By conversion of the acetylene moiety the switching range could be shifted. After cycloaddition of PEG-azide the dual responsive surface allowed a switching in the contact angle range between 29° and 54°. Conversion with azide-functionalized stearic acid shifted the contact angle range to 73° to 115°. As expected, the contact angle hysteresis

(difference between advancing and receding contact angle) is large for measurements performed at pH = 11, due to the deprotonation of the carboxylic acid moieties. The most effective changes in surface wettability was observed if reactivity R_c was converted with azide-functionalized stearic acid, due to the hydrophobic behaviour of stearic acid in combination with two switchable moieties. This simple method offered the possibility to adjust a switchable surface wettability in different contact angle ranges just by conversion with different azide-functionalized moieties.

Conclusions

This simple modular approach of mixing different PMSSQ-based hybrid polymers carrying orthogonal reactivities, demonstrate for the first time a dual- or triple-addressable surface coating to immobilize different functions in a defined ratio on a surface. Defined adjustment of the wetting behaviour and defined dual-responsive surfaces could be obtained by sequential conversion of the orthogonal reactivities present on the surface. Attachment of other surface-relevant functions, like bio-specific binding sites or light-responsive molecules, may benefit from the dual- or triple-reactive character of this approach in the future.

Acknowledgement. D.K. gratefully acknowledges financial support from the FCI, POLYMAT (Graduate School of Excellence “Material Science in Mainz” GSC 266) and the IRTG 1404 (“Self-Organized Materials for Optoelectronic Applications”) funded by the German Science Foundation (DFG). The authors thank Steffen Seibel for synthetic support in monomer synthesis.

Notes and references

† Electronic Supplementary Information (ESI) available: Detailed experimental part and characterization data of the materials used, pH-responsive behaviour of a series of coatings produced from PMSSQ-PFPMA and PMSSQ-PPVB after conversion with 4-benzoic acid methyl azide and isopropylamine, contact angles of different dual-reactive surface coatings and surface wettability characteristics of a series of PMSSQ-PFPMA and PMSSQ-PPVB coatings converted to fully PEGylated surfaces, contact angle values after different conversion sequences of a triple reactive surface. See DOI: 10.1039/b000000x/.

- 1 (a) F. Rusmini, Z. Zhong and J. Feijen, *Biomacromolecules*, 2007, **8**, 1775; (b) W. Göpel and P. Heiduschka, *Biosensors & Bioelectronics*, 1995, **10**, 853; (c) W. Göpel, *Sens. Actuators B*, 1991, **4**, 7; (d) D. Kessler, P. J. Roth and P. Theato, *Langmuir* 2009, accepted.
- 2 (a) A. R. Abate, A. T. Krummel, D. Lee, M. Marquez, C. Holtze and D. A. Weitz, *Lab Chip*, 2008, **8**, 2157; (b) A. R. Abate, D. Lee, T. Do, C. Holtze and D. A. Weitz, *Lab Chip*, 2008, **8**, 516; (c) A. Marmur, *Langmuir*, 2004, **20**, 3517; (d) L. Gao and T. J. McCarthy, *Langmuir* 2006, **22**, 2966.
- 3 (a) F. Xia, L. Feng, S. Wang, T. Sun, W. Song, W. Jiang and L. Jiang, *Adv. Mater.*, 2006, **18**, 432; (b) T. Sun, G. Wang, L. Feng, B. Liu, Y. Ma, L. Liang and D. Zhu, *Angew. Chem. Int. Ed.*, 2004, **43**, 357; (c) M. D. Kurkuri, M. R. Nussio, A. Deslandes and N. H. Voelcker, *Langmuir*,

- 2008, **24**, 4238; (d) V. Papaefthimiou, R. Steitz and G. H. Findegg, *Chem. Unserer Zeit*, 2008, **42**, 102; (e) T. P. Russell, *Science*, 2002, **297**, 964; (f) S. L. Gras, T. Mahmud, G. Rosengarten, A. Mitchell and K. Kalantar-zadeh, *ChemPhysChem*, 2007, **8**, 2036; (g) J. Zimmermann, M. Rabe, G. R. J. Artus and S. Seeger, *Soft Matter*, 2008, **4**, 450.
- 4 (a) D. Beyer, T. M. Bohanon, W. Knoll and H. Ringsdorf, *Langmuir*, 1996, **12**, 2514; (b) S. Cuenot, S. Gabriel, R. Jerome, C. Jerome, C.-A. Fustin, A. M. Jonas and A.-S. Duwez, *Macromolecules*, 2006, **39**, 8428; (c) C. Jerome, S. Gabriel, S. Voccia, C. Detrembleur, M. Ignatova, R. Gouttebaron and R. Jerome, *Chem. Commun.*, 2003, 2500; (d) S. Schiller, J. Hu, A. T. A. Jenkins, R. B. Timmons, F. Sanchez-Estrada, W. Knoll and R. Foerch, *Chem. Mater.*, 2002, **14**, 235.
- 5 (a) J. Lahann, I. S. Choi, J. Lee, K. F. Jensen and R. Langer, *Angew. Chem. Int. Ed.*, 2001, **40**, 3166; (b) J. Lahann, M. Balcells, T. Rodon, K. F. Jensen and R. Langer, *Anal. Chem.*, 2003, **75**, 2117.
- 6 (a) D. Kessler and P. Theato, *Macromolecules*, 2008, **41**, 5237; (b) D. Kessler, N. Metz and P. Theato, *Macromol. Symp.*, 2007, **254**, 34.
- 7 D. Kessler and P. Theato, *Langmuir*, 2009, doi: 10.1021/la9005949.
- 8 M. Eberhardt and P. Theato, *Macromol. Rapid Commun.*, 2005, **26**, 1488.
- 9 K. Nilles and P. Theato, *Eur. Polym. Mater.* 2007, **43**, 2901.
- 10 P. J. Roth, D. Kessler, R. Zentel and P. Theato, *J. Polym. Sci. A:Pol. Chem.*, 2009, **47**, 3118.

Supplementary Information

Experimental Section

Materials. All chemicals and solvents were commercially available (Acros Chemicals, ABCR) and used as received unless otherwise stated. 1,4-Dioxane and THF were distilled from sodium/benzophenone under nitrogen.

Instrumentation. ^1H -NMR and ^{13}C -NMR spectra were recorded on a Bruker 300 MHz FT-NMR spectrometer, ^{19}F -NMR spectra on a Bruker DRX 400 FT-NMR spectrometer. ^{29}Si CPMAS NMR spectra were measured on a Bruker DSX 400 MHz FT-NMR spectrometer (Rotation: 5000 Hz, T = RT, 4 mm rotor). Chemical shifts (δ) were given in ppm relative to TMS. Gel permeation chromatography (GPC) was used to determine molecular weights and molecular weight distributions, M_w/M_n , of polymer samples. (THF used as solvent, polymer concentration: 2 mg/mL, column setup: MZ-Gel-SDplus 10^2 \AA^2 , 10^4 \AA^2 and 10^6 \AA^2 , used detectors: refractive index, UV and light scattering). Thermo gravimetric analysis was performed using a Perkin Elmer Pyris 6 TGA in nitrogen (10 mg pure polymer in aluminum pan). Advancing and receding CA of water were measured using a Dataphysics Contact Angle System OCA 20 and fitted by SCA 20 software. Given CA are average values of 10 individual measurements with an accuracy of 3° . To measure temperature dependent CA, the substrate temperature was controlled with a peltier element underneath (Accuracy of temperature dependent CA measurements 5° , due to complicate temperature adjustment). All chemical reactions were performed in Argon

atmosphere.

Pentafluorophenyl methacrylate (FPMA) was synthesized as explained in [Eberhardt, M.; Theato, P. *Macromol. Rapid Commun.* **2005**, **26**, 1488-1493]. $^1\text{H-NMR}$ (CDCl_3) δ : 6.43 (s, 1H); 5.89 (s, 1H); 2.07 (s, 3H). $^{19}\text{F-NMR}$ (CDCl_3) δ : -153.17; -158.63; -162.90.

Pentafluorophenyl vinylbenzoate (FPVB) was synthesized as explained in [Nilles, K.; Theato, P. *Eur. Polym. Mater.* **2007**, **43**, 2901-2912]. $^1\text{H-NMR}$ (CDCl_3) δ : 8.15 (d, 2H); 7.55 (d, 2H); 6.79 (dd, 1H); 5.94 (d, 1H); 5.47 (d, 1H). $^{19}\text{F-NMR}$ (CDCl_3) δ : -152.89; -158.48; -162.84.

Propargyl vinylbenzoate (PVB). 4.56 g propargyl alcohol (81.3 mmol), 10.3 mL triethylamine and 60 mL dichloromethane were placed in a 100 mL round bottomed flask and stirred magnetically at 0 °C. 12.31 g *p*-vinyl benzoic acid chloride (73.9 mmol) was added slowly and the reaction mixture was stirred for 3 h at room temperature. Afterwards the mixture was washed three times with water and the organic phase was dried over MgSO_4 . The crude product was purified by column chromatography (eluent: hexane : ethyl acetate 1:1). Yield : 67.2 mmol (90.9 %). $^1\text{H-NMR}$ (CDCl_3) δ : 8.01 (d, 2H); 7.45 (d, 2H); 6.73 (dd, 1H); 5.85 (d, 1H); 5.38 (d, 1H); 4.90 (s, 2H); 2.50 (s, 1H).

Poly(methylsilsesquioxane) RAFT macro chain transfer agent (PMSSQ-mCTA). The macro initiator was synthesized as described in [Kessler, D.; Theato, P. *Macromolecules* **2008**, **41**(14), 5237-5244]. $^1\text{H-NMR}$ (CDCl_3) δ : 7.99 (br, 5H); 7.36 (br, 2H); 5.80 (br, 1.9H); 4.55 (br, 2H); 3.48 (br, 1.1H); 2.71 (br, 2H); 0.99 (br, 2H); 0.17 (br, 69.1H). $M_n = 4990$ g/mol, PDI = 1.63.

Poly(methylsilsesquioxane)-poly(pentafluorophenyl methacrylate) (PMSSQ-PFPMA). 0.5 g PMSSQ-mCTA, 10 mg AIBN, 4 mL dioxane and 2 g pentafluorophenyl methacrylate ester were placed in a 20 mL Schlenk flask and degassed for three times. The reaction mixture was stirred magnetically at 80 °C for 4 h and afterwards precipitated into *n*-hexane twice. (Yield: 1.05g). $^1\text{H-NMR}$ (CDCl_3) δ : 7.40 – 6.85 (br); 3.05 (br, 1H); 2; 2.70 – 1.92 (br); 1.50 – 1.27 (br); 0.15 (br). $^{19}\text{F-NMR}$ (CDCl_3) δ : -151.52; -156.11; -161.50. ^{29}Si CPMAS NMR δ : -48.55 (T1); -57.92 (T2); -65.93 (T3). $M_n = 31500$ g/mol, PDI = 1.72.

Poly(methylsilsesquioxane)-poly(pentafluorophenyl vinylbenzoate) (PMSSQ-PFPVB). 0.5 g PMSSQ-mCTA, 10 mg AIBN, 4 mL dioxane and 2 g FPVB were placed in a 20 mL Schlenk flask and degassed for three times. The reaction mixture was stirred magnetically at 80 °C for 4 h and afterwards precipitated into *n*-hexane twice. (Yield: 1.6 g). $^1\text{H-NMR}$ (CDCl_3) δ : 7.95 (br); 6.80 (br); 3.70 (br); 2.90 – 1.0 (br); 0.15 (br). $^{19}\text{F-NMR}$ (CDCl_3) δ : -153.10; -157.90; -163.13. $M_n = 34500$ g/mol, PDI = 1.88.

Poly(methylsilsesquioxane)-poly(propargyl vinylbenzoate) (PMSSQ-PPVB). 0.5 g PMSSQ-mCTA, 10 mg AIBN, 4 mL dioxane and 2 g PVB were placed in a 20 mL Schlenk flask and degassed for three times. The reaction mixture was stirred magnetically at 80 °C for 4 h and afterwards precipitated into *n*-hexane twice. (Yield: 1.3g). $^1\text{H-NMR}$ (CDCl_3) δ : 7.83 (br); 6.45 (br); 4.95 (br); 3.65 (br); 3.45 (br); 2.50 (br); 1.8 – 1.0 (br); 0.15 (br). $M_n = 31000$ g/mol, PDI = 1.94.

Stearic acid pentafluorophenyl ester. 4 g stearic acid (14 mmol) was dissolved in 30 mL DMF, 2.6 mg triethylamine and 5.84 g pentafluorophenyl trifluoro acetate (21 mmol) were added and the solution was stirred for 1h. After removing the solvent and side products at low

pressure the product was obtained as colorless needles. Yield: 4.0 g (46 %).

Stearic acid 2-aminoethaneamide. 4.50 g ethylene diamine (74.9 mmol) was dissolved in 20 mL DMF. 4.0 g Stearic acid pentafluorophenyl ester was added slowly and the solution was stirred magnetically at 0 °C. By precipitation in diethylether the product was obtained as colorless powder. Yield: 2.1 g (quant.). $^1\text{H-NMR}$ (CDCl_3) δ : 7.99 (s, 1H); 3.29 (m, 2H); 2.80 (m, 2H); 2.16 (t, 2H); 1.60 (t, 2H); 1.23 (s, 30H); 0.85 (t, 3H).

Stearic acid 2-azidoethaneamide. 2.34 g sodium azide (36 mmol) was dissolved in 20 mL water at 0 °C. 20 mL dichloromethane and 5.00 g trifluoromethane sulfonic acid anhydride (17.7 mmol) were added to the solution and stirred magnetically for 2 h. 20 mL conc. NaHCO_3 solution was added and the organic phase was separated. After washing with conc. NaHCO_3 solution 1.23 g triethylamine (12.2 mmol) and 98 mg CuSO_4 (0.61 mmol) were added. 2.00 g stearic acid 2-aminoethaneamide was dissolved in 20 mL dichloromethane suspended and added to the reaction mixture. After stirring for 48 h the reaction mixture was washed with conc. NaHCO_3 solution and two times with water. The solvent was removed at low pressure. Yield: 950 mg (44%). $^1\text{H-NMR}$ (CDCl_3) δ : 3.42 (t, 2H); 2.17 (t, 2H); 1.60 (t, 2H); 1.23 (s, 30H); 0.85 (t, 3H).

4-Benzoic acid methyl azide was prepared similarly as explained for stearic acid 2-azidoethaneamide starting from *p*-amino benzoic acid. $^1\text{H-NMR}$ (CDCl_3) δ : 8.01 (d, 2H); 7.49 (d, 2H); 2.71 (m, 2H). $^{13}\text{C-NMR}$ (CDCl_3) δ : 169.45; 144.33; 130.91; 128.99; 50.55.

Poly(ethyleneglycol) methylether azide (PEG- N_3). Poly(ethyleneglycol) monomethylether was purified by column chromatography using methanol, acetone, chloroform (1:2:7) and afterwards dried azeotrop with benzene. 100 g Poly(ethyleneglycol) monomethylether (0.19 mol), 33.2 mL triethylamine (0.24 mol), 22.5 mL methane sulfonic acid chloride (0.29 mmol) and 200 mL THF were stirred mechanically at room temperature. Afterwards, the reaction mixture was filtered, the solvent was removed and the residue was dried in high vacuum. After dissolving in 200 mL ethanol, 24.70 g sodium azide (0.38 mol) was added and the solution was refluxed over night. Ethanol was removed at low pressure and the residue was dissolved in dichloromethane, the mixture was filtered and washed three times with water. The organic phase was dried over MgSO_4 , the solvent was removed and the product was dried in high vacuum. Yield: almost quantitative. $^1\text{H-NMR}$ (CDCl_3) δ : 3.46 (br); 3.17 (br). $^{13}\text{C-NMR}$ (CDCl_3) δ : 70.41; 59.80; 50.47. $M_n = 550$ g/mol.

Surface coating. The PMSSQ-PFPA solution was spin-coated onto clean substrates (15 s, 4000 rpm, 10 wt% solution in THF). To induce the secondary cross-linking of the inorganic block, the samples were annealed at 130 °C for 2 h and afterwards washed with THF for 30 minutes to remove any non-bonded material.

Surface-analogous reaction of PFPMA or PFPVB reactive surfaces. To functionalize the surface afterwards via a polymer analogous reaction, the samples were placed in a solution of the desired amine in THF (10 wt%) at room temperature for 1 h. To remove the excess of the amine, the surface was washed several times with THF. For detailed procedure see [Kessler, D.; Theato, P. *Langmuir* 2009, doi: 10.1021/la9005949].

Surface-analogous reaction of PVB reactive surfaces. The copper-catalyzed 1,3-dipolar cycloaddition between one surface-bounded species and one species in solution was performed as briefly described in [Roth, P. J.; Kessler, D.; Zentel, R.; Theato, P. *J. Polym. Sci. Part A* **2009**, *47*(12), 3118-3130]

Figure S1.

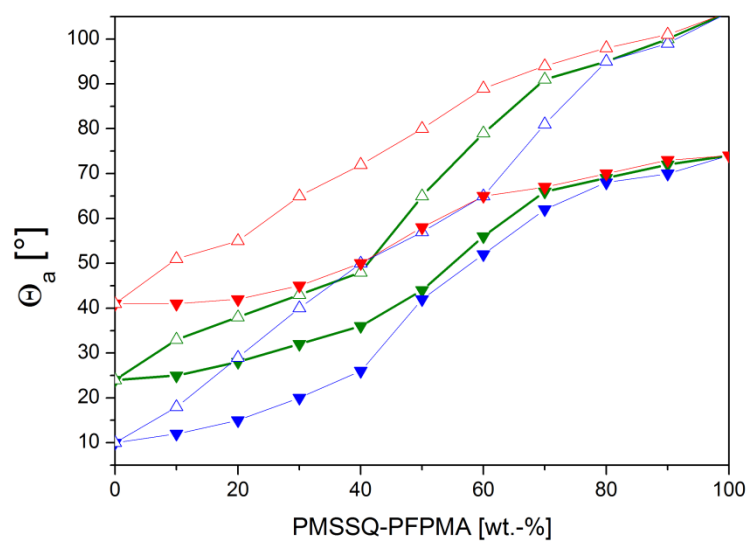


Figure S1. Different mixtures of PMSSQ-PFPMA (R_A) and PMSSQ-PPVB (R_C) were spin-coated onto Si, after conversion with (1) 4-benzoic acid methyl azide and (2) isopropylamine, the advancing contact angles were measured at different temperatures (filled symbols: $T = 15$ °C, free symbols: $T = 60$ °C). Green lines measured at $\text{pH} = 7$, red lines measured at $\text{pH} = 2$, blue lines measured at $\text{pH} = 11$.

Figure S2.

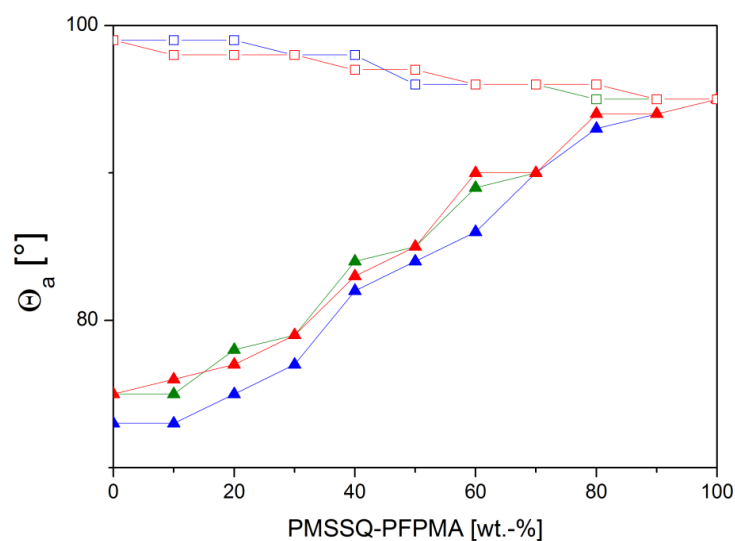


Figure S2. Advancing contact angles of water on silicon surfaces after applying different mixtures of two reactive coating materials. Upper graphs: Mixtures of PMSSQ-PFPVB and PMSSQ-PFPMA (wt.-% PMSSQ-PFPMA between 0% and 100%), green: pH = 7; red: pH = 2; blue: pH = 11. Lower graphs: Mixtures of PMSSQ-PPVB and PMSSQ-PFPMA, green: pH = 7; red: pH = 2; blue: pH = 11.

Figure S3.

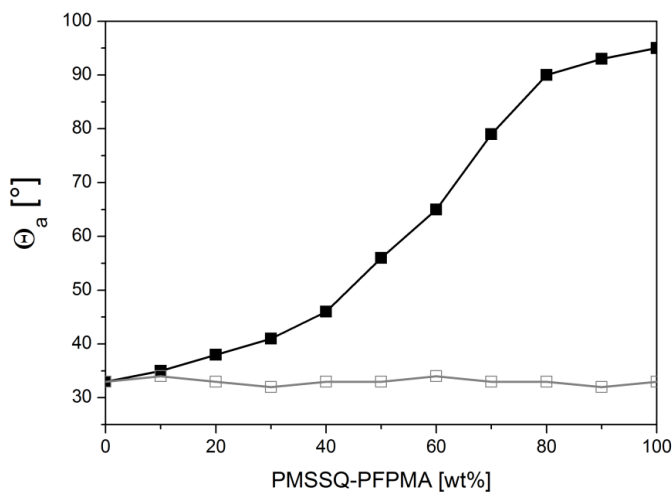


Figure S3. A series of mixtures of PMSSQ-PFPMA and PMSSQ-PPVB were spin coated on silicon wafers. First the cycloaddition with PEG-azide was performed and the contact angle was measured (black line), afterwards the dual-reactive surface was converted with PEG-amine yielding a complete PEGylated surface (grey line).

Table S1. Obtained advancing and receding contact angles on a triple reactive surface with respect to the functionalization of R_C (R_A functionalized with isopropylamine, R_B functionalized with p-amino benzoic acid).

Function at R_C		Θ_a [°]		Θ_r [°]
PEG	pH 2	15 °C	35	31
		60 °C	54	51
	pH 7	15 °C	33	29
		60 °C	52	50
	pH 11	15 °C	29	14
		60 °C	47	32
acetylene	pH 2	15 °C	61	58
		60 °C	92	88
	pH 7	15 °C	59	55
		60 °C	91	84
	pH 11	15 °C	53	34
		60 °C	87	59
Stearic acid	pH 2	15 °C	103	99
		60 °C	115	106
	pH 7	15 °C	99	94
		60 °C	110	100
	pH 11	15 °C	73	39
		60 °C	100	64

5 Conclusion

A new class of inorganic-organic hybrid polymers could successfully be prepared by the combination of different polymerization techniques. The access to a broad range of organic polymers incorporated into the hybrid polymer was realized using two independent approaches.

In the first approach a functional poly(silsesquioxane) (PSSQ) network was pre-formed, which was capable to initiate a controlled radical polymerization to graft organic vinyl-type monomers from the PSSQ precursor. As controlled radical polymerization techniques atom transfer radical polymerization (ATRP), as well as reversible addition fragmentation chain transfer (RAFT) polymerization could be used after defined tuning of the PSSQ precursor either toward a PSSQ macro-initiator or to a PSSQ macro-chain-transfer-agent. The polymerization pathway, consisting of polycondensation of trialkoxy-silanes followed by grafting-from polymerization of different monomers, allowed synthesis of various functional hybrid polymers. A controlled synthesis of the PSSQ precursors could successfully be performed using a microreactor setup; the molecular weight could be adjusted easily while the polydispersity index could be decreased well below 2.

The second approach aimed to incorporate differently derived organic polymers. As examples, polycarbonate and poly(ethylene glycol) were end-group-modified using trialkoxysilanes. After end-group-functionalization these organic polymers could be incorporated into a PSSQ network.

These different hybrid polymers showed extraordinary coating abilities. All polymers could be processed from solution by spin-coating or dip-coating. The high amount of reactive silanol moieties in the PSSQ part could be cross-linked after application by annealing at 130° for 1h. Not only cross-linking of the whole film was achieved, which resulted in mechanical interlocking with the substrate, also chemical bonds to metal or metal oxide surfaces were formed. All coating materials showed high stability and adhesion onto various underlying materials, reaching from metals (like steel or gold) and metal oxides (like glass) to plastics (like polycarbonate or polytetrafluoroethylene).

As the material and the synthetic pathway were very tolerant toward different functionalities, various functional monomers could be incorporated in the final coating material. The incorporation of *N*-isopropylacrylamide yielded in temperature-responsive surface coatings, whereas the incorporation of redox-active monomers allowed the preparation of semi-conductive coatings, capable to produce smooth hole-injection layers on transparent conductive electrodes used in optoelectronic devices.

The range of possible applications could be increased tremendously by incorporation of reactive monomers, capable to undergo fast and quantitative conversions by polymer-analogous reactions. For example, grafting pentafluorophenylacrylate from a PSSQ precursor yielded a reactive surface coating after application onto numerous substrates. Just by dipping the coated substrate into a solution of a functionalized amine, the desired function could be immobilized at the interface as well as throughout the whole film.

The obtained reactive surface coatings could be used as basis for different functional coatings for various applications. The conversion with specifically tuned amines yielded in surfaces with adjustable wetting behaviors, switchable wetting behaviors or as recognition element for surface-oriented bio-analytical devices.

The combination of hybrid materials with orthogonal reactivities allowed for the first time the preparation of multi-reactive surfaces which could be functionalized sequentially with defined fractions of different groups at the interface.

The introduced concept to synthesis functional hybrid polymers unifies the main requirements on an ideal coating material. Strong adhesion on a wide range of underlying materials was achieved by secondary condensation of the PSSQ part, whereas the organic part allowed incorporation of various functionalities. Thus, a flexible platform to create functional and reactive surface coatings was achieved, which could be applied to different substrates.

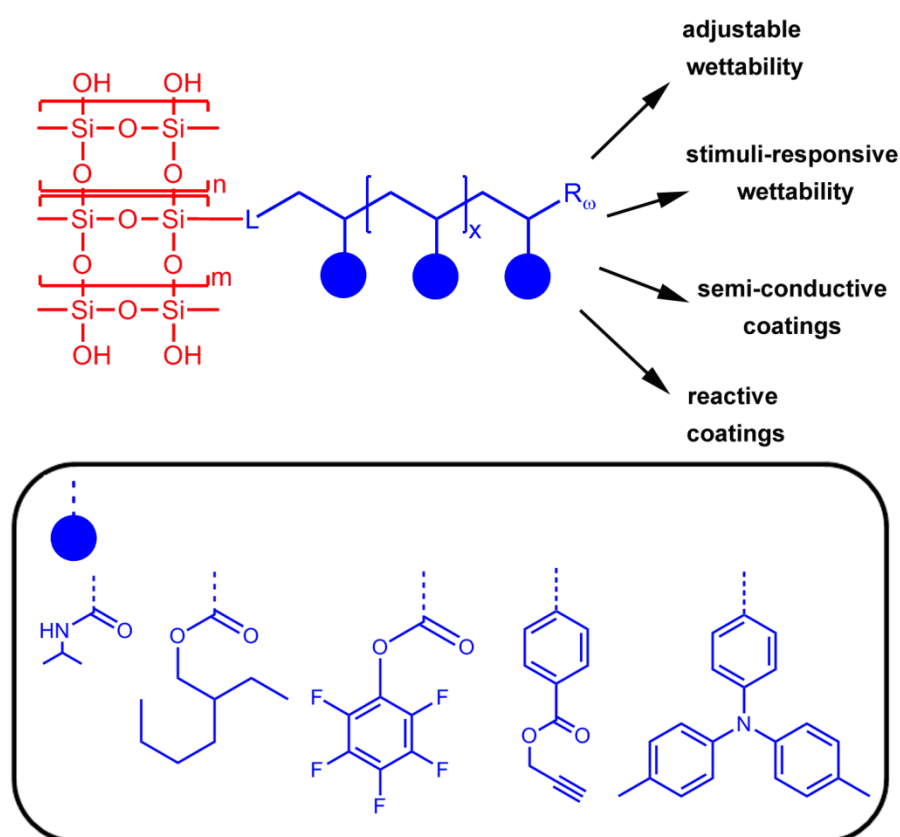


Figure 5.1. General structure of PMSSQ-based hybrid polymers, produced by grafting organic polymers from a PMSSQ pre-cursor and some examples of functional moieties, which could be incorporated into the material (L and R_ω depend on the polymerization technique used).

Papers & Proceedings

1. “Functionalized Surface Coatings Composed of Organic-Inorganic Hybrid Polymers”
Kessler, D.; Bahnmüller, S.; Theato, P. *PMSE Prepr.* **2006**, *95*, 192-193.
2. “Temperature-Responsive Surface Coatings Based on Poly(methylsilsesquioxane)-Hybrid Polymers”
Kessler, D.; Theato, P. *Macromol. Symp.* **2007**, *249-250*, 424-430.
3. “Versatile Surface Coatings Composed of New Inorganic/Organic Hybrid Materials”
Kessler, D.; Theato, P. *PMSE Prepr.* **2007**, *97*, 875-876.
4. “Substrate-Independent Stable and Adherent Reactive Surface Coatings and Their Conversion with Amines”
Kessler, D.; Metz, N.; Theato, P. *Macromol. Symp.* **2007**, *254*, 34-41.
5. “Synthesis of Processable Inorganic-Organic Hybrid Polymers Based on Poly(silsesquioxanes): Grafting from Polymerization Using ATRP”
Kessler, D.; Teutsch, C.; Theato, P. *Macromol. Chem. Phys.* **2008**, *209(14)*, 1437-1446.
Coverpage *Macromol. Chem. Phys.* **2008**, *209(14)*.
6. “Synthesis of Functional Inorganic-Organic Hybrid Polymers Based on Poly(silsesquioxanes) and Their Thin Film Properties”
Kessler, D.; Theato, P. *Macromolecules* **2008**, *41(14)*, 5237-5244.
7. “New Reactive Hybrid Coatings as Versatile Bio-Immobilization Supports”
Kessler, D.; Metz, N.; Theato, P. *PMSE Prepr.* **2008**, *99*, 235-236.
8. “Synthesis of Hybrid Polymers Containing Acetal Side Groups for the Design of Versatile Responsive Surfaces”
Wiss, K.; Kessler, D.; Theato, P. *PMSE Prepr.* **2008**, *99*, 74-75.
9. “Verfahren zur Abtrennung einer organischen von einer elektrolythaltigen wässrigen und organischen Phase”, german patent application **DE 10 2006 050 381.3**
“Method for the Separation of an Organic Phase from an Elektrolyte-Containing Aqueous and Organic Phase”, international patent application **WO/2008/049548, PCT/EP2007/008879**
Meyer, H.; Naberfeld, G.; Rechner, J.; Warsitz, R.; Traving, M.; Bächer, W.; Elsner, T.; Nennemann, A.; Bahnmüller, S.; Langstein, G.; Hitzbleck, J.; Theato, P.; Kessler, D.; Duff, D.-G.; Bayer MaterialScience AG

10. "A Method for Obtaining Defined End Groups of Polymethacrylates Prepared by the RAFT Process During Aminolysis"
Roth, P.; Kessler, D.; Zentel, R.; Theato, P. *Macromolecules* **2008**, *41*(22), 8316-8319.
11. "Synthesis of Defined Poly(silsesquioxanes): Fast Polycondensation of Trialkoxysilanes in a Continuous Flow Microreactor"
Kessler, D.; Löwe, H.; Theato, P. *Macromol. Chem. Phys.* **2009**, *210*(10), 807-813.
Coverpage *Macromol. Chem. Phys.* **2009**, *210*(10).
12. "Versatile ω -End Group Functionalization of RAFT Polymers using Functional Thiosulfonates"
Roth, P.; Kessler, D.; Zentel, R.; Theato, P. *J. Pol. Sci. Part A: Pol. Chem.* **2009**, *47*(12), 3118-3130.
13. "Reactive Surface Coatings Based on Polysilsesquioxanes: Defined Adjustment of Surface Wettability (Part of the "Langmuir 25th year: Wetting and superhydrophobicity" special issue)
Kessler, D.; Theato, P. *Langmuir* **2009**, doi: 10.1021/la9005949.
14. "Surface Coatings Based on Polysilsesquioxanes: Solution Processible Smooth Hole-Injection-Layers for Optoelectronic Applications"
Kessler, D.; Lechmann, M. C.; Noh, S.; Berger, R.; Lee, C.; Gutmann, J. S.; Theato, P. *Macromol. Rapid Commun.* **2009**, doi: 10.1002/marc.200900196.
15. "Surface Coatings Based on Polysilsesquioxanes: Grafting-from Approach Starting from Organic Polymers"
Kessler, D.; Theato, P. *MRS Proc.* **2009**, *1190*, accepted.
16. "Reactive Surface Coatings Based on Polysilsesquioxanes: Controlled Functionalization for Specific Protein Immobilization"
Kessler, D.; Roth, P.; Theato, P. *Langmuir* **2009**, doi: 10.1021/la901878h.
17. "Versatile Responsive Surfaces via Hybrid Polymers Containing Acetal Side Groups"
Wiss, K.; Kessler, D.; Wendorff, T. J.; Theato, P. *Macromol. Chem. Phys.* **2009**, accepted.
18. "Functional Templates for Hybrid Materials with Orthogonal Functionality"
Lechmann, M. C.; Kessler, D.; Gutmann, J. S. *Langmuir* **2009**, accepted.
19. "Modular Approach toward Multi-functional Surfaces with Adjustable and Dual-Responsive Wettability Using a Hybrid Polymer Toolbox"
Kessler, D.; Nilles, K.; Theato, P. *Chem. Commun.*, submitted.

Contributed Oral Presentations

- 1 “Variable Surface Coatings Composed of Organic-Inorganic Hybrid Polymers”
IUPAC International Symposium on Advanced Polymers for Emerging Technologies
Oct. 2006 Busan, Korea
- 2 “Versatile Surface Coatings Composed of New Inorganic/Organic Hybrid Materials”
234th ACS National Meeting
Aug. 2007 Boston, MA, USA
- 3 “Novel Coating Agents Based on Functionalized Hybrid Materials”
Bayreuth Polymer Symposium
Sept. 2007 Bayreuth, Germany
- 4 “Polymeric Nanoobjects Synthesized by Reactive Monomers”
42nd IUPAC World Polymer Congress MACRO 2008
July 2008 Taipei, Taiwan
- 5 “Synthesis and Characterization of Reactive Derivatives of 4-Vinylbenzoic Acid”
42nd IUPAC World Polymer Congress MACRO 2008
July 2008 Taipei, Taiwan
- 6 “New Reactive Hybrid Coatings as Versatile Bio-Immobilization Supports”
236th ACS National Meeting
Aug. 2008 Philadelphia, PA, USA
- 7 “Anorganische-organische Hybridpolymere: Design funktioneller Oberflächen”
Seminar über Forschungsarbeiten am Institut für organische Chemie Mainz
Nov. 2008 Mainz, Germany
- 8 “Hybrid Polymer Coatings: Design of Functional Surfaces”
IMM Young Scientists’ Workshop „Microfluidic Systems and Sensor Applications“
Nov. 2008 Mainz, Germany
- 9 “Stable Semi-conductive Hybrid Coatings: Synthesis in Continuous Flow Process and Characterization of Optoelectronic Properties”
IRTG Spring Meeting
Feb. 2009 Seoul, Korea
- 10 “Reactive Polymer Coatings: Innovative Design of Functional Surfaces”
MRS Spring Meeting
Apr. 2009 San Francisco, CA, USA

Poster Presentations

- 1 “Functional Inorganic-Organic Hybrid Materials Based on PMSSQ”
Korean Polymer Society Fall Meeting
Oct. 2005 Jeju, Korea
- 2 “Flexible Funktionalisierung von Nanoobjekten mit Polymeren” (Poster Award)
Materialwissenschaftliches Forschungszentrum MWFZ Jahrestagung
May 2006 Mainz, Deutschland
- 3 “Variable Synthese von anorganisch-organischen Hybridpolymeren auf PMSSQ-Basis”
GdCh Fachgruppentagung „Polymers and Coatings“
Sept. 2006 Mainz, Deutschland
- 4 “Organic-Inorganic Hybrid Polymers: A Versatile Toolbox for Functional Surface Coatings”
International Symposium on Fundamental and Applied Polymer Science: Toward Next Generation Materials
Jan. 2007 Strasbourg, Frankreich
- 5 “Functional Hybrid Polymers to Create Cross-Linked Interpenetrating Networks of Donor and Acceptor Materials for Optoelectronic Devices”
IRTG Spring Meeting
Feb. 2007 Mainz, Germany
- 6 “Organic-Inorganic Hybrid Polymers: A Versatile Toolbox for Functional Surface Coatings”
Smart Coatings 2007
Feb. 2007 Orlando, FL, USA
- 7 “Functional Polymers for Optoelectronic Applications”
Materialwissenschaftliches Forschungszentrum MWFZ Jahrestagung
May 2007 Mainz, Deutschland
- 8 “Inorganic-Organic Hybrid Polymers: Toward Functional and Reactive Surface Coatings”
REACT 2007
Sept. 2007 Dresden, Deutschland
- 9 “Functional Polymers for Optoelectronic Applications”
IRTG Fall Meeting
Oct. 2007 Seoul, Korea

-
- 10 “From Easy Processable Coating Materials towards Semi-Conductive Surface Layers”
IRTG Spring Meeting
Feb. 2008 Schloß Ringberg, Rottach-Egern, Deutschland
- 11 “Functional Hybrid Polymers: Controlling Wettability, Bio-Compatability and Optoelectronic Behavior of Surfaces”
International Conference on Advanced Functional Polymers and Self-Organized Materials
Sept. 2008 Busan, Korea
- 12 “Reaktive Hybridpolymere: Innovatives Design funktioneller Oberflächen”
(MACRO Award 2009)
Makromolekulares Kolloquium 2009 Freiburg
Feb. 2009 Freiburg, Deutschland
- 13 “Highly Crosslinked Polymer Films for Microfluidic or Optoelectronic Devices”
Frontiers in Polymer Science
June 2009 Mainz, Deutschland
- 14 “Highly Crosslinked Polymer Films for Microfluidic or Optoelectronic Devices”
(accepted)
International Workshop on Self-organized Materials for Optoelectronics
Aug. 2009 Mainz, Germany

7 Acknowledgements

The research presented in this thesis would not have been possible without numerous supports of different people and institutions.

First of all, I would like to acknowledge my advisor [REDACTED] for valuable discussions, suggestions, ideas and support during the last years and [REDACTED] for acceptance to his research group, various suggestions and ideas which contributed to this work.

Most of the ideas and concepts were based on different collaborations. I would like to thank the following collaborators contributing to the successes of the presented work:

- [REDACTED], [REDACTED], [REDACTED], [REDACTED] and [REDACTED] (AK Theato / AK Zentel, University Mainz)
- [REDACTED], [REDACTED], [REDACTED] (Max Planck Institute for Polymer Science)
- [REDACTED], [REDACTED] (Institut für Mikrotechnik Mainz GmbH)
- [REDACTED], [REDACTED] (Organic Semiconductor Laboratory, Seoul National University)
- [REDACTED], [REDACTED], [REDACTED] (Bayer MaterialScience)

Financial support during my doctoral studies was kindly provided by different scholarships. Sincere thanks go to

- the International Research Training Group “Self-Assembled Materials for Optoelectronic Applications” (IRTG 1404) (IRTG-stipend from October 2006 till February 2007).
- the Fund of the Chemical Industry (“Fonds der Chemischen Industrie”), German Chemical Industry Association (VCI) (“Chemiefonds”-stipend from March 2007 till February 2009).
- the Graduate school of excellence “Material Science in Mainz, Polymers in Advanced Materials (POLYMAT)” (GSC 266) (POLYMAT-stipend from March 2009 till August 2009).

For valuable synthetic support, during monomer, polymer, and hybrid polymer synthesis, I thank [REDACTED]

I thank all present and former members of the AK Zentel / AK Theato for generating an extraordinary working atmosphere, valuable discussions and also lots of fun during the entire time. In addition, I thank all members of the IRTG program for making the IRTG an ideal platform for scientific and cultural exchange and furthermore for enjoyable meetings and workshops in Korea and Germany.

Last but most important, I wish to thank my family and my friends for support and encouragement throughout the whole time at university.

